Characterisation of Surfactant Protein A as a Novel Prophylactic Means Against Oncogenic HPV Infections

Sinead Carse

Thesis presented for the Degree of

Doctor of Philosophy

In the Division of

Medical Biochemistry and Structural Biology

Department of Integrative Biomedical Sciences

University of Cape Town

December 2023

Declaration

I, Sinead Carse, hereby declare that the work in which this thesis is based is my original work (except where acknowledgements indicate otherwise), and that neither the whole work nor any part of it has been, is being, or is to be submitted for another degree in this or any other university. My MSc thesis, submitted to the University of Cape Town in February 2020 and published in *Pathogens* in December 2019, is preliminary work foundational to the current work and has been included in this thesis and described as such. I am presenting this thesis for academic examination toward the Degree of Doctor of Philosophy in Medical Biochemistry.

I empower the university to reproduce for the purpose of research either the whole or any portion of the contents in any manner whatsoever.

Signed 

Date: 11/12/2023

Acknowledgments

I would first and foremost like to express my deepest gratitude to my supervisor, Dr Georgia Schäfer. Her constant support and guidance has been instrumental to the progress and success in my academic career. She truly embodies the ultimate mentor – one that encourages independence while always being supportive. Dr Schäfer not only guided me academically but also played a pivotal role during some of the tougher moments in my research journey. Her encouragement during the COVID-19 pandemic and more personal struggles have truly kept me going and helped shape my perspective. I'm immensely grateful for her unwavering support throughout these past few years, which made a world of difference in both my research and personal growth. Thank you, Dr Schäfer, for being a mentor I could always count on.

I would like to thank the members of the Emerging Viruses Group, for their support in the lab. I would like to acknowledge our lab manager, Abeen Chetram, for his role in maintaining the lab. Thank you to all the friends I have made during my time in this group. It is the little moments - from sharing our struggles in the lab to laughing over a coffee on campus – that made it easier to overcome the challenges of a PhD.

I would like to thank the members of the ICGEB. Thank you Reagon Petersen and Justin Henry for their constant support on the technical side, and for their tireless effort in maintaining the labs. Thank you to the administrative staff for their support, and to Dr Luiz Zerbini, our Director, for creating a collaborative environment at the ICGEB.

Thank you to Prof Martina Bergant Marušič for hosting me at her wonderful lab at the University of Nova Gorica, Slovenia. Her guidance and support have been instrumental. My thanks extend to the members of the Laboratory of Environmental and Life Sciences at UNG for making me feel so welcome.

Thank you to Dr Jens Madsen for generously providing the purified human surfactant protein A, and to John Muhiri for providing me with THP-1 cells, and Dr Alta-Albertha Van Zyl for providing me with the HPV-PsVs plasmids.

A thank you to the African Microscopy Initiative (AMI) for supporting the microscopy aspect of my PhD work. A big thank you to Dr Mike Reiche and Dr Viantha Naidoo from the AMI imaging centre for their guidance and support.

Thank you to Tim Reid for his guidance on all my flow cytometry work and for providing me with conjugated antibodies. Thank you to Dr Muki Shey and Dr Nyaradzo Chigorimbo Tsikawa for also providing me with conjugated antibodies and guidance thereof.

Thank you to my family and friends for all their support, and a very special thank you to my partner, Gabriel Stein. He has been with me every step of my PhD, constantly pushing me forward when I struggled to do so myself. His love and support has made one of the most challenging and stressful chapters of my life so far also one of the best. Thank you, Gabe, for being by my side. I would have it no other way.

A final thank you to the Oppenheimer Memorial Trust, the Poliomyelitis Research Foundation, and Dr Georgia Schäfer for providing me with financial assistance. This work was funded by research grants from the National Research Foundation and the Poliomyelitis Research Foundation.

Table of contents

Declaration i

Acknowledgments ii

Table of contents iv

List of figures and tables vii

Abbreviations x

Abstract 1

1 Introduction 2

1.1 Innate Immunity 3

1.1.1 Cellular components 4

1.1.2 The inflammatory response: The role of chemical mediators 7

1.1.3 Pattern recognition receptors 8

1.1.4 Bridging innate and adaptive immunity: The temporal handoff 9

1.1.5 Immune evasion strategies of viruses 10

1.2 Oncogenic HPV genome and structure 11

1.3 HPV life cycle 13

1.4 HPV evasion of the host immune system 18

1.5 HPV vaccines 21

1.6 Cervical cancer prevention and treatment in LMIC 21

1.7 Alternative HPV prophylaxis and therapy 23

1.8 Surfactant Proteins A and D 25

1.8.1 SP-A and SP-D and their role in innate immunity 26

1.8.2 Pathogen agglutination, opsonisation and control by SPs 27

1.8.3 Activation of the complement cascade by SP-A and SP-D 28

1.8.4 SP-A and SP-D interaction with immune cell receptors 28

1.8.5 SPs interaction with immune effectors 29

1.8.6 SP-A and SP-D and their role in adaptive immunity 29

1.9 Identification of SP-A as a novel immune molecule modulating HPV infection 30

1.10 Rationale and aims 33

2 Materials and methods 34

2.1 Cell culture....34
2.1.1 Established cell lines....34
2.1.2 Maintaining and sub-culturing cell lines....34
2.1.3 Cell counting and plating....35
2.1.4 Storage of cell lines....35
2.2 Development of an immune cell panel derived from THP-1 cells....35
2.2.1 Differentiation of THP-1 cells to M0 (steady-state) macrophages....35
2.2.2 Differentiation of M0 to M1, M2c, and M2a macrophages....36
2.2.3 Differentiation of THP-1 cells to immature dendritic cells (DC0s)....36
2.2.4 Validation of immune cell lineages by flow cytometry....36
2.3 Purification of Native Human SP-A....38
2.4 HPV pseudovirus (HPV-PsVs) production....38
2.4.1 Plasmid production....38
2.4.2 Mammalian cell transfection and harvest of HPV-PsVs....39
2.4.3 HPV-PsVs labelling with Alexa Fluor™ 488....39
2.4.4 HPV-PsVs purification – discontinuous caesium chloride gradient....40
2.4.5 Quality checks of the HPV-PsVs preparations....40
2.4.5.1 SDS-PAGE and Silver Stain....40
2.4.5.2 HPV infection and neutralisation assay....41
2.4.5.3 Negative-stain electron microscopy....41
2.4.5.4 Protein quantification by BCA....41
2.5 Experiments with SP-A opsonised HPV-PsVs....42
2.5.1 Assessing HPV-PsVs internalisation with flow cytometry (FACS)....42
2.5.2 Immune and epithelial cell co-cultures....43
2.5.3 Confocal microscopy....43
2.5.3.1 Sample preparation....43
2.5.3.2 Image acquisition....44
2.5.3.3 Image analysis using Fiji (Image J)....45
2.5.4 Assessment of immune modulatory proteins....46
2.6 Statistics....47
3 Results....48
3.1 Development of an immune cell panel derived from THP-1 cells....48
3.2 HPV-PsVs production....57
3.3 Opsonisation and agglutination of HPV-PsVs particles with SP-A....59

3.4 SP-A enhances HPV16-PsVs uptake into immune cells but dampens uptake into epithelial cells 59
3.4.1 Preincubation with SP-A is required for altered HPV16-PsVs uptake 62
3.4.2 Viral uptake is modulated by SP-A in HaCaT and RAW264.7 independently of HPV type 63
3.4.3 SP-A affects internalisation into THP-1 monocytes and immature dendritic cells HPV type-dependently 64
3.5 Monitoring intracellular trafficking of HPV in the presence of SP-A 65
3.6 SP-A modulates HPV-PsVs infection in an *in vitro* immune cell / epithelial cell co-culture system 70
3.6.1 The presence of RAW264.7 or THP-1 cells and SP-A decreases HPV16-PsVs infection of HaCaT cells 71
3.6.2 The presence of M0 macrophages, and to a lesser extent M1 and DC0, results in an SP-A-mediated decrease in HPV16-PsVs infection of HaCaT cells 73
3.6.3 SP-A contributes to the immune cell-mediated reduction of infection by multiple HPV types in HaCaT cells 75
3.7 Assessing altered immune cell cytokine profiles in response to HPV16-PsVs infection: The role of SP-A 77
4 Discussion 90
5 Conclusion 99
6 References 101
7 Appendix 121
7.1 Solution recipes 121
7.2 Additional material 123

List of figures and tables

Figure 1: The immune functions of keratinocytes in pathogen clearance and tissue repair. ...6
Figure 2: Cellular components of the innate and adaptive immune system.. 10
Figure 3: HPV viral genome and capsid structure.. 11
Figure 4: Schematic illustration of the early stages of HPV infection, indicating the sites of inhibition of various anti-HPV molecules.....15
Figure 5: The life cycle of HPV and its key immune evasion mechanisms.....17
Figure 6: Structure of SP-A and SP-D. 26
Figure 7: Binding of HPV16-PsVs to SP-A (but not SP-D) results in increased viral uptake by RAW264.7 macrophages.....30
Figure 8: SP-A reduces HPV16-PsVs infection *in vivo* by increasing macrophage recruitment into the basal epithelium and increased viral uptake by selected immune cell populations. .32
Figure 9: Differentiation scheme of THP-1 cells to produce the immune cell panel. 49
Figure 10: Representative brightfield images of THP-1-derived immune cells in culture. 50
Figure 11: Flow cytometry analysis of the THP-1-derived ICP.. 51
Figure 12: Cell-surface marker expression on THP-1-derived immune cells.....53
Figure 13: Phenotypic analysis of THP-1-derived immune cells using t-SNE. 54
Figure 14: t-SNE analysis of THP-1-derived immune cells with marker expression heatmaps. 56
Figure 15: Representative SDS-PAGE gel of the major and minor capsid proteins for each of the HPV-PsVs types produced. 57
Figure 16: Qualitative comparison of the “band” and “bottom” HPV-PsVs fractions.....58
Figure 17: HPV-PsVs are agglutinated by SP-A to different extents. 59
Figure 18: HPV16-PsVs uptake into various immune cells and HaCaT epithelial cells assessed by FACS.....61
Figure 19: HPV16-PsVs internalisation into HaCaT and various immune cells is altered by preincubation with SP-A.....62
Figure 20: Assessment of HPV16-PsVs preincubation with SP-A versus SP-A priming of cells for modulation of viral internalisation.. 63
Figure 21: SP-A modulates internalisation of multiple HPV-PsVs types into HaCaT and RAW264.7 cells to varying degrees.....64
Figure 22: SP-A modulates internalisation of multiple HPV-PsVs types into THP-1 and DC0 cells to varying degrees. 65
Figure 23: Analysis of HPV16-PsVs uptake and particle size at 3 hpi.....66
Figure 24: HPV16-PsVs particle size and occurrence in HaCaT and RAW264.7 at 3 hpi.. ..67

Figure 25: Colocalisation characteristics of HPV16-PsVs and lysosomes for HaCaT and RAW264.7 at 8 hpi. 69
Figure 26: Representative image of the epithelial cell / immune cell co-culture system. 70
Figure 27: Luciferase activity is indicative of HaCaT epithelial cell, but not immune cell infection 71
Figure 28: HPV16-PsVs infection of HaCaT cells is decreased in the presence RAW264.7 or THP-1, and further dampened by preincubation with SP-A. 72
Figure 29: HPV16-PsVs infection of HaCaT cells is decreased in the presence of M0 or M1 macrophages, or DC0, and further dampened by preincubation with SP-A to different degrees. 74
Figure 30: Infection levels of HaCaT cells by selected oncogenic HPV types is dampened in the presence of SP-A and RAW264.7, THP-1, and DC0 cells 76
Figure 31: Detection of multiple cytokines, chemokines, growth factors and other soluble proteins in cell culture supernatants of THP-1 cells (left) and DC0 cells (right). 78
Figure 32: Venn diagram showing the number of differentially expressed immune modulators as identified by analysis A and analysis B in THP-1 and DC0. 83
Figure 33: Venn diagram showing the number of immune modulators differentially expressed in THP-1 and DC0 cells in the SP-A:HPV16-PsVs group compared to the untreated control. 84
Figure 34: Cytokines, chemokines, and growth factors differentially expressed in the SP-A:HPV16-PsVs group compared to untreated control in THP-1 cells. 85
Figure 35: Cytokines, chemokines, and growth factors differentially expressed in the SP-A:HPV16-PsVs group compared to untreated control in DC0. 88
Figure 36: STRING Protein-Protein Interaction Cluster Network for immune modulators upregulated in DC0 cells in the SP-A:HPV16-PsVs group. 89
Figure 37: Proposed mechanisms of SP-A immunomodulation in the context of HPV infection. 100
Supplementary Figure 1: Restriction enzyme digest of the plasmids used to produce HPV-PsVs 123
Supplementary Figure 2: Gating strategy for the FACS internalisation assay. 124
Supplementary Figure 3: Maps of the expression plasmids for the various L1/L2-specific HPV types prepared in this study. 127
Supplementary Figure 4: HPV16-PsVs internalisation into HaCaT, HeLa, and NIKS cells is altered by SP-A preincubation. 128
Supplementary Figure 5: Transformation of images acquired of multispectral fluorescent beads. 128

Supplementary Figure 6: Cytokines, chemokines, and growth factors that are upregulated by SP-A alone in THP-1 cells.. 132

Table 1: Stimulants used for phenotype biasing of M0 to M1, M2a, and M2c macrophages after 24 h.....36
Table 2: Conjugated antibodies used to phenotype the THP-1-derived immune cell panel. .37
Table 3A: Analysis A - Immune modulators that were differentially expressed in the SP-A:HPV16-PsVs group relative to the untreated control in THP-1 cells. 79
Table 3B: Analysis B - Immune modulators that were differentially expressed in the SP-A:HPV16-PsVs group relative to the HPV16-PsVs only group in THP-1 cells.....79
Table 4A: Analysis A – Immune modulators that were differentially expressed in the SP-A:HPV16-PsVs group relative to the untreated control in DC0 cells.....80
Table 4B: Analysis B – Immune modulators that were differentially expressed in the SP-A:HPV16-PsVs group relative to the HPV16-PsVs only group in DC0 cells..…..82
Supplementary Table 1: Information on the plasmids used for the production of HPV-PsVs. 123
Supplementary Table 2: List of the cytokines, chemokine and growth factors included in the R&D Systems Human XL cytokine array. 129
Supplementary Table 3: Protein information and pathway enrichment predicted by STRING for immune modulators most elevated in DC0 cells in the presence of SP-A and HPV16-PsVs compared to untreated cells.....133

Abbreviations

AF488	Alexa Fluor 488
ALIX	Alg-2-interacting protein X
AMP	Antimicrobial peptide
Angio-1	Angiopoietin 1
ANOVA	Analysis of variance
APC	Antigen presenting cell
ApoA	Apoliprotein A-I
BAL	Bronchoalveolar lavage fluid
BM	Basement membrane
BSA	Bovine serum albumin
C. trachomatis	*Chlamydia trachomatis*
CCD	Charge-coupled-device
CCL	Chemokine ligand
CD	Cluster of differentiation
CLR	C-type lectin receptors
COX-2	Cyclooxygenase 2
CRD	Carbohydrate recognition domain
CRP	C-reactive protein
CSFE	Carboxyfluorescein succinimidyl ester
CTL	Cytotoxic T lymphocyte
CXCL	Chemokine (C-X-C motif) ligand
CyPB	Cyclophilin B
C5	C5 complement component
DAMP	Damage-associated molecular pattern
DC	Dendritic cell
DC0	Immature dendritic cell
DC-SIGN	Dendritic Cell-Specific ICAM-grabbing non-integrin
DNMT	DNA methyltransferase
DOH	Department of health
DMSO	Dimethyl sulfoxide
EEA1	Early antigen 1
EGF	Epidermal growth factor
FACS	Fluorescence-activated cell sorting
FCS	Foetal calf serum

FGF	Fibroblast growth factor
FGT	Female genital tract
FSC-A	Forward scatter area
FSC-H	Forward scatter height
FLT3L	Flt-3 ligand
GAG	Glycosaminoglycan
G-CSF	Granulocyte colony-stimulating factor
GDF-15	Growth/differentiation factor
GH	Growth hormone
GLuc	Gaussia luciferase
GO	Gene ontology
GSI	γ-secretase inhibitor
h	Hour
H. influenza	*Hemophilus influenza*
HIV	Human immunodeficiency virus
HLA	Human Leukocyte Antigen
HLA-DR	Human Leukocyte Antigen-DR isotype
HNC	Head and neck cancer
Hpi	Hour(s) post infection
HR	High-risk
HSPG	Heparan sulphate proteoglycan
HSV	Herpes simplex virus
IAV	Influenza A virus
ICAM-1	Intercellular adhesion molecule 1
ICP	Immune cell panel
IFN	Interferon
IFNAR	IFN-α/β receptor
IGFBP-3	Insulin-like growth factor binding molecule
IL	Interleukin
IL1-ra	Interleukin-1 receptor antagonist
JACoP	Just Another Colocalisation
JAK-STAT	Janus kinase-signal transducer and activator of transcription pathway
kDa	Kilodalton
KLK8	Serine-protease kallikrein-8
LAL	Limulus Amoebocyte Lysate

LC	Langerhans cell
LIF	Leukaemia inhibitory factor
LN332	Laminin 332
LMIC	Low- and middle-income countries
LR	Low-risk
LPS	Lipopolysaccharide
Monoclonal antibody	MAb
Mac-1	Macrophage 1 antigen
MFI	Median fluorescence intensity
MHC	Major histocompatibility complex
min	minutes
M. tb	*Mycobacterium tuberculosis*
MWCO	Molecular weight cut-off
NA	Numerical aperture
NK	Natural killer
NLR	NOD-like receptor
Ori	Origin of replication
P. aeruginosa	*Pseudomonas aeruginosa*
PAMP	Pathogen associated molecular pattern
PBS	Phosphate buffered saline
PCAF	P300/CBP-associated factor
PDGF	Platelet-derived growth factor
PMA	Phorbol 12-myristate 13-acetate
PRR	Pattern recognition receptor
PsVs	Pseudovirus
PV	Papillomavirus
Rb	Retinoblastoma protein
RBP4	Retinoblastoma binding protein 4
rfhSP-A	Recombinant fragments of human SP-A
RLR	RIG-I-like receptor
RSV	Respiratory syncytial virus
rhGM-CSF	Recombinant human Granulocyte-Macrophage Colony-Stimulating Factor
S. aureus	*Staphylococcus aureus*
S. pneumoniae	*Streptococcus pneumoniae*
SAG	Salivary agglutinin
SaliPhe	Saliphenylhalamide

SDS-PAGE	Sodium dodecyl sulphate polyacrylamide gel electrophoresis
sHIV	Simian-human immunodeficiency virus
SNX	Sorting nexin
SP-A	Surfactant protein A
SP-D	Surfactant protein D
SPs	Surfactant proteins
SIRPα	Signal regulatory protein α
SSC	Side scatter
STAT	Signal Transducer and Activator of Transcription
STRING	Search Tool for the Retrieval of Interacting Genes/Proteins
STI	Sexually transmitted infection
TARC	Thymus and activation regulated chemokine
TBS	Tris-buffered saline
TE	Tris-EDTA
Thrombo-1	Thrombospondin 1
TIM-3	T cell immunoglobulin and mucin domain-containing protein 3
TLR	Toll-like receptor
TNF	Tumour necrosis factor
TRAF3	TNF-receptor-associated factor 3
TGN	Trans-Golgi network
TYK2	Tyrosine kinase 2
UCHL1	Ubiquitin C-Terminal Hydrolase L1
URR	Upper regulatory region
VCAM-1	Vascular cell adhesion molecule 1
vDNA	Viral DNA
VEGF	Vascular endothelial growth factor
VLP	Virus-like particle
v-ATPases	Vacuolar ATPases
w/w	Weight per weight

Abstract

Infection with Human papillomavirus (HPV) presents a continuous global health challenge due to its incurable nature, particularly impacting low- and middle-income countries (LMIC). Although highly effective prophylactic vaccines targeting the most prevalent HPV types exist, they do not cover all oncogenic HPV types found in malignant lesions and the extent of cross-protection against other oncogenic HPV types is limited. Moreover, these vaccines are ineffective for women already infected with high-risk HPV types. These limitations are more prominent in LMIC, where limited healthcare access, awareness, and proper transport and storage hinder vaccine accessibility. Cervical cancer's persistent status as the fourth most common cancer in women globally underscores the urgent need for alternative interventions that broadly target HPV infections. In an effort to identify alternative broad-spectrum protective means against HPV infection, our previous research identified surfactant protein A (SP-A), an innate immune opsonin, as a novel molecule capable of recognising HPV16 pseudovirions (HPV16-PsVs) with functional consequences for reduced infection in a murine cervicovaginal HPV challenge model. Building on these findings, our aim was to assess SP-A's suitability as a novel broad-spectrum HPV targeting molecule to prevent initial viral infection of the human keratinocyte cell line, HaCaT. Additionally, we aimed to study SP-A's ability to agglutinate HPV-PsVs and to assess potential consequences of this SP-A coating on immune cell recognition and elicited immune responses in human-derived immune cells.

Our study demonstrated SP-A's ability to agglutinate and opsonise multiple oncogenic HPV-PsVs types, which was accompanied by their enhanced uptake and clearance by RAW264.7 murine macrophages, THP-1 monocytes, and THP-1-derived immature dendritic cells (DC0). Importantly, SP-A-opsonised HPV-PsVs resulted in decreased viral uptake and infection of HaCaT keratinocytes. These results were supported by increased lysosomal accumulation of SP-A-opsonised HPV16-PsVs as observed for both RAW264.7 and HaCaT cells. Co-culturing selected immune cells with HaCaT keratinocytes further reduced HPV-PsV infection in the presence of SP-A which might be explained by SP-A's behaviour in driving a proinflammatory immune response in THP-1 and DC0, in the presence of HPV16-PsVs, as identified by cytokine profiling. These results unveiled SP-A's versatility and substantial influence on various HPV interactions with immune cells and keratinocytes and laid the foundation for future research into the development of alternative prophylactic interventions. Increasing innate immune recognition by exogenous supplementation with SP-A (or SP-A derivatives) holds promise for broader protection against diverse HPV types and potentially other sexually transmitted infections.

1 Introduction

Papillomaviruses (PVs) are a diverse family of viruses known as Papillomaviridae (1). Within this family, there exist over 160 characterised genotypes of human papillomaviruses (HPVs) (2). HPVs are classified into two main categories: low-risk (LR) and high-risk (HR), based on their potential to cause malignancy (3). These viruses are primarily transmitted through sexual activity, making them a global health concern due to their high prevalence and significant disease burden (4, 5). In particular, infection with HR or oncogenic HPVs is a critical public health issue, as it is directly associated with the development of various human cancers. More than 30% of all cancers caused by infectious agents are attributable to HPV (6), where these HPV infections contribute to approximately 5% of all human cancer cases (5).

Among the oncogenic HPV types, 15 have been identified and characterised, namely types 16, 18, 31, 33, 35, 39, 45, 51, 52, 56, 58, 59, 68, 73, and 82. HPV types 16 and 18 are the most prevalent globally (7). These two HR HPV types are responsible for the majority of cervical cancer cases, contributing to approximately 70% of all documented instances (8). HPVs can infect both men and women, and while cervical cancer is the most well-known consequence, HR HPVs are also associated with other anogenital cancers (9). There is also a growing association between HPV infection and the rising incidence of head and neck cancers (HNCs), particularly oropharyngeal cancer (10). However, it is important to note that approximately 570,000 women are diagnosed with cancers related to HPV (including cervical cancer), while the corresponding figure for men is 60,000 (9).

While HPV infection is necessary, it is not the sole determinant in the development of cancer. Many co-factors have been established for the initiation and progression of cervical cancer, some of which include long-term use of contraceptives, tobacco smoking, chronic inflammation, and co-infection with human immunodeficiency virus (HIV) (11-13). Other likely co-factors include co-infection with *Chlamydia trachomatis* (*C. trachomatis*) and herpes simplex virus type-2 (HSV-2), as well as genetic and immunological factors (12, 14).

The higher incidence of cervical cancer in low- and middle-income countries (LMICs) can be attributed to a combination of factors, including a disproportionately high prevalence of HIV, limited access to efficient screening and monitoring systems, and challenges related to healthcare facility accessibility (9). Globally, cervical cancer ranks fourth for both incidence and mortality in women (15). However, it is the second most common cancer in South Africa (16) as well as the leading cause of female cancer- associated deaths in Sub-Saharan Africa (17). In Sub-Saharan Africa, where the burden of HIV is substantial, individuals living with HIV

are at an elevated risk of developing cervical cancer due to weakened immune responses, which can facilitate the persistence of HPV infections (see Section 1.6) (18).

As persistent infection with oncogenic HPVs is strongly linked to cervical cancer, it has the potential to be preventable. Highly efficient vaccines targeting the most common oncogenic HPV types are on the market, but access to these vaccines by the target groups in LMIC has proven challenging for a number of reasons (see Section 1.6). Therefore, alternative means to protect against sexually transmitted HPVs are much needed.

We have previously identified surfactant protein A (SP-A), an innate immune opsonin, as a potentially prophylactic molecule capable of enhancing the innate immune response to HPV16 pseudovirus (HPV16-PsVs) infection in both *in vitro* and *in vivo* mouse models (19). While we have shown SP-A to be capable of opsonising HPV16-PsVs and enhancing its recognition by murine immune cells, it is yet to be determined whether SP-A can enhance immune recognition of human innate immune cells and if this has a functional consequence on the infection of human keratinocytes. Moreover, it is yet unknown if SP-A has broad-spectrum capabilities and can opsonise multiple HPV types with consequences for their infectability.

1.1 Innate Immunity

The immune system is a complex network of cells, tissues, and organs that work together to protect the body from harmful invaders, such as bacteria, viruses, fungi, but also from cancer. Its primary function is to recognise and eliminate foreign substances while distinguishing them from the body's own cells and tissues. The innate immune system is the first line of defence against pathogens and provides immediate, non-specific protection (20). Unlike the adaptive immune system, which develops specific responses to individual pathogens over time, the innate immune system offers a rapid and general response to a wide range of potential threats (21, 22).

There are multiple components of the immune system. The first level of innate immunity includes physical barriers like the skin, cilia, bodily fluids, and mucous membranes. These barriers prevent pathogens from entering the body (20). Chemical barriers, such as stomach acid and antimicrobial substances in bodily fluids, create an inhospitable environment for many microorganisms. The innate immune system is further made up of cellular components, chemical mediators, pattern recognition receptors (PRRs), and the inflammatory response (20, 23).

1.1.1 Cellular components

The cellular components of the innate immune system includes phagocytes of myeloid origin, mast cells, and natural killer (NK) cells (24).

Phagocytes are white blood cells that can engulf and digest pathogens. The two main types of phagocytes are mononuclear and polymorphonuclear phagocytes. Mononuclear phagocytes include monocytes which can differentiate into macrophages, and dendritic cells (DCs) (25, 26): upon infection or inflammation, monocytes migrate to the affected site, differentiate and become actively involved in clearing pathogens and debris, as well as producing inflammatory cytokines (25). Macrophages are larger and more long-lived phagocytes found in various tissues. Equipped with an extensive array of PRRs, which recognise pathogen-associated molecular patterns (PAMPs) and damage-associated molecular patterns (DAMPs), they are pivotal in eliminating pathogens, clearing dead cells, and releasing proinflammatory mediators (25, 27, 28). Macrophages also initiate the adaptive immune response by presenting antigens to T cells. Both monocytes and macrophages are considered antigen-presenting cells (APCs) which play a critical role in the immune system by capturing, processing, and presenting antigens to other immune cells, particularly T cells, as part of the adaptive immune response (29). Macrophages exhibit remarkable functional diversity, and their phenotypic characteristics can be broadly categorised into different subtypes. One commonly used classification system distinguishes between M0, M1, and M2 macrophage subtypes, each associated with specific functions and responses (30). In their resting state, M0 macrophages maintain tissue homeostasis and engage in routine immune surveillance, with the potential to differentiate into specific subtypes (31). Activated by proinflammatory signals, M1 macrophages play a crucial role in early defence, exhibiting potent microbicidal activities and antigen presentation. On the other hand, M2 macrophages, activated by anti-inflammatory cues, contribute to tissue repair and immune regulation. The M2 subtype further divides into M2a, M2b, and M2c, each with unique functions. M2a macrophages, induced by interleukin-4 (IL-4) or IL-13, participate in tissue repair and allergic responses. M2b macrophages, activated by immune complexes, modulate immune responses by balancing proinflammatory and anti-inflammatory signals. M2c macrophages, triggered by anti-inflammatory signals, facilitate inflammation resolution and tissue remodelling. This intricate network of macrophage subtypes underscores their nuanced roles in shaping immune responses, thereby influencing the adaptability of the immune system in diverse physiological contexts.

DCs, however, are often referred to as the most potent APCs in the immune system. They are highly specialised in capturing and processing antigens, and they play a central role in initiating

adaptive immune responses (29). DCs present antigens to T cells, thereby activating the adaptive immune system (32). DCs exist in two main states: immature DCs and mature DCs. Immature DCs, such as Langerhans cells (LCs), are typically found in peripheral tissues, such as the skin, mucosal linings, and other sites where they are exposed to potential pathogens (33). Immature DCs are specialised in capturing antigens from pathogens or other sources, such as damaged cells. They have a high capacity for antigen uptake through phagocytosis or receptor-mediated endocytosis (34). Mature DCs can be found in lymphoid tissues, such as lymph nodes and the spleen, where they migrate after encountering pathogens in peripheral tissues. Mature DCs are specialised in presenting antigens to T cells. They have reduced antigen-capturing ability compared to immature DCs but are highly efficient at antigen presentation and immune activation (35). The transition from immaturity to maturity occurs when DCs encounter pathogens or inflammatory signals and migrate to lymphoid tissues to participate in the activation of specific immune responses (35).

The polymorphonuclear phagocytes (also known as granulocytes) include neutrophils, eosinophils, and basophils (36). Neutrophils are the most abundant type of white blood cells and are typically the first responders to infection. They rapidly migrate to the site of infection and engulf bacteria and fungi (37). Eosinophils and basophils primarily play roles in allergic reactions (38). Eosinophils and basophils are both less abundant than neutrophils but are potent fighters against certain types of infections, especially parasitic infections (39). They release a variety of toxins and enzymes that are effective against parasites and also contribute to inflammation (39).

Mast cells play a similar role to eosinophils and are present in tissues throughout the body, particularly in areas close to the external environment, such as the skin and mucous membranes (40). Mast cells, although sharing characteristics with myeloid cells, are considered a unique category due to their distinct origins and functions. They are not classified as phagocytes but are known for their role in inflammation and allergic responses. They release histamine and other chemicals that increase blood flow and recruit other immune cells to the site of an infection or injury (40).

NK cells are a type of lymphocyte, but unlike B and T cells (which are part of the adaptive immune system), they are considered a part of the innate immune system (41, 42). These cells are responsible for recognising and destroying infected or abnormal host cells, particularly those infected with viruses or cancerous cells. Unlike T cells, NK cells do not require prior exposure to specific antigens to initiate their killing mechanisms (41).

In addition to myeloid cells, mast cells, and NK cells, innate immune responsiveness is a property of the skin and the epithelial cells lining the respiratory, gastrointestinal, and genitourinary tracts (24). Epithelial cells produce a variety of antimicrobial peptides (AMPs) and proteins (43) which can disrupt the integrity of microbial membranes, leading to pathogen death (20). Keratinocytes, for example, possess PRRs and can therefore, upon encountering infection or injury, release pro-inflammatory cytokines and growth factors, which contribute to the inflammation process and tissue repair (28, 44). While primarily part of the innate immune system, keratinocytes can also influence adaptive immunity. By presenting antigens and expressing co-stimulatory molecules, they can interact with DCs and lymphocytes, aiding in the activation and modulation of adaptive immune responses (Figure 1) (44, 45).

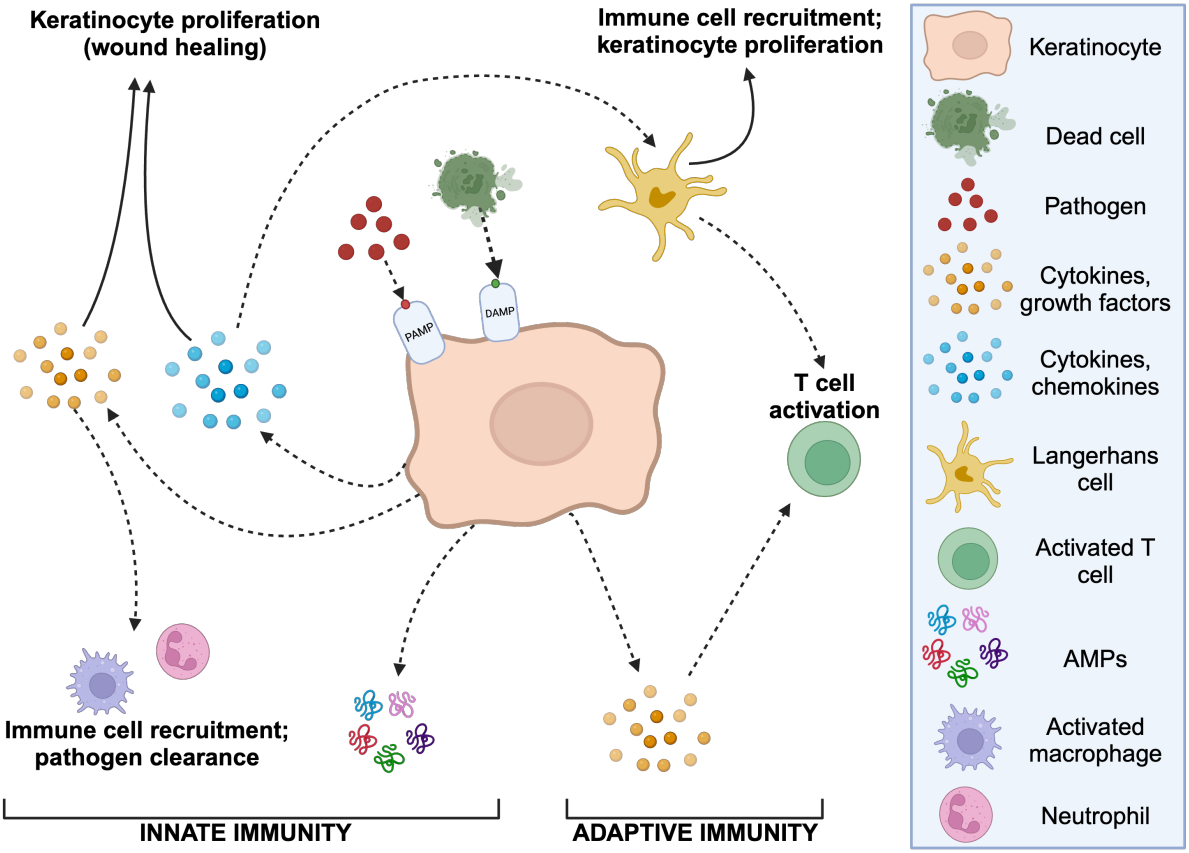

Figure 1: The immune functions of keratinocytes in pathogen clearance and tissue repair. Keratinocytes express various PRRs capable of recognising PAMPs and DAMPs. This leads to the release of cytokines, chemokines, growth factors, and AMPs by keratinocytes. The pro-inflammatory cytokines and chemokines secreted by keratinocytes play a vital role in recruiting neutrophils and macrophages to the site of injury and infection. These immune cells, in turn, eliminate cellular debris and destroy invading pathogens through phagocytosis. The cytokines and chemokines produced by keratinocytes also act as chemoattractants, guiding activated T cells to the wound. Epidermal T cells and dendritic cells respond promptly to tissue injury and infection, producing growth factors that activate keratinocyte proliferation, promoting tissue repair. Figure adapted from (44) and made with BioRender.com.

1.1.2 The inflammatory response: The role of chemical mediators

In response to tissue injury or infection, the innate immune system initiates inflammation. Resident immune cells, like mast cells and macrophages, release mediators such as histamine, cytokines, and chemokines, promoting blood vessel dilation and increased permeability. This enables the influx of immune cells like neutrophils and monocytes from the bloodstream. Chemokines amplify this response, attracting more immune cells to the site, forming a positive feedback loop. Neutrophils and monocytes, in turn, phagocytose pathogens, release antimicrobial substances, and produce enzymes that aid in tissue repair. The accumulation and activation of these cells manifest as the classic signs of inflammation: redness, heat, swelling, and pain.

Soluble factors of innate immunity, also known as chemical mediators, are a critical part of the innate immune system's response to infections and other threats (46). These factors are present in bodily fluids, such as blood, plasma, and tissue interstitial fluid, and they play various roles in defending the body against pathogens. These factors include proteins belonging to the complement system, AMPs, cytokines (including interferons), acute-phase proteins, and surfactant proteins (46-48).

The complement system, comprising over 30 proteins, activates in response to pathogens, playing a vital role in direct pathogen destruction and immune cell-assisted removal. Three pathways—classical, lectin, and alternative—can initiate the complement system, leading to a common set of protein activations (49). Once triggered, a cascade of events results in protein cleavage, enhancing the immune response. Activated complement proteins facilitate opsonisation, making pathogens more recognisable and digestible by phagocytes (49, 50). The system also induces inflammation, releasing cytokines and chemotactic factors that attract immune cells to infection sites. Additionally, it directly attacks pathogens by forming the membrane attack complex (MAC), creating pores in their cell membranes (49). The complement system aids in immune complex clearance, binding to aggregates of antibodies and antigens to facilitate their removal. However, strict regulation prevents excessive activation and damage to the body's cells.

AMPs serve as a crucial component of the innate immune system (20). These small, yet potent, molecules are endowed with the capacity to combat a broad spectrum of pathogens, including bacteria, fungi, and parasites. Their mode of action is diverse and sophisticated, encompassing the destabilisation and rupture of microbial membranes, the formation of pores that compromise cell integrity, and the aggregation of proteins, which disrupts vital cellular processes (20). AMPs not only act at the level of the cell membrane but also penetrate

pathogens to inhibit intracellular targets, including DNA transcription and protein synthesis (20). Defensins, cathelicidins, and hepcidin, among various AMPs, are highly conserved across species, underscoring their vital role in host immunity. Defensins insert into cell membranes, forming pores; cathelicidins exhibit direct antimicrobial actions and modulate immune responses. Hepcidin, with a dual role in iron homeostasis, inhibits microbial growth by sequestering essential iron.

Cytokines are signalling molecules released by various immune cells in response to infection or injury. They play a crucial role in regulating immune responses, including inflammation, immune cell activation and differentiation, and killing of cells (32). They induce chemotaxis, directing cells toward sites of inflammation, infection, and trauma. Key mediators of inflammation include IL-1 and tumour necrosis factor (TNF), promoting vasodilation and vascular permeability for immune cell influx. Interferons (IFNs), primarily responding to viral infections, have antiviral properties and induce resistance in neighbouring cells. IFNs trigger the transcription of interferon-stimulated genes (ISGs), thereby inhibiting various stages of the viral life cycle. Beyond antiviral actions, interferons modulate the immune system, enhancing antigen presentation and affecting immune cell activity. For instance, interferon-γ activates macrophages, increasing phagocytosis and reactive oxygen species production for pathogen elimination.

Acute phase proteins, produced by the liver in response to infection, inflammation, or tissue damage, regulate the inflammatory response and enhance the immune system's ability to combat pathogens. Examples include C-reactive protein (CRP) and serum amyloid A. CRP binds specifically to phosphocholine on the surface of apoptotic cells and certain bacteria, activating the complement system to promote opsonisation and phagocytosis. Serum amyloid A plays roles in lipid metabolism and acts as a chemoattractant, influencing immune cell migration to inflammation sites.

Surfactant proteins A and D are collectins found in the lung's alveoli and help protect against respiratory infections (51). These proteins are key innate immune molecules in the pulmonary environment enhancing the opsonisation of pathogens, thereby facilitating their clearance through phagocytosis by alveolar macrophages (52) (see Section 1.8). Moreover, their non-pulmonary immune functions have attracted considerable attention over the last decade (53).

1.1.3 Pattern recognition receptors

As mentioned earlier (see Section 1.1.1), innate immune cells express PRRs that recognise PAMPs and DAMPs, facilitating rapid responses to potential threats while distinguishing self

from non-self. Toll-like receptors (TLRs), a well-characterised PRR family, are membrane-bound receptors recognising specific PAMPs, triggering signalling pathways that activate transcription factors like NF-κB. This leads to the production of inflammatory cytokines and type I interferons crucial for antiviral responses. C-type lectin receptors (CLRs), another diverse PRR group, recognise carbohydrate structures on pathogen surfaces, contributing to functions like direct microbial killing and modulation of inflammation. For instance, Dectin-1, a CLR, activates immune responses against fungal infections by recognising β-glucans on fungal cell walls (54). Additional PRR groups include NOD-like receptors (NLRs) and RIG-I-like receptors (RLRs). NLRs act as cytoplasmic receptors and detect intracellular PAMPs and DAMPs, while RLRs are cytosolic sensors recognising viral RNA and playing a critical role in antiviral immunity by initiating cascades that induce the production of type I interferons and cytokines. Collectively, these PRRs enable rapid detection and response to a broad range of pathogens, marking early immune defence and shaping subsequent adaptive immune responses. Their ability to discern pathogenic from normal host components is crucial for immune homeostasis and effective immune reactions against invaders.

1.1.4 Bridging innate and adaptive immunity: The temporal handoff

While the innate immune system is traditionally considered non-specific, recent research has suggested that it may have some memory-like features, allowing it to respond more effectively to previously encountered pathogens. Moreover, the innate immune system plays a crucial role in preventing infections and buying time for the adaptive immune system to develop a specific response (20, 21). APCs, such as DCs and macrophages from the innate immune system, capture antigens and present them to T cells. DCs, in particular, are adept at processing captured antigens and presenting them via Major Histocompatibility Complex (MHC) molecules to T cells in the lymph nodes (29, 35).

The adaptive immune system is a highly specialised branch of the immune system that provides specific and targeted defence against pathogens, generating highly specialised cells, chemokines, and antibodies with long-lasting immunologic memory (32). It comprises two main components: the cell-mediated immune system and the humoral immune system. The cell-mediated immune system primarily involves T cells, which play a central role in recognising and destroying infected or abnormal cells. Cytotoxic T cells directly target and kill infected cells, while helper T cells coordinate and regulate the immune response, including the activation of B cells in the humoral immune system. The humoral immune system, on the other hand, is centred around B cells, which produce antibodies (immunoglobulins) that can neutralise pathogens or tag them for destruction by other immune cells. Both components of

the adaptive immune system work in harmony to provide long-term immunity, and they have the ability to "remember" specific pathogens, allowing for a more rapid and effective response upon re-exposure, a key feature of immunological memory (55). While the innate immune system acts within hours of a new infection, the adaptive immune system takes a few days to respond (Figure 2) (21).

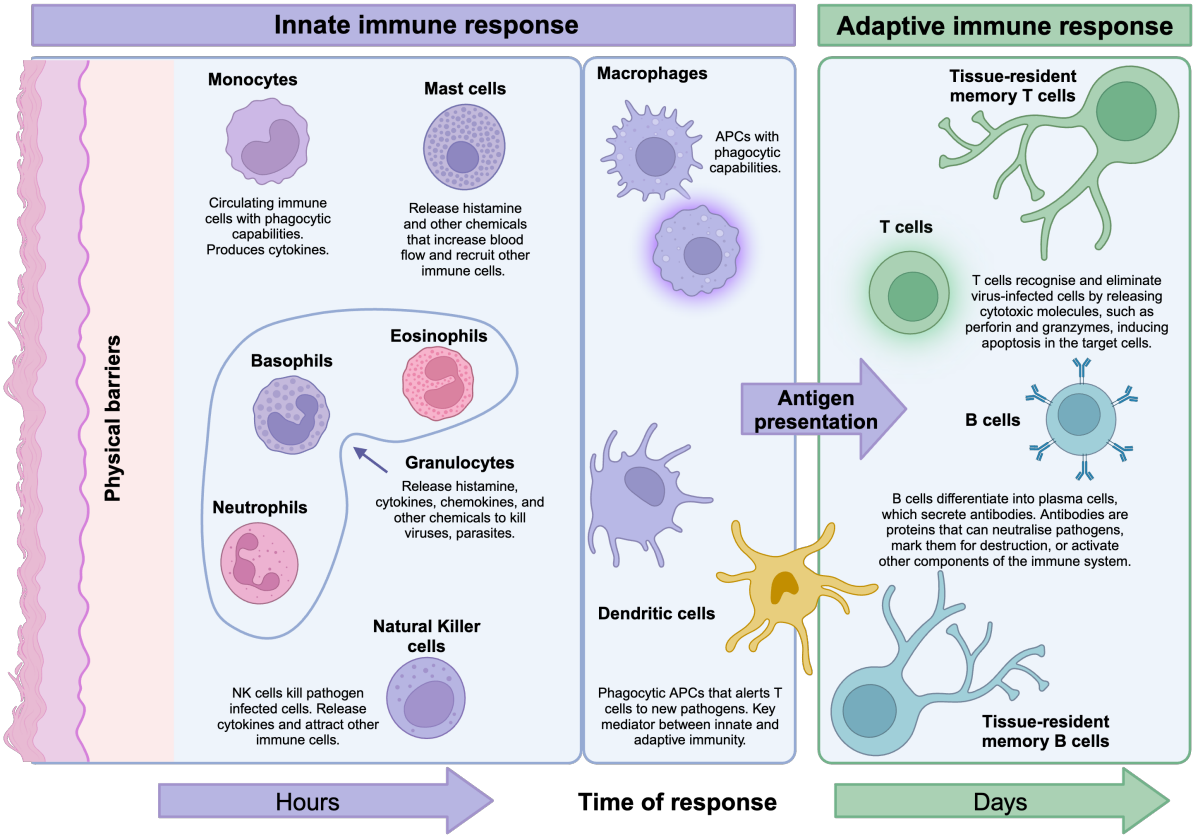

Figure 2: Cellular components of the innate and adaptive immune system. Innate immunity includes physical barriers such as skin and mucosal tissues. The innate arm is orchestrated by basophils, eosinophils, neutrophils, mast cells, natural killer cells, monocytes, macrophages, and dendritic cells, forming the initial defence against bacteria, viruses, and even emerging cancer cells. The adaptive immune system is characterised by antigen-specific responses that take time to develop but confer enduring protection. This includes B cell-mediated humoral immunity and T cell-mediated cellular immunity, both honed towards specific antigens. Macrophages and dendritic cells exhibit a dual nature, possessing traits of both innate and adaptive immune cells. Functioning as APCs, they play a pivotal role in initiating adaptive immunity by presenting antigens to antigen-specific T and B lymphocytes. Together, these cellular immune components, including physical barriers, form a comprehensive defence network against a spectrum of threats. Figure adapted from (56, 57) and made with BioRender.com.

1.1.5 Immune evasion strategies of viruses

Many viruses have evolved multiple mechanisms to circumvent the innate and adaptive immune responses, making them formidable adversaries in the ongoing battle between pathogens and the immune system. These evasion strategies can include inhibiting antigen presentation, downregulating immune recognition markers, and releasing immunomodulatory molecules. Such tactics not only enable viruses to establish persistent infections but also make

them particularly challenging targets for the host's immune system. Understanding these immune evasion mechanisms is crucial for developing effective antiviral strategies, diagnostics, and vaccines (see Section 1.5). The immune evasion strategies of HPV are discussed in more detail in Section 1.4.

1.2 Oncogenic HPV genome and structure

HPVs are small, non-enveloped DNA viruses of 52-55 nm size in diameter with a circular genome of roughly 8 kilo bases (kb) (58). Over 160 genotypes have been characterised (2). The HPV genome is composed of three regions; the “early” (E) gene region, the “late” (L) gene region, and the upstream regulatory region (URR) (58) (Figure 3).

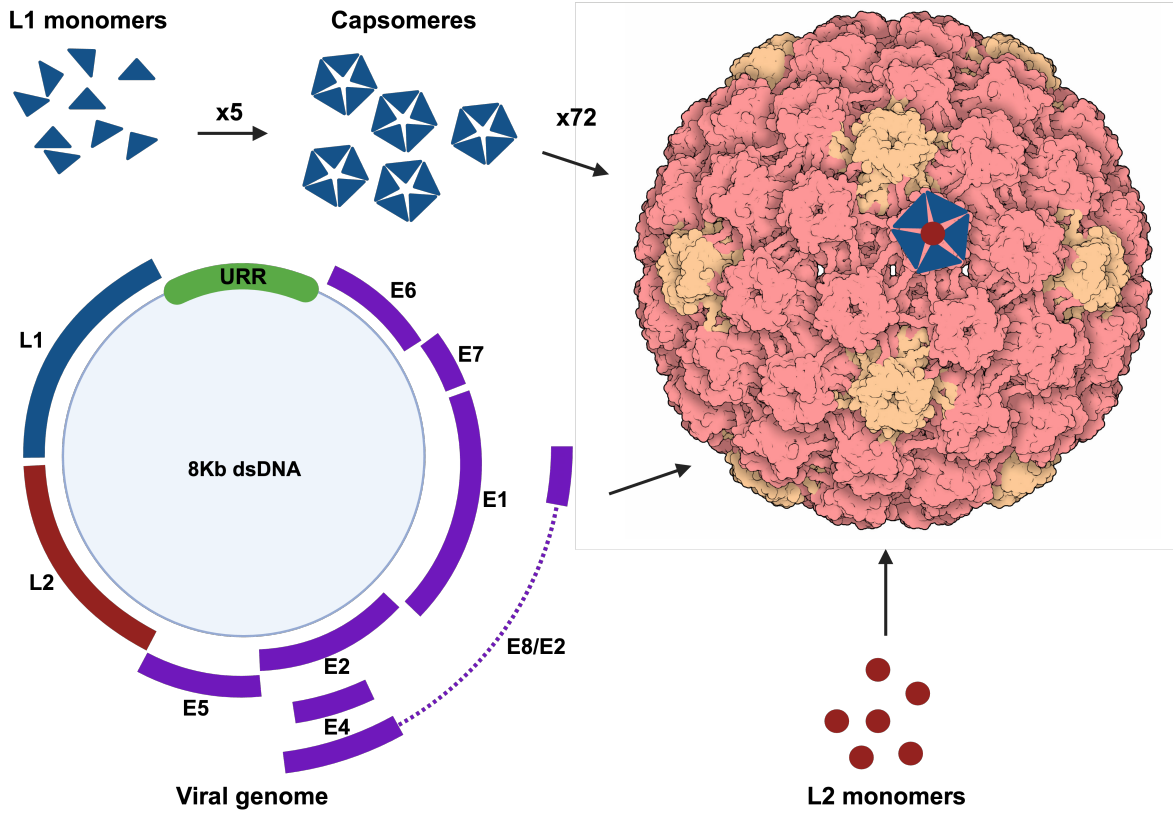

Figure 3: HPV viral genome and capsid structure. The HPV virion consists of its 8 kb circular double-stranded DNA, encased in an icosahedral capsid. The capsid consists of L1 monomers that spontaneously assemble into pentameric capsomeres which assemble into an icosahedral lattice. L2 proteins associate with the L1 capsid proteins. 3D render of the papillomavirus capsid from cryoelectron microscopy was taken from (59).

The URR has binding sites for a number of host cellular factors (60). The viral early proteins E1 and E2 also bind to the URR, which initiates replication and transcription (61). E1 has ATPase, DNA helicase as well as origin of replication (ori)-specific DNA binding and unwinding activities (62). E2 acts as a transcriptional activator protein (62). It has been shown that E1 complexes with E2 for enhanced binding of the ori (61, 62). The E4 gene plays a multifaceted

role in the viral life cycle, including virus synthesis, ensuring the assembly of new virions within the host cell. This process is integral to the production of infectious virus particles capable of infecting new host cells (63).

Some controversy exists around the function of E5 and its role in the HPV life cycle. It is defined as an oncogene and has been implicated in cell immortalisation and transformation, but its function in oncogenesis is much less defined than of E6 and E7 (58), see below. One well-defined implication of E5 in oncogenesis is its interaction with epidermal growth factor (EGF). *In vitro* transformation by HPV16 E5 is mainly facilitated by EGF, where studies have shown that E5 can elevate the levels of vascular endothelial growth factor (VEGF) through the EGF receptor and can enhance cyclooxygenase 2 (Cox-2) expression (64, 65). E5 has also been implicated in immune evasion, as it could selectively downregulates surface human leukocyte antigen (HLA) class I molecules (66). E5 has also been shown to downregulate CD1d found on NK cells (see Section 1.4). This molecule therefore serves as the bridge between innate and adaptive immune defences (67).

The E6 and E7 genes encode oncoproteins and have been implicated in neoplastic transformation of cells (68). Both LR and HR HPV types express E6 and E7, but the differences lie in the strength of their interactions with host cell proteins and their ability to disrupt cellular processes. HR HPV types are more effective at interfering with these processes, making them more likely to lead to cancer development (69-71). E6 specifically forms a complex with the ubiquitin ligase E6-AP and p53, a key tumour suppressor protein involved in controlling the cell cycle, DNA repair and apoptosis (68). Proteasomal degradation of p53 by this complex results in dysregulation of the cell cycle, promotes cell proliferation and increases the frequency of spontaneous mutations, all of which are hallmarks of malignancy (68, 72, 73). E7 targets the retinoblastoma protein (Rb), another major tumour suppressor (68, 74). E7 binding to Rb also leads to proteasomal degradation, resulting in the release of the E2F transcription factor from Rb complexes, which results in the activation of genes that control cell proliferation (68, 72, 73, 75). Furthermore, both E6 and E7 also play a role in immune evasion (detailed in Section 1.4).

Lastly, the E8/E2 fusion protein, in which parts of the E8 gene are linked to the C-terminal half of the E2 gene, is translated from an alternatively spliced viral transcript (58). It has been described for HPV1, 5, 8, 11, 16, and 31 (76). This protein has been shown to inhibit viral gene expression (77).

The late proteins L1 and L2 encode for the major and minor capsid proteins, respectively. L1 spontaneously assembles into pentameric capsomeres, which are five-membered protein

complexes, and comprise the majority of the icosahedral viral capsid (78-80). The capsomeres assemble into an icosahedral lattice. L2 proteins are present in smaller quantities within the capsid. They associate with the L1 pentamers and remain hidden and embedded in the pentamers to stabilises the shape and stability of the capsid (Figure 3) (79). The structure of the L2 protein is less well-defined than that of L1 due to its flexible and disordered nature (80). It is estimated that at least 72 L2 proteins exist in a single HPV capsid (79). Studies on antibody binding indicate that the L2 protein is mostly concealed beneath the surface of native virions, even though its specific configuration is not yet understood (81).

1.3 HPV life cycle

HPV demonstrates a specific affinity for basal keratinocytes within squamous epithelium, particularly in the mucosal epithelial lining of the cervix (78, 82). Approximately 40 HPV types can infect the genital tract (58). *In vivo*, effective HPV infection typically requires prior epithelial damage (83, 84). It is presumed that lesions in the protective outer layers of the epithelium facilitate virion access to mitotically active basal epithelial cells in the inner layers, which can support episomal viral genome replication (82, 83). Although particle-to-infectivity ratios *in vitro* are estimated to be as high as 104:1, HPVs are highly transmissible agents, which suggests much more efficient infectivity *in vivo* (85). Both the major L1 capsid protein and the largely concealed minor L2 capsid protein play roles in the initial binding and entry into basal epithelial cells.

The entry of HPV particles into cultured keratinocytes is unusually asynchronous, with some entering within minutes but many virions remaining on the cell surface for several hours (86). Moreover, it was found that HPV can only infect proliferating, but not senescent cells *in vitro*, but remains viable on the surface of non-dividing cells for extended periods of time (87). Thus, *in vitro* exploration of HPV makes it challenging to discern the specific sequence of events, the precise mechanisms and the cell molecules required for infectious entry and subsequent establishment of infection. It is also not known if the asynchronous entry seen in human keratinocyte monocultures is a limitation of the model or a reflection of infectious transmission *in vivo* (88).

Many infectious pathogens and viruses interact with heparan sulphate proteoglycans (HSPGs) on the cell surface, or on the basement membrane, for attachment and subsequent cellular entry (89). This is also the case for HPV which initially interacts with the glycosaminoglycan (GAG) chains of HSPGs via its L1 capsid protein (27). It has also been proposed that HPV binds in a transient manner to laminin 332 (LN332), a protein secreted into the extracellular matrix by migrating keratinocytes via binding to syndecan HSPG ectodomains attached to

LN332 (90, 91). Binding of L1 induces conformational changes in the capsid and facilitates proteolytic cleavage of L1 by the secreted serine-protease kallikrein-8 (KLK8) (83, 92). This cleavage allows for interactions between the capsid and cyclophilin B, which results in further conformational changes that exposes the L2 N-terminus containing a conserved consensus cleavage site for the host extracellular proprotein convertase furin (1, 93). This interaction has been shown to be essential for successful infection of HPV, as furin cleavage results in the exposure of a binding site on L1, postulated to be recognised by an unknown receptor, or receptor complex (83, 89, 92, 94). The described changes in virion conformation further facilitate the reduction in the binding affinity to HSPGs, thereby facilitating the engagement with the unknown receptor(s), or receptor complex (95). No single molecule has been identified as a necessary entry receptor for HPV although annexin A2, a multifunctional protein that forms a complex with S100A10, has been implicated in the process of HPV internalisation into epithelial cells via L2-dependent pathways and calcium-mediated translocation to the cell surface (96-98).

The mechanisms and pathways used by HPV for intracellular trafficking remains elusive; however, most studies indicate a clathrin-mediated endocytosis pathway for most HPV types, including HPV16 (99). However, HPV has adapted to use many alternative intracellular trafficking pathways. For instance, Schelhaas et al. described a novel endocytic pathway for HPV16 entry in HaCaT and HeLa cells, which was clathrin-, caveolin-, cholesterol- and dynamin-independent (100). Localisation of HPV into early endosomes occurs within 4 hours of cellular internalisation, followed by uncoating of the viral particle within the late endosome (8-12 hours after internalisation) (99). Most studies suggest the insertion and protrusion of L2 across the vesicle membrane (88). Membrane spanning of the L2 capsid protein into the cytosol enables the recruitment of sorting nexins and retromer complexes, which promote the release of a L2/viral DNA (L2/vDNA) complex from the late endosome, followed by retrograde trafficking of the L2/vDNA complex to the trans-Golgi network where it reaches the nucleus in a mitosis-dependent manner for subsequent viral DNA replication and gene expression (88, 101, 102). Furin cleavage has also been implicated in successful endosomal escape prior to transport of the L2/viral DNA complex to the nucleus, emphasising the necessity of furin cleavage for successful infection of HPV. Recently, it was shown that phosphorylation of L2 plays an important role in optimal uncoating of virions during infectious entry (103). In contrast to L2, most of the L1 capsid remains within degradative lysosomal compartments (88). The early stages of HPV infection (binding, uptake, retrograde transport) are depicted in Figure 4.

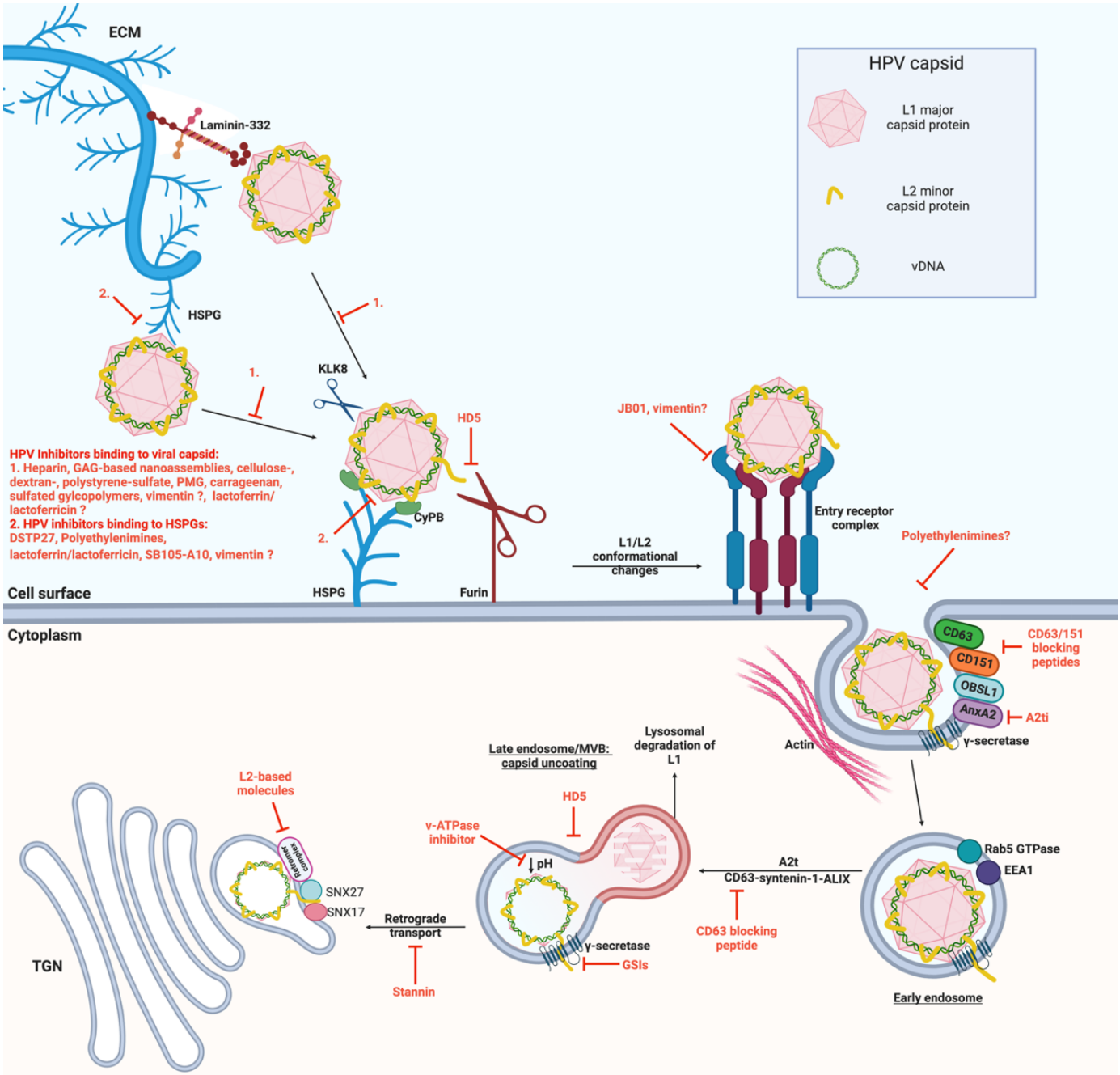

Figure 4: Schematic illustration of the early stages of HPV infection, indicating the sites of inhibition of various anti-HPV molecules. Binding to HSPGs results in conformational changes of the viral capsid, facilitating in interactions between the capsid and CyPB and cleavage by KLK8. This results in the exposure of the L2 N-terminus, and cleavage by furin. The capsid dissociates from HSPGs where exposure of a binding site in L1 is potentially needed for recognition by an unknown entry receptor complex. The viral capsid undergoes ligand induced endocytosis. Membrane protrusion of the L2 capsid protein is chaperoned by γ-secretase, which allows L2 to interact with host cell factors in the cytosol during transport. HPVs localise with EEA1 compartments in a Rab5 GTPase-dependent manner. The early endosome matures into the late endosome when it fuses with lysosomes. Most of the contents are degraded by lysosomal degradation, including the majority of the L1 capsid protein. Endosomal escape and subsequent post-endocytic trafficking of HR HPVs is regulated by CD63-syntenin-1-ALIX, which traffics HPV to these multivesicular endosomes. The capsids disassemble in a pH-dependent manner, and egress from the late endosome. The L2/vDNA complex enters the TGN, where L2 interacts with SNX17, SNX27 and retromer complex. Figure taken from (1) and made with BioRender.com.

The HPV life cycle is closely linked to the differentiation process of host keratinocytes (Figure 5). Initially, low levels of viral DNA are produced in actively dividing basal layer keratinocytes (about 100 genomes per cell). The E1 and E2 proteins play an important role in maintaining this low replication and ensuring the vDNA is distributed to daughter cells (72) which move to the upper layers (spinous layer) and undergo differentiation, leading to increased expression of viral E6 and E7 proteins. These proteins disrupt normal cell cycle control, pushing the cells into the S phase, allowing viral DNA replication and an increase in copy number to thousands per cell. Late viral L1 and L2 capsid proteins are then expressed, and they spontaneously self-assemble to encase the viral genome (104). Newly formed virions are released from the outermost layer of the epithelium (cornified layer) approximately three weeks after infection (105).

In some instances, HPV DNA may integrate into the host genome (106, 107). When this happens, it can disrupt host cell genes near the integration site and further contribute to cancer development. However, not all HPV infections progress to this stage, and integration is not an absolute requirement for carcinogenesis (108). Integration is considered accidental from the virus' perspective as it leads to a dead-end for virus production (109). However, it results in a continuous expression of E6 and E7 oncoproteins (68). Integration also disrupts the expression of E4, E5, and E2, with E2 being responsible for regulating E6 and E7 protein expression (68). Consequently, this suppresses the tumour suppressor proteins, p53 and Rb (see Section 1.2), resulting in uncontrolled cell proliferation and an increased risk of DNA damage (68, 72, 110). The risk of cancer development varies among different HPV types, and the likelihood of integration can also depend on the specific HPV type and host factors (108). While integration can be a factor in the development of some HPV-related cancers, it is not the sole determinant, and other factors, including the persistence of active viral oncogene expression, host immune response, and additional genetic and environmental factors, play significant roles in cancer development and progression.

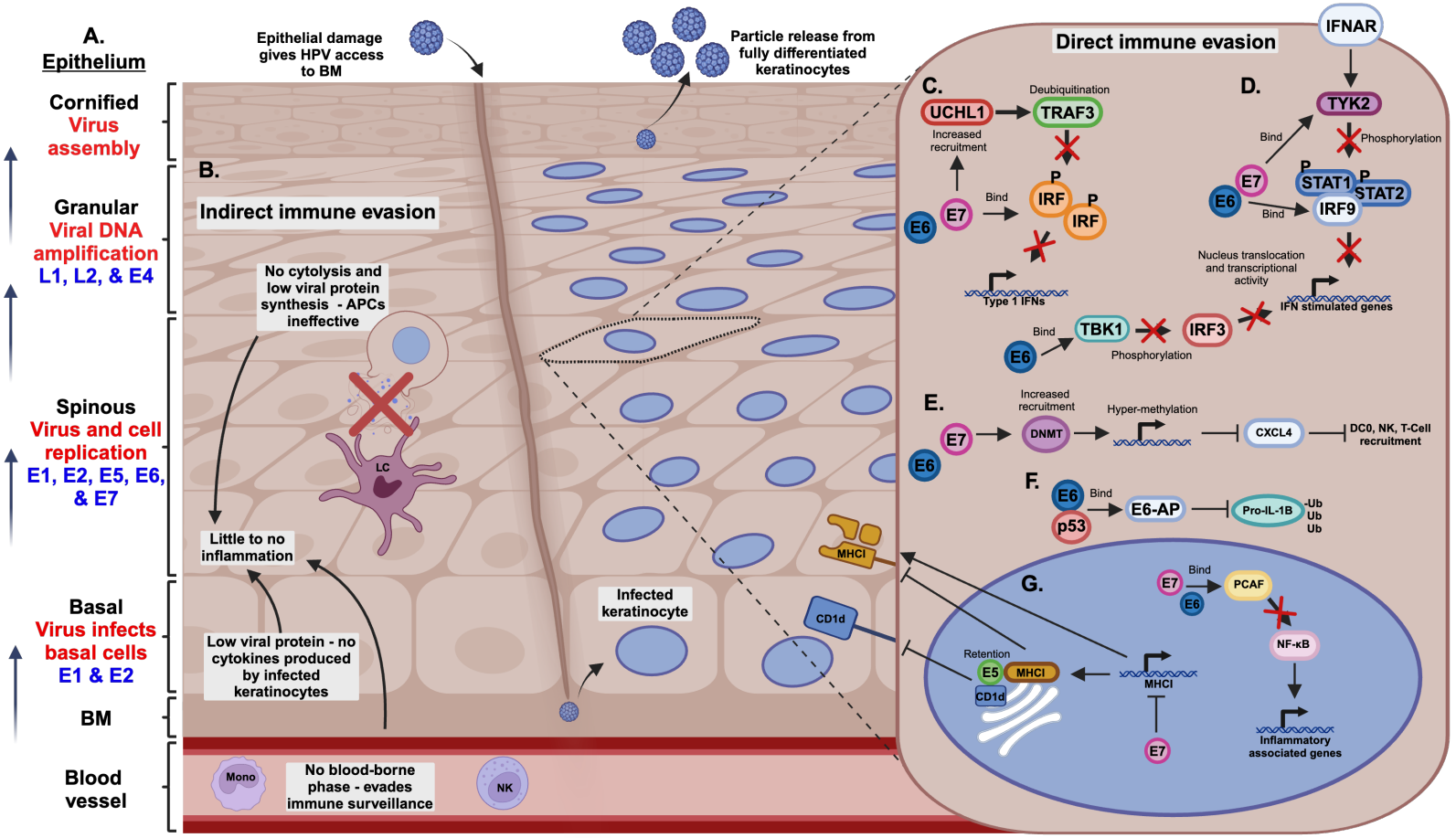

Figure 5: The life cycle of HPV and its key immune evasion mechanisms. A. The HPV life cycle is closely linked to the differentiation of the infected keratinocyte, where HPV gains access to the Basement Membrane (BM) through an abrasion in the epithelium. Basal keratinocytes are infected, where the infected cells travel up the layers of the epithelium until new particles are released from the outermost (cornified) layer of the epithelium. Indicated in red are the stages of the viral life cycle, and in blue the viral proteins that are expressed. **B.** The indirect immune evasion strategies of HPV. There is no cytolysis as a result of low viral replication throughout most of the viral life cycle. Viral particles are therefore only released where immune surveillance is minimal making APCs ineffective. Little to no proinflammatory cytokines are produced and as a result, no immune response is elicited. HPV remains within the epithelium and does not have a blood-borne phase, resulting in minimal exposure to host immune defences. **C-G.** The direct immune evasion strategies exploited by HPV oncoproteins in keratinocytes. **C.** E6 and E7 increase the recruitment of UCHL1 to inhibit TRAF3 activation and bind to IRF to prevent its transcriptional activity. **D.** E6 an E7 bind to TYK2 interfering with the IFNAR signalling pathway to hamper phosphorylation of STAT1 and STAT2, and also by binding to IRF3 to prevent its binding to phosphorylated STAT1 and STAT2 for activating IFN-stimulated genes. E6 binds directly to IRF3 preventing its phosphorylation by TBK1, thereby preventing its transcriptional activity of IFN stimulated genes **E.** HPV E6 and E7 recruit DNMT1 to suppress CXCL14 transcription **F.** E6 and E7 bind to ubiquitin ligase E6-AP, leading to degradation of pro-IL-1β. **G.** HR HPV E6 and E7 prevent the nuclear translocation of NF-κB via upregulation of UCHL1. E6 and E7 are also capable of binding to PCAF, a coactivator of NF-κB in the nucleus, thereby downregulating the NF-κB signalling pathway. HR HPV E7 can interact with the MHC I promoter, leading to repression of MHC1 gene transcription. E5 reduces MHC I and CD1d expression by blocking the transport of MHC I and CD1d proteins to the cell surface via its interactions with host proteins in the Golgi complex and endoplasmic reticulum. Figure adapted from (111, 112) and created with BioRender.com.

1.4 HPV evasion of the host immune system

HPV infections are remarkably common, yet the immune system is typically able to clear the virus through a cell-mediated immune response, often characterised by a Th1-type response (66, 113). In this process, LCs play a pivotal role by capturing viral antigens from infected or dying keratinocytes. These activated LCs then present the antigens to naïve T cells, which in turn become activated effector T cells. These T cells have the capability to home back to the site of infection in the epithelium, where they target and destroy HPV-infected keratinocytes, thereby mitigating the infection (113).

Although cell-mediated immunity controls HPV infection in the majority of cases, about 10% of all infections become persistent, which greatly enhances the risk of progression to disease and malignancy (4). HPV employs several indirect and direct strategies to effectively evade the innate immune responses, as summarised in Figure 5. As stated previously, the infectious life cycle of HPV is closely linked to the differentiation of the infected host keratinocytes (72). There is no cytolysis as a result of low viral replication throughout most of the viral life cycle, where viral release only occurs after the infected basal keratinocyte has migrated to the outer epithelial layers and has fully differentiated. Viral particles are therefore only released where immune surveillance is minimal, thus making APCs, such as intraepithelial DCs, ineffective (114).

Under normal conditions, keratinocytes can either constitutively or be induced to secrete a range of pro-inflammatory cytokines, including IL-1, -6, -10, and -8. IL-1 in particularly plays a vital role in activation of APCs, which in turn present antigens to T-helper cells (115, 116). As low levels of viral proteins are produced at the early stages of the viral life cycle, as well as no cytolysis occurs, little to no pro-inflammatory cytokines are released by infected keratinocytes. As a result, no immune response is elicited as the APCs are ineffective in non-inflammatory environments (115). Throughout its life cycle, HPV remains within the epithelium and does not have a viraemic or blood-borne phase, resulting in minimal exposure to host immune defences (25), and anti-HPV antibodies can usually only be detected in infected individuals after 6 to 12 months (117). This indicates that HPVs employ indirect mechanisms to reduce the efficiency of host immune surveillance, which may increase the susceptibility toward persistent HPV infection when individuals are exposed to additional risk factors (111).

Like many other DNA viruses, HPV has also evolved mechanisms for directly evading the host immune system. HPV oncoproteins E5, E6, and E7 are involved in these direct evasion strategies. Particularly E6 and E7 play central roles in dampening IFN responses by inhibiting PRR signalling pathways through multiple mechanisms: they upregulate the deubiquitinating

enzyme Ubiquitin C-Terminal Hydrolase L1 (UCHL1), block TNF-receptor-associated factor 3 (TRAF3) activation, and they bind to interferon regulatory transcription factor (IRF), thereby suppressing its transcriptional activity of IFN stimulated genes in the nucleus (111, 118). E6 and E7 also interfere with the IFN-α/β receptor (IFNAR) signalling pathway by binding to tyrosine kinase 2 (TYK2) to restrict phosphorylation of the transcription factors STAT1 and STAT2, and by interacting with IRF9 to prevent its binding to phosphorylated STAT1 and STAT2 for activating IFN-stimulated genes (111). E6 and E7 can also inhibit NF-κB nuclear translocation by upregulating UCHL1 (119). They also bind to P300/CBP-associated factor (PCAF), a coactivator of NF-κB in the nucleus, leading to the downregulation of the NF-κB signalling pathway (111).

HPV oncoproteins also directly downregulate the production of IL-1β in keratinocytes. As mentioned previously, HPV16 E6 it forms a complex with ubiquitin ligase E6-AP and the tumour suppressor p53. Another consequence of this complex formation is the degradation of pro-IL-1β and inhibition of IL-1β formation. Clinical studies using human biopsy samples have demonstrated a progressive reduction in IL-1β gene and protein expression, transitioning from normal epithelium to pre-cancerous lesions and to cervical tumours (120). HPV oncoproteins were also found to associate with DNA methyltransferase 1 (DNMT1), leading to hyper-methylation of the CXCL14 promoter (121) and downregulation of CXCL14 which has been observed in HPV-associated cancers (121). It is suggested that CXCL14 may have significant roles in inhibiting angiogenesis and facilitating the recruitment of immature DCs, NK cells, and T cells (122, 123).

The elimination of virus-infected cells by antigen-specific cytotoxic T lymphocytes (CTLs) is a highly efficient and precise mechanism. CTL-mediated killing relies on the presentation of pathogen-derived peptides by MHC class I molecules on the surface of keratinocytes. In the context of HR HPV, E7 interacts with the MHC I promoter, recruiting histone deacetylases to the promoter site, which results in the suppression of MHC I gene expression (124). E7 also represses the expression of antigen processing machinery components (125), leading to impairment of peptide production and transportation in infected cells. In addition, HPV E5 causes retention of MHC class I complexes (HLAs) in the Golgi apparatus and endoplasmic reticulum (ER) and prevents their transport to the cell surface (66), thereby preventing presentation of viral peptides to CTLs (66). E5 also reduces the surface expression of CD1d molecules on keratinocytes, where it is retained with E5 in the ER (67). Reduction of CD1d, a crucial antigen-presenting molecule responsible for activating NK cells is likely to dampen NK cell-mediated antiviral responses, potentially affecting the initial stages of immune activation following HPV infection.

Several co-factors additionally contribute to immune evasion and establishment of persistent HPV infection. The major co-factor relevant to Southern Africa is co-infection with the highly prevalent HIV. Both these viruses share the same route of transmission, and HIV infection has been shown to promote HPV infection in women at both the molecular and cellular levels, such as HPV entry into keratinocytes, establishment of persistent HPV infection, and immune evasion (126). HIV infection and low CD4 count have been shown to be significantly associated with increased risk of HPV infection and HPV-related disease progression. Immune response to HPV infection is modulated by CD4+ T cell-dominated Th1 response as outlined above; therefore in HIV positive individuals who have low CD4 cell counts, HPV immune responses are dampened even further (127). As a result of increased risk of persistent HPV infection in HIV positive women, the risk of cancer development also increases. Indeed, HIV-infected women present with cervical cancer 15 years earlier than HIV negative women (127). Usually, the administration of anti-retroviral therapy decreases the risk of AIDS-defining cancers (such as Kaposi's sarcoma and non-Hodgkin's lymphoma), but this is not the case for HPV-associated cancers (127).

Emerging theories suggest that not all HPV infections are fully eradicated after disease clearance (128). In some instances, a state of equilibrium may be established where memory T cells and the virus co-exist without causing immediate disease, a phenomenon known as viral latency (128). This delicate balance means that the virus is kept in check by the immune system without being completely eliminated. However, should there be a shift due to compromised immune surveillance or immune system failure, such as a result of immunosuppression or hormonal changes, the infection may be reactivated. This reactivation can lead to the progression of the disease, potentially resulting in the recurrence of warts, precancerous lesions, or even cancerous growths, depending on the HPV strain involved and the site of infection (128).

1.5 HPV vaccines

At present, there remains no known treatment or cure for HPV infection. However, there are three highly effective prophylactic vaccines available that target the most prevalent and HR HPV types. In 2006, Merck introduced Gardasil®, a quadrivalent vaccine offering protection against HR HPV types 16 and 18, as well as LR HPV types 6 and 11. The latter are implicated in approximately 90% of genital warts cases (129). Subsequently, in 2007, GlaxoSmithKline produced a bivalent vaccine named Cervarix™, providing prevention against the two primary HR HPV types, 16 and 18 (130). In 2014, Merck released a 9-valent version of their vaccine, known as Gardasil 9, which confers immunity against HPV types 6, 11, 16, 18, 31, 33, 45, 52, and 58 (131). More recently, another bivalent vaccine produced by Xiamen Innovax Biotech, protecting against HPV 16 and 18, was approved by the WHO (132).

As the above-mentioned vaccines are composed of virus-like particles (VLPs) of individual type-specific L1 capsid proteins, they offer minimal cross protection against other HPV types, as the immune response generated is highly type-specific. Moreover, the vaccines cannot eliminate an already established HPV infection. Little is known about their use as a treatment for existing HPV-related cutaneous and mucosal conditions. A reduction in cutaneous lesions (warts) has been reported after receiving the quadrivalent vaccine, as outlined in a review by Pham et al. in 2020 (133). However, most reports on the use of non-commercial HPV vaccines for the treatment of cervical intraepithelial neoplasia, recurrent respiratory papillomatosis, and anal intraepithelial neoplasia did not show promising results (133).

1.6 Cervical cancer prevention and treatment in LMIC

The high prevalence of HPV infection, often coupled with limited access to HPV vaccines and cervical cancer screening programs, places women in low-resource settings at a disproportionately higher risk of developing cervical cancer. Adding to this burden is the co-existence of the HIV epidemic, which has ravaged Sub-Saharan Africa. HIV-positive individuals are particularly vulnerable to HPV-related complications, as their compromised immune systems struggle to control HPV infections, leading to a higher incidence of persistent HPV infections and a heightened risk of cervical cancer (134). Thus, the intersection of HPV and cervical cancer with the HIV epidemic in LMIC underscores the urgent need for innovative prophylactic measures and comprehensive healthcare interventions to reduce the incidence and mortality of cervical cancer in these vulnerable populations.

The South African Department of Health (DOH) began a vaccination program and rolled out Cervarix™ to schoolgirls (Grade 4, approximately 9 years of age) in 2014 (135). In the first

round of vaccinations in April 2014 a coverage rate of 83% was achieved. In 2014, coverage of the second dose later that year dropped to 61%. The vaccine programme, along with cervical cytology screenings provided for women by the state, have not been sufficient to overcome the high HPV infection/cervical cancer rate in South Africa, due to gender inequity, and financial and cultural strains (136, 137). Many people in LMIC are still unaware of HPV infection and protection by vaccination (138, 139). Moreover, young girls are thought to have missed the opportunity to be immunised through the DOH vaccination programme as a result of absenteeism and limited access to school health teams (140). Lack of caregivers' signed consent has also been observed, most likely as a result of inadequate sensitisation campaigns, the social stigma surrounding immunisation of a sexually transmitted virus and overall vaccine hesitancy (139, 141, 142). The need for a cold chain (controlled storage at low temperatures) has been difficult to maintain in South Africa and other LMIC with substandard infrastructure and low funding, which makes administration of vaccines to schoolgirls in rural areas even more challenging (136, 137). The COVID-19 pandemic, which commenced in 2020, also led to a significant decline in the vaccination rate, which plummeted to a mere 3% (143). Lockdowns and school closures clearly contributed to the collapse of school health programmes; and lack of facilities, cold chain issues, and poor vaccine management together explain the low vaccine coverage during the COVID-19 pandemic.

However, there has been a gradual improvement in this situation as the country emerges from the COVID-19 crisis. Coverage of the first vaccine dose has now increased to approximately 38% and 47% in 2021 and 2022, respectively, although this remains significantly lower than the nearly 85% vaccination rate observed in 2014 (144). To address the potential long-term consequences of this disruption to the vaccination program, the SA National Advisory Group on Immunisation recommended a strategic shift. The program is now focused on targeting girls in Grade 5, who were largely unable to receive their shots in 2020 due to the pandemic. The 2023 campaign commenced in February, delivering the first dose to Grade 5 girls aged nine and older at government schools across South Africa.

A modelling study published in 2022 postulated that if the vaccination program in South Africa vaccinated 90% of the target group, incidence of cervical cancer can be reduced from a median incidence of 47.6 in 2020 to 4.5 per 100 000 women-years by 2120, compared to the base case scenario of 26.3 per 100 000 women-years in 2120 (145). In addition, if two life-time cervical screens (Pap smears) are achieved, as currently supported by the DOH in South Africa, the number is further reduced to 3.6 (145).

1.7 Alternative HPV prophylaxis and therapy

Preventive measures such as HPV vaccination and regular cervical cancer screening (Pap smears) play essential roles in reducing the burden of HPV-related diseases. However, given the low vaccine coverage and screening uptake in LMIC, the disease burden resulting from persistent HPV infections is likely to continue. Alternative therapies for the treatment and prevention of HPV infections are required, particularly ones that are more easily accessible to people in LMIC. Topical antiviral microbicides that can block the full spectrum of genital HPV infections (and ideally also other common sexually transmitted infections (STIs)) could either complement the current vaccines, be offered to those without access to these vaccines, or even be given to people who are already infected with HPV. By the early 2000s, the only reagents that had been studied and shown to inhibit HPV infection were monoclonal antibodies (MAbs) with type-specific neutralising activity, and broad-spectrum antiviral agents such as alkyl sulphates and monocaprin (1, 146-149). Over the last two decades, research has delved into discovering and characterising a broad spectrum of molecules with anti-HPV activity. Many approaches are targeting the early steps of HPV infection (i.e. cell-surface binding, entry and intracellular trafficking) as a promising strategy in preventing and treating HPV infections. This is extensively discussed in our review article published in 2021 (Figure 4) (1).

A range of competitive inhibitors have been identified that bind to the viral capsids and prevent their **binding** to HSPGs (1). The most notable molecule that has shown efficacy in human trials and is now commercially available is Carrageenan (150-152). It is an inexpensive, non-toxic anionic polymer that is naturally derived from three species of red algae. Carrageenan primarily blocks HPV infection through two mechanisms. First, it directly binds to the viral capsid, preventing its attachment to cell-surface HSPGs (153). This interference lasts long enough for natural innate defences in the genital tract to inactivate the virus. Second, carrageenan inhibits HPV infection by either occluding virion surfaces involved in binding to cellular proteins crucial for infection or by interfering with the necessary conformational changes within the virion (153). *In vivo* research has also shown a protective effect of carrageenan on herpes simplex virus type 2 (HSV-2) (154) and simian-human immunodeficiency virus (sHIV), but randomised human trials demonstrated no efficacy against vaginal transmission of HIV (155-158). Other HPV-binding molecules that target heparin sulphate binding, such as alginate, heparin, and sulphated glycopolymers (dextran sulphate, cellulose sulphate) have been identified to inhibit HPV infection *in vitro* (159-165). Moreover, dendrimers, dispirotripiperazines, and lactoferins have been demonstrated to block the initial binding of HPV to cells by directly binding to HSPGs (95, 166-168). These compounds have

also shown efficacy against other sexually transmitted viruses (HIV, HSV-1/2, HIV), indicating a broader antiviral potential (161, 169-181).

The **internalisation** step of HPV infection is another target for intervention. Compounds that have been shown to interfere with this process include annexin A2 inhibitors and anhydride modified proteins (97, 182, 183) such as JB01, which has undergone phase IIa clinical trials and showed efficacy intravaginally to treat existing HPV infections in women (183). JB01 has also shown efficacy in inhibiting HIV, HSV-1 and HSV-2 (184-186).

Molecules that inhibit **intracellular trafficking**, such as vacuolar ATPases (v-ATPases) inhibitors, have demonstrated potential to disrupt the HPV lifecycle within host cells (187). Prevention of lysosomal acidification, and therefore retrograde trafficking of L2/vDNA, by saliphenylhalamide (SaliPhe), a derivative of the naturally occurring compound salicylihalamide, was found to be an effective inhibitor against HPV 6, 11, 16, 18 and 31-PsVs infection *in vitro* (187). Human defensin 5 (HD5) has also been found to prevent dissociation of the L2/vDNA complex and redirects the viral particle to lysosomes (188, 189).

The requirement of γ-secretase, a transmembrane protease, for successful infection is a unique feature of HPVs. Knockdown of any of its four subunits were found to potently block HPV infection (190, 191), while treatment with γ-secretase inhibitors (GSIs) prevented the infectivity of several HPV types (HPV16-, HPV11- and HPV31-PsVs) in human keratinocytes at non-cytotoxic doses (190). A strong inhibition of HPV infection was also observed in mouse models using topically applied GSIs, suggesting that GSIs could represent effective microbicides against anogenital HPVs (190).

Stannin, a transmembrane protein, has also been proposed to affect HPV16-PsVs infection. Stannin-deficient mutant cell lines resulted in a 50% increase in HPV16-PsVs infection to that of their wildtype counterparts (192). Further experiments showed that stannin does not affect virus uptake or virus uncoating, but instead blocks virus entry into the trans-Golgi network (TGN) by routing the cargo to lysosomal compartments for degradation, presumably via blocking L2-retromer binding, a critical step for L2/vDNA to enter the TGN (192).

Ongoing research into the molecular mechanisms of HPV infection and the development of therapeutic interventions continue to be critical areas of study in the quest to combat these viruses and their associated cancers. Apart from designing therapies that inhibit HPV binding, uptake and intracellular trafficking, another strategy would be to design therapies that can enhance innate and adaptive immune recognition and viral clearance of HPVs. The role of therapeutic vaccines is to enhance adaptive T cell immunity by initiating naïve T cells to

produce CTL that target HPV infected cells, inducing CD4-positive T cells to produce necessary cytokines, and enhancing APCs (193). There are four main categories of HPV treatment vaccines: live vector-based (bacterial and viral) vaccines, peptide and protein-based vaccines, nucleic acid-based vaccines and whole cell vaccines (e.g., DCs), where the oncoproteins E6 and E7 are the most widely used target antigens for HPV therapeutic vaccines development (194). To enhance innate immune recognition of HPV or other viruses, TLR agonists engaging their respective PRR have been tested (195-197). One such example is AS04, a TLR4 agonist, that has shown effectiveness against HPV infection in clinical trials (198). Additionally, exploring the utilisation of innate immune opsonins stands as a promising avenue to further enhance the recognition of HPV, as detailed in Sections 1.8 and 1.9.

1.8 Surfactant Proteins A and D

SP-A and SP-D are large hydrophilic proteins of the collectins family involved in lung surfactant homeostasis and pulmonary immunity. They are soluble, collagenous C-type lectin PRRs and are calcium dependent (199). Their primary structure consists of an N-terminal non-collagenous domain capable of forming inter-subunit disulphide bonds, a collagenous region of Gly-X-Y repeats, a helical neck domain, and a globular C-terminal carbohydrate recognition domain (CRD), the latter of which is involved in pathogen recognition (199). Monomeric units spontaneously self-assemble into trimers and can form higher order structures (Figure 6) (200). SP-A preferentially binds to mannose, fucose and the lipid ligands on the surface of incoming pathogens (201). SP-D exhibits a preferential binding affinity for inositol, maltose, and glucose (201). SP-A and D have very weak affinities to galactose and sialic acid which is important for distinguishing self from non-self, as these sugars usually form the terminals of carbohydrates on eukaryotic cells (201). SP-A and SP-D recognition and binding of their specific ligands usually takes place via their CRDs and elicits a variety of immune responses, including agglutination of pathogens, opsonisation and enhanced phagocytosis, regulating macrophage function and inflammation, and direct killing (201).

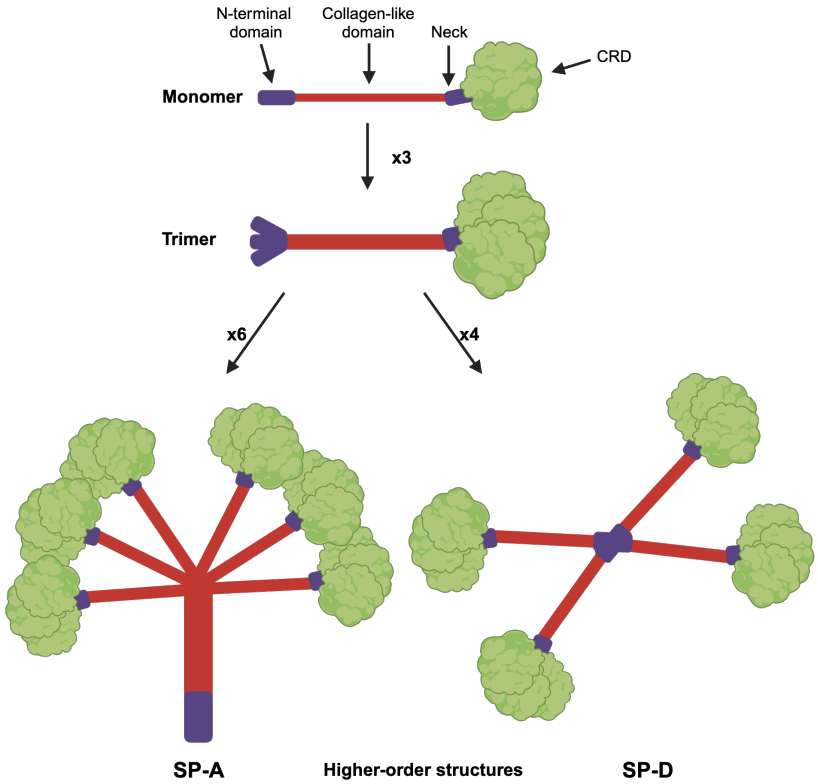

Figure 6: Structure of SP-A and SP-D. Monomers of SP-A and SP-D are composed of a carbohydrate recognition domain (CRD), a neck region, a collagenous region and an N-terminal region. These form trimers which then multimerise to form higher order structures. Figure adapted from (202) and made with BioRender.com.

1.8.1 SP-A and SP-D and their role in innate immunity

SP-A and SP-D play pivotal roles in the innate (and adaptive) immunity of the lung. More recently, the occurrence of non-pulmonary SPs and their immunological roles have been researched (203). SPs exhibit dual roles in the immune response due to their ability to interact with a variety of cell surface receptors and to bind various ligands, which can result in different outcomes depending on the context. They act as first responders to inhaled microorganisms and particulates, triggering a cascade of immune responses that include agglutination and opsonisation for enhanced phagocytosis, modulation of inflammatory mediator release, and direct antimicrobial activity. SP-A and SP-D are therefore often referred to as innate immune scavenge receptors (202). Through these actions, SP-A and SP-D not only contribute to the immediate neutralisation of potential threats but also orchestrate the delicate balance between effective pathogen clearance and limiting inflammation to prevent tissue damage, underscoring their critical function in the innate immune system. The following chapters will highlight the complex nature of SPs in immunomodulation, with primary focus on SP-A.

1.8.2 Pathogen agglutination, opsonisation and control by SPs

SPs have the ability to cluster or agglutinate pathogens. When pathogens are aggregated, they become larger targets that are more easily recognised by phagocytes like macrophages and neutrophils. The aggregated form mimics the natural size preference that phagocytes have for particles, enhancing the efficiency of phagocytosis. A single phagocyte can engulf multiple pathogens in one event of phagocytosis if they are bound together, rather than having to phagocytose each pathogen individually. Aggregation by SPs may additionally physically restrict the movement of pathogens, limiting their ability to spread throughout the respiratory tract and invade host tissues. Aggregation can also neutralise the pathogenicity of microbes as it compromises their ability to bind to host cell receptors preventing infection of host cells (201). The aggregation of pathogens may also facilitate the activation of the complement system, an array of proteins that aids in the opsonisation and destruction of pathogens (see Section 1.1.2).

Opsonisation involves the coating of a pathogen's surface with molecules termed opsonins, thereby tagging the pathogen as a target for phagocytes such as macrophages, neutrophils, and DCs via their surface receptors. SPs are often referred to as innate immune opsonins and have shown the ability to "prime" pathogens for immune cell clearance. For instance, the inflammatory response towards lipopolysaccharides (LPS), an outer-membrane toxin on Gram-negative bacteria, is greatly enhanced when bound to SP-A or SP-D (204). SPs can also agglutinate and opsonise viruses, where SP-A binds, for example, to the glycoproteins of respiratory syncytial virus (RSV), and SP-D opsonises influenza A virus (IAV) (200, 205, 206). Recently, we have shown the ability for SP-A to bind and opsonise HPV16-PsVs, resulting in their increased uptake into murine innate immune cells (19) (see Section 1.9).

Studies have shown that SP-A mediates macrophage phagocytosis and neutrophil uptake of a number of other bacteria, including of *Escherichia coli* (*E. coli*), *Streptococcus pneumoniae* (*S. pneumoniae*), *Staphylococcus aureus* (*S. aureus*), and *Hemophilus influenza* (*H. influenza*) (207). SP-A has also been shown to mediate *Mycobacterium tuberculosis* (*M. tb*) phagocytosis by alveolar macrophages, by binding to macrophage mannose receptors (208). Macrophages, however, serve as the major host cell niche for the growth and survival of *M. tb*, and so these results suggest SP-A assists *M. tb* growth and survival (209). SP-A has also been shown to play an important role in the pathogenesis of mucoid *Pseudomonas aeruginosa* (*P. aeruginosa*) infection in the lung *in vivo*, by enhancing macrophage phagocytosis (210). Likewise, SP-A recognises HSV-1 which generally infects the mucosal layer of the mouth but can also cause infections in the respiratory tract, leading to its enhanced uptake by alveolar macrophages (211).

While surfactant proteins have been historically researched in the context of the pulmonary immune functions they have recently been shown to express at various non-pulmonary sites (63). In the human female genital tract (FGT) SP-A and SP-D have been detected in the myometrium, vaginal epithelium and vaginal lavage fluid (76, 77). It has been suggested that SPs play protective roles during pregnancy as well as contribute to innate defences against sexually transmitted pathogens (78, 79). It has recently been reported that supplementation with SP-A resulted in decreased uropathogenic *E. coli* growth in the urinary tracts of mice (80). Similarly, the addition of SP-A protein has been shown to enhance the phagocytosis of ureaplasma by RAW264.7 murine macrophages and chlamydia by THP-1 human monocytes (212, 213). *In vitro* studies demonstrated SP-A and SP-D interacting with HIV via oligosaccharides on the HIV envelope protein gp120 (78, 81). SP-A binding to HIV inhibits its infectivity of CD4 T cells, presumably by blocking the CD4 binding site of gp120 (78). However, SP-A plays a dual role in HIV infection as SP-A was shown to enhance HIV uptake by DCs *in vitro*, where DCs transfer the virus to CD4 cells, although no *in vivo* studies have validated this (81).

1.8.3 Activation of the complement cascade by SP-A and SP-D

SP-A and SP-D show a high degree of similarity with the complement protein C1q (203), thereby functioning as an "activation-ligand" for the complement cascade pathway (see Section 1.1.2) which facilitates in opsonisation and particle uptake (214). SPs have the ability to directly kill pathogens, a feature shared with C1q. The complement cascade pathway can lead to the formation of the membrane attack complex, which creates pores in the membrane of the pathogen (215). Both SP-A and SP-D demonstrate this ability to target *E. coli* (216). Moreover, SP-A was found to bind to Macrophage 1 antigen (Mac-1), a complement receptor comprising of CD11b and CD18, thereby modulating Mac-1 cell-surface presentation and enhancing Mac-1 mediated phagocytosis (217, 218).

1.8.4 SP-A and SP-D interaction with immune cell receptors

SP-A and SP-D interact with various receptors on innate immune cells to modulate inflammation (202, 203). In the absence of infection, SP-A and SP-D interact with signal-regulatory protein alpha (SIRPα) on myeloid cells (219). This interaction prevents the production of pro-inflammatory cytokines and maintains homeostasis. When challenged with infection and upon pathogen binding to the CRD, SP-A and SP-D preferentially bind to the calrecticulin/CD91 receptor complex and facilitate an inflammatory response (219).

In addition, SP-A and SP-D bind to a number of macrophage receptors, including the Cluster Differentiation 14 receptor (CD14) (203). CD14 acts as a co-receptor with TLR4 for LPS from Gram-negative bacteria leading to a significant inflammatory response (220). However, upon interaction with SP-A and SP-D decreased expression of TNF-α and IL-1 as well as decreased IL-1 and NF-κB DNA binding activity has been observed, indicating a suppression of inflammation (221, 222). This again demonstrates that SP-A and SP-D have important modulatory effects during Gram-negative infection.

SP-A and SP-D were also found to act as direct ligands for TLR2 and TLR4 (203), thereby attenuating cytokine production when exposed to pathogens and their PAMPs (223, 224).

SPs can in turn be regulated by other TLR ligands. LPS from Gram-negative bacteria has been shown to induce expression of both SP-A and SP-D (225-227). Moreover, when exposed to the TLR2 ligand, PamCy3, and the TLR4 ligand, LPS, human retinal Müller cells, were found to upregulate of SP-A protein expression (228).

1.8.5 SPs interaction with immune effectors

SPs can interact with immune effector molecules, such as immunoglobulins, and enhance each other's functions in a synergistic manner within the immune system. Particularly, IgG (via its Fc region) can bind to SP-A (229, 230), facilitating the opsonisation process, where pathogens are marked for destruction and more readily ingested by phagocytes. This interaction links the adaptive immune response with innate defence mechanisms (229, 230).

GP-340, also known as Salivary Agglutinin (SAG), is a member of the scavenger receptor cysteine-rich superfamily. GP-340 is found in various bodily fluids and tissues and has also been reported to play a role in the immune response by binding to a wide array of pathogens, thereby acting as an opsonin to enhance their clearance (231). GP-340 can bind to SP-A, forming complexes that enhance the recognition and clearance of pathogens in the lungs (232). This interaction can help aggregate bacteria and viruses, making them easier targets for phagocytosis by immune cells.

1.8.6 SP-A and SP-D and their role in adaptive immunity

Although their main role is in innate immunity, SPs bridge innate and adaptive immune responses through their functions in modulating the activity of APCs, specifically DCs (202). SP-A, in particular, has been demonstrated to hinder the presentation of *E. coli* antigens, while at the same time enhancing the phagocytosis of the bacteria (233). The influence of SP-D on

DC function has a secondary effect on T cells; by modulating DC chemotaxis, which is essential for T cell activation, SP-D indirectly governs the T cell response (234).

SPs can directly modulate T cells by inhibiting their proliferation and modifying their function and activation state (235-238). By maintaining T cells in a less active state under non-inflammatory conditions, SP-A and SP-D contribute to immune tolerance, preventing excessive inflammation and maintaining homeostasis within the lung environment (239).

1.9 Identification of SP-A as a novel immune molecule modulating HPV infection

In an attempt to identify novel molecules capable of preventing HPV infection by enhancing innate immune recognition and viral clearance we previously demonstrated a direct association between HPV16 pseudovirions (PsVs) and human purified SP-A, but not SP-D, by co-immunoprecipitation assays (19). Moreover, using fluorescently labelled HPV16-PsVs, viral particle uptake into the murine macrophage cell line, RAW264.7, was found to be enhanced at 1 hour post infection (hpi) when preincubated with SP-A, but not SP-D, in the presence of $CaCl_2$ compared to the HPV only and BSA preincubation controls (Figure 7). It was therefore hypothesised that macrophages – and potentially other innate immune cell types – may prevent infection by effectively killing most of the internalised virus in the presence of exogenously added SP-A (19).

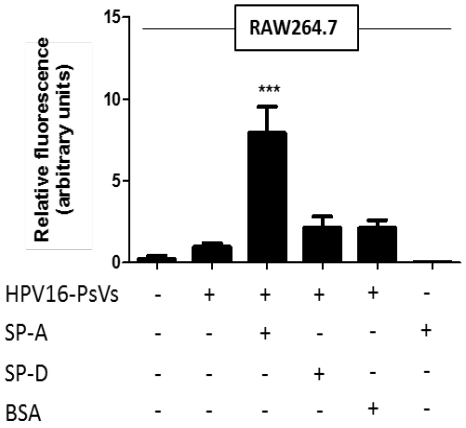

Figure 7: Binding of HPV16-PsVs to SP-A (but not SP-D) results in increased viral uptake by RAW264.7 macrophages (19). RAW264.7 cells were infected for 1 h with fluorescently labelled HPV16-PsVs that had been preincubated with SP-A, SP-D, or BSA for 1 h prior. Viral internalisation was analysed by flow cytometry and is presented as x-fold increase relative to the mean fluorescence intensity of cells infected with untreated HPV16-PsVs which was set as 1. *** = $p < 0.001$; no symbol denotes not significant.

While these *in vitro* findings suggest that SP-A plays a role in enhancing immune recognition of incoming HPV16-PsVs, it is essential to recognise that the natural HPV infection environment within the genital tract is highly complex. Several diverse cell types may be

implicated in immune responses upon viral challenge, including local epithelial cells and other recruited immune cells. To address this complexity, we investigated the impact of SP-A on HPV16-PsVs infection using a murine cervicovaginal challenge model (Figure 8A). This model was chosen for its ability to closely mirror the early events in HPV infection (240).

The absence of endogenous SP-A in the murine FGT allowed us to assess the effects of supplementation with exogenous SP-A on HPV-PsVs infection and macrophage recruitment *in vivo*. As shown in Figure 8B, infection with HPV16-PsVs that were preincubated with SP-A resulted in lower levels of infection at 72 hpi when compared to the BSA control group (19). Moreover, macrophage staining of the FGT from HPV16-PsVs infected mice showed enhanced infiltration of macrophages to the basal epithelium and site of HPV16-PsVs infection in the presence of SP-A (Figure 8C and D) (19). In addition, when using single cell suspensions derived from the FGT of naïve mice to assess HPV16-PsVs uptake into monocytes, macrophages, eosinophils, and neutrophils *ex vivo* (Figure 8E), we observed a significant increase in HPV16-PsVs uptake for all these populations when the viruses had been preincubated with SP-A (Figure 8F-G).

These data suggested an SP-A-mediated opsonisation of incoming HPV16-PsVs, increased phagocytosis, and killing by innate immune cells with an overall effect on dampening the infection. Besides enhanced phagocytosis, SPs are also known to agglutinate (aggregate) pathogens, thereby hindering their entry into host cells. Although we did not study this effect, the inhibitory action of SP-A is not necessarily dependent on agglutination, and our data strongly point toward SP-A-mediated innate immune cell uptake of the virions. While we demonstrated a direct biochemical interaction between HPV16-PsVs and SP-A, suggesting opsonisation as the causal basis for enhanced phagocytosis, we could not exclude the possibility that the mere presence of exogenously supplied SP-A in the murine FGT contributed to enhanced infiltration of innate immune cells to the site of infection and their prompt clearance of the invading viral particles.

To comprehensively investigate the multifaceted interactions between SP-A and various oncogenic HPV types, this thesis assessed the agglutination phenomenon, in addition to opsonisation, and its potential role in inhibiting HPV infection of multiple oncogenic types. Moreover, our research extended into human cell line-based *in vitro* systems, such as co-cultures, to replicate cellular interactions and microenvironments, providing a more clinically relevant platform. *In vitro* systems offer the advantage of covering a wider range of conditions and scenarios efficiently, overcoming the logistical constraints associated with *in vivo* work, ultimately accelerating our progress in understanding SP-A's potential as an anti-HPV therapeutic agent.

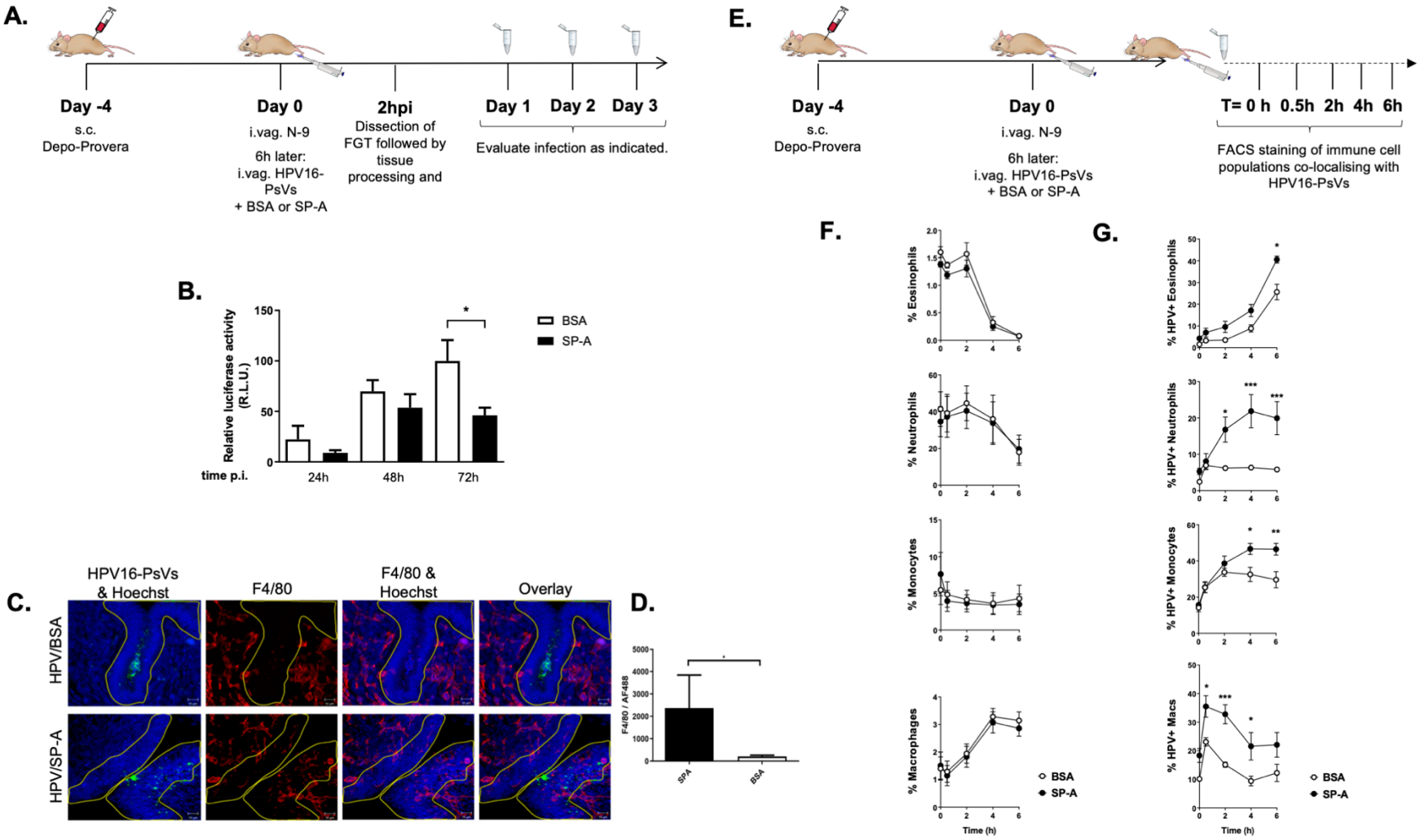

Figure 8: SP-A reduces HPV16-PsVs infection *in vivo* by increasing macrophage recruitment into the basal epithelium and increased viral uptake by selected immune cell populations (19). A. Mouse model for HPV16-PsVs infection using C57BL/6 mice, adapted from (240). **B.** *In vivo* infection levels presented relative to infectivity of the BSA control group at 72 hpi which was set as 100%. **C.** Representative confocal images of epithelial tissue (blue) exposed to fluorescent virions (green) is shown with staining for macrophages in red. The basal epithelium is outlined in yellow. **D.** The area of F4/80 (macrophage) staining in the basal layer of the epithelium was quantified, where macrophage recruitment to the epithelium in response to SP-A coated HPV16-PsVs was compared to the BSA control group. **E.** Mouse model as in A) showing isolation and infection of immune cell population *ex vivo*. Cells were infected with SP-A or BSA-coated HPV16-PsVs. At the indicated time points, cells were stained to visualise and gate the immune cell populations by flow cytometry (eosinophils, neutrophils, inflammatory monocytes, and macrophages). **F.** Shown is the percentage of the indicated immune cell populations over time upon infection with HPV16-PsVs preincubated with BSA (control) or SP-A. **G.** Shown is the uptake of HPV16-PsVs with the indicated immune cell populations over time dependent on preincubation of the viral particles with BSA (control) or SP-A. Depicted are mean values, with error bars showing SEM.* = $p < 0.05$; ** = $p < 0.01$; *** = $p < 0.001$; no symbol denotes not significant.

1.10 Rationale and aims

HPVs are highly prevalent sexually transmitted viruses that cause significant disease burden, with cervical cancer being the fourth most common cancer in women worldwide. Due to multiple mechanisms to effectively escape the host's innate immune response, which therefore delays the activation of adaptive immunity, HPV infections can persist for years, potentially progressing into pathologies. Prophylactic vaccination is considered the most effective control of HPV infections. However, despite the great efforts exerted in HPV-vaccination programs, these vaccines do not cover all the HPV types present in malignant lesions and they have limited benefit for women already infected with HR HPV types. The cost of these vaccines, coupled with limited education and awareness, as well as the challenges in maintaining a cold chain for vaccine transport and storage, impose added burdens on LMICs. This clearly underscores the need for alternative interventions that broadly target HPV infections. Our laboratory has previously identified SP-A as a novel innate immune molecule recognising and binding to HPV16 pseudovirions and dampening infection in a murine cervicovaginal challenge model. Based on these results, we herein aimed to assess the suitability of SP-A as a novel broad-spectrum HPV targeting molecule preventing initial viral infection of human keratinocytes. We also aimed to study the occurrence of agglutination and immune recognition of SP-A-coated HPV-PsVs in human-derived immune cells and to uncover in more detail the immune mechanisms that are affected by SP-A in the context of HPV infections. We hypothesise that SP-A can be developed into a candidate for use in topical microbicides which provide protection against viral genital tract infections.

2 Materials and methods

Chemicals of analytical/reagent grade were used and generally purchased by Merck or Sigma-Aldrich, unless indicated otherwise. Solutions made up in the laboratory are detailed in the Appendix.

2.1 Cell culture

2.1.1 Established cell lines

The human epithelial HPV18-positive cervical adenocarcinoma cell line HeLa (ATCC), the spontaneously immortalised keratinocyte cell line HaCaT (Thermo Scientific), the virus packaging cell line HEK293TT (A kind gift from Lawrence Banks), and the murine leukemic macrophage cell line RAW264.7 (Merck) were cultured in complete Dulbecco's Modified Eagle Medium (cDMEM) (Appendix). The human keratinocyte cell line NIKS was cultured in complete F-Medium (Appendix). The spontaneously immortalised human monocytic-like cell line THP-1 (Merck) was cultured in complete Roswell Park Memorial Institute Medium (cRPMI) (Appendix). This cell line was cultured in suspension, unless stated otherwise.

Cell culture procedures were performed under sterile conditions to prevent the risk of contamination. All cell lines were authenticated by IDEXX BioResearch using the genetic test CellCheck 16 before the study commenced.

2.1.2 Maintaining and sub-culturing cell lines

All cells were cultured in 75 cm^2 cell culture flasks and incubated in a humidified atmosphere containing 5% CO_2 at 37°C. Adherent cell lines were grown in 10 mL cDMEM until 90% confluency before being washed with phosphate-buffered saline (PBS) and removed from the flask enzymatically with trypsin/EDTA (Lonza) or lidocaine/EDTA (Appendix). Adherent cells were pelleted at 3000 rpm for 3 min and resuspended in fresh media at the appropriate ratio.

The suspension cell line THP-1 was grown in 20 mL cRPMI until reaching a concentration of approximately $1.0X10^6$ cells/mL. The cells were split to a density of $2.5X10^5$ cells/mL, by directly transferring the appropriate portion of cells in old media into fresh cRPMI. If necessary, THP-1 cells were spun at 2000 rpm for 4 min. To maintain a homogenic population of monocyte-like cells and to prevent differentiation and heterogeneity over time, a passage number 25 or less was used for all experiments.

Cells in culture were regularly tested for mycoplasma using the LookOut Mycoplasma PCR detection kit (Sigma-Aldrich). All cell-culture flasks and plates used in this project were sourced from SPL Life Sciences.

2.1.3 Cell counting and plating

An automated cell counter (Countess II, Thermo Scientific) was used to count cells and subsequently calculate the appropriate dilutions for each experiment. Total volumes of 2 mL, 1 mL, and 100 µL were used for 6-, 12-, and 96-well plates respectively, unless otherwise stated.

2.1.4 Storage of cell lines

Cells were pelleted at 2000-3000 rpm and gently resuspended in 10% dimethyl sulfoxide (DMSO) in foetal calf serum (FCS, Gibco) at a density of ~$5.0X10^6$ cells/mL. Cells were transferred to cryovials (NEST) in 1 mL aliquots and stored at -80°C before being transferred to liquid nitrogen for long-term storage. To thaw cells, cryotubes were transported on ice before being thawed rapidly in a 37°C water bath. Cells were resuspended in 4 mL pre-warmed media before being pelleted at 2000-3000 rpm for 3 min. Cells were resuspended in 10 mL complete medium and added to a cell culture flask.

2.2 Development of an immune cell panel derived from THP-1 cells

2.2.1 Differentiation of THP-1 cells to M0 (steady-state) macrophages

Differentiation of THP-1 to steady state macrophages (M0) was adapted from published protocols (241, 242). Briefly, THP-1 cells were grown to a confluency of $1.0X10^6$ cells/mL and seeded at a density of $1.0X10^6$ cells/mL in media containing 10 ng/µL phorbol 12-myristate 13-acetate (PMA). The cells were exposed to PMA for 24 h, washed and rested in fresh cRPMI for 48 h before using the cells in experiments, or before further stimulating the cells. The concentration of PMA, exposure and rest times were sufficient to induce the M0 phenotype (see Section 3.1). Depending on the type of experiment, cells were either directly differentiated in the experimental plates, or first differentiated in a T75 flask, lifted gently with lidocaine-EDTA (Appendix) and transferred at the correct cell density to the experimental plate.

2.2.2 Differentiation of M0 to M1, M2c, and M2a macrophages

Phenotype biasing of M0 macrophages was adapted from published protocols (243, 244). Briefly, M0 macrophages that had been resting post-PMA exposure for 24 h were exposed to stimulatory factors for 24 h (Table 1) in RPMI containing 1% penicillin G and streptomycin (Pen-Strep) and 1% foetal calf serum (FCS). The lower percentage FCS was to prevent any interference with the stimulating factors.

Table 1: Stimulants used for phenotype biasing of M0 to M1, M2a, and M2c macrophages after 24 h.

Macrophage phenotype	Stimulating factors	Concentration
M1	LPS (Sigma)	100 ng/mL
	IFN-γ (Peprotech)	20 ng/mL
M2a	IL-4 (Invitrogen)	20 ng/mL
M2c	IL-10 (Peprotech)	20 ng/mL

2.2.3 Differentiation of THP-1 cells to immature dendritic cells (DC0s)

Differentiation of THP-1 cells to immature DCs (DC0) was adapted from published protocols (245, 246). Briefly, THP-1 cells were plated at a density of $0.5X10^6$ cells/mL and stimulated with 10 ng/mL recombinant human Granulocyte-Macrophage Colony-Stimulating Factor (rhGM-CSF, Gibco) and 20 ng/mL IL-4 (Invitrogen) in RPMI containing 1% Pen-Strep and 2% FCS. Cells were stimulated for 6 days, replenishing rhGM-CSF and IL-4 in fresh media on day 3.

2.2.4 Validation of immune cell lineages by flow cytometry

THP-1 cells were differentiated in 6-well plates as described. Cells were lifted gently with lidocaine-EDTA and gentle pipetting, counted and plated in FACS block (Appendix) in a V-shaped 96-well plate, with $5.0X10^5$ cells in 50 µL FACS block per well upon which they were incubated in FACS block for 1 h at 4°C.

The cells were first stained for viability using the Zombie Aqua™ Fixable Viability Kit (BioLegend). Compensation controls were made as follows: one well of cells was treated with 70% ethanol to kill the cells. This was resuspended in a well of viable cells to achieve 50/50 live/dead cells. The viability dye was diluted in PBS to working concentration (Table 2).

The cells were centrifuged for 2 min at 700 g and resuspended in 100 µL viability dye for 15 min at room temperature (RT), before being washed 2 times with FACS wash (Appendix). The cells were then stained with the conjugated antibodies (Table 2) for 30 min at 4°C in the dark. Unstained controls were incubated with FACS block during this incubation step. The cells were washed with FACS wash 3 times, resuspended in 100 µL FACS fix (Appendix), and kept on ice in the dark until acquisition with a BD LSRFortessa™ Cell Analyser using the BD FACSDiva software (BD Biosciences). The cell populations were defined by setting the threshold for forward scatter at 5000 to exclude cell debris; 30 000 gated events were acquired per sample. The FlowJoTM software (v10.7.2; BD Biosciences) was used for post-acquisition analysis. Singlets were gated using a dot plot of the forward scatter height (FSC-H) vs area (FSC-A). The cell population was gated using a dot plot of side scatter (SSC-A) vs. FSC-A. Additionally, the t-SNE analysis FlowJo plugin was employed to visualise the high-dimensional data in a reduced two-dimensional space.

Table 2: Conjugated antibodies used to phenotype the THP-1-derived immune cell panel.

Antibody/Marker	Fluorophore	Excitation and emission peaks (nm)	µL per 50 µL staining volume
Cell viability	BV510 (Zombie Aqua™, BioLegend)	405 and 510	0.25
HLA-DR	PE (BioLegend)	488 and 574	1
CD11c	BV650 (BD Biosciences)	407 and 647	2
CD86	FITC (Biocom)	491 and 516	2.5
CD169	BV605 (Biocom)	407 and 602	2.5
CD206	PE-Cy5 (Biocom)	496 and 667	1.25
DC-SIGN	BV421 (Biocom)	408 and 422	2.5

The BD™ CompBeads Set (anti-Mouse Ig κ; BD Biosciences) was used to account for spectral overlap between the fluorophores. The compensation particles were prepared according to the manufacturer's instructions. Briefly, for each conjugated antibody used, 50 µL of the positive particles and 50 µL of the negative control were added to FACS tubes containing 100 µL FACS block. The same volume of antibody used for staining the samples was added to the FACS tubes. The tubes were incubated for 30 min at 4°C followed by the same washing

procedure as the sample stains. The resuspended beads were stored at 4°C in the dark until they were ready to be used in the flow cytometry experiment.

2.3 Purification of Native Human SP-A

Purified human SP-A was provided by Dr Jens Madsen, University College London, UK. The human SP-A was purified from bronchoalveolar lavage fluid (BAL) obtained from human patients with alveolar proteinosis using a previously described butanol extraction method (247). The collection of BAL was done with informed consent and necessary ethical permission from the Royal Brompton and Harefield Research Ethics Committee NRES10/H0504/9. The patients underwent the procedure for therapeutic purposes.

Native human SP-A was purified from the SP-A-rich BAL pellet through gel chromatography or butanol extraction, following the previously described protocols (248, 249). The purity of SP-A was verified using sodium dodecyl sulphate polyacrylamide gel electrophoresis (SDS-PAGE), Western blotting, and N-terminal sequencing. The purified SP-A protein was diluted with nanopure water or Tris-buffered saline (TBS) with 5 mM $CaCl_2$. The Limulus Amoebocyte Lysate (LAL) chromogenic assay (Lonza) was used to determine the levels of endotoxin in the purified SP-A protein preparation (19). If the butanol-extracted SP-A had low endotoxin levels (<1 pg/µg) it did not require endotoxin treatment. The treated proteins were filtered using a 0.22 µm filter and stored as aliquots at −20°C before being shipped to our laboratory in South Africa.

2.4 HPV pseudovirus (HPV-PsVs) production

HPV pseudovirions are single-cycle infectious particles comprising type-specific L1/L2 capsids enclosing a reporter expression genome (the pseudogenome) that mimic the structure and behaviour of a virus but lack the ability to replicate and cause pathologies (88). This makes them safer for laboratory research and vaccine development, eliminating the risk of accidental infection. The production of HPV-PsVs was adapted from established protocols (160, 250) and is outlined below.

2.4.1 Plasmid production

All plasmids used for transfections were maintained by transformation of chemically competent *E. coli* (TOP10, Invitrogen). Glycerol stocks of these transformed bacteria were used to inoculate liquid LB medium (Appendix) containing selection antibiotics (see Supplementary Table 1) and cultured for approximately 18 h in a shaking incubator at 37°C.

Plasmids were isolated and purified using the Promega PureYield™ Plasmid Maxiprep System. The resulting DNA was quantified using a NanoDrop Microvolume Spectrophotometer (Thermo Fisher) and restriction enzyme digests were performed to ensure the correct plasmid was isolated (Supplementary Table 1, Supplementary Figure 1).

2.4.2 Mammalian cell transfection and harvest of HPV-PsVs

HEK293TT cells were plated out to 50% confluency in 10x T175 flasks and transfected with plasmids encoding for HPV-type specific L1/L2 capsid proteins together with the Gaussia luciferase reporter plasmid pCMV-Gluc (Promega) using the calcium phosphate method. The transfection mixture was set up in a 15 mL falcon tube as follows: 150 µg L1/L2 plasmid, 360 µg pCMV-Gluc, and 750 µL $CaCl_2$ was added to Tris EDTA (TE) buffer (Appendix) to a final volume of 6 mL. The mixture was gently inverted before adding 6 mL 2X HEPES buffered saline (HBS, Appendix). The mixture was incubated at room temperature for 30 min before being added dropwise to the HEK293TT cells. After 48 h, the cell supernatants were collected in 50 mL flacon tubes, and the cells were lifted by trypsinisation and collected in the same 50 mL falcon tubes. The tubes were spun for 5 min at 3000 rpm and resuspended in 1 mL PBS. The cell suspensions were transferred to low protein binding Eppendorf tubes (Thermo Scientific) and spun again. The PBS was removed, and the size of the pellet was assessed. The pellet was resuspended in equal amounts of PBS, followed by 1/105 volumes 1M $MgCl_2$ (final concentration 9.5 mM), 1/28 volumes sterile 10% Brij 58 (Sigma), 2 µL Benzonase (Sigma), and 2 µL Exonuclease V (New England Biolabs). The pellet was incubated at 37°C for 24 h (maturation step), mixing occasionally. After the maturation step, the lysate was chilled on ice for 5 min before adding 0.17 volumes of PBS containing 5 M NaCl. The lysate was chilled on ice for a further 10 min and stored at -80°C until further processing.

Lysates underwent 3 freeze/thaw (-80°C/room temperature) cycles before being spun down at 8000 g for 10 min at 4°C. Supernatants were collected, the pellet (cell debris) washed once in 400 µL 1X high salt buffer (HSB, Appendix) and spun down together with the supernatant in case there was any debris left. The supernatants were either first labelled with Alexa Fluor 488 (AF488, Section 2.4.3) or directly loaded onto the CsCl gradient (Section 2.4.4).

2.4.3 HPV-PsVs labelling with Alexa Fluor™ 488

In order to fluorescently label the virus, the supernatant pH was first adjusted with 1/10 volumes 1 M $NaHCO_3$ (pH 8.3). 1/30 volumes Alexa Fluor™ 488 Succinimidyl Ester (10 mg/mL in DMSO, Invitrogen) was added to the lysate and incubated for 1 h at room temperature

wrapped in aluminium foil on a rotating wheel. The pH was brought back to neutral by adding 1/25 volumes 1 M $NaPO_4$ (pH 6.5).

2.4.4 HPV-PsVs purification – discontinuous caesium chloride gradient

For purification of the HPV-PsVs a discontinuous caesium chloride (CsCl) gradient was prepared as follows: 4 mL of light CsCl (Appendix) was pipetted into a siliconised ultraclear centrifuge tube (Beckman). 4 mL of heavy CsCl (Appendix) was gently underlayed beneath the light CsCl. The virion-containing supernatant was loaded on top of the gradient and topped up with 1X HSB. The positions of the interfaces were marked on the centrifuge tube. The tubes were immediately spun for 8 h at 20 000rpm at 4°C in a Beckman SW40Ti swinging bucket rotor. The sample tubes were carefully removed and placed in a clamp on a ringstand apparatus in a hood. If enough sample was loaded onto the gradient, a faint viral band slightly above the position of the original heavy/light interface could be seen.

To harvest the virions, 18-gauge needles attached to 5 mL syringes were gently inserted into the tube both at a position just below the original heavy/light interface, and 1 cm from the bottom of the tube. Routinely, both the “band” fraction, containing mostly empty particles, was collected (~2 mL), together with a 2 mL fraction positioned at the “bottom” of the tube, containing mostly infectious particles. Both fractions were loaded into individual Amicon Ultra-4 filter devices (100 000 kDa MWCO, Milipore) to remove the CsCl and to concentrate the PsVs. The filters were spun down at 3000 rpm for 10 min, washed with 1X HSB and spun again until the PsVs were concentrated down to approximately 100 µL and stored at -80°C in low binding Eppendorf tubes.

2.4.5 Quality checks of the HPV-PsVs preparations

Each HPV-PsVs preparation underwent the following quality checks (Sections 2.4.5.1 to 2.4.5.4).

2.4.5.1 SDS-PAGE and Silver Stain

10% SDS-PAGE gels were prepared following standard procedures, were loaded with 3 µL denatured HPV-PsVs and were run at 150 V for approximately 1 h. For AF488-labelled PsVs, the SDS-PAGE gel was imaged using the iBright FL1000 fluorescent imager (Invitrogen) prior to staining. The gels were stained using the Pierce™ Silver Stain kit (Thermo Scientific) to assess the purity of the HPV-PsVs. Good quality HPV-PsVs will have clearly defined bands

for the L1 and L2 proteins of the correct size (roughly 55 and 70 kDa respectively, depending on the HPV type), and with little to no contaminant proteins.

2.4.5.2 HPV infection and neutralisation assay

Infectability of the HPV-PsVs were tested using HeLa cells, along with neutralisation assays using antibodies against the various HPV types to determine specificity and quality of the virions. These antibodies were sourced from Neil Christensen (Penn State Cancer Institute, USA) and are primarily type-specific and bind to surface exposed conformational loops (251). HeLa cells were seeded a day prior in a 96-well plate at 5000 cells in 100 µL cDMEM per well. In low protein binding Eppendorf tubes, 0.5 µg PsVs were incubated for 1 h on ice with 0.5 µg of the specific antibody (e.g., HPV16-PsVs with an HPV16 antibody) or an antibody specific for a different type of HPV (e.g., HPV16-PsVs with an HPV18 antibody). The preincubation mixtures were added to the plated HeLa cells, along with an HPV-only positive control and a cell-only negative control. Luciferase activity was assessed 48 hpi using a GloMax® Explorer Multimode Microplate Reader (Promega), following the Pierce™ Gaussia Luciferase Flash Assay Kit (Thermo Scientific) as follows: For each well, freshly prepared Reaction solution was used, which consisted of 0.5 µL of Coelenterazine in 50 µL of Gaussia Flash Assay Buffer. This solution was injected into each well, and the luminescence signal was measured using a 2 sec lag time and a 10 sec integration time.

2.4.5.3 Negative-stain electron microscopy

Negative-stain electron microscopy was employed to visualise the structure of HPV16-PsVs, at a final concentration of 0.1 µg/µL. A 3 µL aliquot of purified HPV16-PsVs was applied to a glow-discharged copper grid coated with carbon (Agar Scientific) for a duration of 30 sec. Following this, the grid was rinsed with two drops of deionized water and stained using two drops of a 2% aqueous uranyl acetate solution (SPI Supplies). The air-dried grid was subsequently examined under a Philips Tecnai F20 transmission electron microscope, which was equipped with a field emission gun operating at 200 kV. Image capture was facilitated by a Gatan US 4000 4kX4k charge-coupled-device (CCD) camera utilizing the Digital Micrograph software suite.

2.4.5.4 Protein quantification by BCA

The Pierce™ BCA Protein Assay (Thermo Scientific) was used to quantify the protein concentration of the HPV-PsVs. Following the manufacturer's instructions, the concentration of the HPV-PsVs ranged from 0.1 to 1.0 µg/µL. 1 ng of HPV-VLPs (-PsVs) consists of

approximately 30 million particles (252). In this study, cells were infected at an HPV-PsVs concentration of 2-4 pg/cell (60 000 to 120 000 particles per cell. For each assay, the HPV-PsVs concentration is stated.

2.5 Experiments with SP-A opsonised HPV-PsVs

Unless otherwise stated, HPV-PsVs were opsonised with SP-A (see Section 1.9) or the control protein BSA by preincubating the viral particles with SP-A (or BSA) at room temperature for 1 h in 2 mL low protein binding Eppendorf tubes at a 1:10 PsVs to SP-A (or BSA) ratio, in the presence of 5 mM sterile filtered $CaCl_2$, before using them in *in vitro* assays (19). Preincubation volumes were kept as low as possible to prevent dilution of the medium, with a maximum preincubation volume of 7 µL added to wells of 96-well plates, and preincubation volumes of 15 and 20 µL for 12- and 6-well plates, respectively.

2.5.1 Assessing HPV-PsVs internalisation with flow cytometry (FACS)

To assess viral binding and internalisation by flow cytometry, cells were plated in triplicates in 1 mL complete media in 12-well plates at a density of 100 000 cells/mL. The cells were grown overnight, unless differentiated from THP-1 cells (see Section 2.2).

AF488-labelled PsVs were preincubated with SP-A (or BSA) at a 1:10 (w/w) ratio for 1 h at room temperature and added to the cells for 1 h at 37°C before lifting with trypsin-EDTA or lidocaine-EDTA. Cell suspensions were harvested in Eppendorf tubes and spun at 750 g at 4°C for 3 min. Cell supernatants were aspirated, and the cell pellets were resuspended in cold FACS wash and transferred to a clear 96-well V-bottom-shaped plate (Thermo Scientific). The plate was spun at 750 g at 4°C for 2 min to pellet the cells which were washed again with FACS wash, before being pelleted again and resuspended in 100 µL FACS fix. The fixed cells were transferred to FACS tubes (BD Falcon) and kept shielded from light on ice until acquisition.

Cells were acquired using a BD LSRFortessa™ Cell Analyser using the BD FACSDiva software in the AF488 channel. Acquisition parameters were set up using an unstained negative control and stained positive control. The cell population was defined by setting the threshold for forward scatter at 5000 to exclude cell debris and 30 000 gated events were acquired per sample. The FlowJoTM software (v10.7.2) was used for post-acquisition analysis. Singlets were gated using a dot plot of the forward scatter height (FSC-H) vs area (FSC-A). The cell population was gated using a dot plot of side scatter (SSC) versus FSC-A. The AF488 positive threshold was set using a dot plot of FSC-A and AF488 of the uninfected

cells (Supplementary Figure 2). This gating strategy was applied to all acquisitions of the same cell type, providing % AF488 (HPV) positive cells.

2.5.2 Immune and epithelial cell co-cultures

A direct cell-to-cell co-culture system was utilised, where HaCaT cells were chosen as the infectible epithelial cell line, and RAW264.7, THP-1 and THP-1-derived immune cells were co-cultured with the HaCaT cells at various ratios.

Co-culture experiments were conducted in 96-well plates, unless stated otherwise. Briefly, HaCaT cells were plated at a density of 5000 cells per well in cDMEM. Immune cells were plated with the HaCaT cells with the following cell numbers: 500, 1000, 5000, 10000 to achieve the approximate epithelial cell to immune cell ratios of 10:1, 5:1, 1:1 and 1:2, respectively. The cells were grown overnight before subsequent infection with HPV-PsVs. Cells were infected with 0.1 µg HPV-PsVs opsonised with 1 µg SP-A or the BSA control.

The Pierce™ Gaussia Luciferase Flash Assay Kit was used for the detection of Gaussia luciferase as a proxy for infection, as described in Section 2.4.5.2.

Carboxyfluorescein succinimidyl ester (CFSE) was used to stain live cells following the manufacturer's instructions (Molecular Probes). Briefly, cells were washed with PBS and then resuspended in 5 µM CFSE in 100 µL PBS. After incubation at room temperature for 5 min, the cells were washed 3 times with PBS to remove any unbound dye and lysed with 100 µL 3% Triton X100. The lysates were transferred to a black 96-well plate. The staining efficiency and viability of the cells was evaluated by measuring fluorescence at 475 nm excitation and 520 nm emission with a Glomax Explorer. CFSE-labelled cells were found to be highly viable and showed a bright, stable fluorescence signal compared to unstained controls. This allowed for the monitoring of cell viability and served to normalise infection levels to live cells (253).

2.5.3 Confocal microscopy

To investigate the uptake of HPV16-PsVs in and around cells following preincubation with either SP-A or BSA, fluorescent and confocal microscopy was performed at the African Microscopy Initiative Imaging Centre at the University of Cape Town. Cellular uptake into HaCaT epithelial cells and RAW264.7 murine macrophages was assessed at 3 hpi, while lysosomal uptake and accumulation of HPV16-PsVs was determined at 8 hpi.

2.5.3.1 Sample preparation

75000 HaCaT or RAW264.7 cells were plated in 12-well plates containing sterile square coverslips (22 X 22 mm, Marienfield Superior) and grown overnight. For each cell type, an experimental condition (HPV16-PsVs + SP-A), and a control condition (HPV16-PsVs + BSA) was plated in duplicate. AF488-labelled HPV16-PsVs were preincubated with SP-A or BSA in the presence of 5 mM $CaCl_2$ for 1 h at room temperature using the optimal HPV:SP-A w:w ratio of 1:10, as previously described (19). Per well, the preincubations consisted of 0.2 µg HPV16-PsVs and 2 µg SP-A (or BSA).

To compare uptake and particle distribution, the HPV preincubations were added to the cells for 3 h, followed by gentle washing with warm PBS and fixing with 2% paraformaldehyde (PFA) for 5 min at 37°C. The cells were washed again and stained with Hoechst 33342 (Thermo Fisher Scientific) for 5 min at RT at a final concentration of 5 µg/mL in PBS. The cells were gently washed and mounted on Lasec Superior Clear Scan microscope slides (76 X 26 X 1.1 mm) with mounting medium (Invitrogen). The mounting medium was allowed to dry overnight at RT before imaging or for long-term storage at 4°C protected from light. For this experiment, an unstained control was made in parallel to determine the baseline fluorescence or background signal in the green channel.

To assess lysosomal accumulation at 8 hpi, the HPV preincubations were added to the cells for 7 h, followed by live staining with LysoTracker™ Deep Red (Thermo Fisher Scientific) in warm cDMEM for 1 h at 37°C at a concentration of 50 nM for HaCaT cells, and 75 nM for RAW264.7. Cells were gently washed with warm PBS before fixing, staining with Hoechst 33342, and mounted as described above. For this experiment, a LysoTracker only and HPV only control was prepared in parallel to determine the baseline fluorescence or background signal of each fluorochrome.

2.5.3.2 Image acquisition

Imaging was performed on a Zeiss LSM 980 with Airyscan 2 confocal laser scanning microscope (Carl Zeiss AG, Germany). Single stains were used to assess the background fluorescence of each channel and acquisition settings were adjusted accordingly. Image acquisition settings were kept constant for all samples. For acquisition, 25 fields of view each for the SP-A and BSA control wells were imaged with a 63x oil immersion objective (1.4 NA) with the emission spectra set to 410-440 nm, 499-529 nm, 567-617 nm and 659-759 nm for Hoechst 33342, AF488-HPV16-PsVs, and LysoTracker™ Deep Red, respectively. The 405 nm, 488 nm, and 639 nm lasers were used to excite Hoechst 33342, AF488-HPV16-PsVs, and LysoTracker™ Deep Red, respectively. Transmitted light images were also captured for the 3 hpi experiment in order to visualise the perimeter of the cell.

1 X sampling was utilised during imaging to ensure accurate representation of specimen details. Pixel size of the image was calculated to be 16.57 µm X 16.57 µm based on the microscope's calibration. Images were acquired at a 16-bit depth to ensure high fidelity in capturing fluorescence intensity variations within samples.

For image acquisition, a scan speed of 6 frames per second was maintained throughout the experiments. Mean averaging was applied with a factor of 4 to reduce noise in the acquired images. Zoom or cropping was not employed in these acquisitions to preserve the true magnification. The magnification for images captured using the 63X objective was calculated as 63 X 10 (for eyepieces) X 1 (no zoom factor). The master gain settings were adjusted individually for each channel as follows: blue – 700 V, green – 590 V, red – 650 V. Laser intensity for each channel was individually optimised for the 3 hpi and 8 hpi series of stains: The 3 hpi experiments used laser intensities set at 0.4% for the 405 nm laser and 2% for the 488 nm laser. The 8 hpi experiments used laser intensities set at 0.3% for the 405 nm laser, 0.3% for the 488 nm laser, and 2.5% for the 639 nm laser. Z-stack intervals were set at 1 µm and a total of 5 slices were acquired.

Chromatic shift, also known as chromatic aberration, occurs when different wavelengths of light do not focus at the same point within the microscope. This phenomenon can lead to misalignment between the images acquired in different channels, resulting in a shift in the location of objects or structures when imaging in multiple channels. Chromatic shift is especially relevant when using multiple fluorophores with varying emission spectra, and it is critical that this is compensated for in colocalisation analyses. To correct for chromatic shift when capturing the blue, green and red channels (i.e., to ensure that all channels were focussed to the same point), we used the calibration MultiSpec™ bead sample (ZEISS). Images of the beads were captured using the same acquisition settings used for the experiment. The necessary transformation was determined as described in Section 2.5.3.3.

2.5.3.3 Image analysis using Fiji (Image J)

Fiji (ImageJ2, v2.14.0/1.54f) was used to perform the particle and colocalisation analyses. To analyse particle occurrence and size, maximum intensity projections were made from the z-stacks, where the cell border was outlined using the transmitted light channel so that only bound or intracellular particles were analysed (see Section 3.5).

To use the “Analyze particles” function, a threshold for the green channel (HPV particles) was set based on the unstained cells control. The lower upper threshold values for the green channel for both HaCaT and RAW264.7 cells (3900-65535 and 2500-65535, respectively)

were manually set and kept constant. The number of cells in the image, the number particles per cell detected, and the area of each particle were recorded.

To calculate the transformation necessary to compensate for chromatic shift, three images of the beads were loaded into Fiji and maximum intensity projects made. The Align.ijm macro script was run to align the green, red and blue channels of the beads. The calculated transformation was saved as a .csv file to be later applied to all experimental images.

For the experimental images, maximum intensity projections were made, and the transformation described above was applied. For each channel (nuclei, HPV and lysosomes) the appropriate threshold was applied to segment the objects of interest. The lower and upper threshold values for the green channel for both HaCaT and RAW264.7 cells (1250-65535 and 811-65535, respectively) and the red channel (2250-65535 and 5010-65535, respectively) were manually set and kept constant to separate the signal from the background by using the single-stained controls.

The “JACoP” (Just Another Colocalisation) plugin (v2.1.4) was used to assess the colocalisation of HPV in lysosomes. The overlap coefficient, Pearson’s correlation coefficient and Manders’ coefficient were recorded to quantify the degree of colocalisation between the red and green channels (lysosomes and HPV, respectively) (254).

2.5.4 Assessment of immune modulatory proteins

Levels of immune modulatory proteins were assessed for THP-1 monocytes and naïve dendritic cells (DC0) using the Proteome Profiler™ Human XL Cytokine Array Kit (R&D Systems, cat: ARY022B). This is a membrane-based antibody array for the parallel determination of the relative levels of selected human cytokines, chemokines and growth factors.

250 000 THP-1 and DC0 cells were plated (in parallel) in 1 mL cRPMI in 12-well plates and cultured overnight. The next day, the cells were treated with the following conditions; one well of each cell type was left untreated to determine baseline cytokine levels; one well of each cell type received HPV16-PsVs preincubated with BSA (as described in Section 2.5); one well of each cell type received HPV16-PsVs preincubated with SP-A (as described in Section 2.5); and one well of each cell type received SP-A without HPV which had been incubated exactly as the two previously mentioned conditions. The cell supernatants were harvested 24 hpi and centrifuged at 500 g for 5 min to remove cells and debris and then used immediately for the protein arrays, following the kit's instructions using the supplied buffers and reagents. First,

the membranes were incubated in blocking buffer for 1 h at RT with gentle shaking, followed by incubation with 500 µL cell supernatants in 1000 µL blocking buffer overnight at 4°C with gentle shaking. The membranes were then washed three times with washing buffer for 10 min on a shaking platform. After washing, the membranes were incubated with 1.5 mL diluted Detection Antibody Cocktail for 1 h at RT with gentle shaking, followed by washing. The membranes were then incubated with 2 mL of 1X Streptavidin-HRP Reagent for 30 min at RT with gentle shaking, followed by washing. Finally, each membrane was laid on a trimmed plastic sheet protector, covered with 1 mL of Chemi Reagent Mix and incubated for 1 min. Excess reagent was removed from the membranes which were then imaged using an iBright FL1000 imager (Thermo Scientific) for 1-10 min on the chemiluminescent setting. The images were exported and analysed using the recommended in-house software, QuickSpots (Western Vision) which aligns the spot array template for this specific kit over the images of the membrane and calculates the pixel density at each site. The fold changes in cytokine expression were calculated and reported as changes relative to the pixel densities for the untreated membrane.

The Search Tool for the Retrieval of Interacting Genes/Proteins (STRING, v12.0) was used to explore protein interactions in our expression data. STRING integrates data from various sources, including experimental studies, computational predictions, and databases, to create a comprehensive network of interactions between proteins and is available at https://string-db.org.

2.6 Statistics

In the statistical analysis of the data, a one-way analysis of variance (ANOVA) was employed to assess the significance of differences among multiple groups. To further examine pairwise comparisons between individual groups, Dunnett's multiple comparison test was applied. Additionally, a two-way ANOVA was performed to investigate the influence of two independent variables on the dependent variable. In this analysis, the main effects of the two factors as well as their interaction were examined. To determine significant differences in pairwise comparisons within the two-way ANOVA, the Sidak multiple comparison test was employed. All calculations were performed with Graph Pad Prism (Version 9).

3 Results

Despite the availability of highly effective HPV vaccines, many people especially those living in LMIC, have limited access. We therefore see a need to explore alternative methods of protection against HPVs, such as stably incorporating HPV-targeting molecules into cost effective and easily accessible topical microbicides. SP-A has been widely identified as an immune opsonin, and we have previously shown its antiviral effects on HPV16-PsVs infection both *in vitro* and *in vivo* mouse models (19). As a continuation of previously published work from our laboratory which included my MSc thesis, we investigated the immune modulatory effects of SP-A in human cells, and its ability to affect infection of multiple oncogenic HPV types. In addition, we further characterised the immune mechanisms associated with SP-A mediated modulation of HPV-PsVs infection on a cellular and molecular level.

3.1 Development of an immune cell panel derived from THP-1 cells

Studying the response to HPV infection within the context of innate immune cell interactions holds significant implications for understanding the immune system's first line of defence in combatting papillomavirus infections, particularly in light of HPV's various strategies to avoid immune recognition (see Section 1.4). The immune cell panel selected for this assessment, encompassing monocytes, resting macrophages (M0) as well as M1, M2a, M2c macrophages, and immature dendritic cells (DC0), offers a comprehensive view of the various responses of innate immune cells during HPV infection. Each of these immune cell types plays distinct roles in the immune response, contributing to a collective defence mechanism against viral threats. Monocytes serve as initial responders, facilitating the recruitment of immune cells to the infection site. Resting macrophages serve as a crucial initial defence and can transition into different functional states based on the cues they receive from the surrounding tissues and the type of immune response required. M1 macrophages exhibit pro-inflammatory properties, aiding in viral clearance and tumour regression, while M2a and M2c macrophages are associated with anti-inflammatory and tissue repair functions, respectively (255). Immature dendritic cells are critical for antigen presentation and the initiation of adaptive immune responses (see Section 1.1.1). The presence of SP-A adds another layer of complexity, as it has been shown to modulate innate immune responses. Investigating how each immune cell subset responds to HPV infection, both in the absence and presence of SP-A, promises to unveil nuanced insights into the orchestrated immune reactions and their potentially modulatory effects. Such knowledge could pave the way for tailored immunotherapeutic strategies aimed at enhancing the immune system's ability to recognise and control HPV infection and related diseases, like cervical cancer.

The human leukaemia monocytic cell line, THP-1, was used as the basis for developing a human immune cell panel. The accessibility, reproducibility, and the established research on THP-1 stimulation made it an obvious candidate (255). THP-1 cells can be differentiated into macrophages or DCs under specific conditions; but while they are frequently used to produce these specialised immune cells, it is important to note that a diverse array of published protocols exists, each offering distinct strategies to modulate their differentiation behaviour. These protocols often vary in terms of differentiation agents, culture conditions, and stimulation cues, resulting in a range of phenotypic outcomes. For this project, a meticulous approach was taken in selecting a protocol that strategically combined elements from various existing methods. The herein established protocol consistently led to distinct immune cell phenotypes, where THP-1 cells have provided a valuable *in vitro* system to investigate the plasticity and diverse functions of innate immune cells (Figure 9).

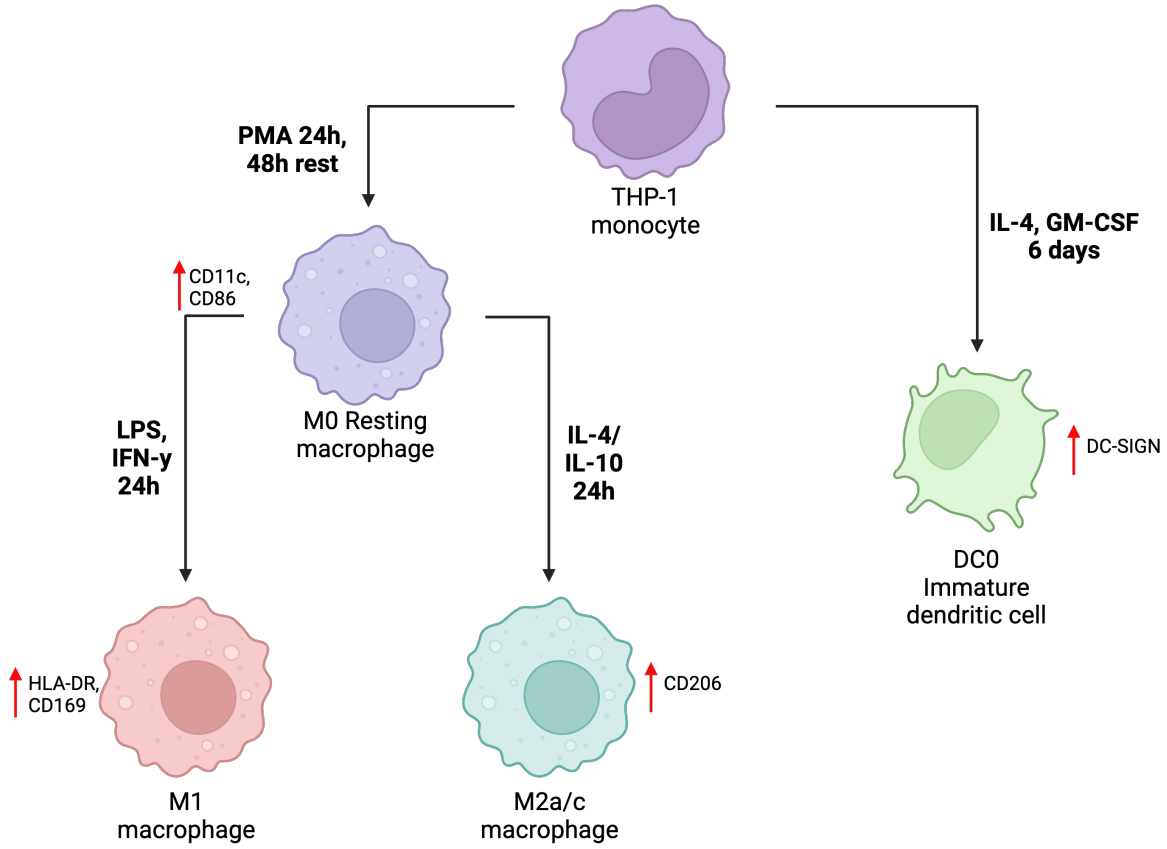

Figure 9: Differentiation scheme of THP-1 cells to produce the immune cell panel. Indicated are the expected changes that were observed in the selected surface marker expression patterns. Made with BioRender.com.

The most common way to differentiate THP-1 cells into resting M0 macrophages is by treatment with PMA followed by a necessary rest period, which has been shown to activate protein kinase C and induces a signalling cascade that leads to the differentiation of monocytes into adherent macrophages (255, 256). At this stage of the differentiation process,

the cells transition from the small round phenotype of the suspension THP-1 cells, to larger, more granular adherent cells (Figure 10A and B).

It is also possible to further differentiate M0 macrophages into M1, M2a, and M2c subtypes by additional treatment with specific cytokines and/or ligands. M1 polarisation can be induced by treatment with IFN-γ or LPS, while M2a and M2c polarisation can be induced by treatment with IL-4 or IL-10, respectively (255, 257, 258). Other than exhibiting a slight increase in granularity and a higher frequency of spindle-shaped cells, these cells looked relatively similar to the resting phenotype (Figure 10C-E). Differentiation of THP-1 cells into immature DCs can be achieved by treatment with GM-CSF and IL-4 (245, 246), where after stimulation, the cells remained in suspension but become more ruffled and granular (245) (Figure 10F). The THP-1 and THP-1 derived immune cells are from here on collectively termed the immune cell panel or ICP.

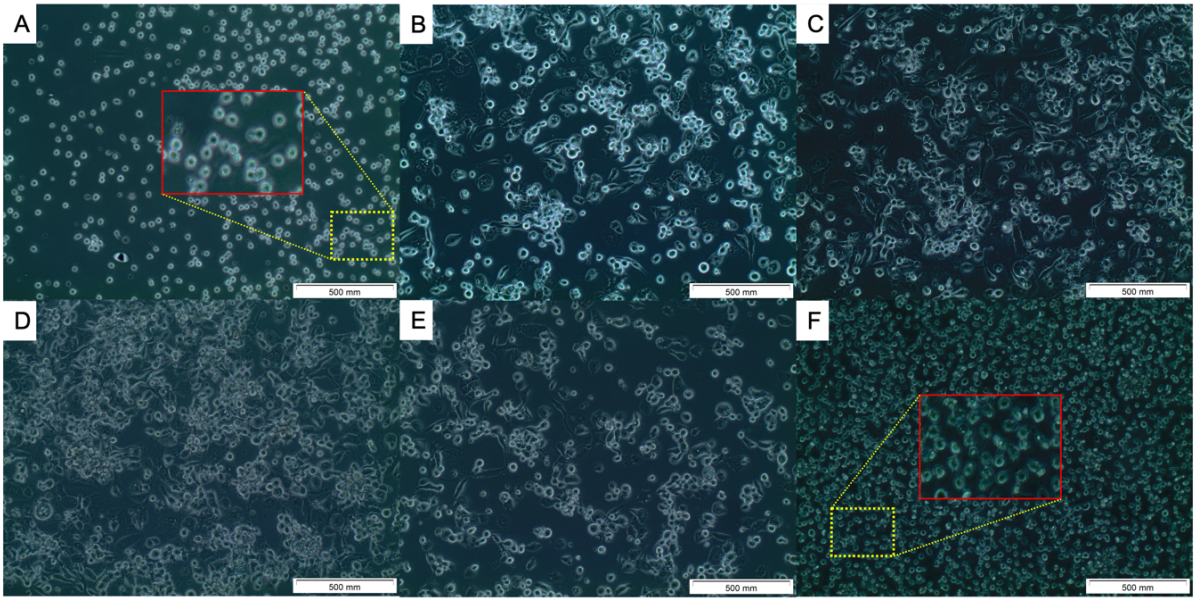

Figure 10: Representative brightfield images of THP-1-derived immune cells in culture. Briefly, THP-1 monocytes were treated with 10 ng/μL PMA for 24 h followed by culture with fresh media for 48 h to produce M0 macrophages. M0 macrophages were treated with stimulating factors (see Section 2.2) for further differentiation. **A.** THP-1 monocytes, **B.** M0 macrophages, **C.** M1 macrophages, **D.** M2a macrophages, **E.** M2c macrophages, **F.** immature dendritic cells. Shown are images taken at 20X magnification.

Flow cytometry can give an indication of the size and complexity of cells. The Forward scatter (FSC-A), which gives an indication of cell size, increases when THP-1 cells have differentiated into M0, M1, M2a and M2c macrophages (241, 242) (Figure 11A-B). Cell size slightly decreased when M0 macrophages were stimulated to an M1 phenotype, as observed previously by Forrester et al. (243). Interestingly, the size of DC0 was found to be smaller than that of the origin cell, THP-1. The Side scatter (SSC-A) gives an indication of cell surface complexity or granularity. Relative to THP-1 cells, all differentiated cell types had increased

surface complexity (Figure 11A-B), where complexity was further increased from immature macrophages to the phenotype-biased M1 and M2a / M2c macrophages. This could result from an increase in membrane-bound organelles (242).

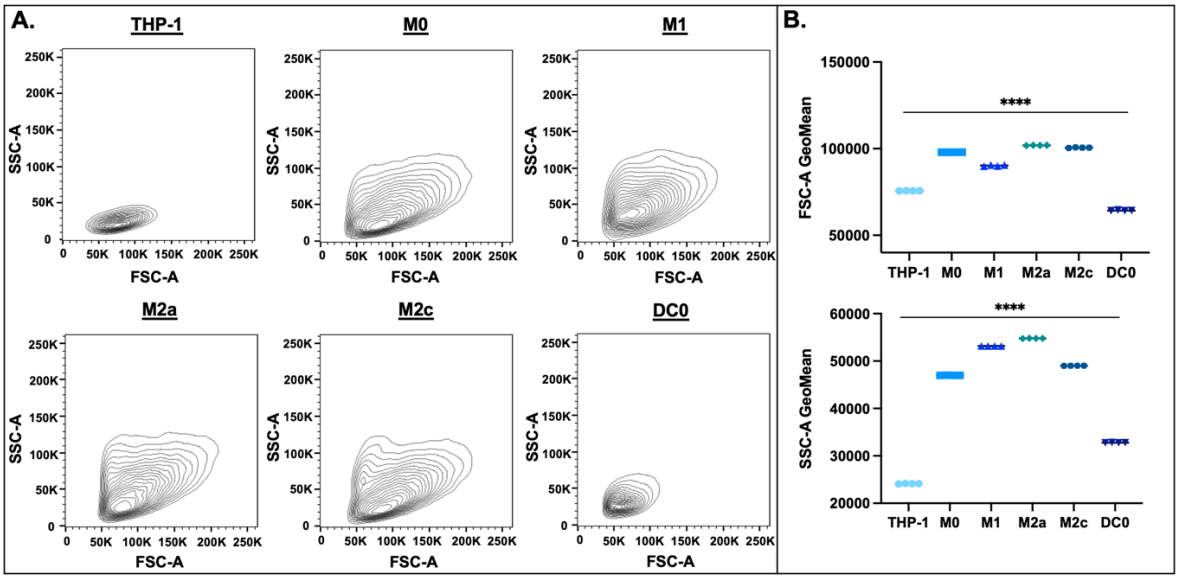

Figure 11: Flow cytometry analysis of the THP-1-derived ICP. Cells were harvested and processed as described in Section 2.2 before acquisition on a BD LSRFortessa. Depicted in **A.** are contour plots of the forward and side scatters (FSC-A and SSC-A), respectively, of the immune cells. **B.** The GeoMean of the FSC-A and SSC-A of the cells are depicted. Acquisition voltages were kept constant when acquiring the different immune cell populations. Statistical significance was determined using one-way ANOVA and Tukey's multiple comparison tests relative to the undifferentiated THP-1 cells. ****= $p<0.0001$.

The resulting macrophages and DCs should exhibit distinct functional and molecular profiles, allowing for the investigation of specific immune cell subsets in various physiological and pathological contexts (see Section 1.1.1). In order to determine successful differentiation and phenotype biasing of the THP-1-derived ICP produced, cell surface staining of selected cell-surface receptors with subsequent flow cytometry analysis was performed. A panel of 6 cell-surface markers was chosen: HLA-DR, CD11c, CD86, CD169, CD206, and DC-SIGN (243, 259, 260).

HLA-DR (Human Leukocyte Antigen-DR) is a class II MHC molecule found on the surface of APCs, including monocytes, macrophages, and DCs (261, 262). In this panel, the THP-1 monocytes and M1 macrophages had the highest surface expression of HLA-DR, with the total live cell populations being 80% positive (Figure 12) (243). All other cell type populations were approximately 30% positive for HLA-DR. **CD11c**, also known as integrin alpha X, is a cell surface protein that is primarily expressed on certain immune cells, particularly DCs and a subset of macrophages (263). An increase in CD11c positivity was observed in the M0 populations compared to the THP-1 population (264). Although CD11c is more associated with M1 macrophages, we did not see an increase in positivity in this population, nor the M2a

and M2c populations. The same observation, however has been published (243). Differentiation to DC0 led to a slight increase in the CD11c positive cell population compared to the THP-1 cells, but not to the same extent as the macrophage populations, as seen previously (245, 259, 264) (Figure 12). **CD86**, also known as B7-2, is a cell surface protein that belongs to the B7 family of co-stimulatory molecules. It is primarily expressed on APCs such as DCs and macrophages (265, 266). All macrophage phenotypes were found to have higher percentage positive CD86 populations compared to the THP-1 population, increasing from 2% to 10% (Figure 12). The DC0 population also had a greater % of CD86 positive cells compared to the THP-1 population (4.5%). **CD169**, also known as Siglec-1, is a lectin-like receptor expressed on certain subsets of macrophages and DCs (267) (260). As observed by Forrester et al. (243), no difference in CD169 expression was observed for THP-1 and M0, but after phenotype biasing to M1, there was a marked increase in CD169 positivity (Figure 12). **CD206**, also known as the mannose receptor, is a cell surface receptor primarily expressed on M2 macrophages, particularly M2a (268, 269). Indeed, the M2a and M2c populations had the highest percentage positivity for CD206 compared to the other cell populations, however, the percentage was low (6%, Figure 12). **DC-SIGN** (Dendritic Cell-Specific ICAM-grabbing non-integrin) is a C-type lectin receptor expressed on DCs and certain macrophages, particularly in mucosal tissues (270, 271). As observed previously, DC0 had the largest population expressing DC-SIGN (40%, Figure 12). Previous studies have also reported a high expression of DC-SIGN in IL-4 polarised THP-1 macrophages (272). Indeed, we also noted a higher percentage of DC-SIGN positive cells in the M2a population compared to the other macrophage populations (Figure 12). Interestingly, we also see a high percentage DC-SIGN positive population in the undifferentiated THP-1 monocytes.

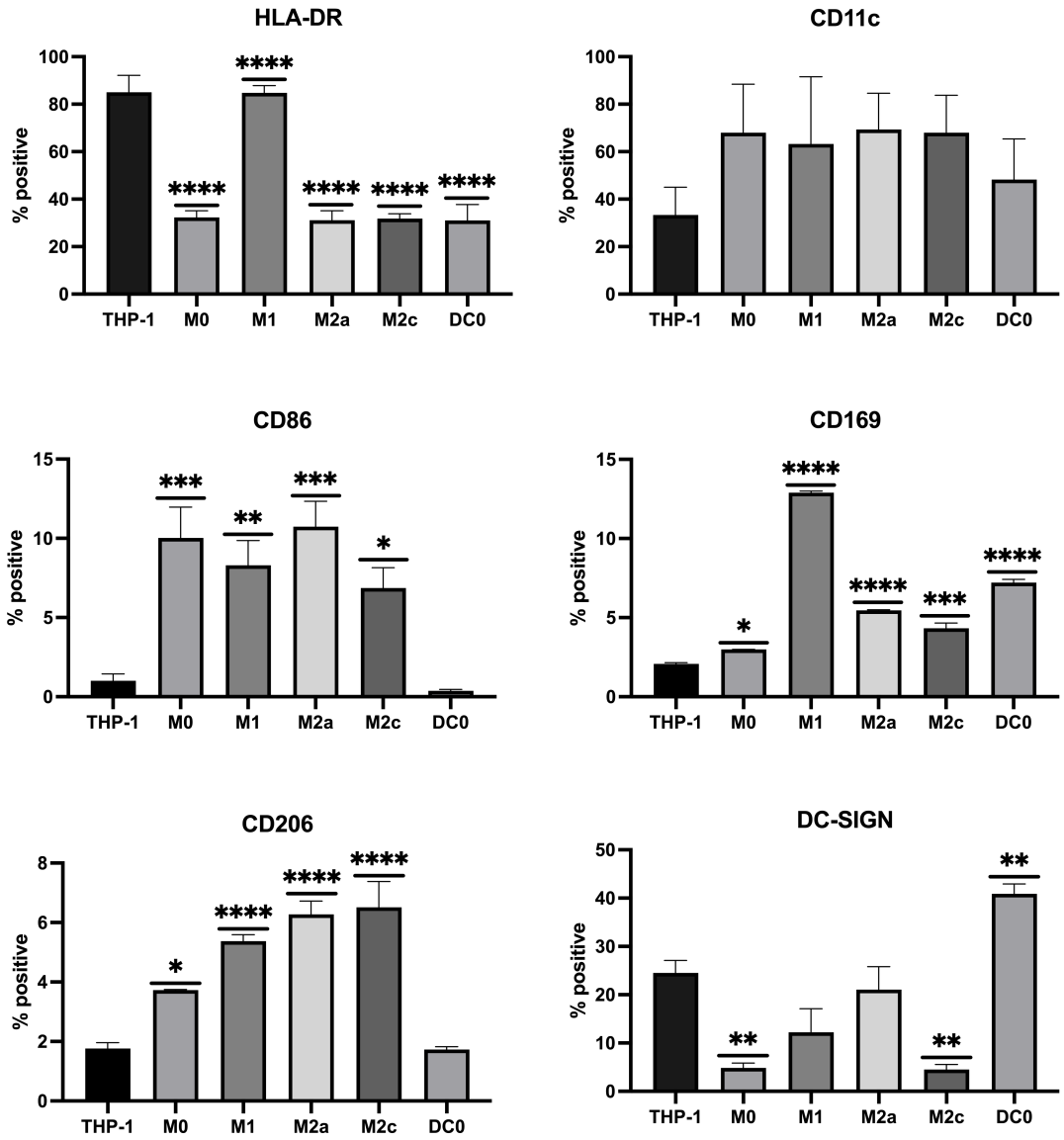

Figure 12: Cell-surface marker expression on THP-1-derived immune cells. Cells were stained as described in Section 2.2.4 before acquisition with the BD LSRFortessa. Percentage positivity relative to the whole live population for CD86, HLA-DR, CD206, CD169, CD11c, and DC-SIGN are shown. Data are from 3 independent experiments where the mean and SEM are plotted. Statistical significance was determined using one-way ANOVA and Tukey's multiple comparison tests relative to the undifferentiated THP-1 cells. *= $p<0.05$; **= $p< 0.005$; ***= $p<0.001$; ****= $p<0.0001$; no symbol denotes not significant.

In order to visualise the high-dimensional data obtained from the multi-cell, multicolour flow cytometry ICP panel as presented in Figure 12, T-Distributed Stochastic Neighbor Embedding (t-SNE) was utilised. t-SNE is a dimensionality reduction technique commonly used for visualising high-dimensional data in a lower-dimensional space. It is particularly useful for revealing underlying patterns, clusters, or relationships within complex datasets. As shown in Figure 13 several distinct cell populations, representing the different subsets of immune cells derived from THP-1 cells, were identified. The t-SNE plot shows that these subsets form distinct clusters, indicating that each group has a unique expression profile. Some cell types have multiple clusters, such as THP-1 monocytes. The presence of two or more clusters might

indicate the inherent heterogeneity within the THP-1 cell line. It is possible that the clusters correspond to different subtypes or subpopulations of THP-1 cells.

There are areas where different populations seem to overlap or where outliers from one population appear close to another, such as the M1 clusters overlapping with other macrophage types. This could indicate transitional states between populations or cells that share characteristics of multiple subsets. The overlap colours may indicate a biological gradient or continuum of states between cell populations. This is likely as the immune cells can differentiate from one type to another; and during this process, they may transiently express a combination of markers that are characteristic of both the original and the target cell types. The overlap is also as a result of populations sharing cell surface markers which are not entirely exclusive to one group (Figure 14). These cells arise from the common progenitor cell THP-1 and the markers used to define the populations are not completely specific. Some overlap may also result from technical variability inherent to the data generation or the t-SNE algorithm itself. t-SNE is a stochastic method where different runs can produce different plots.

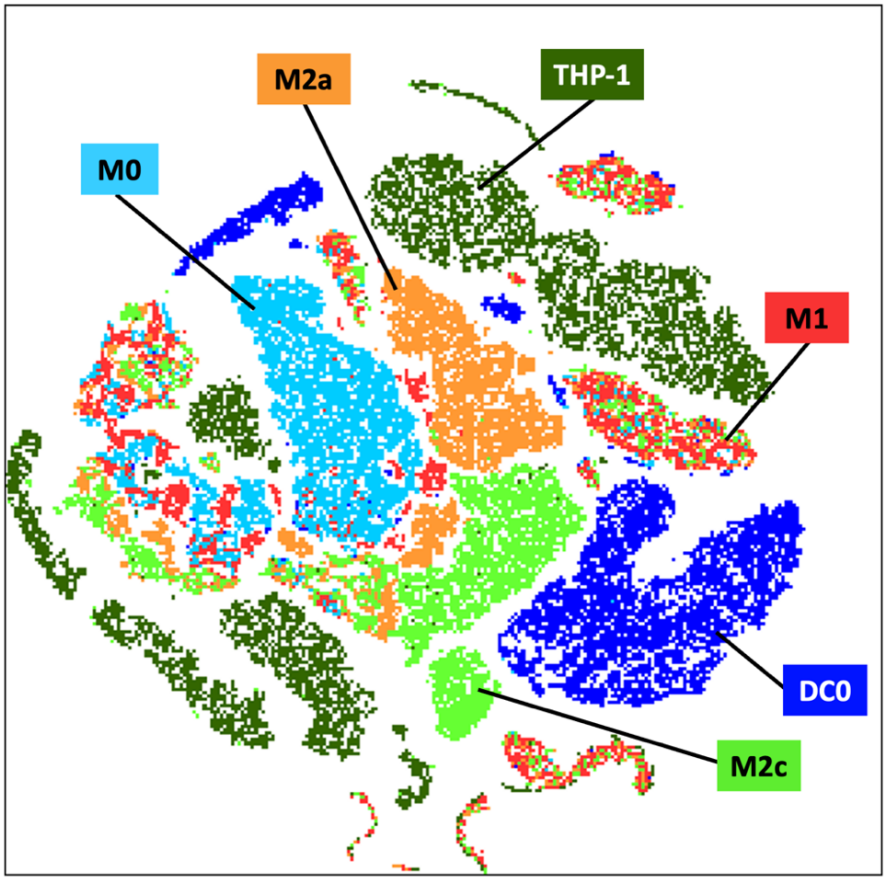

Figure 13: Phenotypic analysis of THP-1-derived immune cells using t-SNE. Dimensionality reduction and clustering analysis of flow cytometry data for the THP-1 cell derived human ICP. Distinct clusters of immune cell populations are color-coded and labelled. The tSNE algorithm was performed in FlowJo (v 10.7.2).

t-SNE was also used to visualise the expression of the cell-surface markers for each cell population, excluding CD169 due to limited antibody availability (Figure 14). High expression levels of HLA-DR (yellow-red) were observed in THP-1, M1, and DC0 cells, suggesting high antigen-presenting capability, which is typical for these cell types. The CD11c and CD86 cell markers show the highest expression in the macrophage populations, as seen with the single stain experiments (Figure 14). Their expression in M1 cells is particularly high, consistent with M1 cells' role as classically activated, pro-inflammatory macrophages. CD206 is typically expressed on M2 macrophages and involved in anti-inflammatory responses. Here, the difference in expression between M1, M2a and M2c was minimal. Further exploration using other M2 markers might be beneficial. DC-SIGN showed a strong expression in DC0 as expected. The expression in the macrophage subsets M0, M1 and M2c was lower, which is consistent with their distinct roles from DCs. M2a showed small areas of high DC-SIGN expression.

As mentioned above, the overlap in marker expression between different populations can indicate shared functions or transitional states between cell types. The intensity and distribution of colours in each plot also suggest that while there are clear distinctions between each cell type's marker expression, there is also heterogeneity within each population, which is a common finding in single-cell analyses. While these plots support the characterisation of the distinct cell types making up the herein described ICP derived from THP-1 cells, they can be valuable for understanding the functional roles of these cells in the immune system, their potential for plasticity, and how they might interact with one another in an immune response.

Taken together, this comprehensive analysis of phenotypic changes in cell size and granularity, together with the expression of a well-defined panel of markers, provides compelling evidence of the successful differentiation of THP-1 cells into the specific cell populations: M0, M1, M2a, M2c, and DC0. These phenotypic changes, in conjunction with the consistent marker expression patterns observed, affirm the accuracy and efficacy of the herein applied protocol as described in Section 2.2 in generating these distinct immune cell populations. Our findings strongly support the conclusion that the differentiation process has effectively yielded the desired cell types, laying the foundation for further studies into the functional characteristics and behaviours of these distinct cell populations in the context of the herein studied immune responses to HPV and the potential therapeutic benefits of SP-A.

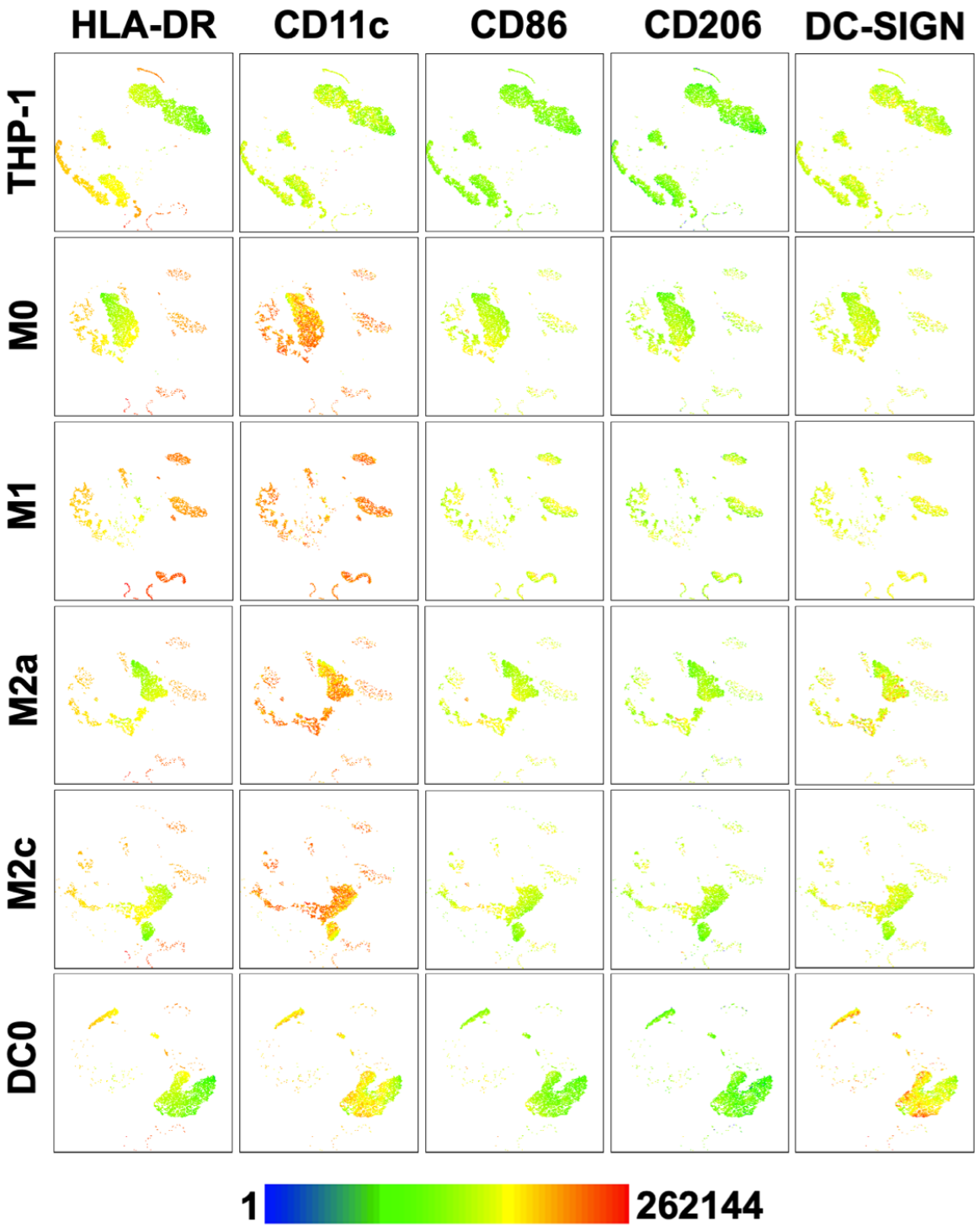

Figure 14: t-SNE analysis of THP-1-derived immune cells with marker expression heatmaps. Shown are median fluorescent intensities for selected markers in the various human immune cell populations derived from THP-1 cells. Each row corresponds to a distinct cell type, and each column represents a specific marker, revealing marker expression levels within the identified cell clusters. The colour gradient, ranging from 1 to 262144, indicates the degree of similarity or proximity between data points in the reduced-dimensional space. Higher colour intensities represent closer proximity or greater similarity among data points, while lower intensities indicate increased dissimilarity or distance.

3.2 HPV-PsVs production

To study HPV infection *in vitro*, non-oncogenic infectious HPV-PsVs were generated according to previously published procedures. The types produced for this study included HPV16, 18, 31, 45, 52, and 58 (see Supplementary Figure 3 for the plasmid maps encoding the major and minor capsid proteins of these HPV types). The type specific L1/L2 plasmids were validated by restriction enzyme digest (Supplementary Figure 1). The foundation work was performed on HPV16-PsVs, whereas the other types were chosen to validate any broad-spectrum capabilities SP-A may have. Incidentally, these types are covered by the second-generation vaccine Gardasil®9 (Merck) and represent the most common oncogenic types. All pseudovirions encapsidated a reporter plasmid representing the pseudogenome, which allowed for the quantification of infection once the pseudovirions had successfully infected cells and reached the host cell nucleus. Here, the Gaussia luciferase (GLuc) reporter plasmid pCMV-GLuc 2 was used to measure infection. Gaussia luciferase is an oxidative enzyme originally produced by the marine copepod *Gaussia princeps* and contains an internal signal peptide for extracellular secretion (273). Because this protein is secreted from the cell cytoplasm, using HPV pseudovirions encapsidating Gaussia luciferase can be beneficial for certain applications, such as time course experiments as luciferase activity can be measured directly from cell culture supernatants without needing to lyse cells (19).

Validation of the quality, purity and specificity of the produced HPV-PsVs was done before any downstream functional experiments. The mature purified particles should solely consist of the major and minor capsid proteins (L1 and L2, respectively) and the reporter genome. Once denatured, the PsVs should therefore consist of two protein bands on an SDS-PAGE gel (Figure 15). The L1 protein is roughly 55-60 kDa, and the L2 band varies in size between the different HPV types, sitting between 70 and 80 kDa. Differences between the HPV types, but also their purity, can be derived from appropriately stained SDS-PAGE gels.

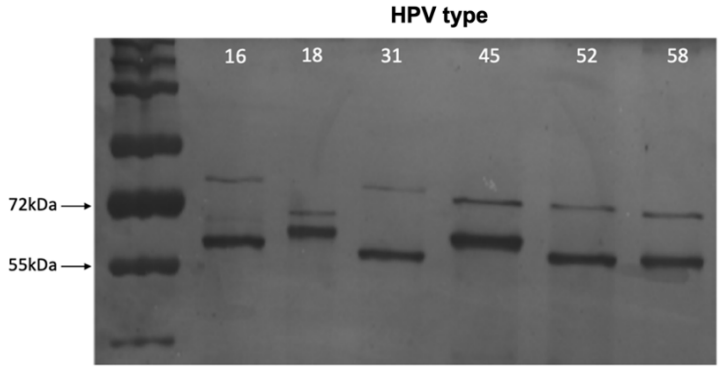

Figure 15: Representative SDS-PAGE gel of the major and minor capsid proteins for each of the HPV-PsVs types produced. The protein bands were visualised by silver stain. The lower more pronounced bands represent the L1 capsid protein, while the thinner bands above are the L2 capsid protein.

Fluorescently labelled HPV-PsVs were also used to determine viral internalisation and cell surface binding by flow cytometry and microscopy. In these experiments, Alexa Fluor 488 (AF488) was used to fluorescently label HPV-PsVs. Figure 16A shows the fluorescent labelling of both the L1 and L2 capsid proteins, and also highlights the difference in quality between the "bottom" fraction and "band" fraction that were harvested after maturation (see Section 2.4.5). The "band" fraction had visible capsid protein bands, but there were more contaminant proteins relative to the "bottom" fraction. While both fractions were of sufficient quality and purity to perform functional assays, the "band" fraction was more heterogeneous, whereas the "bottom" fraction contained uniform particles. This is made evident by negative stain electron microscopy imaging of the particles (Figure 16B). This was also evident based on infection and neutralisation assays (Figure 16C) which were performed to assess the specificity and quality of the HPV types. The "bottom" fractions consistently yielded specific neutralisation, while the "band" fractions could not be completely neutralised with the type-specific antibodies, suggesting incomplete incorporation of the Gaussia luciferase pseudogenome.

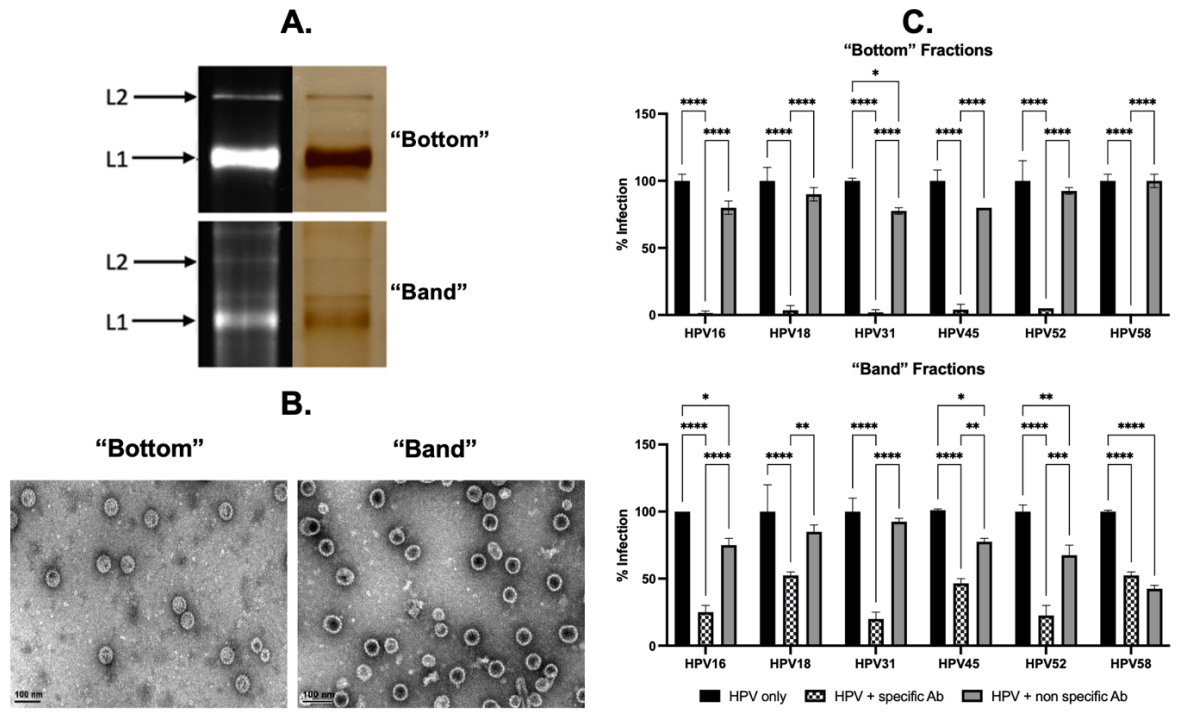

Figure 16: Qualitative comparison of the "band" and "bottom" HPV-PsVs fractions. A. Representative SDS-PAGE gel of the major and minor capsid proteins of HPV16-PsVs. Left: Fluorescent imaging of the SDS-PAGE gel to detect AF488 labelling of the capsid. Right: subsequent silver staining of the gel to visualise protein. Both "bottom" and "band" fractions harvested from caesium chloride gradients are depicted. **B.** Negative-stain electron microscopy of both HPV16-PsVs fractions. **C.** Representative infection and neutralisation assay of all oncogenic HPV-PsVs "bottom" and "band" fractions. HeLa cells were infected with either HPV-PsVs, HPV-PsVs neutralised with a specific antibody, or HPV-PsVs neutralised with an antibody against another HPV type (non-specific). Gaussia luciferase activity was used as a measure of infection. Readings shown are 48 hpi for "bottom" HPV-PsVs fractions (top) and "band" HPV-PsVs fractions (bottom). Experiments were performed in triplicate, where HPV only has been displayed as 100% infection, and other conditions are shown relative to this. Statistical significance was determined using one-way ANOVA and Tukey's multiple comparison tests. *= $p<0.05$; **= $p< 0.005$; ***= $p<0.001$; ****= $p<0.0001$; no symbol denotes not significant.

3.3 Opsonisation and agglutination of HPV-PsVs particles with SP-A

One of the main functions of SP-A is its ability to aggregate pathogens, including viral particles. Primarily, this phenomenon can facilitate the containment and immobilisation of pathogens, thereby impeding their spread and invasion into host tissues. The agglutination process can create larger complexes that are more easily recognised and engulfed by immune cells, leading to enhanced phagocytosis and subsequent degradation of the pathogens.

To investigate whether SP-A can aggregate HPV-PsVs, fluorescent images of SP-A:HPV-PsVs complexes were captured. After incubating with SP-A and $CaCl_2$ for 1 h, HPV-PsVs were observed to cluster together more prominently than in the control samples treated with BSA (Figure 17). The size of clusters and thus the extent to which SP-A agglutinated HPV varied among the types, where HPV16, 18, 31 and 52 particularly formed large complexes compared to the respective BSA controls.

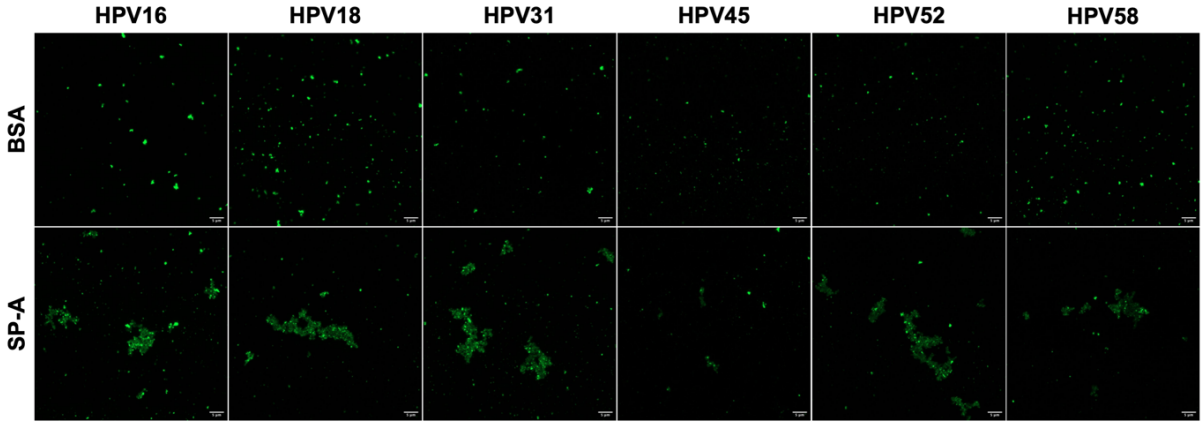

Figure 17: HPV-PsVs are agglutinated by SP-A to different extents. AF488-labelled HPV-PsVs were preincubated with SP-A or the BSA control for 1 h in the presence of 5 mM $CaCl_2$ before imaging with a Zeiss LSM 980 confocal microscope. Shown are representative images taken at the 63x objective. Scale bar = 5 µm.

3.4 SP-A enhances HPV16-PsVs uptake into immune cells but dampens uptake into epithelial cells

We have previously shown that HPV16-PsVs preincubation with SP-A results in its increased uptake into RAW264.7 murine macrophages, and innate immune cells derived from naïve mouse female genital tract tissue (19). The same approach was used to translate these findings to human innate immune cells, specifically the populations of the innate ICP described in Section 3.1, and the host keratinocyte target cells, HaCaT. Cells were infected with HPV-PsVs and processed for FACS as described in Section 2.5.2.

Previously we have only reported on the percentage of cells that were HPV positive at 1 hpi as a measure for internalisation per cell. As SP-A has the ability to aggregate the viral particles (Figure 17), we introduced another statistic: the median fluorescent intensity (MFI) of the HPV positive cells as a measure of internalisation intensity. This additional parameter provides a more comprehensive understanding of the interaction between SP-A and HPV and opens up avenues for exploring its role in viral infection dynamics and intracellular processes. Further investigation of the relationship between HPV-infected cell populations and MFI could yield valuable insights into the mechanistic aspects of SP-A's involvement in modulating viral infections.

As seen previously (19), preincubation of HPV16-PsVs with SP-A increased viral particle uptake in RAW264.7 murine macrophages, as shown by a shift in the positive fluorescent signal (Figure 7, Figure 18 and Figure 19A): the amount of HPV16-PsVs positive cells increased by about 50% in RAW264.7 for the SP-A condition, along with the MFI (Figure 19B). The higher fluorescent signal in the cells indicate a greater number of clustered viral particles which suggests that SP-A may not only influence the overall infection rate, but also potentially impact the viral load within individual infected cells. Among the human immune cell types analysed, DC0 cells showed a significant increase in uptake, while THP-1 monocytes showed a significant increase in MFI (Figures 18 and 19A). Particle uptake and/or MFI in M0, M1, M2a and M2c was not enhanced by SP-A preincubation.

Notably, the response of the keratinocyte cell line, HaCaT, to HPV16-PsVs infection yielded intriguing differences in particle uptake dynamics compared to the ICP, as a decrease in HPV16-PsVs uptake in the presence of SP-A, with a slight decrease in the MFI, was observed. Similar results were obtained with two other epithelial cell lines, HeLa and NIKS (Supplementary Figure 4).

In selecting HaCaT cells as the preferred model for further studying HPV infection, several compelling factors have been taken into consideration. Firstly, HaCaT cells offer the advantage of being non-infected by HPV, ensuring a controlled and unbiased experimental platform. This intrinsic characteristic eliminates potential confounding effects stemming from viral interactions, enabling a clear focus on the mechanisms of HPV entry, replication, and intracellular dynamics. Unlike HeLa cells, which originate from cervical cancer tissue and possess HPV genetic material, HaCaT cells lack this viral influence, allowing for a more accurate representation of initial infection events. Moreover, the choice of HaCaT cells avoids the complexities associated with studying HPV within a cancerous context. Furthermore, HaCaT cells' ease of culture compared to NIKS cells streamlines experimental procedures and accelerates research timelines. NIKS cells, while creating a keratinocyte-like environment,

necessitate more specialized culturing conditions, potentially introducing additional complexities and influencing variability in experimentation. The robustness of the HaCaT cell line, combined with its consistent growth characteristics, makes it widely used and accepted in the field to study HPV entry (100, 274-277) and is an ideal cell line to further investigate the intricate interplay between HPV and host cells. Ultimately, HaCaT cells stand as the optimal choice for unravelling fundamental aspects of HPV infection due to their non-infected status, absence of cancerous attributes, and practical suitability in experimental settings.

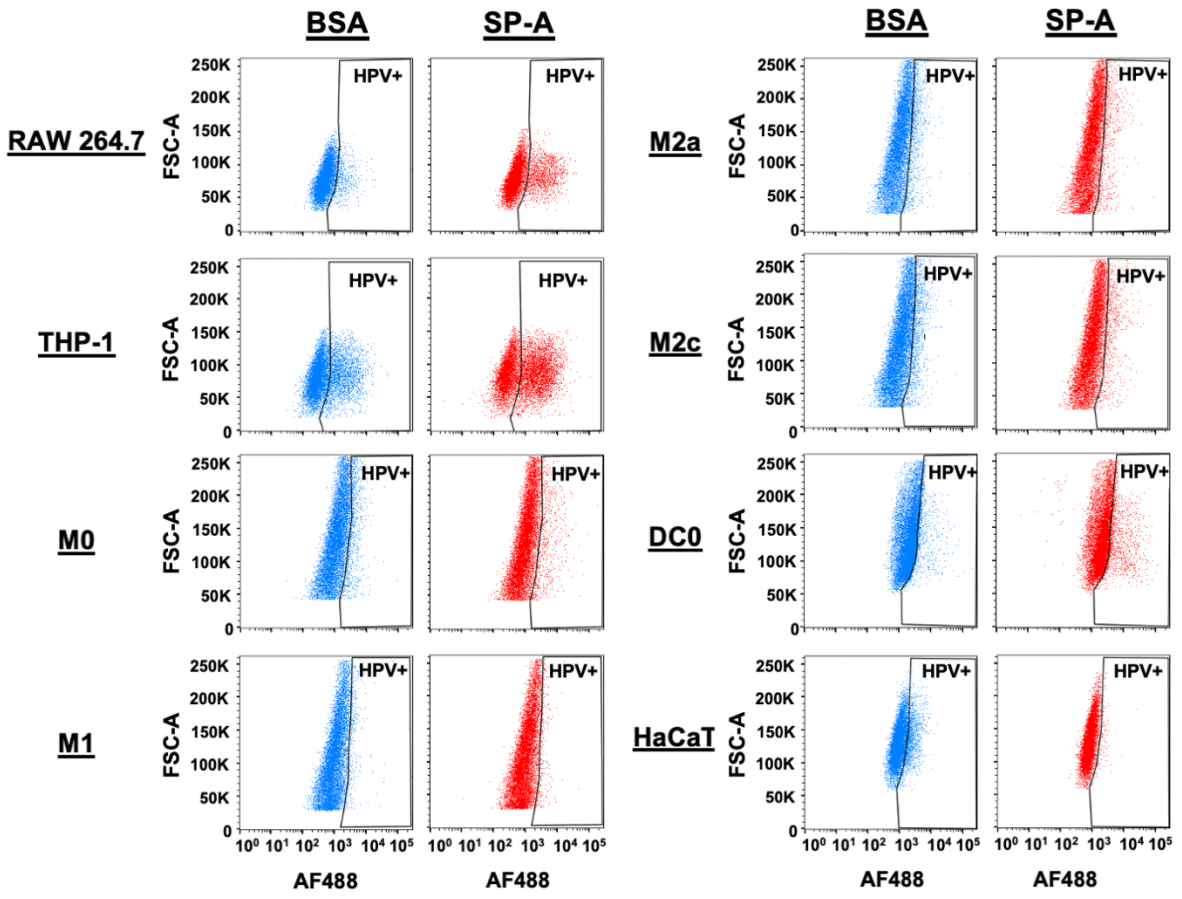

Figure 18: HPV16-PsVs uptake into various immune cells and HaCaT epithelial cells assessed by FACS. Cells were treated as described in Section 2.5.2, before acquisition with a BD Fortessa. Depicted here are dot plots for AF488-HPV16-PsVs uptake after 1 h in various immune and HaCaT cells, with the HPV positive threshold determined by the negative control (untreated cells).

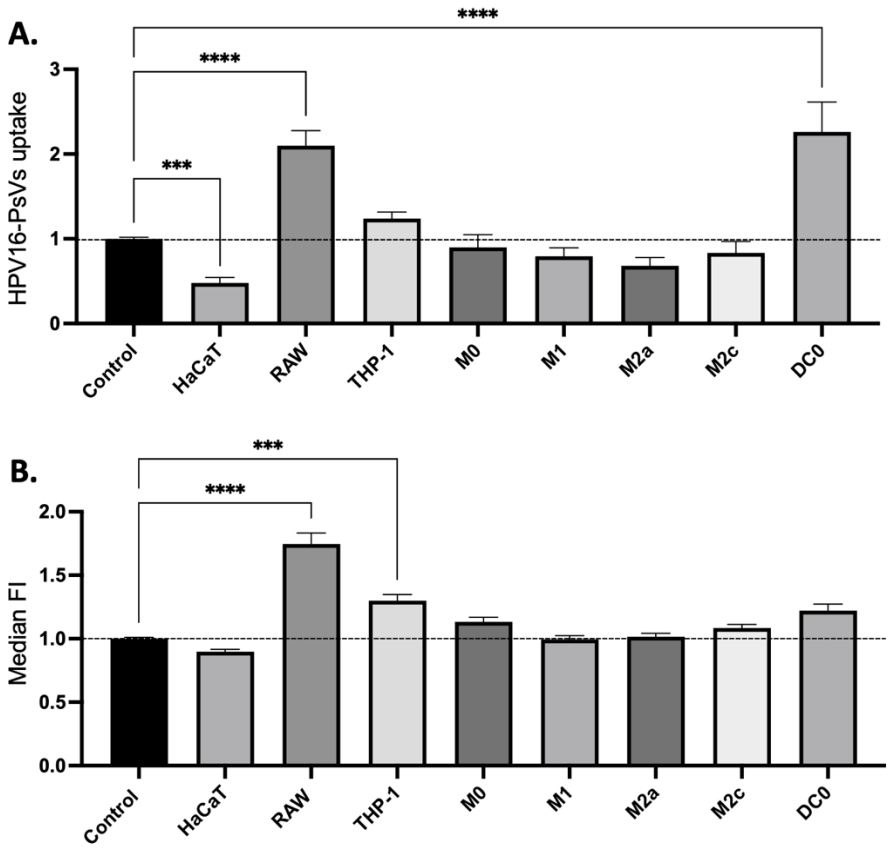

Figure 19: HPV16-PsVs internalisation into HaCaT and various immune cells is altered by preincubation with SP-A. Cells were treated as described in Section 2.5.2, before acquisition with a BD Fortessa. **A.** Fold-change of HPV16-PsVs uptake in the presence of SP-A is depicted with the BSA control set as 1. **B.** Fold-change of the median fluorescent intensity (MFI) of internalised HPV16-PsVs in the presence of SP-A is depicted with the BSA control set as 1 (indicated by the dotted line). Data of three independent experiments are presented relative to uptake of the BSA control group. Statistical significance was determined by one-way ANOVA and Dunnet's multiple comparison tests. ****= $p<0.0001$; no symbol denotes not significant.

3.4.1 Preincubation with SP-A is required for altered HPV16-PsVs uptake

Our previous work consistently applied a 1 h preincubation step of viral particles with SP-A, utilising $CaCl_2$ to facilitate particle opsonisation, before infection of target cells (19) (Figures 7 and 8). Alternative literature suggests an exposure of the target cells to SP-A for 1 h or more prior to subsequent viral infection (278). In order to determine the optimal modulation of viral entry by SP-A, internalisation experiments were performed in HaCaT and RAW264.7 cells subjected to SP-A exposure, in the presence of 5 mM $CaCl_2$, at both 1 h and 24 h prior to introducing HPV16-PsVs. Intriguingly, these conditions failed to elicit the pronounced reduction and increase in particle uptake in HaCaT and RAW264.7 cells, respectively (Figure 20). This observation underscores the essential nature of "priming" the viral particles with SP-A, particularly for modulating particle uptake during the initial stages of infection (205, 279, 280), and was therefore applied to all subsequent experiments.

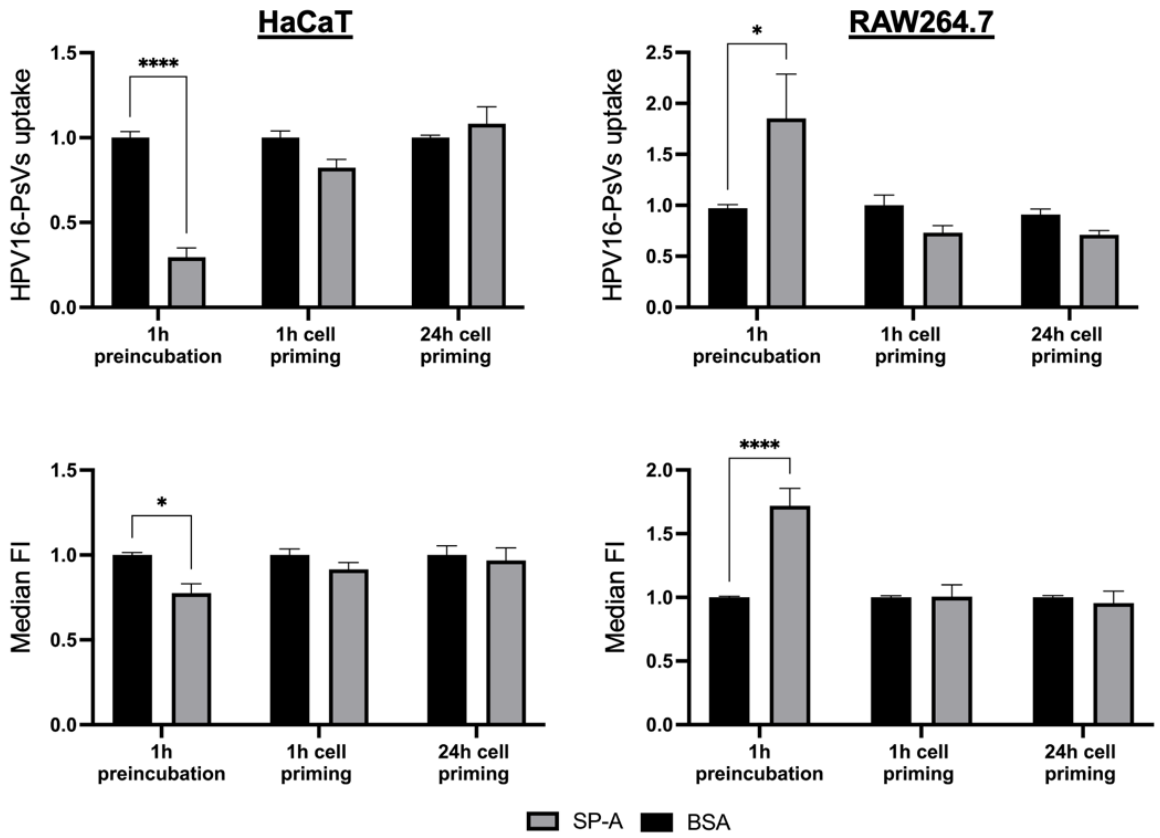

Figure 20: Assessment of HPV16-PsVs preincubation with SP-A versus SP-A priming of cells for modulation of viral internalisation. Three conditions were analysed: **1.** Preincubation of HPV16-PsVs with BSA or SP-A in the presence of $CaCl_2$ 1 h before infection; **2.** Priming of cells with BSA or SP-A in the presence of 5 mM $CaCl_2$ for 1 h prior to HPV16-PsVs infection; **3.** Priming of cells with BSA or SP-A in the presence of 5 mM $CaCl_2$ 24 h prior to HPV16-PsVs infection. All cells were harvested after 1 hpi and acquired as described. HPV16-PsVs uptake in the presence of SP-A is depicted in the top graph and the MFI of internalised HPV16-PsVs is depicted below. Data of three independent experiments are presented relative to uptake of the BSA control group which was set as 1. Statistical significance was determined using two-way ANOVA and Sidak's multiple comparison tests. *=p<0.05; ****= p<0.0001; no symbol denotes not significant.

3.4.2 Viral uptake is modulated by SP-A in HaCaT and RAW264.7 independently of HPV type

In order to assess the broad-spectrum capabilities of SP-A, we tested the uptake of a selection of oncogenic HPV types in HaCaT and RAW264.7 as well as THP-1 and DC0 cells as these were the immune cell types demonstrating a significant alteration in HPV16-PsVs uptake due to the presence of SP-A (Figure 19). Although not as pronounced as seen for HPV16, there was a significant reduction in viral particle uptake in HaCaT cells for HPV types 18, 31, and 45 in the presence of SP-A (Figure 21). Interestingly, the corresponding MFI for all tested HPV types (i.e. 16, 18, 31, 45, 52, and 58) was significantly decreased in HaCaT cells. Viral particle uptake into RAW264.7 was increased for all tested HPV types, with HPV31 displaying the greatest increase in uptake compared to other types, and HPV45 the highest MFI.

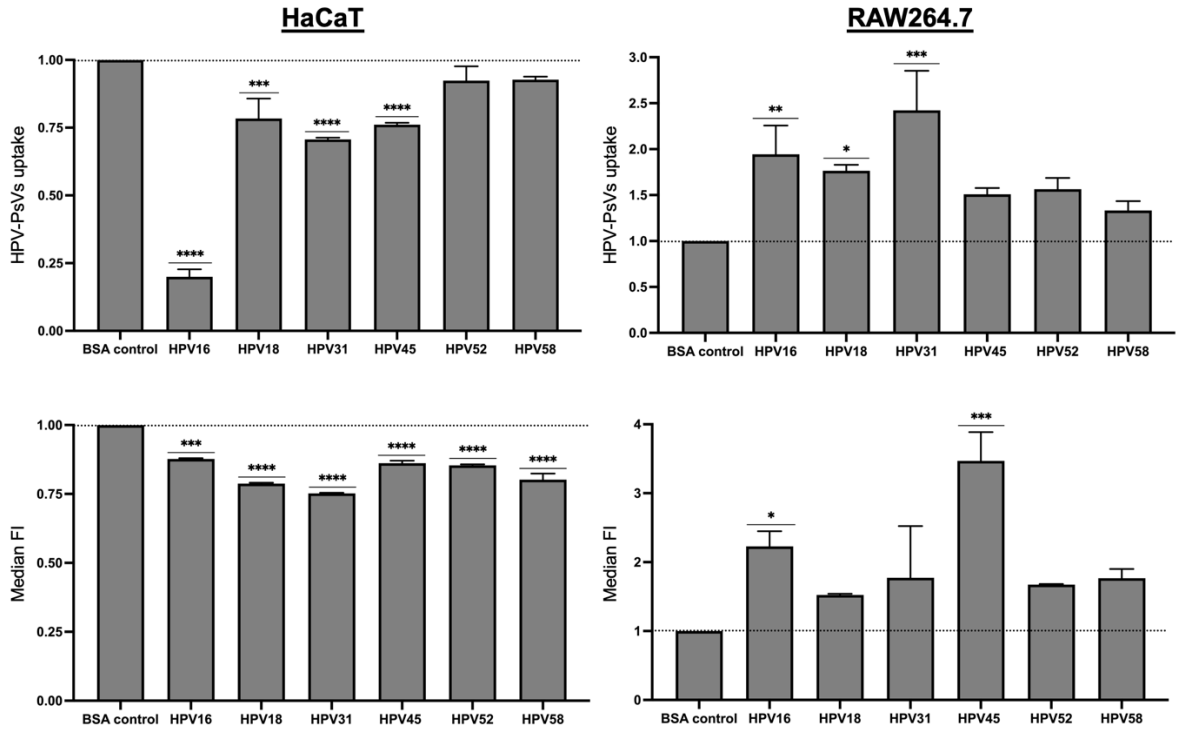

Figure 21: SP-A modulates internalisation of multiple HPV-PsVs types into HaCaT and RAW264.7 cells to varying degrees. Cells were treated as described in Section 2.5.2, before acquisition with a BD Fortessa. HPV-PsVs uptake is depicted on top and the MFI of internalised HPV-PsVs is depicted below. Data of three independent experiments are presented relative to uptake of the BSA control group which was set as 1 (indicated by the dotted line). Statistical significance was determined by one-way ANOVA and Sidak's multiple comparison tests. *= p<0.05; **= p<0.01; ***= p<0.001; ****= p<0.0001; no symbol denotes not significant.

3.4.3 SP-A affects internalisation into THP-1 monocytes and immature dendritic cells HPV type-dependently

The impact of SP-A for internalisation of different HPV types was further tested on THP-1 and DC0 cells (Figure 22). As opposed to HPV16-PsVs, particle uptake into THP-1 monocytes was not increased for any of the other HPV types tested when preincubated with SP-A. In fact, a decrease in MFI was observed for HPV types 18 and 31, although not statistically significant.

Particle uptake in the presence of SP-A in DC0 was also type-dependent and differed to HPV16-PsVs. A notable decrease in uptake for HPV18 was observed, with a decrease in MFI for HPV types 31, 45, 52, and 58 (Figure 22).

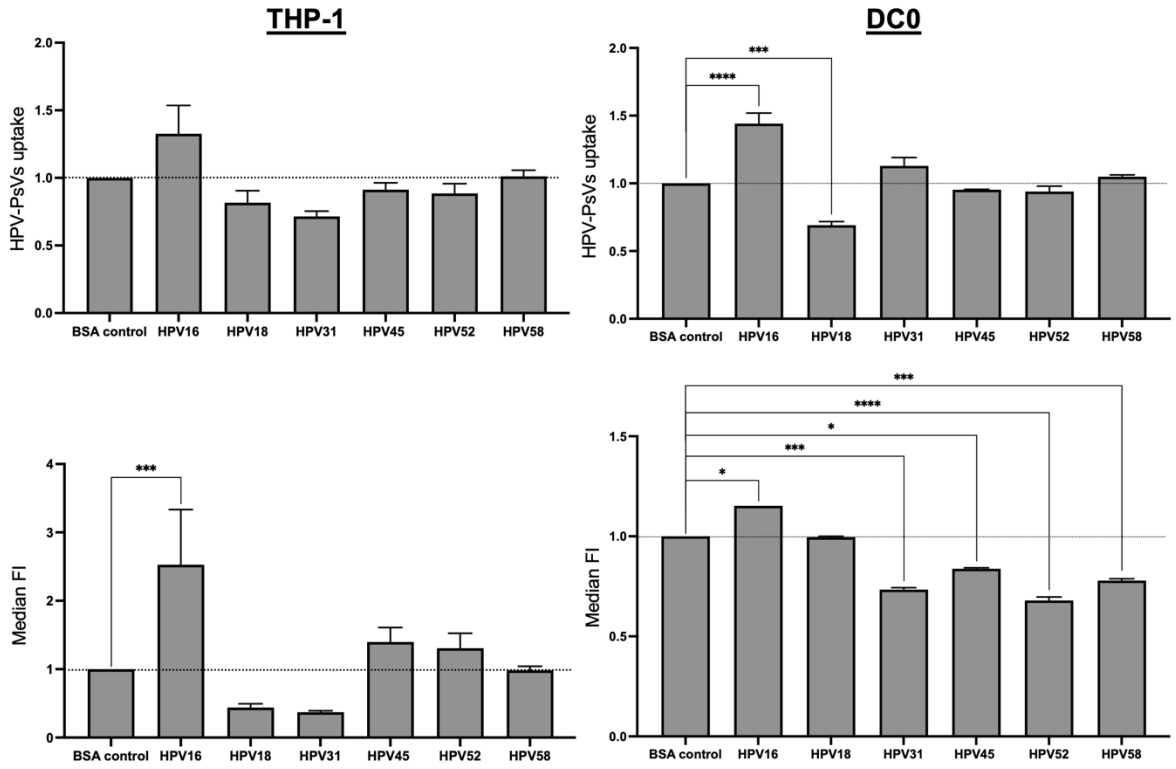

Figure 22: SP-A modulates internalisation of multiple HPV-PsVs types into THP-1 and DC0 cells to varying degrees. Cells were treated as described in Section 2.5.2, before acquisition with a BD Fortessa. HPV-PsVs uptake is depicted on top and the MFI of internalised HPV-PsVs is depicted below. Data of three independent experiments are presented relative to uptake of the BSA control group which was set as 1 (indicated by the dotted line). Statistical significance was determined by one-way ANOVA and Sidak's multiple comparison tests. *= p<0.05; **= p<0.01; ***= p<0.001; ****= p<0.0001; no symbol denotes not significant.

3.5 Monitoring intracellular trafficking of HPV in the presence of SP-A

As illustrated in Figure 17, SP-A demonstrates the ability to agglutinate HPV16-PsVs when preincubated in the presence of $CaCl_2$. Additionally, a notable enhancement in fluorescence intensity was observed in selected immune cells infected with SP-A-coated HPV16-PsVs through FACS analysis, while HaCaT keratinocytes displayed decreased viral uptake (Section 3.4). To validate and gain deeper insights into these findings, we employed confocal microscopy to compare AF488-HPV16 clusters within and surrounding cells preincubated with either SP-A or BSA. HaCaT and RAW264.7 cells were chosen for this analysis, and the time point 3 hpi and 8 hpi (depending on the assessed biological process, see below) was chosen. Using the Fiji "Analyze particles" function allowed us to count each incidence of internalised HPV16-PsVs and measure the size of the clusters (Figure 23).

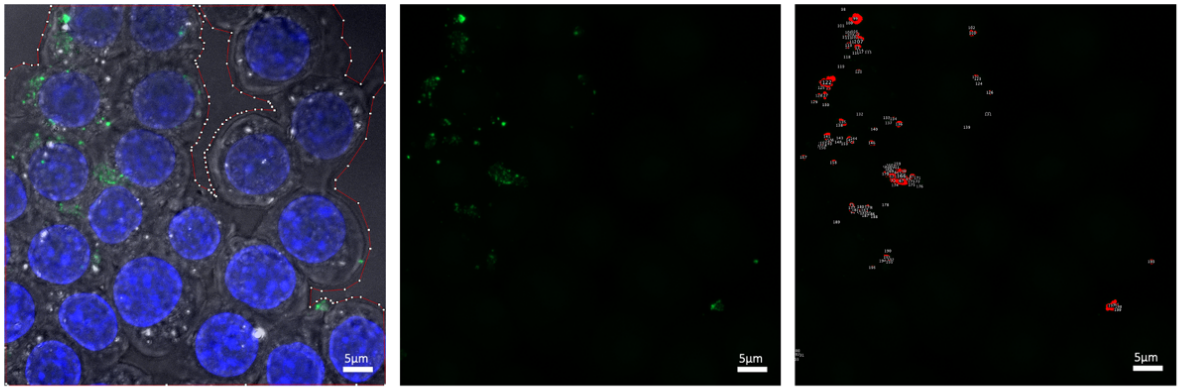

Figure 23: Analysis of HPV16-PsVs uptake and particle size at 3 hpi. Left panel: Hoechst (blue) was used to count cells, and the cell perimeter was defined using the phase contrast images. Middle panel: Incidence of AF488-labelled HPV. Right panel: Thresholds were set to isolate the HPV particles of interest (numbered and indicated in red). Exemplified here are RAW264.7 cells treated with HPV16-PsVs + SP-A for 3 h that were analysed using the Fiji "Analyze particles" tool. Scale bar = 5 µm.

As seen in Figure 24A, the mean size of the detected particles in RAW264.7 was greater in the BSA group, while no significant difference in the mean particle size was observed for the HaCaT cells. However, for both cell lines, the range of particle size in the SP-A groups was greater, and larger clusters were observed (Figure 24A) which supports the agglutination data shown in Figure 17. Moreover, HaCaT cells showed a decrease in particle uptake in the presence of SP-A, while RAW264.7 cells displayed an increased in particle uptake at 3 hpi (Figure 24B), again corroborating the FACS data presented in Figures 18 and 19. Representative images are shown in Figure 24C.

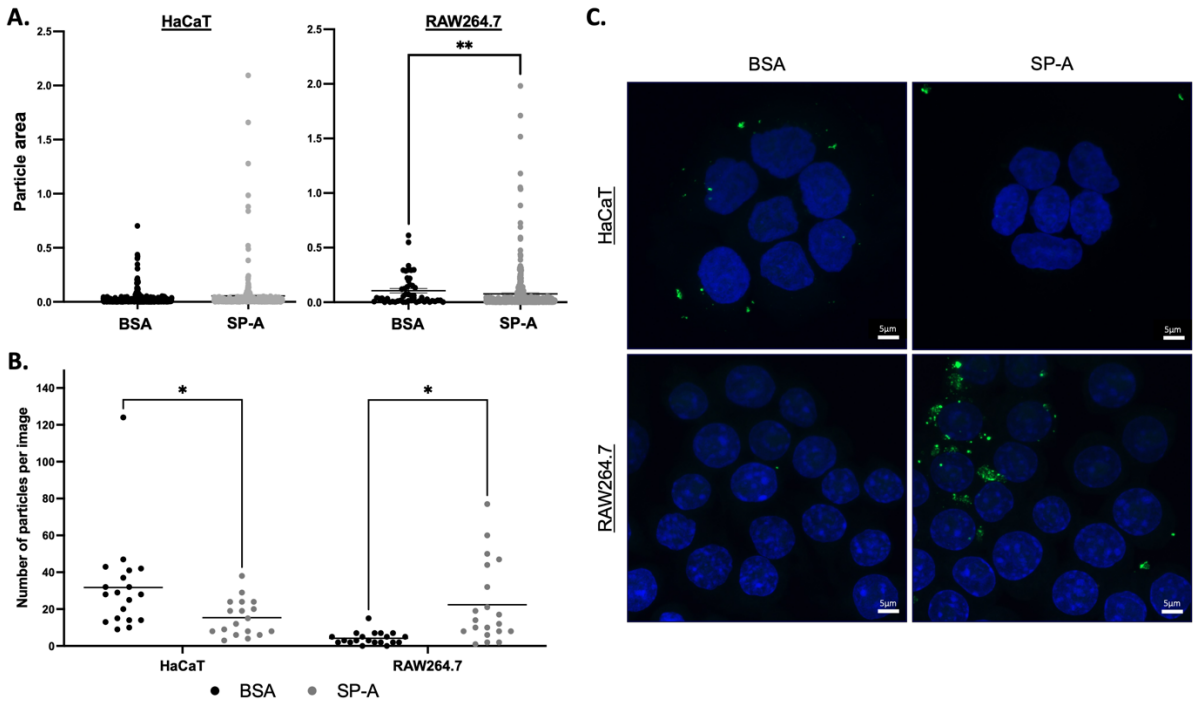

Figure 24: HPV16-PsVs particle size and occurrence in HaCaT and RAW264.7 at 3 hpi. Briefly, 20 z-stacks of HaCaT and RAW264.7 cells infected with BSA- or SP-A-coated HPV16-PsVs were acquired with a Zeiss LSM 980 confocal microscope. Using the Fiji "Analyze particles" function to analyse the maximum intensity projections of the z-stacks (see Figure 23), the **A.** particle area (in μm^2) and **B.** number of particles were determined. Each point on the graphs is the average particle area in pixels or average number of particles for each image. Number of particles was normalised to cell number and cell area. **C.** Representative confocal images of HaCaT and RAW264.7 infected with BSA- or SP-A-coated HPV16-PsVs taken at 3 hpi. Nuclei were stained with Hoechst 33342 (blue), and AF488-HPV16-PsVs are shown in green. Statistical significance was determined by one-way ANOVA and Sidak's multiple comparison tests. *= $p<0.05$; **= $p<0.01$; no symbol denotes not significant. Scale bar = 5 µm.

The way in which SP-A is endocytosed has been previously characterised, and this can provide valuable insights into its ability to modulate intracellular trafficking of pathogens. SP-A has been shown to be rapidly endocytosed by a receptor mediated process through clathrin-coated pits and is trafficked through the endolysosomal pathway in human macrophages (281). Furthermore, SP-A has been shown to enhance the lysosomal delivery of *E. coli* in RAW264.7 cells by regulating Rab7 expression (282). However, it is yet unknown whether SP-A plays a role in the intracellular trafficking of HPV in epithelial cells and/or immune cells. Fluorescent imaging of HPV in the lysosomal compartments will help understand the impact of SP-A on HPV16-PsVs infection by potentially affecting lysosomal escape and degradation and breakdown of particles before trafficking to the nucleus. Using LysoTracker, a dye that accumulates in acidic compartments such as lysosomes, colocolisation with AF488-HPV16-PsVs was performed to assess the difference in accumulation of HPV in these acidic compartments.

Before colocalisation analysis could be performed, chromatic aberration between the different channels needed to be accounted for. Using a macro script in Fiji, a transformation was

calculated using images of multispectral fluorescent beads acquired with the same imaging settings as that of the experimental samples. Compared to the misalignment of the different channels before applying the transformation to the images of the beads, correcting for transformation led to perfect overlap of the channels i.e., they focused to the same position in the image (Supplementary Figure 5). This transformation was applied to each maximum intensity projection used in the analysis.

To assess the colocalisation of HPV at 8 hpi with lysosomes in the absence and presence of SP-A, the JaCoP plugin was employed analysing the Manders', overlap, and Pearson's coefficients, respectively. Importantly, the thresholds for the HPV (green) and lysosome channels (blue) were set to exclude non-specific staining before obtaining the relevant colocalisation statistics (see Section 2.5.3). **Manders' coefficients** measure the fraction of the intensity in one channel that overlaps with the intensity in the other channel. We found that the fraction of the lysosome signal overlapping with the HPV signal was minimal, and no significant difference was seen for either HaCaT or RAW264.7 cells, regardless of the presence of SP-A (Figure 25A). The fraction of the HPV signal overlapping with the lysosome signal, however, was significantly higher in the SP-A groups for both HaCaT cells (mean value of 0.86 compared to BSA value of 0.73) and RAW264.7 cells (mean value of 0.88 compared to BSA value of 0.49), Figure 25A. When assessing the **overlap coefficient**, which measures the spatial overlap of the pixels between two channels irrespective of pixel intensity, we found that the overlap of the HPV signal with the lysosome signal was slightly lower for the SP-A group compared to the BSA control group in HaCaT, but not RAW264.7 cells (Figure 25B). In addition, the **Pearson's coefficient**, which assesses changes in pixel intensities in relating channels but not spatial overlap, was found to be significantly higher in the SP-A group for both HaCaT cells (mean value of 0.26 compared to BSA value of 0.12) and RAW264.7 cells (mean value of 0.84 compared to BSA value of 0.39) (Figure 25B). Taken together, these results indicate that the overall colocalisation pattern was similar in HaCaT and RAW264.7 cells, but the specific intensity correlation between HPV and lysosomes was increased in the presence of SP-A, indicating changes in their interaction dynamics or biological processes.

The occurrence of HPV and localisation with lysosomes for these cell lines in the absence or presence of SP-A is illustrated in Figure 25C. Qualitative analysis of the images for each experimental group showed an increase in the occurrence in the exocytosis of lysosomes (red vesicles that are budding off from the cell membrane). Overall, a more intense LysoTracker signal and larger lysosomes in the presence of SP-A were observed, where these lysosomes were not necessarily carrying HPV particles.

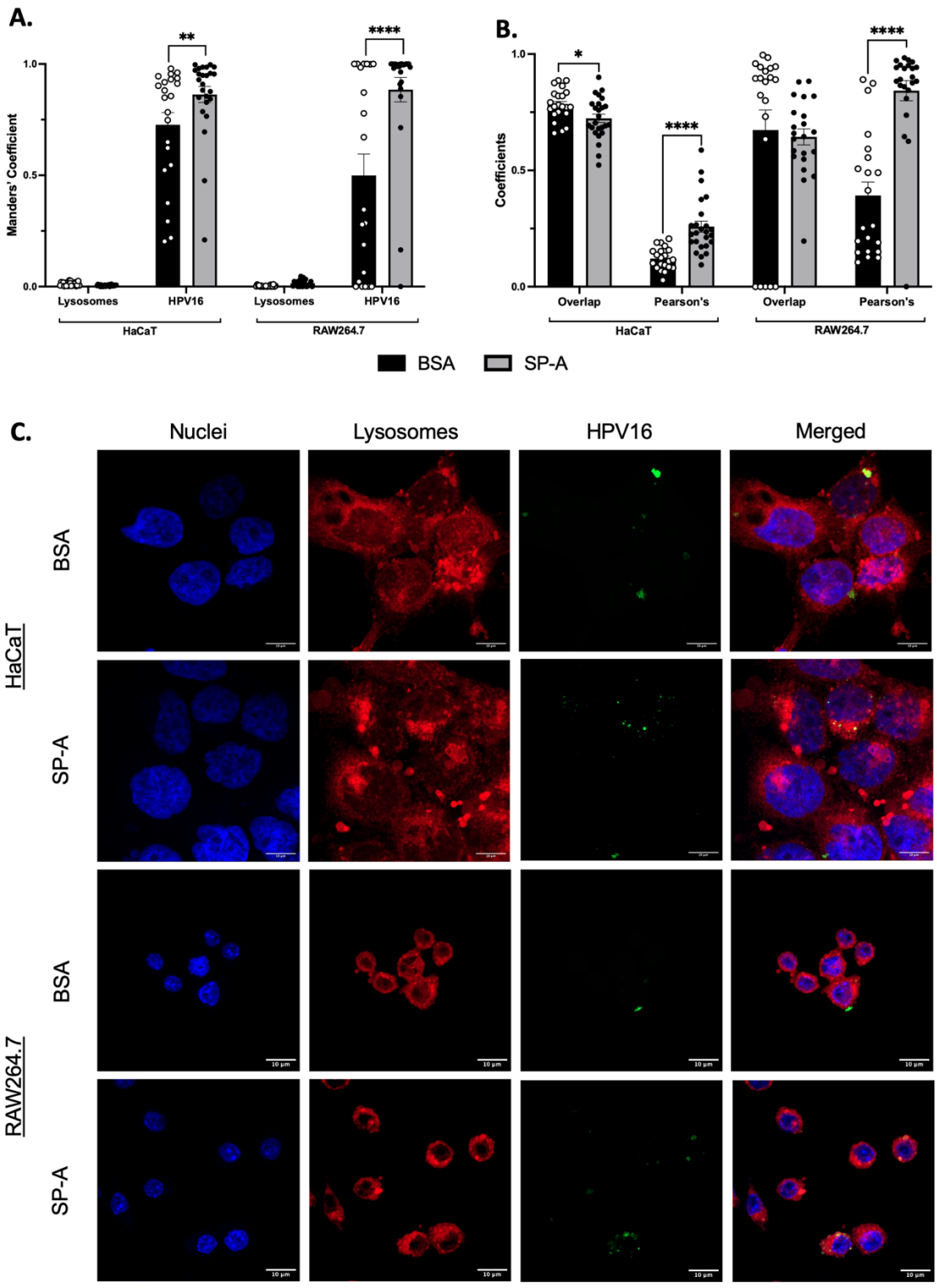

Figure 25: Colocalisation characteristics of HPV16-PsVs and lysosomes for HaCaT and RAW264.7 at 8 hpi. 25 z-stack images were taken for each cell type and experimental condition using a Zeiss LSM 980 confocal microscope, and the resulting maximum intensity projections were used for the analysis. **A.** Manders' coefficients are indicated as Lysosomes (fraction of lysosome signal overlapping with HPV signal) and HPV16 (fraction of HPV signal overlapping with lysosome signal). 0.0 indicates no overlap and 1.0 indicates total overlap. **B.** Overlap and Pearson's coefficients are plotted. Each dot represents a single image, and the bars represent the mean and SEM. **C.** Representative z-stacks of cells infected with AF488-HPV16-PsVs +/- SP-A for 8 h. Cells were stained with LysoTracker™ Deep Red and Hoechst 33342 (blue). AF488-HPV16-PsVs were used and visualised in green. Statistical significance was determined by two-way ANOVA and Sidak's multiple comparison tests. *= $p<0.05$; **= $p<0.01$; ****= $p<0.0001$; no symbol denotes not significant. Scale bar = 10 µm.

3.6 SP-A modulates HPV-PsVs infection in an *in vitro* immune cell / epithelial cell co-culture system

In vitro co-cultures of epithelial cells and other types with immune cells are widely used experimental models for studying the interactions and communication between these cell types (255, 283-286). Co-culture experiments can be performed using various techniques, such as transwell systems, microfluidic devices, or direct cell-to-cell contact, depending on the research question and cell types of interest. Co-culturing epithelial cells with immune cells such as macrophages or DCs can mimic the complex cellular interactions that occur *in vivo* during immune responses and infection. These co-culture models can be used to investigate the mechanisms of immune cell recruitment, activation, and polarisation in response to different stimuli and to evaluate the impact of immune cells on epithelial cell functions, such as cytokine secretion, infection with pathogens and apoptosis. Here, we aimed to establish a co-culture system consisting of the HaCaT epithelial cell line and immune cells (RAW264.7, THP-1, and THP-1 derived immune cells, respectively) in order to assess changes in HPV infection in the presence of innate immune cells and SP-A.

Optimal conditions for the co-culture system were established to ensure cell viability up to 72 hpi. For a 96-well format, 5000 HaCaT cells were seeded and grown overnight as a monoculture or seeded together with varying numbers of immune cells ranging from 500 to 10000 cells per well (Figure 26). This system was designed to determine the level of infection in the target cells, HaCaTs, as the immune cells in monoculture showed no measurable infectivity at 48 hpi as shown in Figure 27. In comparison, infection of HaCaT cells was 100- to 1000-fold higher than the immune cells used in this study.

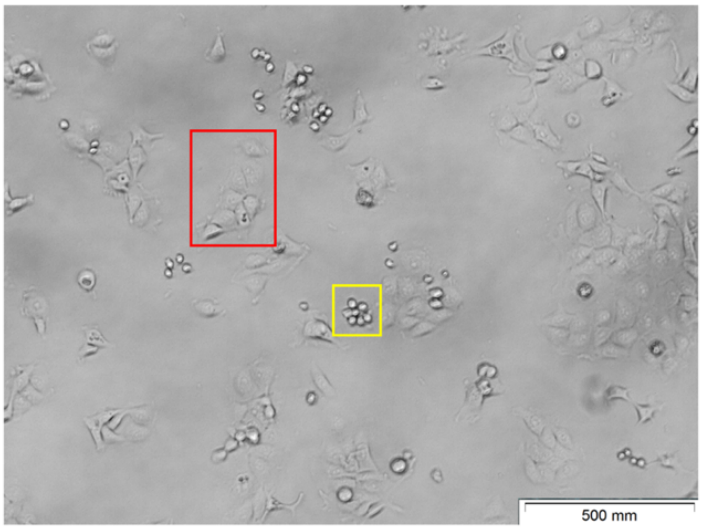

Figure 26: Representative image of the epithelial cell / immune cell co-culture system. Depicted here are 5000 HaCaT cells co-cultured overnight in cDMEM with 1000 RAW264.7 cells. Representative HaCaT cells are boxed in red, and RAW264.7 cells in yellow.

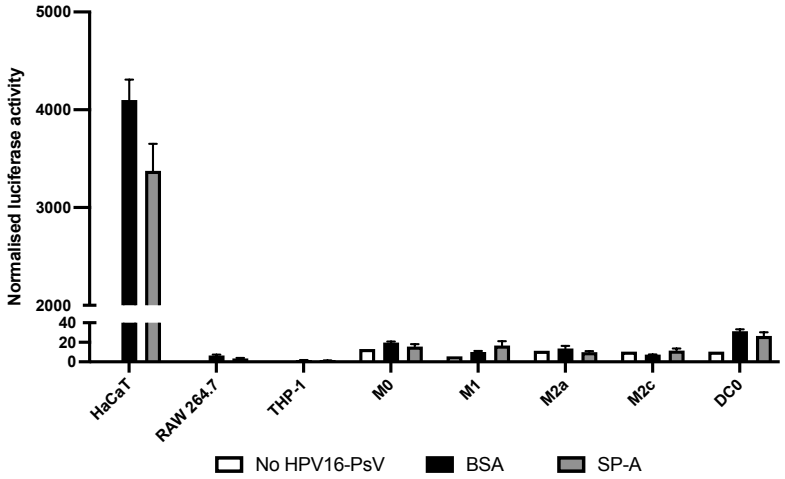

Figure 27: Luciferase activity is indicative of HaCaT epithelial cell, but not immune cell infection. Briefly, 5000 cells were cultured in monoculture in 96-well plates overnight. The cells were infected with HPV16-PsVs encapsidating the Gaussia luciferase reporter gene as described in Section 2.5.1. Gaussia luciferase was quantified in cell culture supernatants at 48 hpi, measured as relative light units and normalised to cell number by staining the cells with CSFE.

3.6.1 The presence of RAW264.7 or THP-1 cells and SP-A decreases HPV16-PsVs infection of HaCaT cells

To assess the effect of RAW264.7 cells on infection of HaCaT cells with SP-A preincubated HPV16-PsVs, the co-culture model was applied as described. Preincubation with SP-A led to a significant 40% decrease in infection in the HaCaT monoculture after 48 h, (Figure 28 A1) which aligns with the FACS data (Section 3.4.2), illustrating a decrease in the initial uptake of HPV-PsVs by HaCaT cells.

The introduction of RAW264.7 murine macrophages led to a significant dose-dependent decrease in infection of HaCaT cells in the BSA control group (Figure 28 A1). Supplementation with SP-A along with the murine macrophages resulted in an additive inhibitory effect of HPV16-PsVs infection, where the lowest infection levels were seen in the co-culture system with the highest number of macrophages (Figure 28 B1). This decrease in infection in the presence of SP-A compared to the BSA control for each co-culture condition suggests a dose-dependent enhanced immune cell clearance of HPV16-PsVs in addition to the inhibitory effect of SP-A seen for HPV16-PsVs infection in HaCaT monocultures.

Similar trends were observed for the THP-1 co-cultures. The introduction of 500, 1000, and 5000 THP-1, but not 10000, cells dose-dependently decreased HPV16-PsVs infection of HaCaT cells in the BSA control group (Figure 28 A2 and B2). Infection in the presence of SP-A and 10000 THP-1 cells was found to be the lowest of all conditions tested, although not significant compared to infection of HaCaT monocultures in the presence of SP-A (Figure 28 B2).

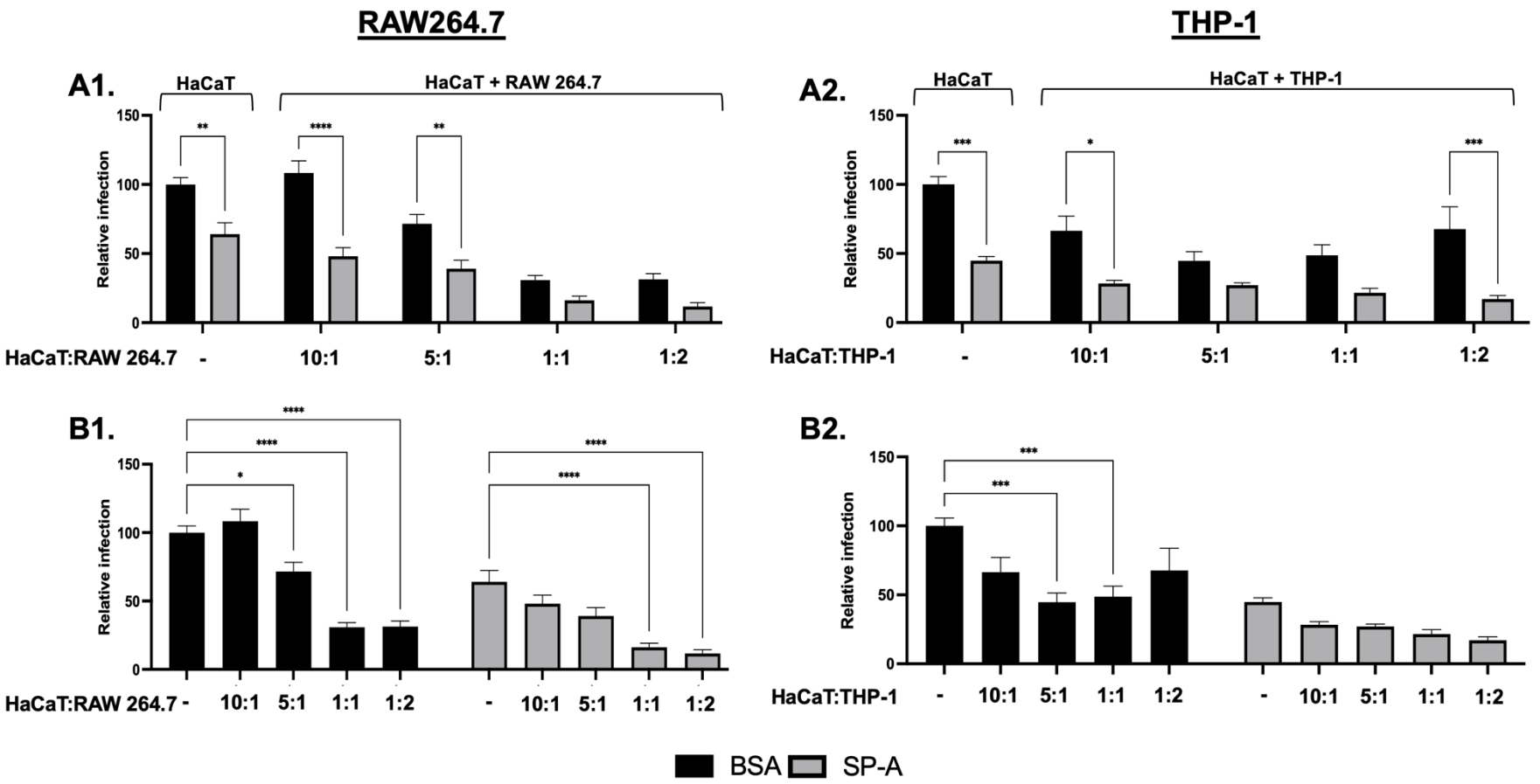

Figure 28: HPV16-PsVs infection of HaCaT cells is decreased in the presence RAW264.7 or THP-1, and further dampened by preincubation with SP-A. Briefly, 5000 HaCaT cells were plated with increasing numbers of RAW264.7 macrophages or THP-1 monocytes (depicted as ratios) the day prior infection. HPV16-PsVs encapsidating the Gaussia luciferase reporter gene were preincubated with SP-A or BSA for 1 h at room temperature before adding to the cells. Depicted here are infection levels of HaCaT cells after 48 h. **A1.** and **A2.** depict comparisons between BSA and SP-A for each culture condition for RAW264.7 and THP-1, respectively. **B1.** and **B2.** depict comparisons between the different culture conditions within the same treatment group for RAW264.7 and THP-1, respectively. Combinatorial analyses of three independent experiments are represented relative to infection of the BSA control group (HaCaT only) which was set as 100%. Statistical significance was determined using 2-way ANOVA with Sidak's test for multiple comparisons. *= $p<0.05$, **= $p<0.01$, ***= $p<0.001$ ****= $p<0.0001$; no symbol denotes not significant.

3.6.2 The presence of M0 macrophages, and to a lesser extent M1 and DC0, results in an SP-A-mediated decrease in HPV16-PsVs infection of HaCaT cells

Similar to the results shown in Figure 28, the introduction of M0 cells also led to a reduction in infection in the BSA control group (Figure 29 A1). SP-A preincubation further decreased infection for each co-culture condition, although not significantly (Figure 29 B1). Co-culture conditions with 5000 M0 cells and more resulted in the lowest level of infection. Although initial HPV16-PsVs uptake into M0 cells was not significantly affected by SP-A preincubation, (Figure 19), M0 clearance of HPV16-PsVs appears to be modulated by the presence of SP-A, as seen by these infection data.

HPV16-PsVs infection was also significantly dampened by the M1 population, as seen by the addition of M1 cells for the BSA control group (Figure 29 A2). However, SP-A preincubation did not seem to further affect infection in the presence of M1 macrophages as much as the previously described immune cell populations (Figure 29 B2). This supports earlier observation where the presence of SP-A did not result in any changes in initial M1 uptake of HPV16-PsVs (Figure 19). Due to their polarisation into a proinflammatory state, we initially hypothesised that M1 cells would be better equipped to recognise, respond to, and combat viral infections by activating immune responses compared to the THP-1 monocytes and naïve M0 macrophages. Interestingly, in this co-culture system, viral clearance mediated by M0 was comparable to that of M1 regardless of SP-A.

HPV16-PsVs infection was also significantly dampened by the DC0 population, as seen by the addition of DC0 for the BSA control group (Figure 29 A3 and B3). Despite the significant increase in initial HPV16-PsVs uptake in DC0 in the presence of SP-A (Figure 22), SP-A only slightly further decreased overall infection of HaCaT cells when co-cultured with DC0 (Figure 29 B3).

Taken together, the different immune cell populations studied here exhibited varying degrees of potency in reducing HPV16-PsVs infection in HaCaT cells, with some, like RAW264.7 macrophages and THP-1 monocytes, showing sensitivity to SP-A enhancement, while others, notably M1 macrophages and DC0, display substantial infection reduction, but relatively independent of SP-A. These findings highlight the differential effectiveness of distinct immune cells in combating HPV16-PsVs infection, with and without SP-A influence.

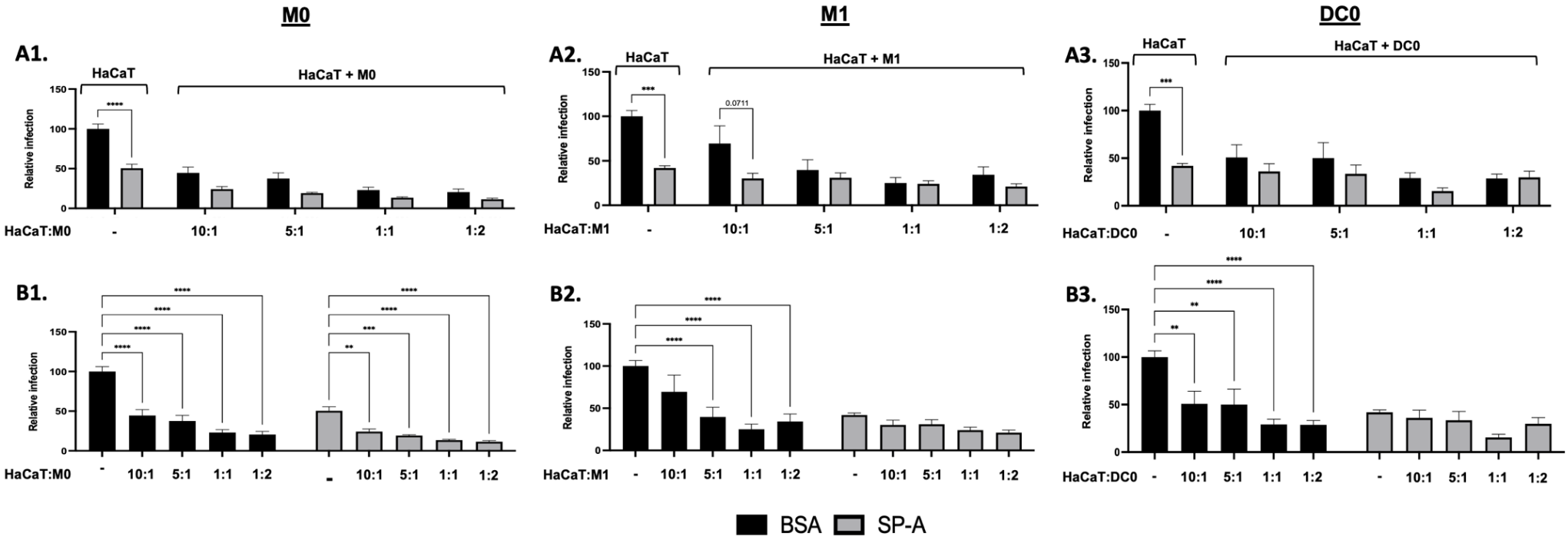

Figure 29: HPV16-PsVs infection of HaCaT cells is decreased in the presence of M0 or M1 macrophages, or DC0, and further dampened by preincubation with SP-A to different degrees. Briefly, 5000 HaCaT cells were plated with increasing numbers of M0, M1, or DC0 the day prior (depicted as ratios). HPV16-PsVs encapsidating the Gaussia luciferase reporter gene were preincubated with SP-A or BSA for 1 h at room temperature before addition to the cells. Depicted here are infection levels after 48 h, where **A1.**, **A2.**, and **A3.** depicts comparisons between BSA and SP-A for each culture, for M0, M1, and DC0, respectively. **B1.**, **B2.**, and **B3.** depict comparisons between the different cultures within the same treatment group for M0, M1, and DC0, respectively. Combinatorial analyses of three independent experiments are represented relative to infection of the BSA control group (HaCaT only) which was set as 100%. Statistical significance was determined using 2-way ANOVA with Sidak's test for multiple comparisons. **= p<0.01, ***= p<0.001, ****= p<0.0001; no symbol denotes not significant.

3.6.3 SP-A contributes to the immune cell-mediated reduction of infection by multiple HPV types in HaCaT cells

Infection of HaCaT cells by other oncogenic HPV-PsVs types in the presence of immune cells and SP-A was also assessed. RAW264.7, THP-1, and DC0 were chosen for this analysis. The highest HaCaT: immune cell ratio that showed a significant reduction in infection for HPV16-PsVs was chosen. This was 5:1 for RAW264.7 and THP-1, and 1:1 for DC0 (Figures 28 and 29).

SP-A reduced infection of the HaCaT monocultures by the different HPV-PsVs types to varying degrees. Infection with HPV-PsVs types 18, 31, 52, and 58 was significantly reduced, comparable to what has been established for HPV16-PsVs (Figure 30 A1). The addition of RAW264.7 did not alter infection levels in the presence of SP-A for any HPV-PsVs type other than HPV16-PsVs. The addition of THP1 and DC0 cells led to significant further changes in infection in the presence of SP-A for all types (THP-1 cells), and types 16, 52, and 58 (DC0 cells) (Figure 30 B2 and B3). Interestingly, infection of HaCaT cells with HPV31-PsVs was increased in the DC0 co-cultures for the SP-A group, although not significantly (Figure 30 B3).

Analysing the infection of HaCaT cells by various oncogenic HPV-PsVs types, our study highlights the inhibitory effect of exogenous SP-A supplementation. The introduction of specific immune cells amplifies this modulation, exerting varying degrees of influence on the infection dynamics of selected HPV types in this HaCaT-immune cell co-culture model. This differential impact underscores the distinct potency of diverse immune cell populations in shaping HPV-PsVs infection, with SP-A often augmenting their effects.

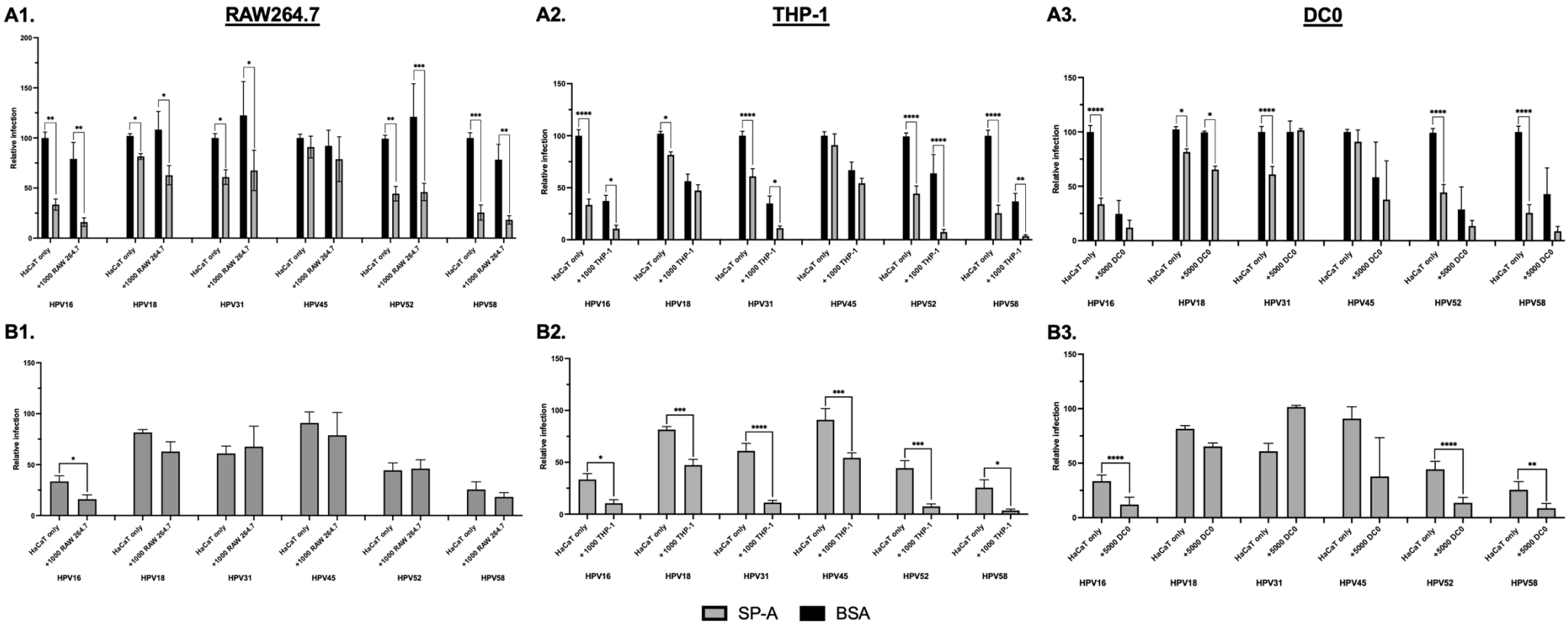

Figure 30: Infection levels of HaCaT cells by selected oncogenic HPV types is dampened in the presence of SP-A and RAW264.7, THP-1, and DC0 cells. Briefly, 5000 HaCaT cells were seeded with 1000 RAW264.7 cells, 1000 THP-1 cells or 5000 DC0 the day prior. HPV-PsVs types 16, 18, 31, 45, 52, and 58 encapsidating the Gaussia luciferase reporter gene were preincubated with SP-A or BSA for 1 h at room temperature before addition to the co-cultures. Depicted here are infection levels 72 hpi, where **A.** depicts comparisons between BSA and SP-A for each culture, and **B.** depicts comparisons between HaCaT monocultures and the addition of the respective immune cells in the SP-A group. Combinatorial analyses of three independent experiments are represented. Statistical significance was determined using 2-way ANOVA with Sidak's test for multiple comparisons. *= $p<0.05$, ***= $p<0.001$ ****= $p<0.0001$; no symbol denotes not significant.

3.7 Assessing altered immune cell cytokine profiles in response to HPV16-PsVs infection: The role of SP-A

Our study sought to investigate the impact of HPV16-PsVs infection on immune cell cytokine, chemokine and growth factor profiles, particularly in the presence of SP-A. Cytokines are signalling molecules released by immune cells and other cell types that play a pivotal role in regulating immune responses, while chemokines are molecules that specifically attract immune cells to sites of inflammation or infection, and growth factors are signalling proteins that stimulate cell growth, proliferation, and differentiation in various tissues and cell types. Alterations in these immune regulatory molecules' profiles can provide insights into the immune system's reaction to specific stimuli or pathogens. SP-A, on the other hand, is a critical component of the pulmonary innate immune system and has also been implicated in modulating immune responses in non-pulmonary sites. We selected undifferentiated THP-1 monocytes and immature DCs for our immune modulator response towards HPV16-PsVs pre-incubated with or without SP-A due to their high phagocytic activity (Figure 22) and their ability to directly reduce HPV16-PsVs infection in HaCaT cells (Figure 20 and 30).

To assess changes in immune modulatory proteins, we utilised the Proteome Profiler™ Human XL Cytokine Array Kit, which comprises 105 different antibodies targeting human cytokines, chemokines, and growth factors immobilised on a membrane (for a complete list of proteins, please refer to Supplementary Table 2). This kit facilitates the detection of relative changes in immune mediator expression in cell culture supernatants. Our experimental conditions were as follows: An '**untreated'** immune cell control served as the baseline immune mediator profile for unstimulated cells (Figure 31). An **'SP-A only'** condition was employed to evaluate the impact of SP-A on immune mediator expression in isolation. Furthermore, we exposed cells to HPV16-PsVs preincubated with BSA and SP-A (termed **HPV16-PsVs only** and '**SP-A:HPV16-PsVs'**, respectively), to both assess the effects of HPV16-PsVs alone on THP-1 and DC0 cells (BSA:HPV16-PsVs), and to compare how preincubation of HPV16-PsVs with SP-A influenced their immune response compared to control (SP-A:HPV16-PsVs).

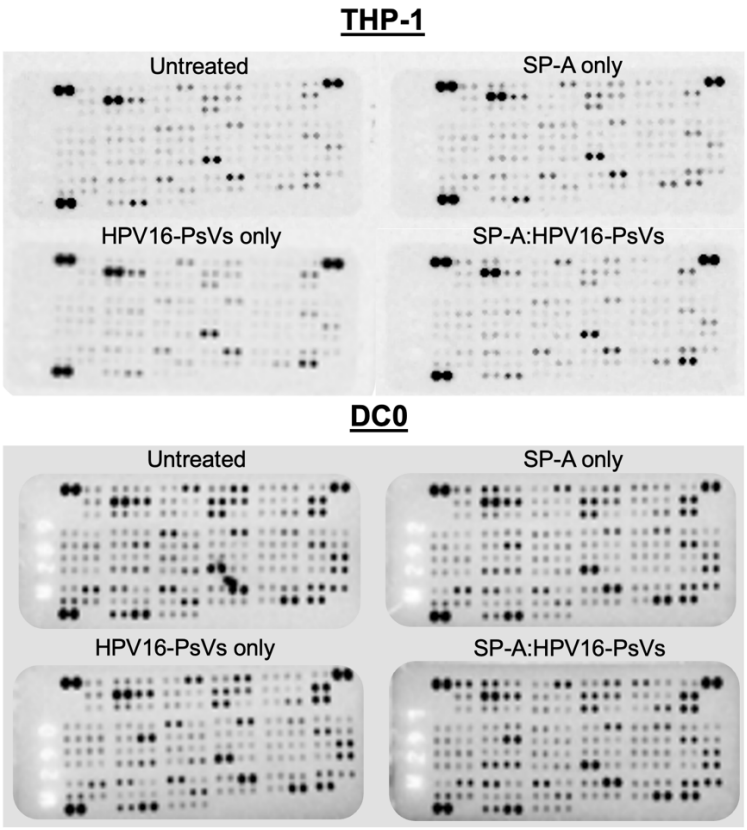

Figure 31: Detection of multiple cytokines, chemokines, growth factors and other soluble proteins in cell culture supernatants of THP-1 cells (top) and DC0 cells (bottom). Briefly, undifferentiated THP-1 cells and THP-1-derived DC0 were grown overnight as described in Section 2.5.4, and were left untreated, treated with SP-A or infected with HPV16-PsVs preincubated with either BSA or SP-A for 24 h. Cell supernatants were harvested and used on the Proteome Profiler™ Human XL Cytokine Array which contained 105 different capture antibodies spotted in duplicate, as described by the manufacturer. Shown are the membranes simultaneously imaged for chemiluminescence using the iBright FL1000. Relative levels of the selected immune modulatory proteins were determined from these images using the QuickSpots software (Ideal Eyes Systems).

The analysis of the Proteome Profiler™ Human XL Cytokine Array was performed as follows: All immune modulators that showed at least a 0.5-fold change in expression (i.e. 50% reduction or increase in expression) of **A**) the SP-A:HPV16-PsVs group relative to the untreated control (analysis A) and/or **B**) the SP-A:HPV16-PsVs group relative to the HPV16-PsVs only group (analysis B) were included.

Of the 105 immune modulators analysed, only 8 were differentially expressed in the SP-A:HPV16-PsVs group relative to the untreated control (analysis A, Table 3A), while 5 were differentially expressed in the SP-A:HPV16-PsVs group compared to HPV16-PsVs only (analysis B, Table 3B) in THP-1 cells. Interestingly, all the immune modulators identified by analysis B were also identified in analysis A as shown in the Venn diagram (Figure 32), of which the same 2 were downregulated in the respective analysis and the remaining were upregulated. Due to this overlap and the lower number of differentially regulated immune modulators identified in analysis B, all subsequent analyses focussed on differentially regulated proteins in the SP-A:HPV16-PsVs group compared to control (analysis A).

Table 3A: Analysis A - Immune modulators that were differentially expressed in the SP-A:HPV16-PsVs group relative to the untreated control in THP-1 cells. A 0.5-fold change in expression was used as the cut-off value. Shown are mean values obtained from the duplicate dots on the membranes (Figure 31). Proteins are ordered from highest to lowest according to the fold-change in expression of SP-A:HPV16-PsVs relative to the untreated control.

Name	**Analysis A: Fold expression relative to untreated condition**		
	SP-A only	HPV16-PsVs only	SP-A:HPV16-PsVs
VEGF	1.19	2.82	3.28
C5	4.04	1.49	2.97
Apoliprotein A-I	2.43	1.22	2.53
Lipocalin-2	2.04	1.31	1.69
FGF-7	0.97	2.22	1.59
Adiponectin	2.29	0.95	2.09
Growth hormone	0.57	1.09	0.50
GRO-α	0.64	1.02	0.42

Table 3B: Analysis B - Immune modulators that were differentially expressed in the SP-A:HPV16-PsVs group relative to the HPV16-PsVs only group in THP-1 cells. A 0.5-fold change in expression was used as the cut-off value. Shown are mean values obtained from the duplicate dots on the membranes (Figure 31). Proteins are ordered from highest to lowest according to the fold-change in expression of SP-A:HPV16-PsVs relative to the HPV16-PsVs group.

Name	**Analysis B: Fold expression relative to HPV16-PsVs only**		
	Untreated control	SP-A only	SP-A:HPV16-PsVs
Adiponectin	1.06	2.42	2.21
Apoliprotein A-I	0.82	1.90	2.08
C5	0.67	2.72	2.00
Growth hormone	0.92	0.53	0.47
GRO-α	0.97	0.63	0.41

The analyses of the immune modulator profiles for DC0 cells were similarly performed and revealed 43 proteins being upregulated (none downregulated) in the SP-A:HPV16-PsVs group compared to untreated control (analysis A, table 4A) and 34 proteins found upregulated (none downregulated) in the SP-A:HPV16-PsVs group compared to HPV16-PsVs only (analysis B,

Table 4B). As seen for THP-1 cells, all immune modulators identified by analysis B were also identified by analysis A (Figure 32). Again, all subsequent analyses focussed therefore on differentially regulated proteins in the SP-A:HPV16-PsVs group compared to control (analysis A).

Table 4A: Analysis A – Immune modulators that were differentially expressed in the SP-A:HPV16-PsVs group relative to the untreated control in DC0 cells. A 0.5-fold change in expression was used as the cut-off value. Shown are mean values obtained from the duplicate dots on the membranes (Figure 31). Proteins are ordered from highest to lowest according to the fold-change in expression of SP-A:HPV16-PsVs relative to the untreated control.

Name	**Analysis A: Fold expression relative to untreated condition**		
	SP-A only	HPV16-PsVs only	SP-A:HPV16-PsVs
Cripto-1	5.43	5.22	14.12
EGF	3.45	1.20	5.47
FGF-7	1.58	2.38	5.35
IL-8	1.28	4.03	4.59
FLT3L	2.45	1.67	4.58
CD26	3.03	1.18	4.60
C5	2.48	0.94	4.21
Adiponectin	2.12	0.99	3.45
Apoliprotein A-I	2.89	1.15	3.24
CD30	1.43	1.52	3.20
Angiopoietin-1	1.34	1.68	3.18
G-CSF	1.38	1.36	3.02
IL-1β	1.44	1.07	2.59
LIF	0.91	1.02	2.28
TNFα	1.50	1.67	2.27
CRP	0.91	1.44	2.24
Growth hormone	0.79	1.31	2.23
Angiogenin	1.61	1.15	2.14
CCL20	0.91	1.02	2.12

TIM-3	1.17	1.54	2.09
IL-2	1.32	1.23	2.04
IL-13	0.82	0.93	1.98
CCL3	0.74	1.15	1.94
ICAM-1	1.14	0.75	1.93
IL-15	0.98	1.92	1.92
VCAM-1	1.03	1.39	1.89
PDG	1.20	1.01	1.89
FGF-2	0.88	1.06	1.87
IGFBP-3	1.03	1.01	1.79
IL-3	0.92	1.23	1.79
RBP4	1.37	1.30	1.77
TGFα	1.20	1.42	1.77
IL-12	0.99	0.88	1.74
CD40 ligand	0.99	1.06	1.72
IL-16	0.96	1.69	1.69
IL-22	0.93	1.66	1.66
IL-19	0.82	1.64	1.64
Fas Ligand	0.98	1.16	1.63
IL-24	0.73	1.58	1.58
Thrombospondin-1	1.12	1.18	1.57
TARC	0.92	1.02	1.56

Table 4B: Analysis B – Immune modulators that were differentially expressed in the SP-A:HPV16-PsVs group relative to the HPV16-PsVs only group in DC0 cells. A 0.5-fold change in expression was used as the cut-off value. Shown are mean values obtained from the duplicate dots on the membranes (Figure 31). Proteins are ordered from highest to lowest according to the fold-change in expression of SP-A:HPV16-PsVs relative to the HPV16-PsVs group.

Name	**Analysis B: Fold expression relative to HPV16-PsVs only**		
	Untreated control	SP-A only	SP-A + HPV16-PsVs
EGF	0.83	2.89	4.57
C5	1.06	2.62	4.47
CD26	0.85	2.56	3.88
Adiponectin	1.05	2.22	3.61
Apoliprotein A-I	0.94	2.72	3.05
FLT3L	0.60	1.46	2.74
Cripto-1	0.19	1.04	2.70
ICAM-1	1.33	1.50	2.56
IL-1β	0.93	1.33	2.41
Lipocalin-2	1.17	1.5	2.38
IL-15	1.21	1.18	2.31
FGF-7	0.42	0.66	2.25
LIF	0.98	0.89	2.23
G-CSF	0.74	1.01	2.21
IL-13	1.08	0.88	2.12
CD30	0.66	0.94	2.10
IL-12	1.14	1.12	1.97
IL-24	1.21	0.88	1.90
Angiopoietin-1	0.59	0.79	1.88
PDGF	0.99	1.18	1.87
Angiogenin	0.87	1.39	1.85
CCL20	0.85	0.76	1.78

IGFBP-3	0.99	1.01	1.77
FGF-2	0.95	0.83	1.76
IL-19	1.04	0.85	1.70
Growth hormone	0.76	0.60	1.70
GDF-15	0.81	1.06	1.66
IL-2	0.82	1.08	1.66
CCL3	0.85	0.68	1.64
CRP	0.69	0.63	1.62
CD40 ligand	0.94	0.93	1.61
IL16	0.94	0.89	1.58
TARC	0.98	0.90	1.53
IL22	0.91	0.84	1.50

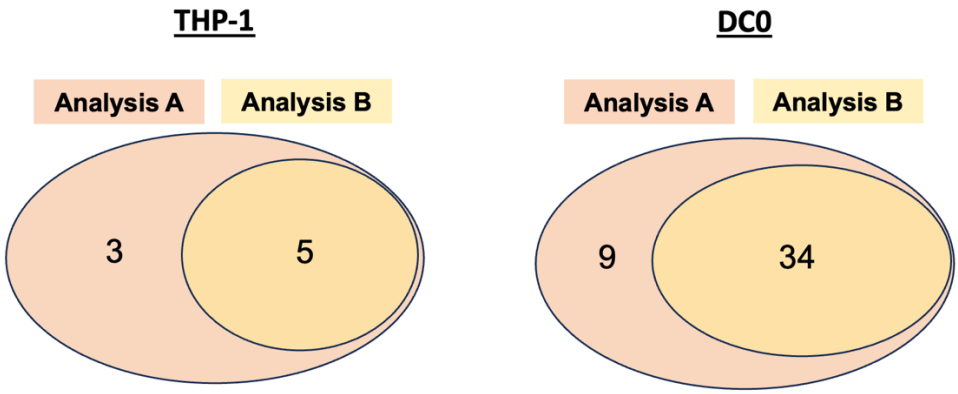

Figure 32: Venn diagram showing the number of differentially expressed immune modulators as identified by analysis A and analysis B in THP-1 and DC0.

A few proteins only responded to SP-A and showed a striking increase in expression relative to the untreated control in THP-1, but not DC0 cells. This response was neither observed in the HPV16-PsVs nor the SP-A:HPV16-PsVs groups (Supplementary Figure 6). As these proteins did not show an SP-A-mediated response to HPV16, they were not included in the analysis.

As illustrated in Figure 33, DC0 cells displayed a much higher degree of differential expression compared to THP-1 cells, with more than 40 immune modulatory proteins exhibiting alternate

expression in the SP-A:HPV16-PsVs group with a higher fold-change relative to the untreated group on average (Tables 4A and Figure 32). All differentially expressed immune modulators identified in THP-1 cells (except VEGF and GRO-α) were also differentially expressed in DC0 following the same trends with the exception of GH which was downregulated by SP-A:HPV16-PsVs in THP1 cells but upregulated in DC0 cells. (Figure 34 and 35).

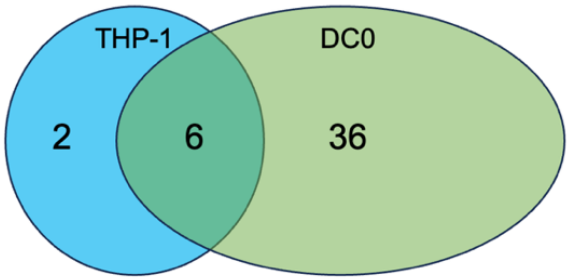

Figure 33: Venn diagram showing the number of immune modulators differentially expressed in THP-1 and DC0 cells in the SP-A:HPV16-PsVs group compared to the untreated control. The depicted proteins were identified by analysis A (Tables 3A and 4A).

All data derived from analysis A are also further presented in Figures 34 and 35. For THP1 cells, we found that the majority of proteins was differentially expressed due to the presence of SP-A irrespective of the presence of HPV16-PsVs (i.e. C5/C5a complement component, Apoliprotein A-I, Lipocalin-2, Apidonectin, GH, and GRO-α). In addition, HPV16-PsVs alone was found to have a positive effect on the expression of VEGF and FGF-7 irrespective of the presence of SP-A (Figure 34). Overall, it is therefore evident that the effects driven by SP-A are more prevalent than those induced by HPV-PsVs16 which was expected given the low immunogenicity of HPV. The differentially expressed proteins in Figure 34 are linked to the inflammatory response, modulation of inflammation, and cell growth and repair: the upregulation of **C5/C5a** (key components in the late stages of the complement cascade) in THP-1 cells challenged with SP-A opsonised HPV16 suggests an activated immune response involving complement activation, potential inflammation, enhanced immune recognition, and potential immunomodulation by SP-A. Likewise, **Apolipoprotein A-I** (ApoA), being the main constituent of lipoprotein has been shown to regulate activated complement (287). **Adiponectin**, a crucial adipokine, has been shown to reduce TNF-α expression in macrophages, effectively counteracting its detrimental effects. It also suppresses endothelial inflammation via a cAMP-dependent pathway, particularly inhibiting NF-κB signalling (288). The increase in Adiponectin found here suggests safeguarding against systemic inflammation (289). **Lipocalin-2** is a protein highly expressed in barrier tissues and is known for its antimicrobial activity by sequestering iron, regulating cell death, and modulating the inflammatory response (290, 291). Its upregulation may indicate protection from excessive

inflammation. Both **VEGF** and **FGF-7** (also known as keratinocyte growth factor) were found to be upregulated in THP-1 when challenged with SP-A opsonised HPV16-PsVs or challenged with HPV16-PsVs alone. Their upregulation may indicate their involvement in cell growth, tissue repair, angiogenesis, and the regulation of cellular differentiation, which collectively support innate immunity and the body's ability to heal and recover from injuries or damage. Interestingly**, Growth hormone** (GH) and **GRO-α** were downregulated in the SP-A:HPV16-PsVs group compared to both the untreated and HPV16-PsVs only group. GH influences the immune system by regulating the production, differentiation, and function of immune cells involved in innate immunity, such as monocytes, macrophages, DCs, and natural killer cells (292-294). GRO-α belongs to the CXC chemokine family and acts as a chemoattractant for neutrophils and other inflammatory cells (295, 296). Its primary role involves recruiting neutrophils to sites of inflammation or injury, thereby amplifying the inflammatory response.

These changes collectively suggest a dynamic environment with a potential decrease in certain aspects of immune regulation in the presence of SP-A (e.g. due to reduced growth hormone and GRO-α) alongside an increase in factors associated with tissue repair and angiogenesis (e.g. FGF-7 and VEGF). This scenario might point toward a context where the body is responding to tissue damage, stress, or a need for repair, potentially balancing immune responses with tissue regeneration processes. This again highlights the dual immune functions of SP-A when responding to infection.

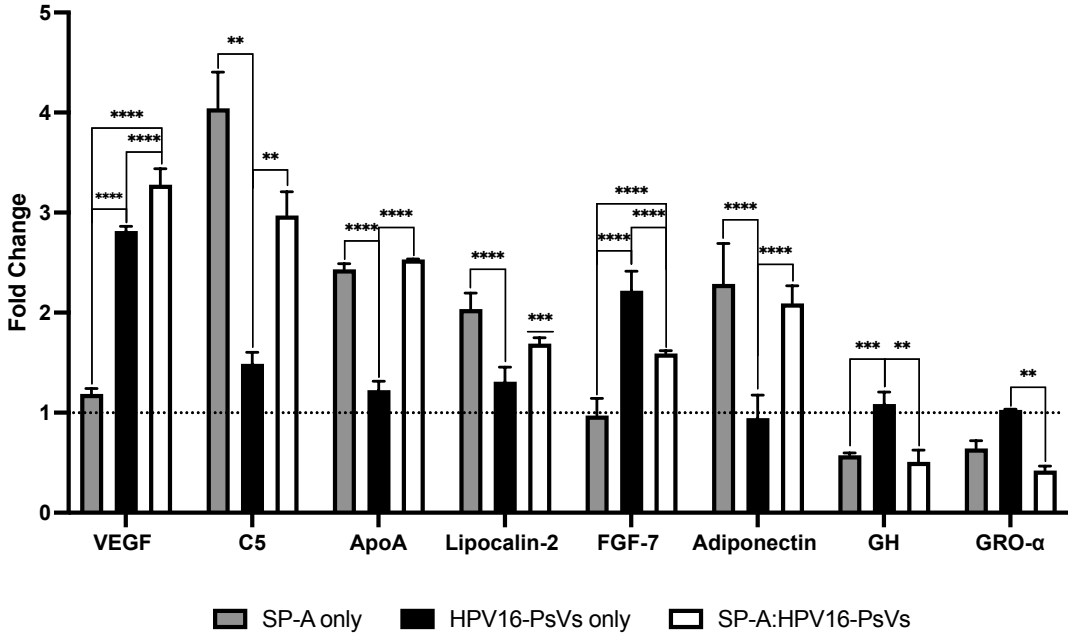

Figure 34: Cytokines, chemokines, and growth factors differentially expressed in the SP-A:HPV16-PsVs group compared to untreated control in THP-1 cells. Proteins shown were identified by analysis A (Table 3A). Data are represented as mean fold-change relative to the untreated control group which was set as 1 (dotted line). Statistical significance was determined using 2-way ANOVA with Tukey's test for multiple comparisons. *= p<0.05, **= p<0.001, ***= p<0.001 ****= p<0.0001; no symbol denotes not significant.

For DC0 cells, we observed many proinflammatory cytokines and mediators of the inflammatory response to be upregulated when challenged with SP-A opsonised HPV16-PsVs. Interestingly, we identified half of the proteins (n=21) to be differentially regulated in the presence of SP-A alone or HPV16-PsVs alone, respectively, with an overall increase in the presence of SP-A:HPV16-PsVs (Figure 35A). The other n=22 proteins were found to be irresponsive to the presence of both SP-A and HPV-16-PsVs alone but induced when HPV16-PsVs was pre-coated with SP-A (Figure 35B).

For further analysis of these rather complex data, we employed the STRING (Search Tool for the Retrieval of Interacting Genes/Proteins) database, a valuable resource for exploring known and predicted protein-protein interactions (297). We utilised it to investigate the complex network of interactions among cytokines, chemokines, and growth factors. This allowed us to delve into the molecular connections that underlie the complex biology of the immune modulators in our study. Additionally, we harnessed the power of the K-means clustering algorithm. This approach was instrumental in unravelling the intricate protein interactions within the unique context of HPV and SP-A, shedding light on the underlying mechanisms that drive the observed immune modulatory protein dynamics. The known functions of the assessed proteins are described, and the predicted functional enrichments, gene ontology (GO), STRING network clusters and associated KEGG pathways for these clusters that may have any relevance in SP-A mediated enhanced immune recognition of HPV are documented in detail in Supplementary Table 3.

The DC0 immune modulators were clustered into 4 groups which were found to have predicted interactions with other cytokines within the same cluster or other clusters with high certainty, where many were associated with enhancing inflammation (Figure 36). Every immune modulator in this cluster analysis was upregulated in the SP-A:HPV16-PsVs condition compared any other condition tested (Figure 35), emphasising heightened (Figure 35A) or induced (Figure 35B) HPV16-PsVs immune responses when opsonised with SP-A. **Cluster I** is composed of proteins displaying prominent roles in promoting epithelial and endothelial cell proliferation and migration (Figure 36). These proteins collectively exert their functions through positive regulation of epithelial and endothelial tube formation, thereby implicating their crucial involvement in tissue repair in response to HPV16-PsVs infection. **Cluster II** proteins exhibit roles in orchestrating immune cell chemotaxis and fostering inflammatory responses. These proteins are closely associated with regulating the migration of macrophages, monocytes, lymphocytes, and neutrophils, indicating their pivotal role in the innate and adaptive immune responses. Pathway analyses reveal their involvement in signalling cascades such as the C-type lectin receptor and JAK-STAT pathways, crucial in mediating immune cell activation and

cytokine interactions. **Cluster III** proteins are primarily characterised by their cytokine activities and signalling pathway involvement. These proteins are linked to the regulation of cytokine-mediated pathways like JAK-STAT signalling and IL-20 family signalling, hinting at their potential impact on Th17 cell differentiation and cytokine-cytokine receptor interactions. Meanwhile, **Cluster IV** includes an extensive array of proteins and showcases a multifaceted involvement in immune responses, spanning from the regulation of inflammatory processes to the modulation of various immune cell activities. Notably, these proteins are associated with pathways like toll-like receptor signalling, NF-κB signalling, and cytokine interactions, underscoring their crucial role in orchestrating immune cell activation, migration, and inflammatory signalling cascades.

Overall, many of the proteins upregulated in DC0 in the presence of HPV16-PsVs and SP-A have specific functions in B cell maturation, T cell proliferation, and act as chemokines for adaptive immune cells (Supplementary Table 3). This emphasizes SP-A's ability to activate the link between innate and adaptive immunity in DCs.

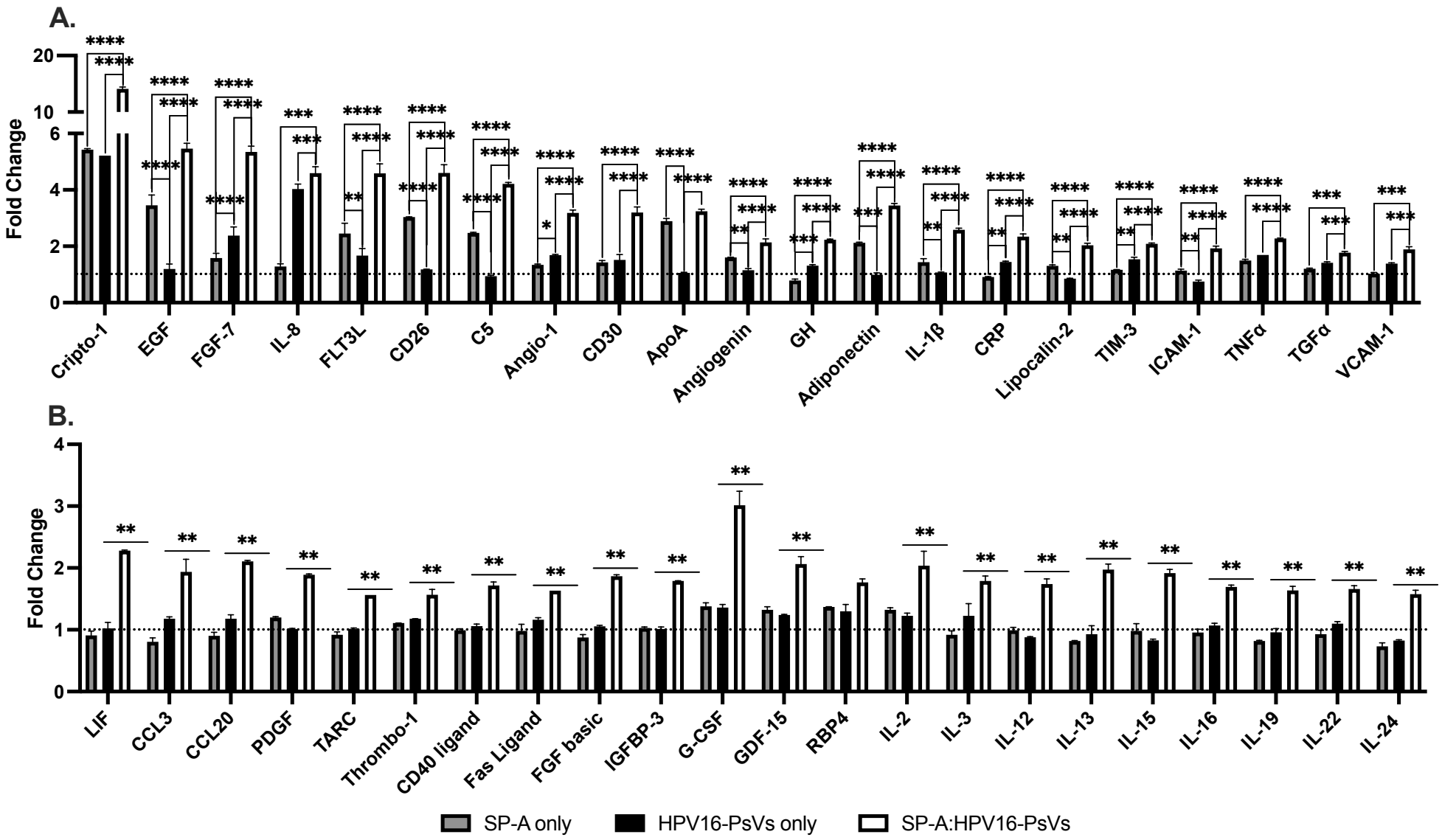

Figure 35: Cytokines, chemokines, and growth factors differentially expressed in the SP-A:HPV16-PsVs group compared to untreated control in DC0. Proteins shown were identified by analysis A (Table 4A). Data are represented as mean fold-change relative to the untreated control group which was set as 1 (dotted line). **A.** Immune modulators differentially expressed in SP-A alone and/or HPV16-PsVs alone, and further modified by HPV16-PsVs in the presence of SP-A. **B.** Immune modulators upregulated only in the dual presence of SP-A and HPV16-PsVs. Statistical significance was determined using 2-way ANOVA with Tukey's test for multiple comparisons. *= $p<0.05$, **= $p<0.001$, ***= $p<0.001$ ****= $p<0.0001$; no symbol denotes not significant.

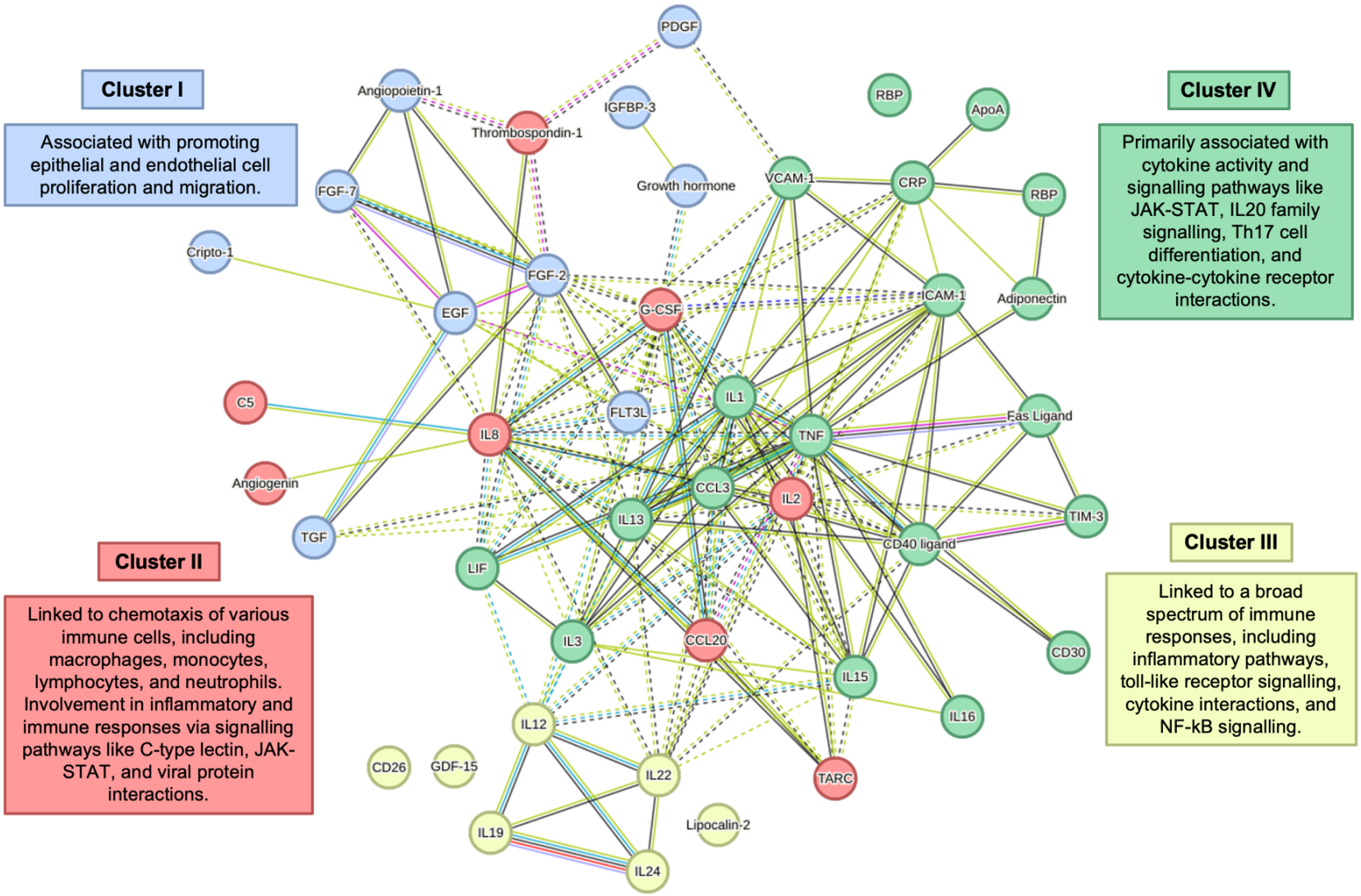

Figure 36: STRING Protein-Protein Interaction Cluster Network for immune modulators upregulated in DC0 cells in the SP-A:HPV16-PsVs group. This network map illustrates predicted functional interactions among the upregulated cytokines, chemokines, and growth factors identified in DC0, when exposed to HPV16-PsVs and SP-A compared to untreated cells, as analysed using the STRING database. Nodes represent individual molecules, lines connecting nodes indicate known or predicted interactions. Proteins were grouped as indicated by the colour of the nodes, using kmeans clustering. Predicted interactions were determined as follows: from **curated databases**, **experimentally determined**, **textmining**, **co-expression**, and **protein homology**. Solid lines represent interactions within clusters, and dotted lines connect proteins between clusters. Predicted protein-protein interactions were set to a high confidence threshold score. Abbreviations are specified in Supplementary Table 2.

4 Discussion

Infection with HPV presents an ongoing global health challenge as a result of its incurable nature and heightened impact when co-existing with HIV, especially in regions such as Southern Africa with elevated HIV prevalence. Prophylactic vaccination is considered the most effective control of viral infections. Highly efficacious prophylactic vaccines against the most prevalent oncogenic HPV types have been developed (see Section 1.5). However, despite the great efforts exerted in HPV vaccination programs, these vaccines do not cover all the oncogenic HPV types present in malignant lesions and the extent of cross-protection against other oncogenic HPV types, of which there are more than twenty that have been identified, is largely unknown. In addition, the vaccines are ineffective for women already infected with HR HPV types. The limitations of these vaccines are especially prevalent in LMIC regions such as Sub-Sharan Africa, where limited access to healthcare, awareness, and proper transport and storage all negatively affect the accessibility of these vaccines. The persistence of cervical cancer as the fourth most common cancer in women globally underscores the urgent demand for alternative interventions that can more broadly target HPV infection, especially in regions facing challenges of limited healthcare access and awareness. Over the last couple of decades, research has been underway to explore alternative means of protection against HPV that are broad-spectrum, easily accessible, and affordable (1).

In response to the dire need for alternative intervention, our research has previously identified SP-A, an innate immune opsonin, capable of recognising HPV16-PsVs (19). We have shown that SP-A opsonisation of HPV16-PsVs resulted in increased viral uptake by mouse immune cells and was capable of recruiting macrophages to the site of infection in a murine cervicovaginal HPV challenge model. Moreover, these *in vivo* data also suggested that SP-A was capable of reducing HPV16-PsVs infection. We hypothesised that this could be translated to human cells, and that exogenous supplementation with SP-A could lead to a reduction in HPV infection of human keratinocytes.

By using *in vitro* monoculture and co-culture systems, together with various molecular and imaging techniques, we set out to describe the broad-spectrum recognition capabilities of SP-A using multiple oncogenic HPV-PsVs types. We also aimed to describe in further detail the immune mechanisms of SP-A in the context of HPV infections by exploring the intracellular trafficking of HPV in the presence of SP-A, and the regulation of cytokine and chemokine production. Given the myriad of immune evasion mechanisms evolved by HPV, we propose that harnessing innate immune molecules, such as SP-A, to enhance HPV immune recognition holds great promise. This approach not only addresses the challenges posed by

HPV's immune evasion strategies but also opens new avenues for developing effective interventions in combating this persistent viral threat. We are currently in the process of preparing a manuscript for publication to disseminate these findings to the scientific community.

3.1. Examining SP-A-mediated innate immune responses to HPV-PsVs using murine and human immune cell lines

The innate immune response against HPV infections remains a critical area of study for developing effective intervention and therapeutic strategies, where numerous studies have utilised receptor agonists to enhance immune responses in both prophylactic and therapeutic vaccines targeting HPV-associated diseases (195-198). The herein described research focused on utilising the murine macrophage cell line, RAW264.7, and human THP-1-derived immune cells as a foundational platform to explore the interplay between the innate immune response towards HPV-PsVs and the modulatory effects of SP-A. Despite its murine origin, RAW264.7 cells have been pivotal in our previous research endeavours, serving as a foundational model for investigating immune regulation (19) (Section 1.9). Therefore, in the continuation of our studies, we have chosen to delve deeper into understanding the immune responses and regulatory mechanisms within this well-characterised cell line. THP-1 cells are a human monocytic cell line that have been widely used in research to study innate immunity due to their ability to differentiate into macrophage-like cells upon stimulation with PMA. Moreover, THP-1 cells possess the remarkable capacity to differentiate into various myeloid populations, which are represented by specific cell surface marker expression profiles, allowing for a broader exploration of immune cell functions in controlled *in vitro* environments. Both RAW264.7 and THP-1 cells are commercially available and can be cultured and manipulated easily, providing a consistent and reproducible cell source for experiments and eliminating the need of frequent isolation of primary murine or human immune cells which can introduce great experimental variability. While acknowledging that engineered cell lines and *in vitro* systems may not perfectly replicate the entirety of native immune cell heterogeneity, they remain indispensable tools in uncovering fundamental immune mechanisms and providing preliminary insights into immune responses in controlled settings.

As mentioned previously, innate immunity serves as the frontline defence against pathogens, initiating rapid responses upon encountering threats like infection with HPV (see Section 1.1). However, HPV has evolved several strategies to evade host immune surveillance and innate immune detection which could be targeted to develop potential prophylactic and therapeutic intervention (see Section 1.4). Through a series of comprehensive analyses, this research

delineated the impact of SP-A on the innate immune response against HPV-PsVs in RAW264.7 and THP-1-derived immune cells, and how SP-A might influence immune cell recognition of HPV-PsVs, impact response pathways, and subsequent antiviral mechanisms. We indeed found that SP-A facilitates enhanced uptake of HPV-PsVs by selected innate immune cells while reducing viral uptake and infection of keratinocytes through agglutination and opsonisation.

Agglutination occurs when particles, such as pathogens or cells, clump together due to the binding action of certain molecules, such as SP-A. Studying SP-A's potential broad-spectrum activities we observed that it could indeed induce agglutination of the full panel of oncogenic HPV-PsVs types studied here (i.e. 16, 18, 31, 45, 52, and 58), leading to the formation of viral clusters or aggregates at varying degrees (Figure 17). This process may have a dual effect on the subsequent outcome of HPV infection and immune responses: while agglutination enhances the recognition of these clusters by selected immune cell populations followed by their engulfment, it might simultaneously reduce the ability of individual HPV particles to enter susceptible cells like keratinocytes as observed in this study.

Opsonisation refers to the process by which molecules, such as SP-A, bind to pathogens, marking them for recognition and subsequent engulfment and destruction by immune cells. SP-A, as a part of the innate immune system, can recognize certain structures on pathogens, including HPV16-PsVs in this context, and coat them. This coating, along with particle aggregation is proposed to enhance the herein observed recognition of HPV-PsVs by selected immune cells, leading to their enhanced uptake. This study also confirmed the necessity of "priming" the HPV-PsVs with SP-A prior to infection of target cells in the presence of $CaCl_2$ (Figure 20). Being a C-type lectin, SP-A typically recognises carbohydrate residues; however, the specific pattern and recognition of glycosylated sites on HPV remains enigmatic due to the limited glycoproteins on the HPV surface (298-300). Further investigation into the precise structural elements and functional implications of this interaction is crucial for a deeper understanding of SP-A / HPV dynamics and for the development of potential therapeutic targets against HPV infections.

In contrast to the enhanced uptake of SP-A agglutinated HPV-PsVs into immune cells, particle entry into HaCaT keratinocytes was greatly hindered (Figure 21). This phenomenon was also observed in HeLa and NIKS (Supplementary Figure 4). It is reasonable to assume that the above-described agglutination prevented HPV-PsVs binding to host cellular receptors. This is supported by the observation that HPV45-PsVs formed the smallest fragments in the presence of SP-A (Figure 17) which correlates with its much lower reduction in uptake and infection of HaCaT cells when compared to SP-A coated HPV16-PsVs (Figure 21 and 30, respectively).

As mentioned above, the SP-A mediated increase in HPV-PsVs uptake was only observed for selected immune cell populations: THP-1 monocytes, and THP-1-derived immature DCs showed a significant increase in HPV16-PsVs uptake in the presence of SP-A which was comparable to that of RAW264.7 cells (Figure 19), while entry into the other immune cell populations was not substantially affected. THP-1 monocytes, DC0 and RAW264.7 cells were therefore further explored in their recognition and uptake of other oncogenic HPV types besides the prototype 16. While RAW264.7 displayed increased uptake of the whole HPV-PsVs panel in the presence of SP-A, THP-1 and DC0 were found to only SP-A dependently enhance type 16 entry but showed no differential uptake towards any of the other studied HPV types (Figure 22). This differential response highlights SP-A's distinct potency on viral uptake across cell lines, demonstrating a robust effect on RAW264.7 cells and a more limited influence on THP-1 and DC0. While our focus was on the very initial uptake of particles at 1 hpi, it remains plausible that THP-1 and DC0 cells could potentially exhibit a delayed response to SP-A for HPV types other than type 16 at later time points. This is supported by the observation that infection of HaCaT cells by selected HPV-PsVs types was dampened by THP-1 or DC0 cells, and further reduced in the presence of SP-A (Figure 30), highlighting the necessity for further investigations beyond this early uptake phase.

Overall, SP-A's properties of opsonisation and agglutination play a crucial role in modulating the interactions between HPV-PsVs and various cell types, potentially influencing the immune response against the virus and its ability to infect specific cell populations.

3.2. SP-A alters lysosomal accumulation of HPV-PsVs in keratinocytes and macrophages

Intracellular trafficking of HPV has been explored to identify potential targets for anti-HPV molecule design, with particular focus on understanding and preventing lysosomal escape which is essential for successful infection (101, 275). We were particularly interested in studying lysosomal interaction and accumulation of the prototype HPV16-PsVs in the presence of SP-A and to understand if and how SP-A influences lysosomal processing of the virions within cells. Understanding this interaction may provide insights into how SP-A affects the virus's degradation or survival pathways within lysosomes, offering potential strategies for combating HPV infections.

SP-A has been shown to increase pathogen delivery to lysosomes which are intracellular compartments responsible for breaking down and recycling molecules (282, 301); therefore, we set out to elucidate any potential modulations in lysosome accumulation of HPV when preincubated with SP-A making use of confocal imaging of AF488-labelled HPV16-PsVs and

staining cells for lysosomes using LysoTracker™ Deep Red (Figure 25). When analysing selected colocalisation parameters such as HPV Manders' coefficient and the Pearson's coefficients, we saw both increase in the presence of SP-A suggesting a more pronounced association between HPV-PsVs and lysosomes both in keratinocytes and macrophages. This correlation indicates a potential enhancement in the targeting or trafficking of HPV-PsVs towards lysosomal compartments within these cells. However, we did not observe any changes in the spatial arrangement or the extent of overlap between the signals in these cells in the presence of SP-A, as seen by the overlap coefficient. This suggests that while SP-A appears to enhance the association between HPV-PsVs and lysosomes within keratinocytes and macrophages, it might not significantly alter the physical proximity or closeness of these entities.

These results indicate that in the context of both keratinocytes and macrophages, SP-A may modulate various endocytic pathways, potentially contributing to increased lysosomal accumulation and alterations in lysosomal dynamics with different biological outcomes in these cell types. In macrophages, SP-A might specifically impact lysosomal phagocytosis, a process where macrophages internalise large particles or pathogens by forming phagosomes that fuse with lysosomes for degradation. SP-A's influence on this pathway could enhance the formation of larger lysosomes, possibly due to increased fusion events between phagosomes and lysosomes. This may result in augmented lysosomal accumulation, promoting a more efficient degradation or processing of internalised materials, including HPV particles. In keratinocytes, SP-A's effects on endocytic pathways might involve alterations in general endocytosis or autophagocytosis. Changes in these pathways could lead to the accumulation of larger lysosomes within the cells. While the specific implications are less clear, SP-A's impact on endocytic processes in keratinocytes seems to promote the formation of larger lysosomes, as indicated by increased lysosomal size and accumulation (Figure 25). SP-A's observed ability to induce larger lysosomes and stimulate lysosomal exocytosis, leading to the release of lysosomal content outside the cell, might suggest a broader influence on endocytic trafficking. This could involve alterations in recycling pathways or lysosomal exocytosis mechanisms across both macrophages and keratinocytes. The observed increase in lysosomal accumulation of HPV16-PsVs, larger lysosomes, and lysosomal exocytosis in both cell types in the presence of SP-A implies a multifaceted influence on endocytic processes. However, our analysis does not allow a conclusion as to whether the increased association of HPV-PsVs with lysosomes in the presence of SP-A had consequences for increased capsid degradation or any changes in the L2/vDNA dissociation from these acidic organelles, unlike HD5, an anti-HPV molecule that was shown to prevent the dissociation of the L2/vDNA complex thereby redirecting the viral particles to lysosomes (188).

Access to additional lysosomal markers like LAMP1 and 2, the staining for degrading capsids using the L1-7 antibody, and the labelling of the viral genome could further enhance our understanding of the specific mechanisms governing HPV trafficking, lysosomal dynamics and HPV capsid disassembly in different cell types under the influence of SP-A (302).

3.3. SP-A reduces HPV-PsVs infection of keratinocytes which is further reduced in the presence of immune cells

In an attempt to elucidate the impact of both selected innate immune cell populations and the presence of the innate immune molecule SP-A on HPV-PsVs infection of human keratinocytes, we established a co-culture system which allowed us to study the intricate interactions between different cell types, mirroring the complex interplay during an actual infection scenario.

Supporting our earlier observations of SP-A mediated decreased HPV-PsVs uptake into HaCaT keratinocytes 1 hpi, we also saw decreased infection levels (as measured by Gaussia luciferase reporter gene activity 48 hpi) in HaCaT monocultures in the presence of SP-A. Importantly, we consistently observed a decrease in HaCaT infection for HPV-PsVs types 16, 18, 31, 52, and 58, but not 45, in the presence of SP-A (Figure 30), which might be correlated to the different agglutination patterns observed for the different HPV types in the presence of SP-A as mentioned above.

Co-culturing of selected immune cells alongside HaCaT keratinocytes further reduced their infection by HPV-PsVs to varying extents when pre-coated with SP-A. This synergistic effect seen for some immune cells (particularly RAW264.7 macrophages and THP-1 monocytes) might be due to immune cell-mediated clearance of HPV-PsVs, or due to enhancing the anti-viral environment in the co-culture system. This effect was most pronounced for co-culturing RAW264.7 with HaCaT cells and appeared to be rather specific for HPV type 16. The widespread prevalence of HPV16 may have led to the evolution of a more robust immune response and the development of a highly effective recognition system by immune effectors against HPV16 due to repeated exposures. Additionally, variations in viral antigens might have made HPV16 more immunogenic, further contributing to the evolution of a heightened immune response. Potential immune evasion strategies by HPV16 could have reinforced this evolved immune recognition, while host-specific factors may have also played a role in fostering this heightened response.

These findings highlight the complex interplay of SP-A, immune cells, and their joint effect on HPV infection in a physiologically relevant cellular setting. However, it is important to note that

the co-culture system used here involved the co-culturing of only a single immune cell type per experimental condition and may not encompass the diverse array of immune cells and their interactions found in the human body. Moreover, the focus here was on macrophage populations and DC0 while other innate immune cell populations (such as selected granulocytes) which also potentially respond to SP-A opsonised HPV-PsVs (Figure 8) were not included. Therefore, balancing the benefits and limitations is crucial when interpreting the results derived from co-culture systems. While they offer valuable initial insights into cellular interactions during infection avoiding the use of animal models or primary cells, their constraints must be acknowledged and further complementation using alternative experimental models or clinical data for a comprehensive understanding of HPV is necessary.

3.4. SP-A regulates immune mediator production in the context of HPV infection

In the absence of infection, SP-A primarily functions as an anti-inflammatory molecule (200), contributing to maintaining immune homeostasis by regulating the inflammatory response. SP-A has been observed to dampen excessive immune reactions, acting as a modulator that helps prevent unnecessary inflammation (200). This anti-inflammatory role often involves the suppression of immune cell activation, reduction in pro-inflammatory cytokine production, and the regulation of immune cell functions to maintain a balanced immune environment.

Conversely, in the presence of infection or microbial challenge, SP-A's role shifts towards promoting inflammation and triggering immune responses. When encountering pathogens like viruses, bacteria, or other infectious agents, SP-A functions as a pattern recognition molecule. It binds to these pathogens, initiating signalling pathways that lead to the activation of immune cells and the production of pro-inflammatory cytokines (202). This pro-inflammatory function aims to combat the invading pathogens by recruiting immune cells, enhancing their activity, and orchestrating an effective immune response to eliminate the threat.

The ability of SP-A to switch between anti-inflammatory and pro-inflammatory roles highlights its context-dependent modulation of immune responses. This dynamic behaviour allows SP-A to finely regulate immune reactions, adapting its function based on the presence or absence of infection (200), which is crucial in mounting appropriate immune responses against pathogens while preventing excessive or harmful inflammation. Our research elucidated the SP-A mediated changes in immune modulatory protein expression in the context of HPV16-PsVs immune recognition. THP-1 monocytes and DC0 were again chosen, as a result of their substantial increase in HPV16-PsVs uptake in the presence of SP-A (Figure 19), and their ability to aid in the reduced infection of keratinocytes (Figure 30). While monocytes are highly versatile and can adapt their cytokine and mediator production based on their

microenvironment, DC0 cells are effective antigen presenting cells which also possess the capability to produce cytokines and chemical mediators.

Our overall analysis of relative changes in cytokine, chemokine and growth factor expression using the Proteome Profiler™ Human XL Cytokine Array Kit showed a substantially more potent inflammatory response in DC0 compared to THP-1 cells, with multiple inflammatory mediators being upregulated, when DC0 were exposed to HPV16-PsVs in the presence of SP-A (Figures 34 and 35). STRING analysis indicated an SP-A mediated effect on the upregulation of the JAK-STAT pathway, on macrophage differentiation, neutrophil activation, TNF-signalling, NF-κB-signalling, complement cascade activation, and activation of the Th1 immune response in DC0, highlighting DC's role in bridging innate and adaptive immune responses (Figure 36). Interestingly, many proteins were only upregulated in the SP-A:HPV16-PsVs group, but not by SP-A or HPV16-PsVs alone (Figure 35B), indicating that upon binding to HPV16-PsVs, SP-A drives a heightened immune response towards immune cell activation and pathogen recognition and clearance.

While our study sheds light on SP-A's pivotal role in modulating inflammatory responses in the context of HPV-PsVs exposure, it is essential to acknowledge the inherent limitations of our experimental design. Notably, by using a pseudovirus system our explorations were restricted to the effects of SP-A on immune responses triggered by the initial encounter with these particles which lack any HPV oncogenes. Therefore, our study did not encompass the investigation of HPV E5, E6, and E7 proteins' immune evasion mechanisms and their potential interplay with SP-A-mediated immune modulation. Understanding the intricate ways in which these viral proteins might influence SP-A's impact on inflammatory responses remains an unexplored area. Moreover, we focussed these studies on isolated immune cell populations (THP-1 and DC0, respectively) and did not similarly characterise immune modulator profiles of HaCaT keratinocytes which potentially (but most likely to a lower extent) contribute to immune responses to HPV infection and its potential evasion strategies.

3.5. Potential for SP-A as a component in topical microbicides against HPV infection

SP-A's ability to act as an innate immune molecule recognising and targeting incoming pathogens while modulating immune responses, emphasizes its significance in maintaining immune balance and combating infections while avoiding immune-related pathologies. This is particularly important in the context of infection with HPV as this virus has successfully evolved several immune evasion strategies. Our herein presented data indicate that SP-A is capable to render incoming HPV more visible to the immune system, potentially inhibiting viral infection.

Developing small molecule inhibitors and their incorporation into topical microbicides is a targeted approach in fighting viral infections, particularly those that are sexually transmitted. Vaginal lubricants containing carrageenan have been successfully developed to prevent HPV and HSV-2, but not HIV, infection and are commercially available (150, 151). Our study demonstrating SP-A's interaction with HPV offers potential new avenues for alternative prophylactic means. By identifying which parts of SP-A interact with HPV, possibly through advanced imaging and mutational analysis, small peptide inhibitors could be designed and incorporated into topical lubricants. As isolation of full-length SP-A derived from human sources (as used in this study) is not sustainable, developing small molecules would be more cost-effective and easier to scale up. Established production methods, such as demonstrated for recombinant fragments of human SP-A (rfhSP-A) (199, 303), could pave the way for exploring scaled-up production of biologically active fragments. Harnessing SP-A's inhibitory mechanisms extends beyond HPV to other sexually transmitted infections (STIs), which should be addressed in further studies. This potential broad-spectrum inhibition of various STIs by SP-A and its viability in therapeutic interventions promises a broader impact on infectious disease management.

5 Conclusion

This thesis represents a substantial step forward in unravelling the intricate interactions between SP-A, innate immunity, and HPV infection dynamics. Our exploration has unveiled the versatile nature of SP-A and its significant influence on various aspects of HPV interactions with immune cells and keratinocytes. Importantly, we could show that SP-A is capable in recognising multiple oncogenic HPV types, leading to their agglutination with consequences for increased human innate immune cell uptake, while concurrently impeding viral entry into keratinocytes. This dual action potentially orchestrates immune cell clearance of incoming HPV while limiting viral infection in susceptible cells. Moreover, our studies shed light on SP-A's impact on lysosomal accumulation of HPV-PsVs within keratinocytes and macrophages. This aspect introduces an additional layer of complexity, suggesting that SP-A not only influences viral degradation pathways but also augments immune cell phagocytosis, contributing to potential strategies for viral clearance. Further, our investigations unveiled SP-A's ability to trigger a pro-inflammatory response in innate immune cells upon encountering HPV-PsVs, potentially enhancing their capacity to combat HPV infections. Figure 37 summaries these mechanisms.

In resource-limited settings grappling with HPV-related challenges, effective therapies are urgently needed, given limitations in existing vaccines and the high prevalence of HPV-linked malignancies. Exploring SP-A-associated pathways offers hope for broader protection against diverse HPV types and sexually transmitted infections. Understanding how SP-A influences immune responses, its interactions with HPV evasion strategies, and its modulation of immune cell signalling during HPV recognition stands as crucial avenues for future research in these contexts.

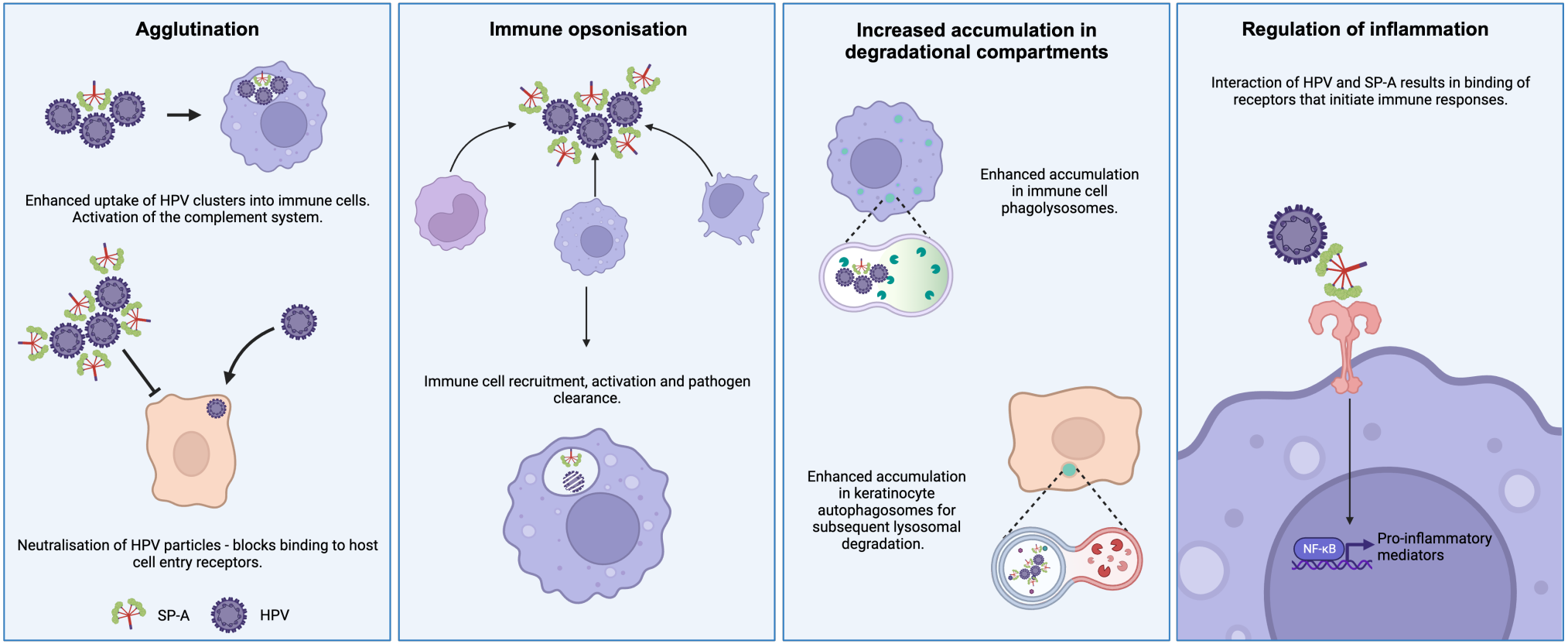

Figure 37: Proposed mechanisms of SP-A immunomodulation in the context of HPV infection. SP-A binds and agglutinates HPV resulting in increased uptake of larger HPV clusters into immune cells, and a decreased uptake into keratinocytes as a result of hindering HPV binding to cell surface receptors. SP-A opsonises HPV resulting in immune cell recruitment, activation and pathogen clearance. SP-A affects intracellular trafficking of HPV, by enhancing accumulation of viral particles in the phagolysosomes of immune cells and redirecting HPV endocytosis to autophagosomes and subsequent lysosomal degradation. SP-A opsonisation of HPV results in SP-A binding to immune cell receptors and subsequent initiation of a proinflammatory response. Image made with BioRender.com.

6 References

1. Carse S, Bergant M, Schäfer G. 2021. Advances in targeting hpv infection as potential alternative prophylactic means. International journal of molecular sciences 22:2201.
2. Burk RD, Harari A, Chen Z. 2013. Human papillomavirus genome variants. Virology 445:232-243.
3. De Villiers E-M, Fauquet C, Broker TR, Bernard H-U, Zur Hausen H. 2004. Classification of papillomaviruses. Virology 324:17-27.
4. Bosch FX, Manos MM, Muñoz N, Sherman M, Jansen AM, Peto J, Schiffman MH, Moreno V, Kurman R, Shan KV. 1995. Prevalence of human papillomavirus in cervical cancer: a worldwide perspective. JNCI: Journal of the National Cancer Institute 87:796-802.
5. de Martel C, Georges D, Bray F, Ferlay J, Clifford GM. 2020. Global burden of cancer attributable to infections in 2018: a worldwide incidence analysis. The Lancet Global Health 8:e180-e190.
6. Plummer M, de Martel C, Vignat J, Ferlay J, Bray F, Franceschi S. 2016. Global burden of cancers attributable to infections in 2012: a synthetic analysis. The Lancet Global Health 4:e609-e616.
7. Muñoz N, Bosch FX, De Sanjosé S, Herrero R, Castellsagué X, Shah KV, Snijders PJ, Meijer CJ. 2003. Epidemiologic classification of human papillomavirus types associated with cervical cancer. New England journal of medicine 348:518-527.
8. Munoz N, Bosch FX, Castellsagué X, Díaz M, De Sanjose S, Hammouda D, Shah KV, Meijer CJ. 2004. Against which human papillomavirus types shall we vaccinate and screen? The international perspective. International journal of cancer 111:278-285.
9. NCI. 2023. HPV and Cancer. National Institutes of Health,
10. Szymonowicz KA, Chen J. 2020. Biological and clinical aspects of HPV-related cancers. Cancer biology & medicine 17:864.
11. Yetimalar H, Kasap B, Cukurova K, Yildiz A, Keklik A, Soylu F. 2012. Cofactors in human papillomavirus infection and cervical carcinogenesis. Archives of gynecology and obstetrics 285:805-810.
12. Castle PE, Giuliano AR. 2003. Chapter 4: Genital Tract Infections, Cervical Inflammation, and Antioxidant Nutrients—Assessing Their Roles as Human Papillomavirus Cofactors. JNCI Monographs 2003:29-34.
13. Castellsagué X, Muñoz N. 2003. Chapter 3: Cofactors in Human Papillomavirus Carcinogenesis—Role of Parity, Oral Contraceptives, and Tobacco Smoking. JNCI Monographs 2003:20-28.
14. Zhao Y, Cao X, Zheng Y, Tang J, Cai W, Wang H, Gao Y, Wang Y. 2012. Relationship between cervical disease and infection with human papillomavirus types 16 and 18, and herpes simplex virus 1 and 2. Journal of medical virology 84:1920-1927.
15. Sung H, Ferlay J, Siegel RL, Laversanne M, Soerjomataram I, Jemal A, Bray F. 2021. Global Cancer Statistics 2020: GLOBOCAN Estimates of Incidence and Mortality Worldwide for 36 Cancers in 185 Countries. CA Cancer J Clin 71:209-249.
16. Bruni L AG, Serrano B, Mena M, Collado JJ, Gómez D, Muñoz J, Bosch FX, de Sanjosé S. 2023. Human Papillomavirus and Related Diseases in South Africa. Summary Report. ICO/IARC Information Centre on HPV and Cancer (HPV Information Centre),
17. De Vuyst H, Alemany L, Lacey C, Chibwesha CJ, Sahasrabuddhe V, Banura C, Denny L, Parham GP. 2013. The burden of human papillomavirus infections and related diseases in sub-saharan Africa. Vaccine 31:F32-F46.
18. Williamson AL. 2015. The interaction between human immunodeficiency virus and human papillomaviruses in heterosexuals in Africa. Journal of clinical medicine 4:579-592.

19. Ujma S, Carse S, Chetty A, Horsnell W, Clark H, Madsen J, Mackay R-M, Watson A, Griffiths M, Katz AA, Schäfer G. 2019. Surfactant Protein A Impairs Genital HPV16 Pseudovirus Infection by Innate Immune Cell Activation in A Murine Model. Pathogens. 8(4):
20. Riera Romo M, Pérez-Martínez D, Castillo Ferrer C. 2016. Innate immunity in vertebrates: an overview. Immunology 148:125-139.
21. Medzhitov R, Janeway Jr CA. 1997. Innate immunity: impact on the adaptive immune response. Current opinion in immunology 9:4-9.
22. Marshall JS, Warrington R, Watson W, Kim HL. 2018. An introduction to immunology and immunopathology. Allergy, Asthma & Clinical Immunology 14:1-10.
23. Aristizábal B, González Á. 2013. Innate immune system, Autoimmunity: From Bench to Bedside El Rosario University Press.
24. Turvey SE, Broide DH. 2010. Innate immunity. Journal of Allergy and Clinical Immunology 125:S24-S32.
25. Geissmann F, Manz MG, Jung S, Sieweke MH, Merad M, Ley K. 2010. Development of monocytes, macrophages, and dendritic cells. Science 327:656-661.
26. Hume DA, Ross IL, Himes SR, Sasmono RT, Wells CA, Ravasi T. 2002. The mononuclear phagocyte system revisited. Journal of leukocyte biology 72:621-627.
27. Hirayama D, Iida T, Nakase H. 2017. The phagocytic function of macrophage-enforcing innate immunity and tissue homeostasis. International journal of molecular sciences 19:92.
28. Pivarcsi A, Kemény L, Dobozy A. 2004. Innate immune functions of the keratinocytes. Acta microbiologica et immunologica Hungarica 51:303-310.
29. Germic N, Frangez Z, Yousefi S, Simon HU. 2019. Regulation of the innate immune system by autophagy: monocytes, macrophages, dendritic cells and antigen presentation. Cell Death & Differentiation 26:715-727.
30. Yunna C, Mengru H, Lei W, Weidong C. 2020. Macrophage M1/M2 polarization. European Journal of Pharmacology 877:173090.
31. Zhang Y, Zou J, Chen R. 2022. An M0 macrophage-related prognostic model for hepatocellular carcinoma. BMC cancer 22:791.
32. Yatim KM, Lakkis FG. 2015. A brief journey through the immune system. Clinical journal of the American Society of Nephrology: CJASN 10:1274.
33. Hume DA. 2006. The mononuclear phagocyte system. Current opinion in immunology 18:49-53.
34. Wilson NS, El-Sukkari D, Villadangos JA. 2004. Dendritic cells constitutively present self antigens in their immature state in vivo and regulate antigen presentation by controlling the rates of MHC class II synthesis and endocytosis. Blood 103:2187-2195.
35. Cella M, Engering A, Pinet V, Pieters J, Lanzavecchia A. 1997. Inflammatory stimuli induce accumulation of MHC class II complexes on dendritic cells. Nature 388:782-787.
36. Tigner A, Ibrahim SA, Murray I. 2020. Histology, white blood cell.
37. Rosales C. 2018. Neutrophil: a cell with many roles in inflammation or several cell types? Frontiers in physiology 9:113.
38. Bochner BS. 2000. Systemic activation of basophils and eosinophils: markers and consequences. Journal of allergy and clinical immunology 106:S292-S302.
39. Leichner T, Kambayashi T. 2014. White Blood Cells and Lymphoid Tissue, Reference Module in Biomedical Sciences. Elsevier.
40. Stone KD, Prussin C, Metcalfe DD. 2010. IgE, mast cells, basophils, and eosinophils. Journal of Allergy and Clinical Immunology 125:S73-S80.
41. Vivier E, Raulet DH, Moretta A, Caligiuri MA, Zitvogel L, Lanier LL, Yokoyama WM, Ugolini S. 2011. Innate or adaptive immunity? The example of natural killer cells. science 331:44-49.
42. Yokoyama WM. 2005. Natural killer cell immune responses. Immunologic research 32:317-325.

43. Bals R, Hiemstra P. 2004. Innate immunity in the lung: how epithelial cells fight against respiratory pathogens. European Respiratory Journal 23:327-333.
44. Piipponen M, Li D, Landén NX. 2020. The immune functions of keratinocytes in skin wound healing. International journal of molecular sciences 21:8790.
45. Sugita K, Kabashima K, Atarashi K, Shimauchi T, Kobayashi M, Tokura Y. 2007. Innate immunity mediated by epidermal keratinocytes promotes acquired immunity involving Langerhans cells and T cells in the skin. Clinical & Experimental Immunology 147:176-183.
46. Cruvinel WdM, Mesquita Júnior D, Araújo JAP, Catelan TTT, Souza AWSd, Silva NPd, Andrade LEC. 2010. Immune system: Part I. Fundamentals of innate immunity with emphasis on molecular and cellular mechanisms of inflammatory response. Revista brasileira de reumatologia 50:434-447.
47. Pasupuleti M, Schmidtchen A, Malmsten M. 2012. Antimicrobial peptides: key components of the innate immune system. Critical reviews in biotechnology 32:143-171.
48. Haagsman HP, Hogenkamp A, Van Eijk M, Veldhuizen EJ. 2008. Surfactant collectins and innate immunity. Neonatology 93:288-294.
49. Rus H, Cudrici C, Niculescu F. 2005. The role of the complement system in innate immunity. Immunologic research 33:103-112.
50. Janeway Jr CA, Travers P, Walport M, Shlomchik MJ. 2001. The complement system and innate immunity, Immunobiology: The Immune System in Health and Disease 5th edition. Garland Science.
51. Han S, Mallampalli RK. 2015. The role of surfactant in lung disease and host defense against pulmonary infections. Annals of the American Thoracic Society 12:765-774.
52. Lawson PR, Reid KB. 2000. The roles of surfactant proteins A and D in innate immunity. Immunological reviews 173:66-78.
53. Ujma S, Horsnell WG, Katz AA, Clark HW, Schäfer G. 2017. Non-pulmonary immune functions of surfactant proteins A and D. Journal of innate immunity 9:3-11.
54. Drummond RA, Brown GD. 2011. The role of Dectin-1 in the host defence against fungal infections. Current opinion in microbiology 14:392-399.
55. Clark EA, Ledbetter JA. 1994. How B and T cells talk to each other. Nature 367:425-428.
56. Newton K, Dixit VM. 2012. Signaling in innate immunity and inflammation. Cold Spring Harbor perspectives in biology 4:a006049.
57. Yamauchi T, Moroishi T. 2019. Hippo pathway in mammalian adaptive immune system. 8:398.
58. Yu L, Majerciak V, Zheng ZM. 2022. HPV16 and HPV18 Genome Structure, Expression, and Post-Transcriptional Regulation. International Journal of Molecular Sciences 23:4943.
59. Books C, Corner E, Geis I, Goodsell D. Molecule of the Month: Human Papillomavirus and Vaccines.
60. O'Connor M, Chan S-Y, Bernard H-U. 1995. Transcription factor binding sites in the long control region of genital HPVs. Human papillomaviruses:21-40.
61. Berg M, Stenlund A. 1997. Functional interactions between papillomavirus E1 and E2 proteins. Journal of Virology 71:3853-3863.
62. Sverdrup F, Khan SA. 1994. Replication of human papillomavirus (HPV) DNAs supported by the HPV type 18 E1 and E2 proteins. Journal of virology 68:505-509.
63. Doorbar J. 2013. The E4 protein; structure, function and patterns of expression. Virology 445:80-98.
64. Pim D, Collins M, Banks L. 1992. Human papillomavirus type 16 E5 gene stimulates the transforming activity of the epidermal growth factor receptor. Oncogene 7:27-32.
65. Oh J-M, Kim S-H, Lee Y-I, Seo M, Kim S-Y, Song Y-S, Kim W-H, Juhnn Y-S. 2008. Human papillomavirus E5 protein induces expression of the EP4 subtype of prostaglandin E2 receptor in cyclic AMP response element-dependent pathways in cervical cancer cells. Carcinogenesis 30:141-149.

66. Ashrafi GH, Haghshenas MR, Marchetti B, O'Brien PM, Campo MS. 2005. E5 protein of human papillomavirus type 16 selectively downregulates surface HLA class I. International journal of cancer 113:276-283.
67. Miura S, Kawana K, Schust DJ, Fujii T, Yokoyama T, Iwasawa Y, Nagamatsu T, Adachi K, Tomio A, Tomio K, Kojima S, Yasugi T, Kozuma S, Taketani Y. 2010. CD1d, a Sentinel Molecule Bridging Innate and Adaptive Immunity, Is Downregulated by the Human Papillomavirus (HPV) E5 Protein: a Possible Mechanism for Immune Evasion by HPV. Journal of Virology 84:11614-11623.
68. Ciesielska U, Nowińska K, Podhorska-Okołów M, Dzięgiel P. 2012. The role of human papillomavirus in the malignant transformation of cervix epithelial cells and the importance of vaccination against this virus. Advances in Clinical and Experimental Medicine 21:235-244.
69. Münger K, Yee CL, Phelps WC, Pietenpol JA, Moses HL, Howley PM. 1991. Biochemical and biological differences between E7 oncoproteins of the high- and low-risk human papillomavirus types are determined by amino-terminal sequences. Journal of Virology 65:3943-3948.
70. Barbosa MS, Vass WC, Lowy DR, Schiller JT. 1991. In vitro biological activities of the E6 and E7 genes vary among human papillomaviruses of different oncogenic potential. Journal of Virology 65:292-298.
71. Đukić A, Lulić L, Thomas M, Skelin J, Bennett Saidu NE, Grce M, Banks L, Tomaić V. 2020. HPV Oncoproteins and the Ubiquitin Proteasome System: A Signature of Malignancy? Pathogens 9:133.
72. Narisawa-Saito M, Kiyono T. 2007. Basic mechanisms of high-risk human papillomavirus-induced carcinogenesis: roles of E6 and E7 proteins. Cancer science 98:1505-1511.
73. Gonzalez SL, Stremlau M, He X, Basile JR, Münger K. 2001. Degradation of the retinoblastoma tumor suppressor by the human papillomavirus type 16 E7 oncoprotein is important for functional inactivation and is separable from proteasomal degradation of E7. J Virol 75:7583-91.
74. Dyson N, Howley PM, Münger K, Harlow E. 1989. The human papilloma virus-16 E7 oncoprotein is able to bind to the retinoblastoma gene product. Science 243:934-937.
75. Chellappan S, Kraus VB, Kroger B, Munger K, Howley PM, Phelps W, Nevins J. 1992. Adenovirus E1A, simian virus 40 tumor antigen, and human papillomavirus E7 protein share the capacity to disrupt the interaction between transcription factor E2F and the retinoblastoma gene product. Proceedings of the National Academy of Sciences 89:4549-4553.
76. Dreer M, van de Poel S, Stubenrauch F. 2017. Control of viral replication and transcription by the papillomavirus E8^ E2 protein. Virus Research 231:96-102.
77. Stubenrauch F, Zobel T, Iftner T. 2001. The E8 Domain Confers a Novel Long-Distance Transcriptional Repression Activity on the E8^E2C Protein of High-Risk Human Papillomavirus Type 31. Journal of Virology 75:4139-4149.
78. Chow LT, Broker TR, Steinberg BM. 2010. The natural history of human papillomavirus infections of the mucosal epithelia. Apmis 118:422-449.
79. Buck CB, Cheng N, Thompson CD, Lowy DR, Steven AC, Schiller JT, Trus BL. 2008. Arrangement of L2 within the Papillomavirus Capsid. Journal of Virology 82:5190-5197.
80. Goetschius DJ, Hartmann SR, Subramanian S, Bator CM, Christensen ND, Hafenstein SL. 2021. High resolution cryo EM analysis of HPV16 identifies minor structural protein L2 and describes capsid flexibility. Scientific Reports 11:3498.
81. Wang JW, Roden RB. 2013. L2, the minor capsid protein of papillomavirus. Virology 445:175-186.
82. Stanley M. 2010. HPV-immune response to infection and vaccination. Infectious agents and cancer 5:1-6.

83. Ozbun MA. 2019. Extracellular events impacting human papillomavirus infections: Epithelial wounding to cell signaling involved in virus entry. Papillomavirus research 7:188-192.
84. Roberts JN, Buck CB, Thompson CD, Kines R, Bernardo M, Choyke PL, Lowy DR, Schiller JT. 2007. Genital transmission of HPV in a mouse model is potentiated by nonoxynol-9 and inhibited by carrageenan. Nature medicine 13:857-861.
85. Ozbun MA, Bondu V, Patterson NA, Sterk RT, Waxman AG, Bennett EC, McKee R, Sharma A, Yarwood J, Rogers M. 2021. Infectious titres of human papillomaviruses (HPVs) in patient lesions, methodological considerations in evaluating HPV infectivity and implications for the efficacy of high-level disinfectants. EBioMedicine 63.
86. Becker M, Greune L, Schmidt MA, Schelhaas M. 2018. Extracellular conformational changes in the capsid of human papillomaviruses contribute to asynchronous uptake into host cells. Journal of virology 92:e02106-17.
87. Broniarczyk J, Ring N, Massimi P, Giacca M, Banks L. 2018. HPV-16 virions can remain infectious for 2 weeks on senescent cells but require cell cycle re-activation to allow virus entry. Scientific Reports 8:811.
88. Ozbun MA, Campos SK. 2021. The long and winding road: Human papillomavirus entry and subcellular trafficking. Current Opinion in Virology 50:76-86.
89. Schäfer G, Blumenthal MJ, Katz AA. 2015. Interaction of human tumor viruses with host cell surface receptors and cell entry. Viruses 7:2592-2617.
90. Shafti-Keramat S, Handisurya A, Kriehuber E, Meneguzzi G, Slupetzky K, Kirnbauer R. 2003. Different Heparan Sulfate Proteoglycans Serve asCellular Receptors for HumanPapillomaviruses. Journal of virology 77:13125-13135.
91. Culp TD, Budgeon LR, Christensen ND. 2006. Human papillomaviruses bind a basal extracellular matrix component secreted by keratinocytes which is distinct from a membrane-associated receptor. Virology 347:147-159.
92. Cerqueira C, Samperio Ventayol P, Vogeley C, Schelhaas M. 2015. Kallikrein-8 proteolytically processes human papillomaviruses in the extracellular space to facilitate entry into host cells. Journal of virology 89:7038-7052.
93. Bienkowska-Haba M, Patel HD, Sapp M. 2009. Target cell cyclophilins facilitate human papillomavirus type 16 infection. PLoS pathogens 5:e1000524.
94. Richards RM, Lowy DR, Schiller JT, Day PM. 2006. Cleavage of the papillomavirus minor capsid protein, L2, at a furin consensus site is necessary for infection. Proceedings of the National Academy of Sciences 103:1522-1527.
95. Selinka H-C, Florin L, Patel HD, Freitag K, Schmidtke M, Makarov VA, Sapp M. 2007. Inhibition of transfer to secondary receptors by heparan sulfate-binding drug or antibody induces noninfectious uptake of human papillomavirus. Journal of virology 81:10970-10980.
96. Dziduszko A, Ozbun MA. 2013. Annexin A2 and S100A10 Regulate Human Papillomavirus Type 16 Entry and Intracellular Trafficking in Human Keratinocytes. Journal of Virology 87:7502-7515.
97. Woodham AW, Da Silva DM, Skeate JG, Raff AB, Ambroso MR, Brand HE, Isas JM, Langen R, Kast WM. 2012. The S100A10 subunit of the annexin A2 heterotetramer facilitates L2-mediated human papillomavirus infection.
98. Bharadwaj A, Bydoun M, Holloway R, Waisman D. 2013. Annexin A2 Heterotetramer: Structure and Function. International Journal of Molecular Sciences 14:6259-6305.
99. Schiller JT, Day PM, Kines RC. 2010. Current understanding of the mechanism of HPV infection. Gynecologic oncology 118:S12-S17.
100. Schelhaas M, Shah B, Holzer M, Blattmann P, Kühling L, Day PM, Schiller JT, Helenius A. 2012. Entry of human papillomavirus type 16 by actin-dependent, clathrin-and lipid raft-independent endocytosis. PLoS pathogens 8:e1002657.
101. Siddiqa A, Broniarczyk J, Banks L. 2018. Papillomaviruses and endocytic trafficking. International journal of molecular sciences 19:2619.
102. Aydin I, Weber S, Snijder B, Samperio Ventayol P, Kühbacher A, Becker M, Day PM, Schiller JT, Kann M, Pelkmans L. 2014. Large scale RNAi reveals the requirement of

nuclear envelope breakdown for nuclear import of human papillomaviruses. PLoS pathogens 10:e1004162.
103. Broniarczyk J, Massimi P, Pim D, Bergant Marušič M, Myers MP, Garcea RL, Banks L. 2019. Phosphorylation of human papillomavirus type 16 L2 contributes to efficient virus infectious entry. Journal of Virology 93:10.1128/jvi. 00128-19.
104. Kirnbauer R, Booy F, Cheng N, Lowy D, Schiller J. 1992. Papillomavirus L1 major capsid protein self-assembles into virus-like particles that are highly immunogenic. Proceedings of the National Academy of Sciences 89:12180-12184.
105. Doorbar J. 2005. The papillomavirus life cycle. Journal of clinical virology 32:7-15.
106. Pinatti L, Walline H, Carey T. 2018. Human papillomavirus genome integration and head and neck cancer. Journal of dental research 97:691-700.
107. Wentzensen N, Vinokurova S, Doeberitz MvK. 2004. Systematic review of genomic integration sites of human papillomavirus genomes in epithelial dysplasia and invasive cancer of the female lower genital tract. Cancer research 64:3878-3884.
108. Bodelon C, Untereiner ME, Machiela MJ, Vinokurova S, Wentzensen N. 2016. Genomic characterization of viral integration sites in HPV-related cancers. International journal of cancer 139:2001-2011.
109. McBride AA. 2017. Playing with fire: consequences of human papillomavirus DNA replication adjacent to genetically unstable regions of host chromatin. Current Opinion in Virology 26:63-68.
110. Moody CA, Laimins LA. 2010. Human papillomavirus oncoproteins: pathways to transformation. Nature Reviews Cancer 10:550-560.
111. Zhou C, Tuong ZK, Frazer IH. 2019. Papillomavirus immune evasion strategies target the infected cell and the local immune system. Frontiers in oncology 9:682.
112. Roden RBS, Stern PL. 2018. Opportunities and challenges for human papillomavirus vaccination in cancer. Nature Reviews Cancer 18:240-254.
113. Stanley M. 2006. Immune responses to human papillomavirus. Vaccine 24:S16-S22.
114. Stanley M. 2008. Immunobiology of HPV and HPV vaccines. Gynecologic oncology 109:S15-S21.
115. Stanley MA. 2012. Epithelial cell responses to infection with human papillomavirus. Clinical microbiology reviews 25:215-222.
116. Arend WP, Palmer G, Gabay C. 2008. IL-1, IL-18, and IL-33 families of cytokines. Immunological reviews 223:20-38.
117. Carter JJ, Koutsky LA, Wipf GC, Christensen ND, Lee S-K, Kuypers J, Kiviat N, Galloway DA. 1996. The natural history of human papillomavirus type 16 capsid antibodies among a cohort of university women. Journal of Infectious Diseases 174:927-936.
118. Park J-S, Kim E-J, Kwon H-J, Hwang E-S, Namkoong S-E, Um S-J. 2000. Inactivation of interferon regulatory factor-1 tumor suppressor protein by HPV E7 oncoprotein: implication for the E7-mediated immune evasion mechanism in cervical carcinogenesis. Journal of Biological Chemistry 275:6764-6769.
119. Karim R, Tummers B, Meyers C, Biryukov JL, Alam S, Backendorf C, Jha V, Offringa R, van Ommen G-JB, Melief CJ. 2013. Human papillomavirus (HPV) upregulates the cellular deubiquitinase UCHL1 to suppress the keratinocyte's innate immune response. PLoS pathogens 9:e1003384.
120. Niebler M, Qian X, Höfler D, Kogosov V, Kaewprag J, Kaufmann AM, Ly R, Böhmer G, Zawatzky R, Rösl F. 2013. Post-translational control of IL-1β via the human papillomavirus type 16 E6 oncoprotein: a novel mechanism of innate immune escape mediated by the E3-ubiquitin ligase E6-AP and p53. PLoS pathogens 9:e1003536.
121. Cicchini L, Westrich JA, Xu T, Vermeer DW, Berger JN, Clambey ET, Lee D, Song JI, Lambert PF, Greer RO. 2016. Suppression of antitumor immune responses by human papillomavirus through epigenetic downregulation of CXCL14. MBio 7:e00270-16.
122. Shellenberger TD, Wang M, Gujrati M, Jayakumar A, Strieter RM, Burdick MD, Ioannides CG, Efferson CL, El-Naggar AK, Roberts D. 2004. BRAK/CXCL14 is a

potent inhibitor of angiogenesis and a chemotactic factor for immature dendritic cells. Cancer research 64:8262-8270.
123. Starnes T, Rasila KK, Robertson MJ, Brahmi Z, Dahl R, Christopherson K, Hromas R. 2006. The chemokine CXCL14 (BRAK) stimulates activated NK cell migration: implications for the downregulation of CXCL14 in malignancy. Experimental hematology 34:1101-1105.
124. Li H, Ou X, Xiong J, Wang T. 2006. HPV16E7 mediates HADC chromatin repression and downregulation of MHC class I genes in HPV16 tumorigenic cells through interaction with an MHC class I promoter. Biochemical and biophysical research communications 349:1315-1321.
125. Georgopoulos NT, Proffitt JL, Blair GE. 2000. Transcriptional regulation of the major histocompatibility complex (MHC) class I heavy chain, TAP1 and LMP2 genes by the human papillomavirus (HPV) type 6b, 16 and 18 E7 oncoproteins. Oncogene 19:4930-4935.
126. Konopnicki D, De Wit S, Clumeck N. 2013. HPV and HIV coinfection: a complex interaction resulting in epidemiological, clinical and therapeutic implications. Future Virology 8:903-915.
127. Williamson A-L. 2015. The interaction between human immunodeficiency virus and human papillomaviruses in heterosexuals in Africa. Journal of clinical medicine 4:579-592.
128. Doorbar J. 2023. The human Papillomavirus twilight zone – Latency, immune control and subclinical infection. Tumour Virus Research 16:200268.
129. Siddiqui MAA, Perry CM. 2006. Human papillomavirus quadrivalent (types 6, 11, 16, 18) recombinant vaccine (Gardasil®). Drugs 66:1263-1271.
130. Monie A, Hung C-F, Roden R, Wu TC. 2008. Cervarix™: a vaccine for the prevention of HPV 16, 18-associated cervical cancer. Biologics: Targets and Therapy 2:107-113.
131. Zhai L, Tumban E. 2016. Gardasil-9: A global survey of projected efficacy. Antiviral research 130:101-109.
132. BioPharm W. 2020. Cecolin. https://www.ystwt.cn/cecolin/. Accessed 8 Ferbruary 2024.
133. Pham CT, Juhasz M, Sung CT, Mesinkovska NA. 2020. The human papillomavirus vaccine as a treatment for human papillomavirus–related dysplastic and neoplastic conditions: A literature review. Journal of the American Academy of Dermatology 82:202-212.
134. Palefsky J. 2006. Biology of HPV in HIV Infection. Advances in Dental Research 19:99-105.
135. Delany-Moretlwe S, Kelley KF, James S, Scorgie F, Subedar H, Dlamini NR, Pillay Y, Naidoo N, Chikandiwa A, Rees H. 2018. Human Papillomavirus Vaccine Introduction in South Africa: Implementation Lessons From an Evaluation of the National School-Based Vaccination Campaign. Global Health: Science and Practice 6:425-438.
136. Sharma K, Machalek DA, Toh ZQ, Amenu D, Muchengeti M, Ndlovu AK, Mremi A, Mchome B, Vallely AJ, Denny L. 2023. No woman left behind: achieving cervical cancer elimination among women living with HIV. The Lancet HIV 10:e412-e420.
137. Denny L. 2015. Control of cancer of the cervix in low-and middle-income countries. Annals of surgical oncology 22:728-733.
138. Amzat J, Kanmodi KK, Aminu K, Egbedina EA. 2023. School-Based Interventions on Human Papillomavirus in Africa: A Systematic Scoping Review. Venereology 2:43-58.
139. Milondzo T, Meyer JC, Dochez C, Burnett RJ. 2022. Human papillomavirus vaccine hesitancy highly evident among caregivers of girls attending South African private schools. Vaccines 10:503.
140. Tathiah N, Naidoo M, Moodley I. 2015. Human papillomavirus (HPV) vaccination of adolescents in the South African private health sector: Lessons from the HPV demonstration project in KwaZulu-Natal. South African Medical Journal 105:954-954.

141. Ngcobo N, Burnett R, Cooper S, Wiysonge C. 2019. Human papillomavirus vaccination acceptance and hesitancy in South Africa: Research and policy agenda. South African Medical Journal 109:13-15.
142. Ledibane TD, Ledibane NR, Matlala M. 2023. Performance of the school-based human papillomavirus vaccine uptake in Tshwane, South Africa. Southern African Journal of Infectious Diseases 38:1-6.
143. Amponsah-Dacosta E, Blose N, Nkwinika VV, Chepkurui V. 2022. Human papillomavirus vaccination in South Africa: programmatic challenges and opportunities for integration with other adolescent health services? Frontiers in Public Health 10:799984.
144. WHO, UNICEF. 2023. Joint Reporting Form on HPV Immunization.
145. Boily M-C, Barnabas RV, Rönn MM, Bayer CJ, van Schalkwyk C, Soni N, Rao DW, Staadegaard L, Liu G, Silhol R. 2022. Estimating the effect of HIV on cervical cancer elimination in South Africa: Comparative modelling of the impact of vaccination and screening. EClinicalMedicine 54.
146. Christensen N, Kreider J, Cladel N, Patrick S, Welsh P. 1990. Monoclonal antibody-mediated neutralization of infectious human papillomavirus type 11. Journal of Virology 64:5678-5681.
147. Christensen ND, Cladel NM, Reed CA. 1995. Postattachment neutralization of papillomaviruses by monoclonal and polyclonal antibodies. Virology 207:136-142.
148. Howett M, Neely E, Christensen N, Wigdahl B, Krebs F, Malamud D, Patrick S, Pickel M, Welsh P, Reed C. 1999. A broad-spectrum microbicide with virucidal activity against sexually transmitted viruses. Antimicrobial agents and chemotherapy 43:314-321.
149. Howett M, Wigdahl B, Malamud D, Christensen N, Wyrick P, Krebs F, Catalone B. 2000. Alkyl sulfates: a new family of broad spectrum microbicides, abstr 13th International AIDS Conference
150. Magnan S, Tota J, El-Zein M, Burchell A, Schiller J, Ferenczy A, Tellier P-P, Coutlee F, Franco E, Rodrigues A. 2019. Efficacy of a Carrageenan gel Against Transmission of Cervical HPV (CATCH): Interim analysis of a randomized, double-blind, placebo-controlled, phase 2B trial. Clinical Microbiology and Infection 25:210-216.
151. Perino A, Consiglio P, Maranto M, De Franciscis P, Marci R, Restivo V, Manzone M, Capra G, Cucinella G, Calagna G. 2019. Impact of a new carrageenan-based vaginal microbicide in a female population with genital HPV-infection: first experimental results. European Review for Medical & Pharmacological Sciences 23.
152. Calagna G, Maranto M, Paola C, Capra G, Perino A, Chiantera V, Cucinella G. 2020. 'Secondary prevention'against female HPV infection: literature review of the role of carrageenan. Expert Review of Anti-infective Therapy 18:865-874.
153. Buck CB, Thompson CD, Roberts JN, Müller M, Lowy DR, Schiller JT. 2006. Carrageenan is a potent inhibitor of papillomavirus infection. PLoS pathogens 2:e69.
154. Carlucci MJ, Scolaro LA, Noseda MD, Cerezo AS, Damonte EB. 2004. Protective effect of a natural carrageenan on genital herpes simplex virus infection in mice. Antiviral Research 64:137-141.
155. McLean CA, van de Wijgert JHHM, Jones HE, Karon JM, McNicoll JM, Whitehead SJ, Braunstein S, Achalapong J, Chaikummao S, Tappero JW, Markowitz LE, Kilmarx PH. 2010. HIV genital shedding and safety of Carraguard use by HIV-infected women: a crossover trial in Thailand. AIDS 24.
156. Skoler-Karpoff S, Ramjee G, Ahmed K, Altini L, Plagianos MG, Friedland B, Govender S, De Kock A, Cassim N, Palanee T. 2008. Efficacy of Carraguard for prevention of HIV infection in women in South Africa: a randomised, double-blind, placebo-controlled trial. The Lancet 372:1977-1987.
157. Derby N, Lal M, Aravantinou M, Kizima L, Barnable P, Rodriguez A, Lai M, Wesenberg A, Ugaonkar S, Levendosky K, Mizenina O, Kleinbeck K, Lifson JD, Peet MM, Lloyd Z, Benson M, Heneine W, O'Keefe BR, Robbiani M, Martinelli E, Grasperge B, Blanchard J, Gettie A, Teleshova N, Fernández-Romero JA, Zydowsky TM. 2018.

Griffithsin carrageenan fast dissolving inserts prevent SHIV HSV-2 and HPV infections in vivo. Nature Communications 9:3881.
158. Kizima L, Rodriguez A, Kenney J, Derby N, Mizenina O, Menon R, Seidor S, Zhang S, Levendosky K, Jean-Pierre N. 2014. A potent combination microbicide that targets SHIV-RT, HSV-2 and HPV. Plos one 9:e94547.
159. Drobni P, Mistry N, McMillan N, Evander M. 2003. Carboxy-fluorescein diacetate, succinimidyl ester labeled papillomavirus virus-like particles fluoresce after internalization and interact with heparan sulfate for binding and entry. Virology 310:163-172.
160. Joyce JG, Tung J-S, Przysiecki CT, Cook JC, Lehman ED, Sands JA, Jansen KU, Keller PM. 1999. The L1 major capsid protein of human papillomavirus type 11 recombinant virus-like particles interacts with heparin and cell-surface glycosaminoglycans on human keratinocytes. Journal of Biological Chemistry 274:5810-5822.
161. Herold BC, Bourne N, Marcellino D, Kirkpatrick R, Strauss DM, Zaneveld LJ, Waller DP, Anderson RA, Chany CJ, Barham BJ. 2000. Poly (sodium 4-styrene sulfonate): an effective candidate topical antimicrobial for the prevention of sexually transmitted diseases. The Journal of infectious diseases 181:770-773.
162. Herold BC, Siston A, Bremer J, Kirkpatrick R, Wilbanks G, Fugedi P, Peto C, Cooper M. 1997. Sulfated carbohydrate compounds prevent microbial adherence by sexually transmitted disease pathogens. Antimicrobial agents and chemotherapy 41:2776-2780.
163. Lembo D, Donalisio M, Rusnati M, Bugatti A, Cornaglia M, Cappello P, Giovarelli M, Oreste P, Landolfo S. 2008. Sulfated K5 Escherichia coli polysaccharide derivatives as wide-range inhibitors of genital types of human papillomavirus. Antimicrobial agents and chemotherapy 52:1374-1381.
164. Wang S, Lu Z, Wang S, Liu W, Gao J, Tian L, Wang L, Zhang X, Zhao X, Wang W. 2020. The inhibitory effects and mechanisms of polymannuroguluronate sulfate against human papillomavirus infection in vitro and in vivo. Carbohydrate polymers 241:116365.
165. Christensen ND, Reed CA, Culp TD, Hermonat PL, Howett MK, Anderson RA, Zaneveld LJ. 2001. Papillomavirus microbicidal activities of high-molecular-weight cellulose sulfate, dextran sulfate, and polystyrene sulfonate. Antimicrobial agents and chemotherapy 45:3427-3432.
166. Drobni P, Näslund J, Evander M. 2004. Lactoferrin inhibits human papillomavirus binding and uptake in vitro. Antiviral research 64:63-68.
167. Mistry N, Drobni P, Näslund J, Sunkari VG, Jenssen H, Evander M. 2007. The anti-papillomavirus activity of human and bovine lactoferricin. Antiviral research 75:258-265.
168. Donalisio M, Rusnati M, Civra A, Bugatti A, Allemand D, Pirri G, Giuliani A, Landolfo S, Lembo D. 2010. Identification of a dendrimeric heparan sulfate-binding peptide that inhibits infectivity of genital types of human papillomaviruses. Antimicrobial agents and chemotherapy 54:4290-4299.
169. Schmidtke M, Karger A, Meerbach A, Egerer R, Stelzner A, Makarov V. 2003. Binding of a N, N′-bisheteryl derivative of dispirotripiperazine to heparan sulfate residues on the cell surface specifically prevents infection of viruses from different families. Virology 311:134-143.
170. Andersen JH, Jenssen H, Gutteberg TJ. 2003. Lactoferrin and lactoferricin inhibit Herpes simplex 1 and 2 infection and exhibit synergy when combined with acyclovir. Antiviral research 58:209-215.
171. Van der Strate B, Beljaars L, Molema G, Harmsen M, Meijer D. 2001. Antiviral activities of lactoferrin. Antiviral research 52:225-239.
172. Bon I, Lembo D, Rusnati M, Clo A, Morini S, Miserocchi A, Bugatti A, Grigolon S, Musumeci G, Landolfo S. 2013. Peptide-derivatized SB105-A10 dendrimer inhibits the

infectivity of R5 and X4 HIV-1 strains in primary PBMCs and cervicovaginal histocultures. PLoS One 8:e76482.
173. Sepúlveda-Crespo D, Ceña-Díez R, Jiménez JL, Ángeles Muñoz-Fernández M. 2017. Mechanistic studies of viral entry: An overview of dendrimer-based microbicides as entry inhibitors against both HIV and HSV-2 overlapped infections. Medicinal research reviews 37:149-179.
174. Luganini A, Nicoletto SF, Pizzuto L, Pirri G, Giuliani A, Landolfo S, Gribaudo G. 2011. Inhibition of herpes simplex virus type 1 and type 2 infections by peptide-derivatized dendrimers. Antimicrobial agents and chemotherapy 55:3231-3239.
175. Ito M, Baba M, Sato A, Pauwels R, De Clercq E, Shigeta S. 1987. Inhibitory effect of dextran sulfate and heparin on the replication of human immunodeficiency virus (HIV) in vitro. Antiviral research 7:361-367.
176. Rider CC. 1997. The potential for heparin and its derivatives in the therapy and prevention of HIV-1 infection. Glycoconjugate journal 14:639-642.
177. Howell A, Taylor T, Miller J, Groveman D, Eccles E, Zacharski L. 1996. Inhibition of HIV-1 infectivity by low molecular weight heparin: Results of in vitro studies and a pilot clinical trial in patients with advanced AIDS. International Journal of Clinical and Laboratory Research 26:124-131.
178. Piret J, Lamontagne J, Bestman-Smith J, Roy S, Gourde P, Désormeaux A, Omar RF, Juhász J, Bergeron MG. 2000. In vitro and in vivo evaluations of sodium lauryl sulfate and dextran sulfate as microbicides against herpes simplex and human immunodeficiency viruses. Journal of clinical microbiology 38:110-119.
179. Anderson RA, Feathergill K, X D, Cooper M, Kirkpatrick R, Spear P, Waller DP, Chany CJ, Doncel GF, Herold BC. 2000. Evaluation of Poly (Styrene-4-Sulfonate) as a Preventive Agent for Conception and Sexually Transmitted Diseases. Journal of andrology 21:862-875.
180. Thuy TTT, Ly BM, Van TTT, Van Quang N, Tu HC, Zheng Y, Seguin-Devaux C, Mi B, Ai U. 2015. Anti-HIV activity of fucoidans from three brown seaweed species. Carbohydrate polymers 115:122-128.
181. Sinha S, Astani A, Ghosh T, Schnitzler P, Ray B. 2010. Polysaccharides from Sargassum tenerrimum: Structural features, chemical modification and anti-viral activity. Phytochemistry 71:235-242.
182. Hua C, Zhu Y, Wu C, Si L, Wang Q, Sui L, Jiang S. 2019. The underlying mechanism of 3-hydroxyphthalic anhydride-modified bovine beta-lactoglobulin to block human papillomavirus entry into the host cell. Frontiers in Microbiology 10:2188.
183. Guo X, Qiu L, Wang Y, Wang Y, Wang Q, Song L, Li Y, Huang K, Du X, Fan W. 2016. A randomized open-label clinical trial of an anti-HPV biological dressing (JB01-BD) administered intravaginally to treat high-risk HPV infection. Microbes and Infection 18:148-152.
184. Neurath AR, Debnath AK, Strick N, Li YY, Lin K, Jiang S. 1995. Blocking of CD4 cell receptors for the human immunodeficiency virus type 1 (HIV-1) by chemically modified bovine milk proteins: Potential for AIDS prophylaxis. Journal of Molecular Recognition 8:304-316.
185. Neurath A, Strick N, Li Y. 1998. 3-Hydroxyphthaloyl β-lactoglobulin. III. Antiviral activity against herpesviruses. Antiviral Chemistry and Chemotherapy 9:177-184.
186. Kokuba H, Aurelian L, Neurath A. 1998. 3-Hydroxyphthaloyl β-lactoglobulin. IV. Antiviral activity in the mouse model of genital herpesvirus infection. Antiviral Chemistry and Chemotherapy 9:69-79.
187. Müller KH, Spoden GA, Scheffer KD, Brunnhöfer R, De Brabander JK, Maier ME, Florin L, Muller CP. 2014. Inhibition by cellular vacuolar ATPase impairs human papillomavirus uncoating and infection. Antimicrobial agents and chemotherapy 58:2905-2911.
188. Wiens ME, Smith JG. 2017. α-Defensin HD5 inhibits human papillomavirus 16 infection via capsid stabilization and redirection to the lysosome. MBio 8:10.1128/mbio. 02304-16.

189. Gulati NM, Miyagi M, Wiens ME, Smith JG, Stewart PL. 2019. α-Defensin HD5 stabilizes human papillomavirus 16 capsid/core interactions. Pathogens and Immunity 4:196.
190. Huang H-S, Buck CB, Lambert PF. 2010. Inhibition of gamma secretase blocks HPV infection. Virology 407:391-396.
191. Karanam B, Peng S, Li T, Buck C, Day PM, Roden RB. 2010. Papillomavirus infection requires γ secretase. Journal of virology 84:10661-10670.
192. Lipovsky A, Erden A, Kanaya E, Zhang W, Crite M, Bradfield C, MacMicking J, DiMaio D, Schoggins JW, Iwasaki A. 2017. The cellular endosomal protein stannin inhibits intracellular trafficking of human papillomavirus during virus entry. The Journal of General Virology 98:2821.
193. Lee S-J, Yang A, Wu T-C, Hung C-F. 2016. Immunotherapy for human papillomavirus-associated disease and cervical cancer: review of clinical and translational research. Journal of gynecologic oncology 27.
194. Mo Y, Ma J, Zhang H, Shen J, Chen J, Hong J, Xu Y, Qian C. 2022. Prophylactic and therapeutic HPV vaccines: current scenario and perspectives. Front Cell Infect Microbiol. 2022; 12: 909223.
195. Shen K-Y, Song Y-C, Chen I-H, Chong P, Liu S-J. 2014. Depletion of tumor-associated macrophages enhances the anti-tumor immunity induced by a Toll-like receptor agonist-conjugated peptide. Human Vaccines & Immunotherapeutics 10:3241-3250.
196. Lescaille G, Pitoiset F, Macedo R, Baillou C, Huret C, Klatzmann D, Tartour E, Lemoine FM, Bellier B. 2013. Efficacy of DNA vaccines forming e7 recombinant retroviral virus-like particles for the treatment of human papillomavirus-induced cancers. Human gene therapy 24:533-544.
197. Sajadian A, Tabarraei A, Soleimanjahi H, Fotouhi F, Gorji A, Ghaemi A. 2014. Comparing the effect of Toll-like receptor agonist adjuvants on the efficiency of a DNA vaccine. Archives of virology 159:1951-1960.
198. Garçon N, Morel S, Didierlaurent A, Descamps D, Wettendorff M, Van Mechelen M. 2011. Development of an AS04-adjuvanted HPV vaccine with the adjuvant system approach. BioDrugs 25:217-226.
199. Watson A, Sørensen GL, Holmskov U, Whitwell HJ, Madsen J, Clark H. 2020. Generation of novel trimeric fragments of human SP-A and SP-D after recombinant soluble expression in E. coli. Immunobiology 225:151953.
200. Kishore U, Greenhough TJ, Waters P, Shrive AK, Ghai R, Kamran MF, Bernal AL, Reid KB, Madan T, Chakraborty T. 2006. Surfactant proteins SP-A and SP-D: structure, function and receptors. Molecular immunology 43:1293-1315.
201. Wright JR. 2005. Immunoregulatory functions of surfactant proteins. Nature Reviews Immunology 5:58-68.
202. Watson A, Madsen J, Clark HW. 2021. SP-A and SP-D: dual functioning immune molecules with antiviral and immunomodulatory properties. Frontiers in Immunology 11:622598.
203. Vieira F, Kung JW, Bhatti F. 2017. Structure, genetics and function of the pulmonary associated surfactant proteins A and D: The extra-pulmonary role of these C type lectins. Annals of Anatomy-Anatomischer Anzeiger 211:184-201.
204. McIntosh JC, Swyers AH, Fisher JH, Wright JR. 1996. Surfactant proteins A and D increase in response to intratracheal lipopolysaccharide. American journal of respiratory cell and molecular biology 15:509-519.
205. Ghildyal R, Hartley C, Varrasso A, Meanger J, Voelker DR, Anders EM, Mills J. 1999. Surfactant protein A binds to the fusion glycoprotein of respiratory syncytial virus and neutralizes virion infectivity. Journal of Infectious Diseases 180:2009-2013.
206. Hartshorn KL, White MR, Shepherd V, Reid K, Jensenius JC, Crouch E. 1997. Mechanisms of anti-influenza activity of surfactant proteins A and D: comparison with serum collectins. American Journal of Physiology-Lung Cellular and Molecular Physiology 273:L1156-L1166.

207. Hartshorn KL, Crouch E, White MR, Colamussi ML, Kakkanatt A, Tauber B, Shepherd V, Sastry KN. 1998. Pulmonary surfactant proteins A and D enhance neutrophil uptake of bacteria. American Journal of Physiology-Lung Cellular and Molecular Physiology 274:L958-L969.
208. Gaynor CD, Mccormack FX, Voelker DR, Mcgowan SE, Schlesinger LS. 1995. Pulmonary surfactant protein A mediates enhanced phagocytosis of Mycobacterium tuberculosis by a direct interaction with human macrophages. Journal of immunology (Baltimore, Md: 1950) 155:5343-5351.
209. McDonough K, Kress Y, Bloom B. 1993. The interaction of Mycobacterium tuberculosis with macrophages: a study of phagolysosome fusion. Infectious agents and disease 2:232-235.
210. LeVine AM, Kurak KE, Bruno MD, Stark JM, Whitsett JA, Korfhagen TR. 1998. Surfactant protein-A-deficient mice are susceptible to Pseudomonas aeruginosa infection. American journal of respiratory cell and molecular biology 19:700-708.
211. Simoons-Smit A, Kraan E, Beishuizen A, van Schijndel RS, Vandenbroucke-Grauls C. 2006. Herpes simplex virus type 1 and respiratory disease in critically-ill patients: real pathogen or innocent bystander? Clinical microbiology and infection 12:1050-1059.
212. Okogbule-Wonodi AC, Chesko KL, Famuyide ME, Viscardi RM. 2011. Surfactant protein-A enhances ureaplasmacidal activity in vitro. Innate immunity 17:145-151.
213. Oberley RE, Ault KA, Neff TL, Khubchandani KR, Crouch EC, Snyder JM. 2004. Surfactant proteins A and D enhance the phagocytosis of Chlamydia into THP-1 cells. American Journal of Physiology-Lung Cellular and Molecular Physiology 287:L296-L306.
214. Tenner AJ, Robinson SL, Borchelt J, Wright J. 1989. Human pulmonary surfactant protein (SP-A), a protein structurally homologous to C1q, can enhance FcR-and CR1-mediated phagocytosis. Journal of Biological Chemistry 264:13923-13928.
215. Endo M, Ohi H, Ohsawa I, Fujita T, Matsushita M, Fujita T. 1998. Glomerular deposition of mannose-binding lectin (MBL) indicates a novel mechanism of complement activation in IgA nephropathy. Nephrology, dialysis, transplantation: official publication of the European Dialysis and Transplant Association-European Renal Association 13:1984-1990.
216. Wu H, Kuzmenko A, Wan S, Schaffer L, Weiss A, Fisher JH, Kim KS, McCormack FX. 2003. Surfactant proteins A and D inhibit the growth of Gram-negative bacteria by increasing membrane permeability. The Journal of clinical investigation 111:1589-1602.
217. Brown EJ. 1995. Phagocytosis. Bioessays 17:109-117.
218. Gil M, McCormack FX, LeVine AM. 2009. Surfactant protein A modulates cell surface expression of CR3 on alveolar macrophages and enhances CR3-mediated phagocytosis. Journal of Biological Chemistry 284:7495-7504.
219. Gardai SJ, Xiao Y-Q, Dickinson M, Nick JA, Voelker DR, Greene KE, Henson PM. 2003. By binding SIRPα or calreticulin/CD91, lung collectins act as dual function surveillance molecules to suppress or enhance inflammation. Cell 115:13-23.
220. Zanoni I, Granucci F. 2013. Role of CD14 in host protection against infections and in metabolism regulation. Frontiers in cellular and infection microbiology 3:32.
221. Alcorn JF, Wright JR. 2004. Surfactant protein A inhibits alveolar macrophage cytokine production by CD14-independent pathway. American Journal of Physiology-Lung Cellular and Molecular Physiology 286:L129-L136.
222. Senft AP, Korfhagen TR, Whitsett JA, Shapiro SD, LeVine AM. 2005. Surfactant protein-D regulates soluble CD14 through matrix metalloproteinase-12. The Journal of Immunology 174:4953-4959.
223. Sato M, Sano H, Iwaki D, Kudo K, Konishi M, Takahashi H, Takahashi T, Imaizumi H, Asai Y, Kuroki Y. 2003. Direct binding of Toll-like receptor 2 to zymosan, and zymosan-induced NF-κB activation and TNF-α secretion are down-regulated by lung collectin surfactant protein A. The Journal of Immunology 171:417-425.

224. Yamada C, Sano H, Shimizu T, Mitsuzawa H, Nishitani C, Himi T, Kuroki Y. 2006. Surfactant protein A directly interacts with TLR4 and MD-2 and regulates inflammatory cellular response: importance of supratrimeric oligomerization. Journal of Biological Chemistry 281:21771-21780.
225. Herbein JF, Wright JR. 2001. Enhanced clearance of surfactant protein D during LPS-induced acute inflammation in rat lung. American Journal of Physiology-Lung Cellular and Molecular Physiology 281:L268-L277.
226. Saka R, Wakimoto T, Nishiumi F, Sasaki T, Nose S, Fukuzawa M, Oue T, Yanagihara I, Okuyama H. 2016. Surfactant protein-D attenuates the lipopolysaccharide-induced inflammation in human intestinal cells overexpressing toll-like receptor 4. Pediatric surgery international 32:59-63.
227. Vayrynen O, Glumoff V, Hallman M. 2002. Regulation of surfactant proteins by LPS and proinflammatory cytokines in fetal and newborn lung. American Journal of Physiology-Lung Cellular and Molecular Physiology 282:L803-L810.
228. Bhatti F, Ball G, Hobbs R, Linens A, Munzar S, Akram R, Barber AJ, Anderson M, Elliott M, Edwards M. 2015. Pulmonary surfactant protein a is expressed in mouse retina by Müller cells and impacts neovascularization in oxygen-induced retinopathy. Investigative ophthalmology & visual science 56:232-242.
229. Lin PM, Wright JR. 2006. Surfactant protein A binds to IgG and enhances phagocytosis of IgG-opsonized erythrocytes. American Journal of Physiology-Lung Cellular and Molecular Physiology 291:L1199-L1206.
230. Wofford JA, Wright JR. 2007. Surfactant protein A regulates IgG-mediated phagocytosis in inflammatory neutrophils. American Journal of Physiology-Lung Cellular and Molecular Physiology 293:L1437-L1443.
231. Madsen J, Mollenhauer J, Holmskov U. 2010. Gp-340/DMBT1 in mucosal innate immunity. Innate immunity 16:160-167.
232. Jakel A, Qaseem AS, Kishore U, Sim RB. 2013. Ligands and receptors of lung surfactant proteins SP-A and SP-D. Front Biosci (Landmark Ed) 18:1129-40.
233. Brinker KG, Garner H, Wright JR. 2003. Surfactant protein A modulates the differentiation of murine bone marrow-derived dendritic cells. American Journal of Physiology-Lung Cellular and Molecular Physiology 284:L232-L241.
234. Haczku A, Cao Y, Vass G, Kierstein S, Nath P, Atochina-Vasserman EN, Scanlon ST, Li L, Griswold DE, Chung KF. 2006. IL-4 and IL-13 form a negative feedback circuit with surfactant protein-D in the allergic airway response. The Journal of Immunology 176:3557-3565.
235. Borron P, Veldhuizen R, Lewis JF, Possmayer F, Caveney A, Inchley K, McFadden RG, Fraher LJ. 1996. Surfactant associated protein-A inhibits human lymphocyte proliferation and IL-2 production. American journal of respiratory cell and molecular biology 15:115-121.
236. Borron PJ, Mostaghel EA, Doyle C, Walsh ES, McHeyzer-Williams MG, Wright JR. 2002. Pulmonary surfactant proteins A and D directly suppress CD3+/CD4+ cell function: evidence for two shared mechanisms. The Journal of Immunology 169:5844-5850.
237. Mukherjee S, Giamberardino C, Thomas J, Evans K, Goto H, Ledford JG, Hsia B, Pastva AM, Wright JR. 2012. Surfactant protein A integrates activation signal strength to differentially modulate T cell proliferation. The Journal of Immunology 188:957-967.
238. Yang S, Milla C, Panoskaltsis-Mortari A, Ingbar DH, Blazar BR, Haddad IY. 2001. Human surfactant protein a suppresses T cell–dependent inflammation and attenuates the manifestations of idiopathic pneumonia syndrome in mice. American journal of respiratory cell and molecular biology 24:527-536.
239. Watson A, Spalluto CM, McCrae C, Cellura D, Burke H, Cunoosamy D, Freeman A, Hicks A, Hühn M, Ostridge K. 2020. Dynamics of IFN-β responses during respiratory viral infection. Insights for therapeutic strategies. American journal of respiratory and critical care medicine 201:83-94.

240. Roberts J. 2007. Infection of murine vaginal or endocervical mucosa with human papillomavirus pseudovirions.
241. Aldo PB, Craveiro V, Guller S, Mor G. 2013. Effect of culture conditions on the phenotype of THP-1 monocyte cell line. Wiley Online Library,
242. Daigneault M, Preston JA, Marriott HM, Whyte MK, Dockrell DH. 2010. The identification of markers of macrophage differentiation in PMA-stimulated THP-1 cells and monocyte-derived macrophages. PloS one 5:e8668.
243. Forrester MA, Wassall HJ, Hall LS, Cao H, Wilson HM, Barker RN, Vickers MA. 2018. Similarities and differences in surface receptor expression by THP-1 monocytes and differentiated macrophages polarized using seven different conditioning regimens. Cellular immunology 332:58-76.
244. Qin Z. 2012. The use of THP-1 cells as a model for mimicking the function and regulation of monocytes and macrophages in the vasculature. Atherosclerosis 221:2-11.
245. Berges C, Naujokat C, Tinapp S, Wieczorek H, Höh A, Sadeghi M, Opelz G, Daniel V. 2005. A cell line model for the differentiation of human dendritic cells. Biochemical and Biophysical Research Communications 333:896-907.
246. Li L, Wang S, Zou Z, Tao A, Ai Y. 2018. Activation profile of THP-1 derived dendritic cells stimulated by allergen Mal f 1 beyond its IgE-binding ability. International Immunopharmacology 62:139-146.
247. Watson A, Kronqvist N, Spalluto CM, Griffiths M, Staples KJ, Wilkinson T, Holmskov U, Sorensen GL, Rising A, Johansson J. 2017. Novel expression of a functional trimeric fragment of human SP-A with efficacy in neutralisation of RSV. Immunobiology 222:111-118.
248. Dobbs LG, Wright JR, Hawgood S, Gonzalez R, Venstrom K, Nellenbogen J. 1987. Pulmonary surfactant and its components inhibit secretion of phosphatidylcholine from cultured rat alveolar type II cells. Proceedings of the National Academy of Sciences 84:1010-1014.
249. Suwabe A, Mason RJ, Voelker DR. 1996. Calcium dependent association of surfactant protein A with pulmonary surfactant: application to simple surfactant protein A purification. Archives of biochemistry and biophysics 327:285-291.
250. Buck CB, Pastrana DV, Lowy DR, Schiller JT. 2005. Generation of HPV pseudovirions using transfection and their use in neutralization assays, p 445-462, Human Papillomaviruses. Springer.
251. Christensen ND, Cladel NM, Reed CA, Budgeon LR, Embers ME, Skulsky DM, McClements WL, Ludmerer SW, Jansen KU. 2001. Hybrid papillomavirus L1 molecules assemble into virus-like particles that reconstitute conformational epitopes and induce neutralizing antibodies to distinct HPV types. Virology 291:324-334.
252. Buck CB. 2015. Production of Papillomaviral Vectors (Pseudoviruses), *on* NCI. Accessed 9 February.
253. Schäfer G, Guler R, Murray G, Brombacher F, Brown GD. 2009. The role of scavenger receptor B1 in infection with Mycobacterium tuberculosis in a murine model. PloS one 4:e8448.
254. Bolte S, Cordelières FP. 2006. A guided tour into subcellular colocalization analysis in light microscopy. Journal of microscopy 224:213-232.
255. Chanput W, Mes JJ, Wichers HJ. 2014. THP-1 cell line: An in vitro cell model for immune modulation approach. International Immunopharmacology 23:37-45.
256. Park E, Jung H, Yang H, Yoo M, Kim C, Kim K. 2007. Optimized THP-1 differentiation is required for the detection of responses to weak stimuli. Inflammation research 56:45-50.
257. Gordon S. 2003. Alternative activation of macrophages. Nature Reviews Immunology 3:23-35.
258. Mantovani A, Sozzani S, Locati M, Allavena P, Sica A. 2002. Macrophage polarization: tumor-associated macrophages as a paradigm for polarized M2 mononuclear phagocytes. Trends in Immunology 23:549-555.

259. Deng Y, Govers C, Beest Et, Van Dijk A-J, Hettinga K, Wichers HJ. 2021. A THP-1 cell line-based exploration of immune responses toward heat-treated BLG. Frontiers in Nutrition 7:612397.
260. Liu Y, Xia Y, Qiu C-H. 2021. Functions of CD169 positive macrophages in human diseases. Biomedical Reports 14:1-1.
261. Crux NB, Elahi S. 2017. Human leukocyte antigen (HLA) and immune regulation: how do classical and non-classical HLA alleles modulate immune response to human immunodeficiency virus and hepatitis C virus infections? Frontiers in immunology 8:832.
262. Bishara N. 2012. The use of biomarkers for detection of early-and late-onset neonatal sepsis. Hematology, immunology and infectious disease: neonatology questions and controversies:303-315.
263. Martin AW. 2011. Chapter 6 - Immunohistology of Non-Hodgkin Lymphoma, p 156-188. *In* Dabbs DJ (ed), Diagnostic Immunohistochemistry (Third Edition). W.B. Saunders, Philadelphia.
264. Czernek L, Chworos A, Duechler M. 2015. The uptake of extracellular vesicles is affected by the differentiation status of myeloid cells. Scandinavian journal of immunology 82:506-514.
265. Brzostek J, Gascoigne NR, Rybakin V. 2016. Cell type-specific regulation of immunological synapse dynamics by B7 ligand recognition. Frontiers in Immunology 7:24.
266. Chen R, Yang D, Shen L, Fang J, Khan R, Liu D. 2022. Overexpression of CD86 enhances the ability of THP-1 macrophages to defend against Talaromyces marneffei. Immunity, inflammation and disease 10:e740.
267. Oetke C, Vinson MC, Jones C, Crocker PR. 2006. Sialoadhesin-deficient mice exhibit subtle changes in B-and T-cell populations and reduced immunoglobulin M levels. Molecular and cellular biology.
268. Morón-Calvente V, Romero-Pinedo S, Toribio-Castelló S, Plaza-Díaz J, Abadía-Molina AC, Rojas-Barros DI, Beug ST, LaCasse EC, MacKenzie A, Korneluk R. 2018. Inhibitor of apoptosis proteins, NAIP, cIAP1 and cIAP2 expression during macrophage differentiation and M1/M2 polarization. PLoS One 13:e0193643.
269. Mantovani A, Sica A, Sozzani S, Allavena P, Vecchi A, Locati M. 2004. The chemokine system in diverse forms of macrophage activation and polarization. Trends in immunology 25:677-686.
270. Geijtenbeek TB, Torensma R, van Vliet SJ, van Duijnhoven GC, Adema GJ, van Kooyk Y, Figdor CG. 2000. Identification of DC-SIGN, a novel dendritic cell–specific ICAM-3 receptor that supports primary immune responses. Cell 100:575-585.
271. Zhou T, Chen Y, Hao L, Zhang Y. 2006. DC-SIGN and immunoregulation. Cell Mol Immunol 3:279-283.
272. Dominguez-Soto A, Sierra-Filardi E, Puig-Kröger A, Pérez-Maceda B, Gómez-Aguado F, Corcuera MT, Sánchez-Mateos P, Corbí AL. 2011. Dendritic cell-specific ICAM-3–grabbing nonintegrin expression on M2-polarized and tumor-associated macrophages is macrophage-CSF dependent and enhanced by tumor-derived IL-6 and IL-10. The Journal of Immunology 186:2192-2200.
273. Verhaegen M, Christopoulos TK. 2002. Recombinant Gaussia luciferase. Overexpression, purification, and analytical application of a bioluminescent reporter for DNA hybridization. Analytical chemistry 74:4378-4385.
274. Broniarczyk J, Massimi P, Bergant M, Banks L. 2015. Human papillomavirus infectious entry and trafficking is a rapid process. Journal of virology 89:8727-8732.
275. Bergant Marušič M, Ozbun MA, Campos SK, Myers MP, Banks L. 2012. Human papillomavirus L2 facilitates viral escape from late endosomes via sorting nexin 17. Traffic 13:455-467.
276. Young JM, Zine El Abidine A, Gómez-Martinez RA, Bondu V, Sterk RT, Surviladze Z, Ozbun MA. 2022. Protamine Sulfate Is a Potent Inhibitor of Human Papillomavirus Infection In Vitro and In Vivo. Antimicrobial Agents and Chemotherapy 66:e01513-21.

277. Molenberghs F, Verschuuren M, Barbier M, Bogers JJ, Cools N, Delputte P, Schelhaas M, De Vos WH. 2022. Cells infected with human papilloma pseudovirus display nuclear reorganization and heterogenous infection kinetics. Cytometry Part A 101:1035-1048.
278. Yau E, Yang L, Chen Y, Umstead TM, Atkins H, Katz ZE, Yewdell JW, Gandhi CK, Halstead ES, Chroneos ZC. 2023. Surfactant protein A alters endosomal trafficking of influenza A virus in macrophages. Frontiers in immunology 14:919800.
279. Funk CJ, Wang J, Ito Y, Travanty EA, Voelker DR, Holmes KV, Mason RJ. 2012. Infection of human alveolar macrophages by human coronavirus strain 229E. The Journal of general virology 93:494.
280. Hartshorn KL, White MR, Voelker DR, Coburn J, Zaner K, Crouch EC. 2000. Mechanism of binding of surfactant protein D to influenza A viruses: importance of binding to haemagglutinin to antiviral activity. Biochemical Journal 351:449-458.
281. Crowther JE, Schlesinger LS. 2006. Endocytic pathway for surfactant protein A in human macrophages: binding, clathrin-mediated uptake, and trafficking through the endolysosomal pathway. American Journal of Physiology-Lung Cellular and Molecular Physiology 290:L334-L342.
282. Sender V, Moulakakis C, Stamme C. 2011. Pulmonary surfactant protein A enhances endolysosomal trafficking in alveolar macrophages through regulation of Rab7. The Journal of Immunology 186:2397-2411.
283. Zoumpopoulou G, Tsakalidou E, Dewulf J, Pot B, Grangette C. 2009. Differential crosstalk between epithelial cells, dendritic cells and bacteria in a co-culture model. International Journal of Food Microbiology 131:40-51.
284. Lisi S, Sisto M, D'Amore M, Lofrumento DD. 2014. Co-culture system of human salivary gland epithelial cells and immune cells from primary Sjögren's syndrome patients: an in vitro approach to study the effects of Rituximab on the activation of the Raf-1/ERK1/2 pathway. International Immunology 27:183-194.
285. Bodet C, Chandad F, Grenier D. 2005. Modulation of cytokine production by Porphyromonas gingivalis in a macrophage and epithelial cell co-culture model. Microbes and Infection 7:448-456.
286. Loss H, Aschenbach JR, Ebner F, Tedin K, Lodemann U. 2020. Inflammatory responses of porcine MoDC and intestinal epithelial cells in a direct-contact co-culture system following a bacterial challenge. Inflammation 43:552-567.
287. Hamilton K, Zhao J, Sims P. 1993. Interaction between apolipoproteins AI and A-II and the membrane attack complex of complement. Affinity of the apoproteins for polymeric C9. Journal of Biological Chemistry 268:3632-3638.
288. Tang CH, Lu ME. 2009. Adiponectin increases motility of human prostate cancer cells via adipoR, p38, AMPK, and NF-κB pathways. The Prostate 69:1781-1789.
289. Takemura Y, Ouchi N, Shibata R, Aprahamian T, Kirber MT, Summer RS, Kihara S, Walsh K. 2007. Adiponectin modulates inflammatory reactions via calreticulin receptor–dependent clearance of early apoptotic bodies. The Journal of clinical investigation 117:375-386.
290. Eller K, Schroll A, Banas M, Kirsch AH, Huber JM, Nairz M, Skvortsov S, Weiss G, Rosenkranz AR, Theurl I. 2013. Lipocalin-2 expressed in innate immune cells is an endogenous inhibitor of inflammation in murine nephrotoxic serum nephritis. PloS one 8:e67693.
291. Flo TH, Smith KD, Sato S, Rodriguez DJ, Holmes MA, Strong RK, Akira S, Aderem A. 2004. Lipocalin 2 mediates an innate immune response to bacterial infection by sequestrating iron. Nature 432:917-921.
292. McCubrey JA, Steelman LS, Mayo MW, Algate PA, Dellow RA, Kaleko M. 1991. Growth-promoting effects of insulin-like growth factor-1 (IGF-1) on hematopoietic cells: overexpression of introduced IGF-1 receptor abrogates interleukin-3 dependency of murine factor-dependent cells by a ligand-dependent mechanism.
293. Kooijman R, Willems M, De Haas C, Rijkers GT, Schuurmans A, Van Buul-Offers SC, Heijnen CJ, Zegers B. 1992. Expression of type I insulin-like growth factor receptors on human peripheral blood mononuclear cells. Endocrinology 131:2244-2250.

294. Renier G, Clement I, Desfaits A, Lambert A. 1996. Direct stimulatory effect of insulin-like growth factor-I on monocyte and macrophage tumor necrosis factor-alpha production. Endocrinology 137:4611-4618.
295. Smith DF, Galkina E, Ley K, Huo Y. 2005. GRO family chemokines are specialized for monocyte arrest from flow. American Journal of Physiology-Heart and Circulatory Physiology 289:H1976-H1984.
296. Glynn P, Henney E, Hall I. 2001. Peripheral blood neutrophils are hyperresponsive to IL-8 and Gro-α in cryptogenic fibrosing alveolitis. European Respiratory Journal 18:522-529.
297. Jensen LJ, Kuhn M, Stark M, Chaffron S, Creevey C, Muller J, Doerks T, Julien P, Roth A, Simonovic M, Bork P, von Mering C. 2008. STRING 8—a global view on proteins and their functional interactions in 630 organisms. Nucleic Acids Research 37:D412-D416.
298. Zhou J, Sun XY, Frazer IH. 1993. Glycosylation of Human Papillomavirus Type 16 L1 Protein. Virology 194:210-218.
299. Liu W, Li J, Du H, Ou Z. 2021. Mutation profiles, glycosylation site distribution and codon usage bias of human papillomavirus type 16. Viruses 13:1281.
300. Mobini Kesheh M, Shavandi S, Azami J, Esghaei M, Keyvani H. 2023. Genetic diversity and bioinformatic analysis in the L1 gene of HPV genotypes 31, 33, and 58 circulating in women with normal cervical cytology. Infectious Agents and Cancer 18:19.
301. Sawada K, Ariki S, Kojima T, Saito A, Yamazoe M, Nishitani C, Shimizu T, Takahashi M, Mitsuzawa H, Yokota S-i. 2010. Pulmonary collectins protect macrophages against pore-forming activity of Legionella pneumophila and suppress its intracellular growth. Journal of Biological Chemistry 285:8434-8443.
302. Bienkowska-Haba M, Williams C, Kim SM, Garcea RL, Sapp M. 2012. Cyclophilins facilitate dissociation of the human papillomavirus type 16 capsid protein L1 from the L2/DNA complex following virus entry. Journal of virology 86:9875-9887.
303. Watson A, Phipps MJ, Clark HW, Skylaris C-K, Madsen J. 2018. Surfactant proteins A and D: trimerized innate immunity proteins with an affinity for viral fusion proteins. Journal of innate immunity 11:13-28.
304. Dong J, McPherson CM, Stambrook PJ. 2002. Flt-3 ligand: a potent dendritic cell stimulator and novel antitumor. Cancer biology & therapy 1:486-489.
305. Powers C, McLeskey S, Wellstein A. 2000. Fibroblast growth factors, their receptors and signaling. Endocrine-related cancer 7:165-197.
306. Wells A. 1999. EGF receptor. The International Journal of Biochemistry & Cell Biology 31:637-643.
307. Schultz G, Clark W, Rotatori DS. 1991. EGF and TGF-α in wound healing and repair. Journal of cellular biochemistry 45:346-352.
308. De Castro NP, Rangel MC, Nagaoka T, Salomon DS, Bianco C. 2010. Cripto-1: an embryonic gene that promotes tumorigenesis. Future oncology 6:1127-1142.
309. Koh GY. 2013. Orchestral actions of angiopoietin-1 in vascular regeneration. Trends in molecular medicine 19:31-39.
310. Chen CL, Huang FW, Huang SS, San Huang J. 2021. IGFBP-3 and TGF-β inhibit growth in epithelial cells by stimulating type V TGF-β receptor (TβR-V)-mediated tumor suppressor signaling. FASEB BioAdvances 3:709.
311. Laron Z. 2001. Insulin-like growth factor 1 (IGF-1): a growth hormone. Molecular Pathology 54:311.
312. Hannink M, Donoghue DJ. 1989. Structure and function of platelet-derived growth factor (PDGF) and related proteins. Biochimica et Biophysica Acta (BBA)-Reviews on Cancer 989:1-10.
313. Gao X, Xu Z. 2008. Mechanisms of action of angiogenin. Acta biochimica et biophysica Sinica 40:619-624.
314. Manthey HD, Woodruff TM, Taylor SM, Monk PN. 2009. Complement component 5a (c5a). The international journal of biochemistry & cell biology 41:2114-2117.

315. Sadik CD, Miyabe Y, Sezin T, Luster AD. 2018. The critical role of C5a as an initiator of neutrophil-mediated autoimmune inflammation of the joint and skin. Seminars in Immunology 37:21-29.
316. Krzysiek R, Lefevre EA, Bernard J, Foussat A, Galanaud P, Louache F, Richard Y. 2000. Regulation of CCR6 chemokine receptor expression and responsiveness to macrophage inflammatory protein-3α/CCL20 in human B cells. Blood, The Journal of the American Society of Hematology 96:2338-2345.
317. Lee AY, Körner H. 2019. The CCR6-CCL20 axis in humoral immunity and TB cell immunobiology. Immunobiology 224:449-454.
318. Roberts AW. 2005. G-CSF: a key regulator of neutrophil production, but that's not all! Growth factors 23:33-41.
319. Nelson BH. 2004. IL-2, regulatory T cells, and tolerance. The Journal of Immunology 172:3983-3988.
320. Handa K, Suzuki R, Matsui H, Shimizu Y, Kumagai K. 1983. Natural killer (NK) cells as a responder to interleukin 2 (IL 2). II. IL 2-induced interferon gamma production. Journal of immunology (Baltimore, Md: 1950) 130:988-992.
321. Baggiolini M, Loetscher P, Moser B. 1995. Interleukin-8 and the chemokine family. International journal of immunopharmacology 17:103-108.
322. Tsuda H, Michimata T, Hayakawa S, Tanebe K, Sakai M, Fujimura M, Matsushima K, Saito S. 2002. A Th2 chemokine, TARC, produced by trophoblasts and endometrial gland cells, regulates the infiltration of CCR4+ T lymphocytes into human decidua at early pregnancy. American journal of reproductive immunology 48:1-8.
323. Saeki H, Tamaki K. 2006. Thymus and activation regulated chemokine (TARC)/CCL17 and skin diseases. Journal of dermatological science 43:75-84.
324. Doroudgar S, Glembotski CC. 2013. ATF6 and thrombospondin 4: the dynamic duo of the adaptive endoplasmic reticulum stress response. Circulation research 112:9-12.
325. Ohnuma K, Dang NH, Morimoto C. 2008. Revisiting an old acquaintance: CD26 and its molecular mechanisms in T cell function. Trends in immunology 29:295-301.
326. Fleischer B. 1994. CD26: a surface protease involved in T-cell activation. Immunology today 15:180-184.
327. Emmerson PJ, Duffin KL, Chintharlapalli S, Wu X. 2018. GDF15 and growth control. Frontiers in physiology 9:1712.
328. Maruo S, Oh-Hora M, Ahn H-J, Ono S, Wysocka M, Kaneko Y, Yagita H, Okumura K, Kikutani H, Kishimoto T. 1997. B cells regulate CD40 ligand-induced IL-12 production in antigen-presenting cells (APC) during T cell/APC interactions. Journal of immunology (Baltimore, Md: 1950) 158:120-126.
329. Macatonia SE, Hosken NA, Litton M, Vieira P, Hsieh C-S, Culpepper JA, Wysocka M, Trinchieri G, Murphy KM, O'Garra A. 1995. Dendritic cells produce IL-12 and direct the development of Th1 cells from naive CD4+ T cells. Journal of immunology (Baltimore, Md: 1950) 154:5071-5079.
330. Liao Y-C, Liang W-G, Chen F-W, Hsu J-H, Yang J-J, Chang M-S. 2002. IL-19 induces production of IL-6 and TNF-α and results in cell apoptosis through TNF-α. The Journal of Immunology 169:4288-4297.
331. Leigh T, Scalia RG, Autieri MV. 2020. Resolution of inflammation in immune and nonimmune cells by interleukin-19. American Journal of Physiology-Cell Physiology 319:C457-C464.
332. Zenewicz LA, Flavell RA. 2008. IL-22 and inflammation: Leukin'through a glass onion. European journal of immunology 38:3265-3268.
333. Poindexter NJ, Williams RR, Powis G, Jen E, Caudle AS, Chada S, Grimm EA. 2010. IL-24 is expressed during wound repair and inhibits TGFα-induced migration and proliferation of keratinocytes. Experimental dermatology 19:714-722.
334. Wolk K, Witte K, Witte E, Proesch S, Schulze-Tanzil G, Nasilowska K, Thilo J, Asadullah K, Sterry W, Volk H-D, Sabat R. 2008. Maturing dendritic cells are an important source of IL-29 and IL-20 that may cooperatively increase the innate immunity of keratinocytes. Journal of Leukocyte Biology 83:1181-1193.

335. Dikmen K, Bostanci H, Gobut H, Yavuz A, Alper M, Kerem M. 2018. Recombinant adiponectin inhibits inflammation processes via NF-kB pathway in acute pancreatitis. Bratislava Medical Journal-Bratislavske Lekarske Listy 119.
336. Febriza A, Ridwan R, As' ad S, Kasim VN, Idrus HH. 2019. Adiponectin and its role in inflammatory process of obesity. Molecular and Cellular Biomedical Sciences 3:60-6.
337. Yang P, Skiba NP, Tewkesbury GM, Treboschi VM, Baciu P, Jaffe GJ. 2017. Complement-mediated regulation of apolipoprotein E in cultured human RPE cells. Investigative ophthalmology & visual science 58:3073-3085.
338. Dieu M-C, Vanbervliet B, Vicari A, Bridon J-M, Oldham E, Aït-Yahia S, Brière F, Zlotnik A, Lebecque S, Caux C. 1998. Selective recruitment of immature and mature dendritic cells by distinct chemokines expressed in different anatomic sites. The Journal of experimental medicine 188:373-386.
339. Øynebråten I, Hinkula J, Fredriksen AB, Bogen B. 2014. Increased generation of HIV-1 gp120-reactive CD8+ T cells by a DNA vaccine construct encoding the chemokine CCL3. PloS one 9:e104814.
340. Lee SY, Lee SY, Kandala G, Liou M-L, Liou H-C, Choi Y. 1996. CD30/TNF receptor-associated factor interaction: NF-kappa B activation and binding specificity. Proceedings of the National Academy of Sciences 93:9699-9703.
341. Grewal IS, Flavell RA. 1996. The role of CD40 ligand in costimulation and T-cell activation. Immunological reviews 153:85-106.
342. Karnell JL, Rieder SA, Ettinger R, Kolbeck R. 2019. Targeting the CD40-CD40L pathway in autoimmune diseases: Humoral immunity and beyond. Advanced Drug Delivery Reviews 141:92-103.
343. Tan SSH, Ng PML, Ho B, Ding JL. 2005. The antimicrobial properties of C-reactive protein (CRP). Journal of Endotoxin Research 11:249-256.
344. Mortensen RF, Duszkiewicz JA. 1977. Mediation of CRP-dependent phagocytosis through mouse macrophage Fc-receptors. The Journal of Immunology 119:1611-1616.
345. Alderson MR, Tough TW, Davis-Smith T, Braddy S, Falk B, Schooley KA, Goodwin RG, Smith C, Ramsdell F, Lynch DH. 1995. Fas ligand mediates activation-induced cell death in human T lymphocytes. The Journal of experimental medicine 181:71-77.
346. van Buul JD, Allingham MJ, Samson T, Meller J, Boulter E, García-Mata R, Burridge K. 2007. RhoG regulates endothelial apical cup assembly downstream from ICAM1 engagement and is involved in leukocyte trans-endothelial migration. The Journal of cell biology 178:1279-1293.
347. Jelinek DF, Lipsky PE. 1987. Enhancement of human B cell proliferation and differentiation by tumor necrosis factor-alpha and interleukin 1. Journal of immunology (Baltimore, Md: 1950) 139:2970-2976.
348. Munitz A, Brandt E, Mingler M, Finkelman F, Rothenberg M. 2008. Distinct roles for IL-13 and IL-4 via IL-13 receptor α1 and the type II IL-4 receptor in asthma pathogenesis. Proceedings of the National Academy of Sciences 105:7240-7245.
349. Tan J, Deleuran B, Gesser B, Maare H, Deleuran M, Larsen CG, Thestrup-Pedersen K. 1995. Regulation of human T lymphocyte chemotaxis in vitro by T cell-derived cytokines IL-2, IFN-gamma, IL-4, IL-10, and IL-13. Journal of immunology (Baltimore, Md: 1950) 154:3742-3752.
350. Girard D, Paquet M-E, Paquin R, Beaulieu AD. 1996. Differential effects of interleukin-15 (IL-15) and IL-2 on human neutrophils: modulation of phagocytosis, cytoskeleton rearrangement, gene expression, and apoptosis by IL-15.
351. Perera LP, K Goldman C, Waldmann TA. 1999. IL-15 induces the expression of chemokines and their receptors in T lymphocytes. The Journal of Immunology 162:2606-2612.
352. Lim KG, Wan H-C, Bozza PT, Resnick MB, Wong D, Cruikshank W, Kornfeld H, Center DM, Weller PF. 1996. Human eosinophils elaborate the lymphocyte chemoattractants. IL-16 (lymphocyte chemoattractant factor) and RANTES. Journal of immunology (Baltimore, Md: 1950) 156:2566-2570.

353. Kaser A, Dunzendorfer S, Offner FA, Ryan T, Schwabegger A, Cruikshank WW, Wiedermann CJ, Tilg H. 1999. A role for IL-16 in the cross-talk between dendritic cells and T cells. The Journal of Immunology 163:3232-3238.
354. Hara T, Miyajima A. 1996. Function and signal transduction mediated by the interleukin 3 receptor system in hematopoiesis. Stem cells 14:605-618.
355. Elliott MJ, Vadas MA, Cleland LG, Gamble JR, Lopez AF. 1990. IL-3 and granulocyte-macrophage colony-stimulating factor stimulate two distinct phases of adhesion in human monocytes. Journal of immunology (Baltimore, Md: 1950) 145:167-176.
356. Shih C-C, Hu MC-T, Hu J, Weng Y, Yazaki PJ, Medeiros J, Forman SJ. 2000. A secreted and LIF-mediated stromal cell–derived activity that promotes ex vivo expansion of human hematopoietic stem cells. Blood, The Journal of the American Society of Hematology 95:1957-1966.
357. Steinhoff JS, Lass A, Schupp M. 2021. Biological functions of RBP4 and its relevance for human diseases. Frontiers in Physiology 12:659977.
358. Moraes-Vieira PM, Yore MM, Dwyer PM, Syed I, Aryal P, Kahn BB. 2014. RBP4 activates antigen-presenting cells, leading to adipose tissue inflammation and systemic insulin resistance. Cell metabolism 19:512-526.
359. Banerjee H, Kane LP. 2018. Immune regulation by Tim-3. F1000Research 7.
360. Monney L, Sabatos CA, Gaglia JL, Ryu A, Waldner H, Chernova T, Manning S, Greenfield EA, Coyle AJ, Sobel RA. 2002. Th1-specific cell surface protein Tim-3 regulates macrophage activation and severity of an autoimmune disease. Nature 415:536-541.
361. Ocana-Guzman R, Torre-Bouscoulet L, Sada-Ovalle I. 2016. TIM-3 regulates distinct functions in macrophages. Frontiers in immunology 7:229.
362. Park SH, Kang K, Giannopoulou E, Qiao Y, Kang K, Kim G, Park-Min K-H, Ivashkiv LB. 2017. Type I interferons and the cytokine TNF cooperatively reprogram the macrophage epigenome to promote inflammatory activation. Nature immunology 18:1104-1116.
363. Dinarello CA. 1987. The biology of interleukin 1 and comparison to tumor necrosis factor. Immunology letters 16:227-231.
364. Cook-Mills JM. 2002. VCAM-1 signals during lymphocyte migration: role of reactive oxygen species. Molecular immunology 39:499-508.
365. Walsh GM, Symon F, Lazarovits A, Wardlaw A. 1996. Integrin α4β7 mediates human eosinophil interaction with MAdCAM-1, VCAM-1 and fibronectin. Immunology 89:112-119.
366. Rüegg C, Postigo AA, Sikorski EE, Butcher EC, Pytela R, Erle DJ. 1992. Role of integrin alpha 4 beta 7/alpha 4 beta P in lymphocyte adherence to fibronectin and VCAM-1 and in homotypic cell clustering. The Journal of cell biology 117:179-189.

7 Appendix

7.1 Solution recipes

cDMEM

1% Penicillin-Streptomycin (10000 U/mL, Lonza)

10% Foetal calf serum (FCS, Gibco)

In 500 mL Dulbecco's Modified Eagle Medium (DMEM), high Glucose (Capricorn Scientific)

F-Medium

3 volume Ham's F12, with L-glutamine (Capricorn Scientific)

1 volume DMEM, high Glucose (Capricorn Scientific)

5% FCS (Gibco)

1% Pen/Strep (10000 U/mL, Lonza)

0.4 µg/mL hydrocortisone

5 µg/mL insulin

8.4 ng/mL cholera toxin

10 ng/mL Epidermal Growth Factor (Invitrogen)

24 µg/mL adenine

cRPMI

1% Penicillin-Streptomycin (10000 U/mL, Lonza)

10% Foetal calf serum (FCS, Gibco)

In 500 mL RPMI 1640, with L-glutamine (Capricorn Scientific)

Lidocaine-EDTA

Lidocaine hydrochloride (Sigma) 4 mg/mL

10 mM EDTA

In PBS

FACS block

5% Bovine serum albumin (BSA) in PBS

FACS wash

0.5% BSA in PBS

FACS fix

1% paraformaldehyde in FACS wash

Luria-Bertani (LB) medium

10 g Tryptone

10 g Sodium Chloride (NaCl)

5 g Yeast extract

To 1L dH_2O

The pH was adjusted to 7.0 and the volume adjusted to 1L. The LB was sterilised by autoclaving for 20 min at 15 psi on liquid cycle.

2X HEPES buffered saline (HBS)

50 mM HEPES

280 mM NaCl

1.5 mM Na_2HPO_4

The pH was adjusted to 7.1, and filter sterilised.

5X High salt buffer (HSB)

125 mM HEPES, pH = 7.5

2.5 M NaCl

0.1 % Brij58

5 mM MgCl2

500 µM EDTA

Light caesium chloride (CsCl) solution

54 g CsCl

Up to 200 mL in 1X HSB

Heavy CsCl solution

77.6 g CsCl

Up to 200 mL in 1X HSB

7.2 Additional material

Supplementary Table 1: Information on the plasmids used for the production of HPV-PsVs.

Plasmid name	Gene/insert	Source	Selection antibiotic	Restriction Enzymes	RE products
pXULL	HPV16 L1 and L2	John T Schiller[1]	50 µg/mL zeocin	HindIII	1.6 kb + 1.6 kb + 2.4 kb + 2.8 kb
pV18cap	HPV18 L1 and L2	John T Schiller[1]	50 µg/mL kanamycin	XhoI, Not I	2.2 kb + 6.7 kb
p31sheLL	HPV31 L1 and L2	John T Schiller[1]	100 µg/mL ampicillin	NotI, EcoRV	9.28 kb + 1.45 kb
p45sheLL	HPV45 L1 and L2	John T Schiller[1]	100 µg/mL ampicillin	KpnI, HpaI	5.5 kb + 5.29 kb
p52sheLL	HPV 52 L1 and L2	John T Schiller[1]	100 µg/mL ampicillin	NotI, EcoRV	9.28 kb + 1.44 kb
p58sheLL	HPV 58 L1 and L2	John T Schiller[1]	100 µg/mL ampicillin	EcoRV, XhoI	8.63 kb +2.1 kb
pCMV-Gluc	Gaussia (Gau) luciferase Reporter	New England Biolabs	75 µg/mL ampicillin	StuI, Not I	0.94 kb + 4.86 kb

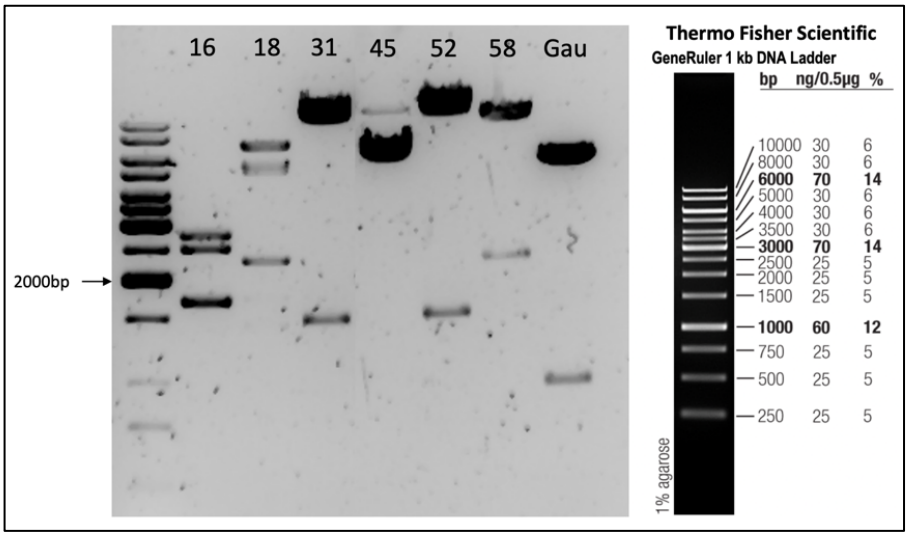

Supplementary Figure 1: Restriction enzyme digest of the plasmids used to produce HPV-PsVs. HPV types 16, 18, 31, 45, 52, and 58 were produced encapsidating the Gaussia luciferase reporter gene (Gau). Note: Some digests are incomplete and full plasmid constructs are detected along with the RE fragments.

[1] National Cancer Institute, NIH

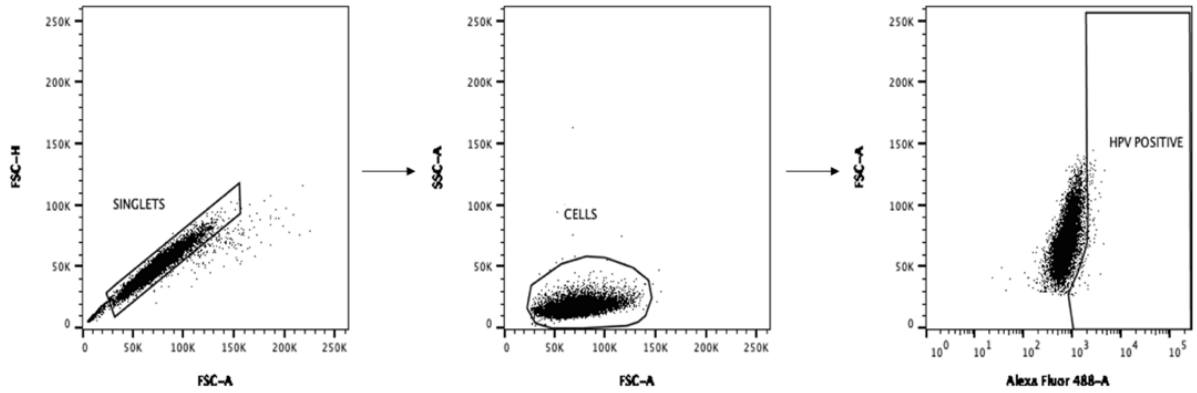

Supplementary Figure 2: Gating strategy for the FACS internalisation assay. Cells were treated as described in Section 2.5.2 before FACS analysis with a BD Fortessa. Singlets were gated based on the FSC-H/FSC-A plot, Singlets were further gated as cells based on the FSC-A/SSC-A plot. The HPV positive threshold in the AF488 channel was determined using untreated cells, where the same gating strategy was applied to all samples of the same cell type. Depicted here are uninfected RAW264.7 cells.

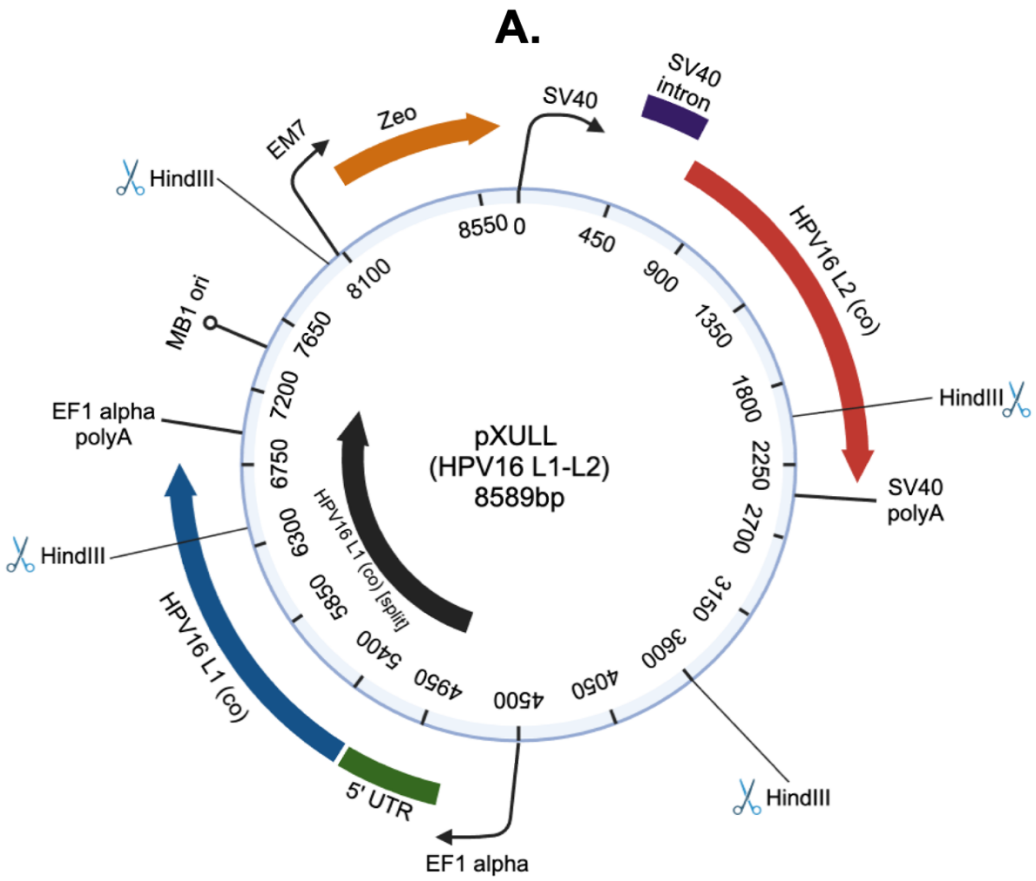

B.

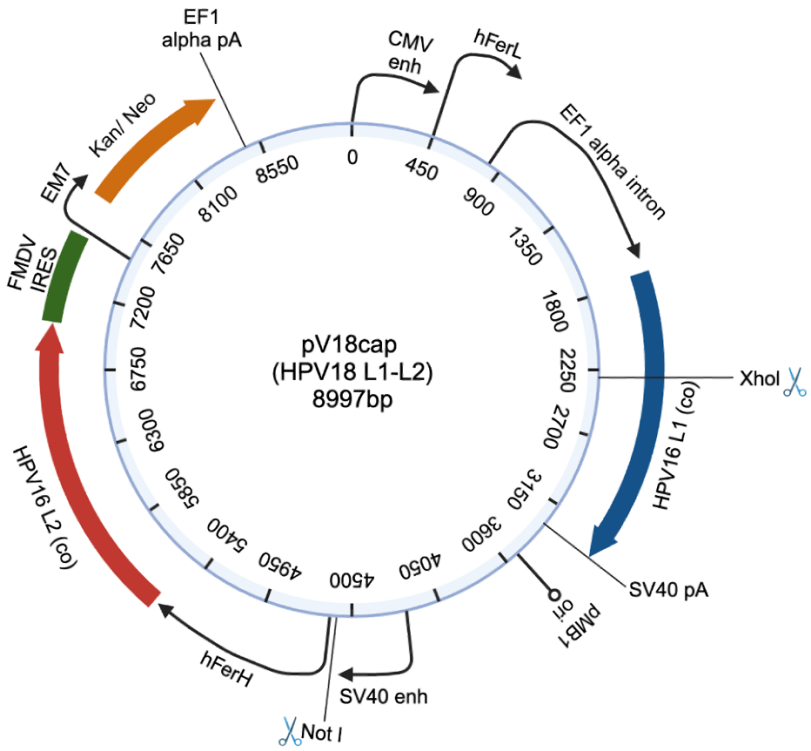
EF1
alpha pA
CMV
enh
hFerL
EF1 alpha intron
Kan/ Neo
EM7
FMDV
IRES
pV18cap
(HPV18 L1-L2)
8997bp
XhoI
HPV16 L1 (co)
HPV16 L2 (co)
SV40 pA
pMB1
ori
hFerH
SV40 enh
NotI
0
450
900
1350
1800
2250
2700
3150
3600
4050
4500
4950
5400
5850
6300
6750
7200
7650
8100
8550

C.

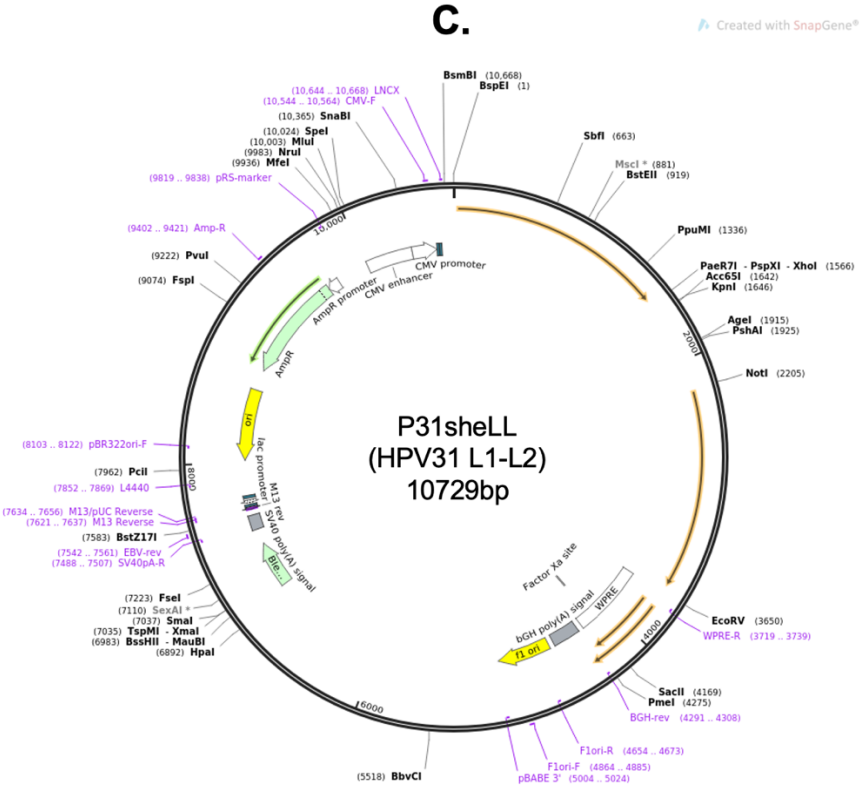
Created with SnapGene®
P31sheLL
(HPV31 L1-L2)
10729bp
BsmBI (10,668)
BspEI (1)
SbfI (663)
MscI * (881)
BstEII (919)
PpuMI (1336)
PaeR7I - PspXI - XhoI (1566)
Acc65I (1642)
KpnI (1646)
AgeI (1915)
PshAI (1925)
NotI (2205)
EcoRV (3650)
WPRE-R (3719 .. 3739)
SacII (4169)
PmeI (4275)
BGH-rev (4291 .. 4308)
F1ori-R (4654 .. 4673)
F1ori-F (4864 .. 4885)
pBABE 3' (5004 .. 5024)
(5518) BbvCI
(6892) HpaI
(6983) BssHII - MauBI
(7035) TspMI - XmaI
(7037) SmaI
(7110) SexAI *
(7223) FseI
(7583) BstZ17I
(7962) PciI
(8103 .. 8122) pBR322ori-F
(9074) FspI
(9222) PvuI
(9402 .. 9421) Amp-R
(9819 .. 9838) pRS-marker
(9936) MfeI
(9983) NruI
(10,003) MluI
(10,024) SpeI
(10,365) SnaBI
(10,544 .. 10,564) CMV-F
(10,644 .. 10,668) LNCX
CMV promoter
CMV enhancer
AmpR promoter
AmpR
ori
lac promoter
M13 rev
SV40 poly(A) signal
bGH poly(A) signal
WPRE
f1 ori
Factor Xa site
(7852 .. 7869) L4440
(7634 .. 7656) M13/pUC Reverse
(7621 .. 7637) M13 Reverse
(7542 .. 7561) EBV-rev
(7488 .. 7507) SV40pA-R

D.

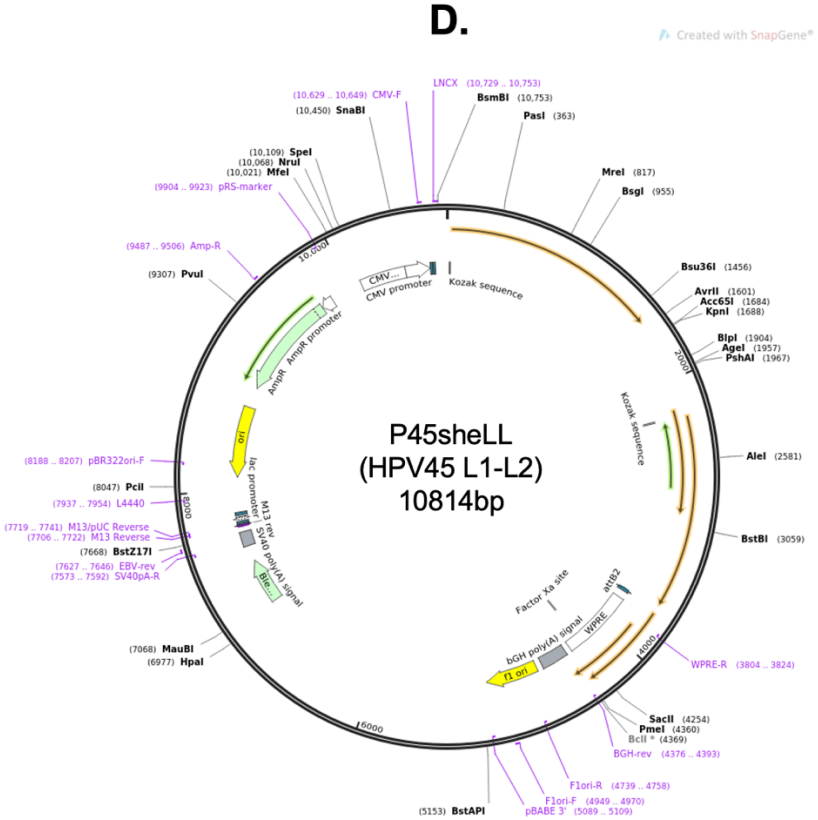
Created with SnapGene®
P45sheLL
(HPV45 L1-L2)
10814bp
LNCX (10,729 .. 10,753)
BsmBI (10,753)
PasI (363)
MreI (817)
BsgI (955)
Bsu36I (1456)
AvrII (1601)
Acc65I (1684)
KpnI (1688)
BlpI (1904)
AgeI (1957)
PshAI (1967)
AleI (2581)
BstBI (3059)
WPRE-R (3804 .. 3824)
SacII (4254)
PmeI (4360)
BclI * (4369)
BGH-rev (4376 .. 4393)
F1ori-R (4739 .. 4758)
F1ori-F (4949 .. 4970)
pBABE 3' (5089 .. 5109)
(5153) BstAPI
(7068) MauBI
(6977) HpaI
(7719 .. 7741) M13/pUC Reverse
(7706 .. 7722) M13 Reverse
(7668) BstZ17I
(7627 .. 7646) EBV-rev
(7573 .. 7592) SV40pA-R
(8188 .. 8207) pBR322ori-F
(8047) PciI
(7937 .. 7954) L4440
(9904 .. 9923) pRS-marker
(10,109) SpeI
(10,068) NruI
(10,021) MfeI
(10,450) SnaBI
(10,629 .. 10,649) CMV-F
(9487 .. 9506) Amp-R
(9307) PvuI
CMV promoter
Kozak sequence
AmpR promoter
AmpR
ori
lac promoter
M13 rev
SV40 poly(A) signal
Ble
Factor Xa site
attB2
WPRE
bGH poly(A) signal
f1 ori
Kozak sequence
10,000
2000
4000
6000
8000

E.

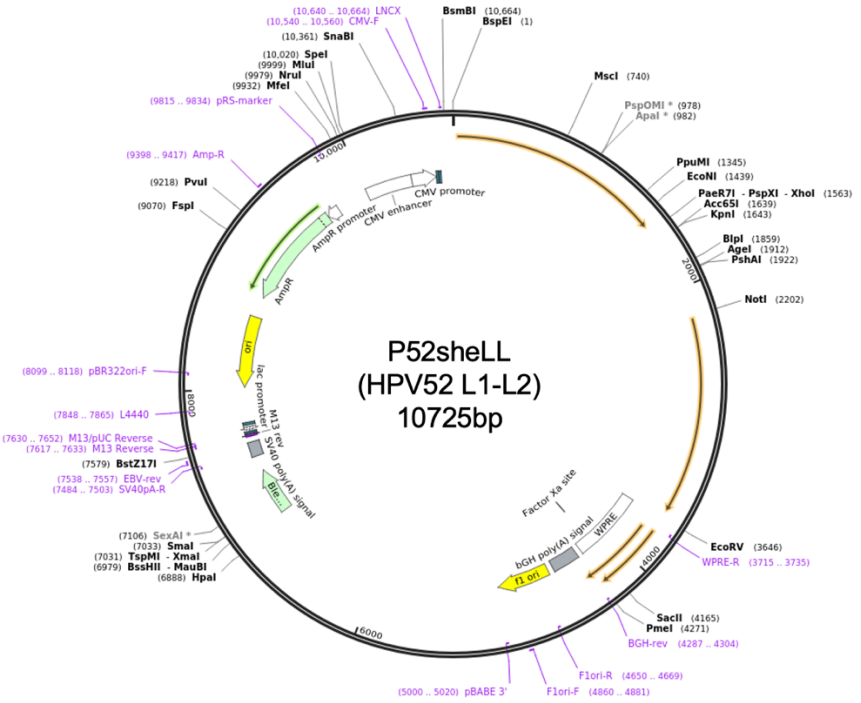
Created with SnapGene®
P52sheLL
(HPV52 L1-L2)
10725bp
BsmBI (10,664)
BspEI (1)
MscI (740)
PspOMI * (978)
ApaI * (982)
PpuMI (1345)
EcoNI (1439)
PaeR7I - PspXI - XhoI (1563)
Acc65I (1639)
KpnI (1643)
BlpI (1859)
AgeI (1912)
PshAI (1922)
NotI (2202)
EcoRV (3646)
WPRE-R (3715 .. 3735)
SacII (4165)
PmeI (4271)
BGH-rev (4287 .. 4304)
F1ori-R (4650 .. 4669)
F1ori-F (4860 .. 4881)
(5000 .. 5020) pBABE 3'
(7106) SexAI *
(7033) SmaI
(7031) TspMI - XmaI
(6979) BssHII - MauBI
(6888) HpaI
(7630 .. 7652) M13/pUC Reverse
(7617 .. 7633) M13 Reverse
(7579) BstZ17I
(7538 .. 7557) EBV-rev
(7484 .. 7503) SV40pA-R
(8099 .. 8118) pBR322ori-F
(7848 .. 7865) L4440
(9815 .. 9834) pRS-marker
(10,020) SpeI
(9999) MluI
(9979) NruI
(9932) MfeI
(10,361) SnaBI
(10,640 .. 10,664) LNCX
(10,540 .. 10,560) CMV-F
(9398 .. 9417) Amp-R
(9218) PvuI
(9070) FspI
CMV promoter
CMV enhancer
AmpR promoter
AmpR
ori
lac promoter
M13 rev
SV40 poly(A) signal
Ble
Factor Xa site
WPRE
bGH poly(A) signal
f1 ori
10,000
2000
4000
6000
8000

F.

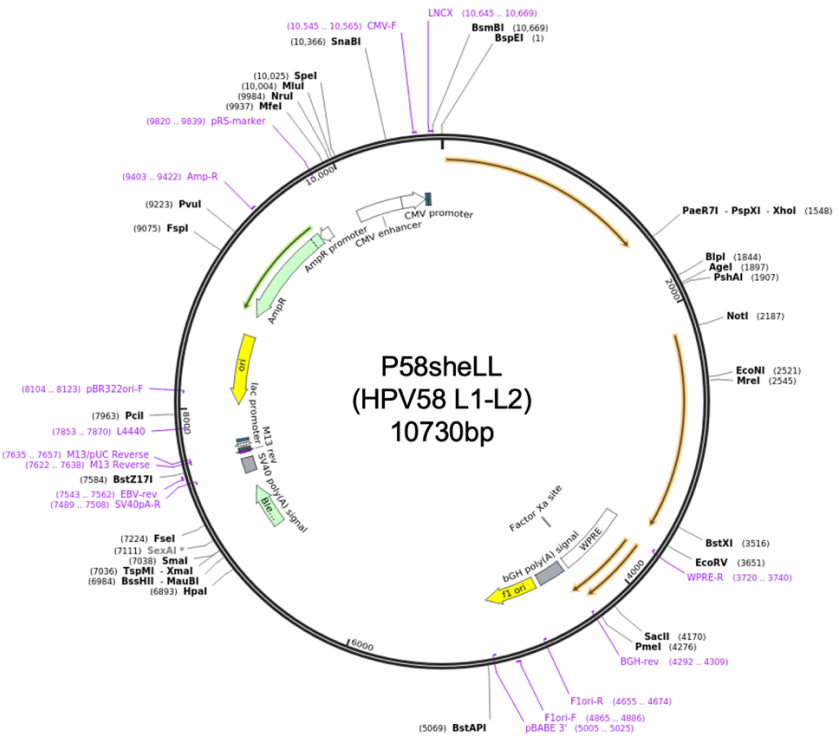

G.

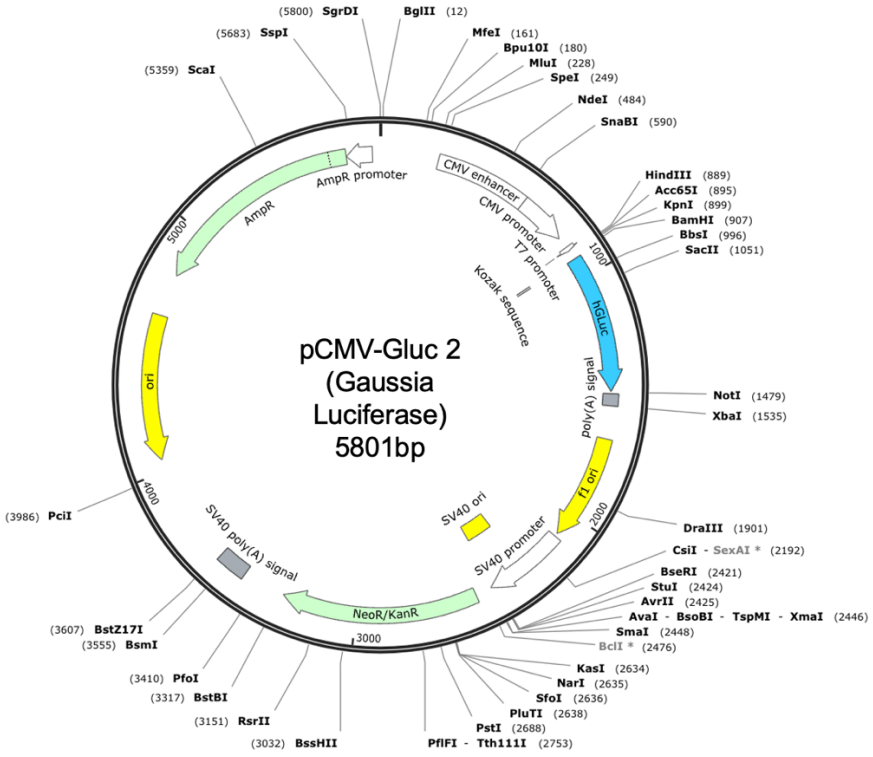

Supplementary Figure 3: Maps of the expression plasmids for the various L1/L2-specific HPV types prepared in this study. A. - **F.** L1-L2 expression plasmids for oncogenic HPV types 16, 18, 31, 45, 52, and 58. **G.** Gaussia luciferase reporter gene expression plasmid.

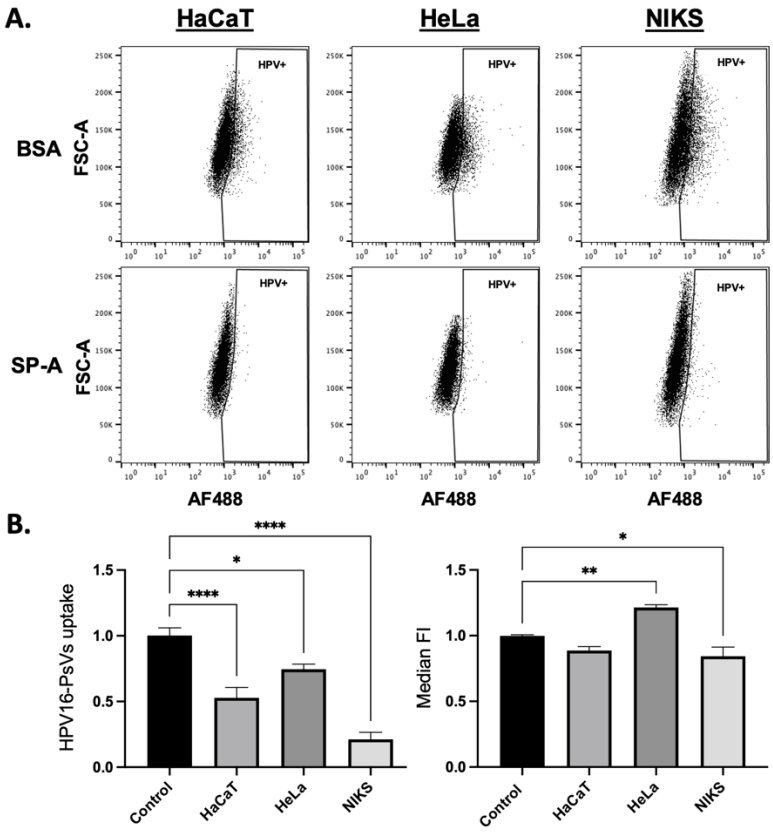

Supplementary Figure 4: HPV16-PsVs internalisation into HaCaT, HeLa, and NIKS cells is altered by SP-A preincubation. Cells were treated as described in Section 2.5.2, before acquisition with a BD Fortessa. **A.** Dot plots for AF488-HPV16-PsVs uptake after 1 h into the epithelial cell lines HaCaT, HeLa, and NIKS in the presence of BSA (top) or SP-A (bottom). **B.** HPV16-PsVs uptake on the left and the median fluorescent intensity (MFI) on the right is depicted. Data of three independent experiments are presented relative to uptake of the BSA control group which was set as 1. Statistical significance was determined by two-way Anova and Tukey's multiple comparison tests. *= p<0.05; **= p< 0.01; ****= p<0.0001; no symbol denotes not significant.

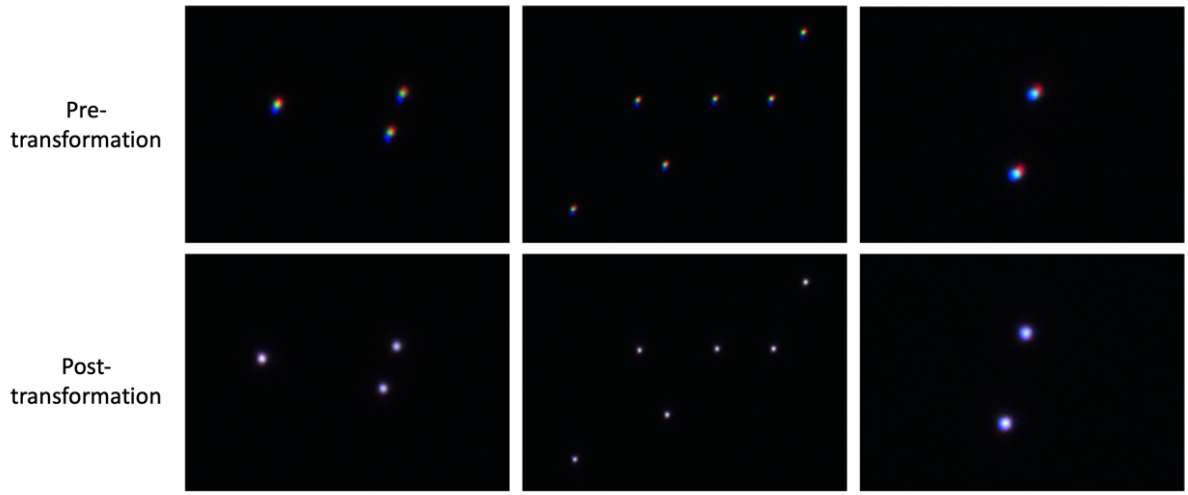

Supplementary Figure 5: Transformation of images acquired of multispectral fluorescent beads. Chromatic shift was accounted for using chromatic beads that fluoresced in the experimental channels: green, red, and blue. The top panel shows misalignment of these channels before the calculation was applied, and the bottom panel shows the channels aligning once the calculation was applied. The Align_Channels MacroScript created by Jerome Boulanger and available at https://github.com/jboulanger/imagej-macro.

Supplementary Table 2: List of the cytokines, chemokine and growth factors included in the R&D Systems Human XL cytokine array. Shown are the co-ordinates of each analyte on the membranes, the Entrez Gene ID, and the alternative nomenclature.

Coordinate	Analyte/Control	Entrez Gene ID	Alternate Nomenclature
A1, A2	Reference Spots	N/A	RS
A3, A4	Adiponectin	9370	Acrp30
A5, A6	Apolipoprotein A-I	335	ApoA1
A7, A8	Angiogenin	283	_____
A9, A10	Angiopoietin-1	284	Ang-1, ANGPT1
A11, A12	Angiopoietin-2	285	Ang-2, ANGPT2
A13, A14	BAFF	10673	BLyS, TNFSF13B
A15, A16	BDNF	627	Brain-derived Neurotrophic Factor
A17, A18	Complement Component C5/C5a	727	C5/C5a
A19, A20	CD14	929	_____
A21, A22	CD30	943	TNFRSF8
A23, A24	Reference Spots	N/A	RS
B3, B4	CD40 ligand	959	CD40L, TNFSF5, CD154, TRAP
B5, B6	Chitinase 3-like 1	1116	CHI3L1, YKL-40
B7, B8	Complement Factor D	1675	Adipsin, CFD
B9, B10	C-Reactive Protein	1401	CRP
B11, B12	Cripto-1	6997	Teratocarcinoma-derived Growth Factor
B13, B14	Cystatin C	1471	CST3, ARMD11
B15, B16	Dkk-1	22943	Dickkopf-1
B17, B18	DPPIV	1803	CD26, DPP4, Dipeptidyl-peptidase IV
B19, B20	EGF	1950	Epidermal Growth Factor
B21, B22	EMMPRIN	682	CD147, Basigin
C3, C4	ENA-78	6374	CXCL5
C5, C6	Endoglin	2022	CD105, ENG
C7, C8	Fas Ligand	356	TNFSF6, CD178, CD95L
C9, C10	FGF basic	2247	FGF-2

C11, C12	FGF-7	2252	KGF
C13, C14	FGF-19	9965	_____
C15, C16	Flt-3 Ligand	2323	FLT3LG
C17, C18	G-CSF	1440	CSF3
C19, C20	GDF-15	9518	MIC-1
C21, C22	GM-CSF	1437	CSF2
D1, D2	GROα	2919	CXCL1, MSGA-α
D3, D4	Growth Hormone	2688	GH, Somatotropin
D5, D6	HGF	3082	Scatter Factor, SF
D7, D8	ICAM-1	3383	CD54
D9, D10	IFN-γ	3458	IFNG
D11, D12	IGFBP-2	3485	_____
D13, D14	IGFBP-3	3486	_____
D15, D16	IL-1α	3552	IL-1F1
D17, D18	IL-1β	3553	IL-1F2
D19, D20	IL-1ra	3557	IL-1F3
D21, D22	IL-2	3558	_____
D23, D24	IL-3	3562	_____
E1, E2	IL-4	3565	_____
E3, E4	IL-5	3567	_____
E5, E6	IL-6	3569	_____
E7, E8	IL-8	3576	CXCL8
E9, E10	IL-10	3586	_____
E11, E12	IL-11	3589	_____
E13, E14	IL-12 p70	3593	_____
E15, E16	IL-13	3596	_____
E17, E18	IL-15	3600	_____
E19, E20	IL-16	3603	_____
E21, E22	IL-17A	3605	IL-17, CTLA8
E23, E24	IL-18 Bpa	10068	_____
F1, F2	IL-19	29949	_____
F3, F4	IL-22	50616	IL-TIF
F5, F6	IL-23	51561	IL-23A, SGRF
F7, F8	IL-24	11009	C49A, FISP, MDA-7, MOB-5, ST16
F9, F10	IL-27	246778	_____
F11, F12	IL-31	386653	_____
F13, F14	IL-32	9235	_____

F15, F16	IL-33	90865	C9orf26, DVS27, NF-HEV
F17, F18	IL-34	146433	C16orf77
F19, F20	IP-10	3627	CXCL10
F21, F22	I-TAC	6373	CXCL11, SCYB9B
F23, F24	Kallikrein 3	354	PSA, KLK3
G1, G2	Leptin	3952	OB
G3, G4	LIF	3976	_____
G5, G6	Lipocalin-2	3934	NGAL, LCN2, Siderocalin
G7, G8	MCP-1	6347	CCL2, MCAF
G9, G10	MCP-3	6354	CCL7, MARC
G11, G12	M-CSF	1435	CSF1
G13, G14	MIF	4282	_____
G15, G16	MIG	4283	CXCL9
G17, G18	MIP-1α/MIP-1β	6348/6351	CCL3/CCL4
G19, G20	MIP-3α	6364	CCL20, Exodus-1, LARC
G21, G22	MIP-3β	6363	CCL19, ELC
G23, G24	MMP-9	4318	CLG4B, Gelatinase B
H1, H2	Myeloperoxidase	4353	MPO, Lactoperoxidase
H3, H4	Osteopontin	6696	OPN
H5, H6	PDGF-AA	5154	_____
H7, H8	PDGF-AB/BB	5154/5155	_____
H9, H10	Pentraxin 3	5806	PTX3, TSG-14
H11, H12	PF4	5196	CXCL4
H13, H14	RAGE	177	_____
H15, H16	RANTES	6352	CCL5
H17, H18	RBP-4	5950	_____
H19, H20	Relaxin-2	6019	RLN2, RLXH2
H21, H22	Resistin	56729	ADSF, FIZZ3, RETN
H23, H24	SDF-1α	6387	CXCL12, PBSF
I1, I2	Serpin E1	5054	PAI-I, PAI-1, Nexin
I3, I4	SHBG	6462	ABP
I5, I6	ST2	9173	IL-1 R4, IL1RL1, ST2L
I7, I8	TARC	6361	CCL17
I9, I10	TFF3	7033	ITF, TFI
I11, I12	TfR	7037	CD71, TFR1, TFRC, TRFR

I13, I14	TGF-α	7039	TGFA
I15, I16	Thrombospondin-1	7057	THBS1, TSP-1
I17, I18	TNF-α	7124	TNFSF1A
I19, I20	uPAR	5329	PLAUR
I21, I22	VEGF	7422	BEGFA
J1, J2	Reference Spots	N/A	RS
J5, J6	Vitamin D BP	2638	VDB, DBP, VDBP
J7, J8	CD31	5175	PECAM-1
J9, J10	TIM-3	84868	HAVCR2
J11, J12	VCAM-1	7412	CD106
J23, J24	Negative Controls	N/A	Control (-)

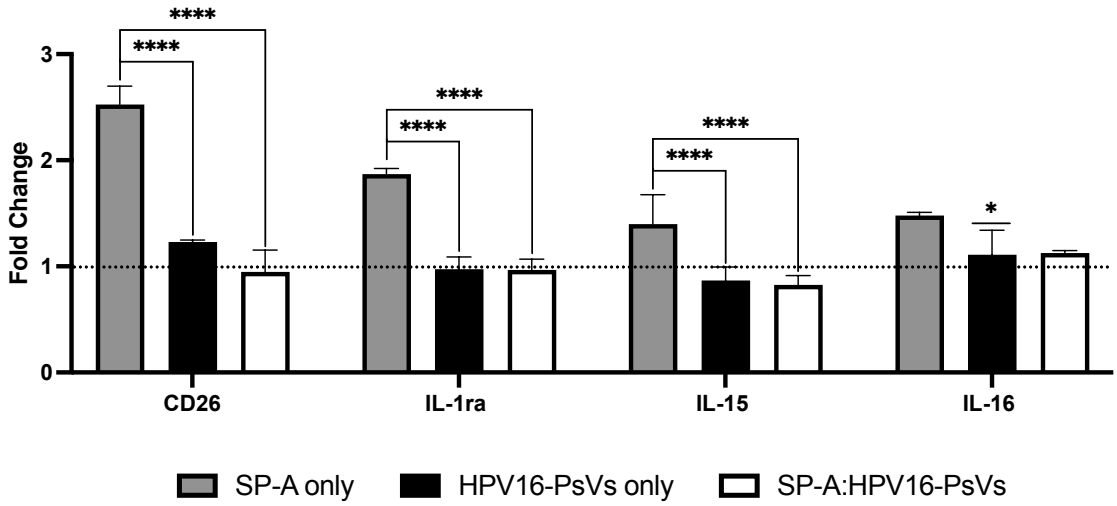

Supplementary Figure 6: Cytokines, chemokines, and growth factors that are upregulated by SP-A alone in THP-1 cells. Data are represented as mean fold-change relative to the untreated control group which was set as 1 (dotted line). Statistical significance was determined using 2-way ANOVA with Tukey's test for multiple comparisons. *= $p<0.05$, ****= $p<0.0001$; no symbol denotes not significant.

Supplementary Table 3: Protein information and pathway enrichment predicted by STRING for immune modulators most elevated in DC0 cells in the presence of SP-A and HPV16-PsVs compared to untreated cells. Elevated proteins were submitted to the STRING database and grouped using kmeans clustering, set to a high confidence threshold score for protein interactions (297). The relevant functional enrichments for GO biological and molecular function, STRING network clusters and KEGG pathways are listed. Only functional enrichments with a *strength of 1.75 or higher and a false discovery rate of $p<0.05$ are shown.

Name	Function Definition	Top Cluster GO enrichments, STRING and KEGG pathways
FLT3L (Flt-3 ligand)	Regulates haematopoiesis. The activated receptor kinase subsequently phosphorylates and activates multiple cytoplasmic effector molecules in pathways involved in apoptosis, proliferation, and differentiation of hematopoietic cells in bone marrow. Potent DC stimulator (304).	**GO:** Positive regulation of epithelial tube formation and epithelial cell proliferation and migration. Positive regulation of endothelial cell proliferation.
FGF-7 (fibroblast growth factor 7)	Keratinocyte growth factor that also acts as an integrin ligand which is required for FGF2 signalling (305).	
FGF-2 (fibroblast growth factor basic)	Plays an important role in the regulation of cell survival, cell division, cell differentiation and cell migration (24).	
EGF (epidermal growth factor)	Acts as a potent mitogenic factor that plays an important role in the growth, proliferation and differentiation of numerous cell types (306, 307).	
TGF-α (transforming growth factor alpha)	A growth factor which activates a signalling pathway for cell proliferation, differentiation and development (307).	
Cripto-1	Membrane-bound signalling protein that plays an essential role in embryonic development and tumour growth (308).	
Angio-1 (Angiopoietin-1)	Roles in vascular development, angiogenesis, endothelial cell survival, proliferation, migration, adhesion and cell spreading, reorganization of the actin cytoskeleton (309).	
IGFBP3 (insulin-like growth factor binding protein)	Exhibits IGF-independent antiproliferative and apoptotic effects mediated by its receptor TMEM219/IGFBP-3R (310).	
GH (growth hormone)	Plays an important role in growth control by stimulating secretion of insulin-like growth factor (IGF-1) (311).	
PDGF (platelet-derived growth factor)	A growth factor that regulates cell growth and division (312).	
Angiogenin	This protein induces angiogenesis after binding to actin on the surface of endothelial cells (313).	**GO:** Regulation of macrophage chemotaxis. Monocyte chemotaxis. Lymphocyte chemotaxis.
C5 complement component	A mediator of local inflammatory process. Binding to the receptor C5AR1 induces a variety of responses including intracellular calcium release, contraction of smooth muscle, increased vascular permeability, and histamine release from mast cells and basophilic leukocytes. C5a is also a potent chemokine which stimulates the locomotion of polymorphonuclear leukocytes and directs their migration toward sites of inflammation (314, 315).	

CCL20 (chemokine ligand 20)	Signals through binding and activation of CCR6 and induces a strong chemotactic response and mobilisation of intracellular calcium ions. The ligand- receptor pair CCL20-CCR6 is responsible for the chemotaxis of DCs, effector/memory T cells and B cells. Acts as a chemotactic factor that attracts lymphocytes (316, 317).	Regulation of granulocyte chemotaxis. Neutrophil chemotaxis. Regulation of leukocyte chemotaxis. Inflammatory response. Innate immune response. Defence response to other organisms. **KEGG:** C-type lectin receptor signalling pathway. JAK-STAT signalling pathway. Viral protein interaction with cytokine and cytokine receptor.
G-CSF (Granulocyte colony-stimulating factor)	Acts in haematopoiesis by controlling the production, differentiation, and function of granulocytes and the monocytes-macrophages (318).	
IL-2	Required for T cell proliferation and other activities crucial to regulation of the immune response. Can stimulate B cells, monocytes, lymphokine-activated killer cells, natural killer cells, and glioma cells (319, 320).	
IL-8	Attracts neutrophils, basophils, and T cells. It is also involved in neutrophil activation. It is released from several cell types in response to an inflammatory stimulus (296, 321).	
TARC (Thymus and activation regulated chemokine)	Chemotactic factor for T lymphocytes. May play a role in T cell development in thymus and in trafficking and activation of mature T cells (322, 323).	
Thrombo-1 (thrombospondin 1)	Plays a role in ER stress response, via its interaction with the activating transcription factor 6α (ATF6) which produces adaptive ER stress response factors (324).	
CD26	Essential for T cell receptor-mediated T cell activation. Acts as a positive regulator of T cell coactivation. Induces T cell proliferation and NF-κB activation in a T cell receptor/CD3-dependent manner (325, 326).	**GO:** Cytokine activity. **STRING:** JAK-STAT signalling pathway. IL20 family signalling. **KEGG:** JAK-STAT signalling pathway. Viral protein interaction with cytokine and cytokine receptor. Th17 cell differentiation. Cytokine-cytokine receptor interaction.
GDF-15 (Growth/Differentiation Factor-15)	Member of the TGFβ superfamily and is a stress-induced cytokine released in response to tissue injury (327).	
IL-12	It is produced by APCs and plays a critical role in host defence against intracellular microbial infection and control of malignancy via its ability to stimulate both innate and adaptive immune effector cells (328, 329).	
IL-19	May play some important roles in inflammatory responses. Upregulates IL-6 and TNF-α and induces apoptosis (330, 331).	
IL-22	Cytokine that contributes to the inflammatory response (332).	
IL-24	Has antiproliferative properties on melanoma cells and may contribute to terminal cell differentiation. Belongs to the IL-10 family. DCs not known to produce IL-24 (333, 334).	
Lipocalin-2	Iron-trafficking protein involved in multiple processes such as apoptosis, innate immunity and renal development (291).	
Adiponectin	Inhibits endothelial NF-κB signalling through a cAMP-dependent pathway (335, 336).	**GO:**
ApoA (Apoliprotein A-I)	It has serine proteinase activity and is able of autoproteolysis. Regulates activated complement (337).	

CCL3 (chemokine ligand 3)	Has inflammatory and chemokinetic properties. Binds to CCR1, CCR4 and CCR5. One of the major HIV-suppressive factors produced by CD8+ T cells (338, 339).	Positive regulation of neutrophil activation. Toll-like receptor 3 signalling pathway. Positive regulation of macrophage activation and differentiation. T cell migration. Acute inflammatory response. Calcium-mediated signalling. Positive regulation of defence response. Cytokine receptor binding. NF-κB signalling pathway. Positive regulation of I-κB kinase/NF-κB signalling. **STRING:** JAK-STAT signalling pathway Toll-like receptor signalling pathway.
CD30	May play a role in the regulation of cellular growth and transformation of activated lymphoblasts. Regulates gene expression through activation of NF-κB (340).	
CD40 ligand	Costimulates T cell proliferation and cytokine production. Induces the activation of NF-κB. Induces the activation of kinases MAPK8 and PAK2 in T-cells (341, 342).	
CRP (C-reactive protein)	Promotes agglutination, bacterial capsular swelling, phagocytosis and complement fixation through its calcium-dependent binding to phosphorylcholine (343, 344).	
Fas ligand	Involved in cytotoxic T cell-mediated apoptosis, natural killer cell-mediated apoptosis and in T cell development. Initiates fratricidal/suicidal activation-induced cell death (AICD) in antigen- activated T cells contributing to the termination of immune responses (345).	
ICAM-1	During leukocyte trans-endothelial migration, ICAM1 engagement promotes the assembly of endothelial apical cups through ARHGEF26/SGEF and RHOG activation (346).	
IL-1	Stimulates thymocyte proliferation by inducing IL-2 release, B cell maturation and proliferation, and fibroblast growth factor activity. IL-1 proteins are involved in the inflammatory response (338, 347).	
IL-13	Inhibits inflammatory cytokine production. Synergizes with IL-2 in regulating IFN- γ synthesis. May be critical in regulating inflammatory and immune responses. Positively regulates IL-31RA expression in macrophages (348, 349).	
IL-15	Stimulates the proliferation of T lymphocytes. In neutrophils, stimulates phagocytosis probably by signalling through the IL-15 receptor (350, 351).	
IL-16	Stimulates a migratory response in CD4+ lymphocytes, monocytes, and eosinophils. Primes CD4+ T cells for IL-2 and IL-15 responsiveness. Also induces T lymphocyte expression of IL-2 receptor. Ligand for CD4. Involved in cell cycle progression in T cells (352, 353).	
IL-3	Act in haematopoiesis by controlling the production, differentiation, and function of granulocytes and the monocytes-macrophages (354, 355).	
LIF (leukaemia inhibitory factor)	Has the capacity to induce terminal differentiation in leukemic cells. Its activities include the induction of haematopoietic differentiation in normal and myeloid leukaemia cells (356).	
RBP4 (retinol binding protein)	Mediates retinol transport in blood plasma (357). Shown to activate APCs leading to inflammation (358).	
TIM-3 (T cell immunoglobulin and	Modulates innate and adaptive immune responses and regulates macrophage activation. Inhibits Th1-mediated auto- and alloimmune responses and promotes immunological tolerance (359-361).	

mucin domain-containing protein 3)		
TNF (tumour necrosis factor)	It is mainly secreted by macrophages and can induce cell death of certain tumour cell lines. It is a potent pyrogen causing fever by direct action or by stimulation of IL-1 secretion and is implicated in the induction of cachexia and under certain conditions it can stimulate cell proliferation and induce cell differentiation (362, 363).	
VCAM-1 (Vascular cell adhesion molecule 1)	Important in cell-cell recognition. Appears to function in leukocyte-endothelial cell adhesion. Interacts with integrin α-4/ β-1 on leukocytes and mediates both adhesion and signal transduction (364-366).	

* Strength: Log10(observed / expected). This measure describes how large the enrichment effect is. It's the ratio between the number of proteins in the network that are annotated with a term and the number of proteins that we expect to be annotated with this term in a random network of the same size. False Discovery Rate: This measure describes how significant the enrichment is. P-values corrected for multiple testing within each category using the Benjamini–Hochberg procedure